

## University of Bradford eThesis

This thesis is hosted in [Bradford Scholars](#) – The University of Bradford Open Access repository. Visit the repository for full metadata or to contact the repository team



© University of Bradford. This work is licenced for reuse under a [Creative Commons Licence](#).

**REGULATION OF HAIR GROWTH:  
PROSTAGLANDINS AND PROSTAMIDES**

**KARZAN KHIDHIR**

**PhD**

**2010**

# **REGULATION OF HAIR GROWTH: PROSTAGLANDINS AND PROSTAMIDES**

Studies confirming the growth stimulating effects of prostanoids and prostamides on human hair follicles in organ culture and locating their receptors using lipidomics, molecular biological and immunohistological approaches

**Karzan Ghafur Khidhir**

Principal Supervisor: Professor V.A. Randall

Associate Supervisor: Dr S. Picksley

**Submitted for the degree of  
Doctor of Philosophy**

**Department of Biomedical Sciences**

**School of Life Sciences**

**University of Bradford**

**2010**

## Abstract

### Regulation of hair growth: prostaglandins and prostamides

**Keywords:** Alopecia, balding, bimatoprost, hair follicle, human, organ culture, prostaglandin  $F_{2\alpha}$ , treatment.

Hair growth disorders cause significant psychological distress, but are poorly controlled. Since prostaglandin  $F_{2\alpha}$  ( $PGF_{2\alpha}$ ) and prostamide  $F_{2\alpha}$  analogue glaucoma treatments cause eyelash growth as side-effects, they may be useful for alopecia. How they function is unknown; possibilities include direct action on hair follicles or stimulating follicular blood flow. It is important to clarify whether scalp follicles can also respond as human follicle response to androgens differ with body site. Therefore, human scalp follicles were grown *in vitro* in organ culture with  $PGF_{2\alpha}$ , latanoprost, a  $PGF_{2\alpha}$  analogue, and bimatoprost, a prostamide  $F_{2\alpha}$  analogue, with, or without, appropriate antagonists, and the presence of  $PGF_{2\alpha}$  (FP) and prostamide  $F_{2\alpha}$  receptors were investigated using molecular biological and immunohistochemical methods.

Each treatment significantly stimulated follicle growth rate, the percentage of growing follicles, and the amount of hair produced in a dose-responsive manner (10nM-1 $\mu$ M); the receptor antagonists blocked these effects.

Immunohistochemistry of frozen scalp sections demonstrated FP protein only in dermal papillae and connective tissue sheaths. RT-PCR identified FP and various prostamide  $F_{2\alpha}$  receptors in anagen follicles and isolated dermal papillae and bulbar connective tissue sheath, but not in bulb matrix or other epithelial tissues.

Therefore, isolated human scalp hair follicles can respond biologically to  $PGF_{2\alpha}$  and related pharmaceuticals in organ culture via follicular receptors and express the genes and protein for FP and prostamide  $F_{2\alpha}$  receptors.  $PGF_{2\alpha}$ -related drugs appear to act directly on follicles via receptors in the regulatory dermal papilla. They offer an exciting, novel approach for treating alopecia and merit clinical investigation.



## **Acknowledgements**

First and foremost I thank God.

I would like to pay special praise, thanks and appreciation to my principal supervisor, Professor Val Randall, for her support, co-operation and guidance in organising this project. I would also like to thank my second supervisor, Dr Steve Picksley, for his advice and being there when I needed help with molecular biology area.

I must also thank Professor Anna Nicolaou, Dr Joanne Durn and Dr Karen Massey for all the help with lipidomics area. I am also grateful to Dr Tayyebah Vafaei and Dr Katie Shorter for their help and advice throughout my learning period until I mastered the techniques that enabled this project to be successful. I would also like to thank all the technical staff within the Biomedical Sciences Division for their help and assistance.

I would also like to acknowledge the gift of latanoprost, bimatoprost and various receptor antagonists to Professor Randall by Dr David Woodward of Allergan Inc., Irvine, California, USA.

I would like to thank the Kurdistan Regional Government/Ministry of Higher Education and Scientific Research for funding my research studentship.

Last, but not least, I am very grateful to my family for all the support and encouragement without whom reaching such heights in life would surely have been impossible. Thank you for your support that you have given me.

Finally, to anyone that I have mistakenly forgotten, thanks for the help!

# Contents

<b>Abstract.....</b>	<b>3</b>
<b>Acknowledgements.....</b>	<b>4</b>
<b>Table of Contents.....</b>	<b>5</b>
<b>List of Figures.....</b>	<b>9</b>
<b>List of Tables .....</b>	<b>11</b>
<b>List of Abbreviations .....</b>	<b>12</b>
<b>1. Overall introduction .....</b>	<b>15</b>
1.1 The importance of hair.....	16
1.2 The structure and function of the hair follicle .....	18
1.2.1 Structure of the hair follicle .....	18
1.2.2 The hair follicle growth cycle .....	24
1.2.3 Embryogenesis of the hair follicle.....	28
1.2.4 Mesenchymal and epithelial interactions in the hair follicle.....	30
1.3 Regulation of hair growth.....	33
1.3.1 Hormonal regulation of hair growth .....	33
1.3.2 Potential paracrine factors produced by hair follicles .....	41
1.4 Hair disorders .....	44
1.5 Prostanoids and hair growth.....	51
1.5.1 Glaucoma treatments stimulate eyelash growth .....	51
1.5.2 The prostanoids.....	53
1.5.2.1 Prostanoid biosynthesis .....	534
1.5.2.2 The roles of prostanoids .....	536
1.5.3 Prostaglandins .....	58
1.5.4 Prostaglandins and hair growth.....	62
1.5.5 Prostamides and hair growth.....	64
1.5.5.1 Prostamides .....	645
1.5.5.2 Prostamide biosynthesis.....	645
1.5.5.3 Prostamide analogues and their therapeutic roles .....	647
1.6 Aims and experimental design .....	70
<b>2 Materials and Methods.....</b>	<b>76</b>
2.1 Histological and immunohistological staining of human and red deer hair follicles.....	76
2.1.1 Tissue samples.....	76
2.1.1.1 Deer skin .....	76
2.1.1.2 Human skin .....	767
2.1.2 Preparation of poly-l-lysine coated slides .....	78
2.1.3 Tissue sectioning .....	79

2.1.4 Histological study of skin and hair follicle structure using Saccpic staining .....	79
2.1.5 Immunohistochemical studies .....	81
2.1.5.1 Immunohistochemical localisation of cytokeratins 5 & 6.....	81
2.1.5.2 Localisation of melanoma-associated antigen, NKI-beteb, in human hair follicles.....	813
2.1.5.3 Localisation of PGF <sub>2α</sub> receptor (FP) in human hair follicles by immunohistochemistry.....	814
2.1.5.4 Localisation of PGE <sub>2</sub> receptor (EP <sub>2</sub> ) expression in human hair follicles.....	814
2.1.6 Visualising the staining.....	85
2.2 Detection of gene expression in human hair follicles by reverse transcription - polymerase chain reaction (RT-PCR) .....	85
2.2.1 Investigations into whether human hair follicles express the genes for prostaglandin and prostamide F <sub>2α</sub> receptors using RT-PCR.....	88
2.2.1.1 Tissue collection .....	89
2.2.1.2 Hair follicle microdissection.....	89
2.2.1.3 Microdissection of human hair follicle components .....	92
2.2.1.3.1 Experiment to determine follicle area including the bulge .....	92
2.2.1.3.2 Microdissection procedure to isolate human follicle components .....	93
2.2.1.4 RNA isolation, DNase treatment and cDNA synthesis.....	98
2.2.1.4.1 Total RNA extraction.....	985
2.2.1.4.2 Agarose gel electrophoresis .....	100
2.2.1.4.3 Spectrophotometric analysis .....	100
2.2.1.4.4 Poly(A) <sup>+</sup> RNA isolation.....	101
2.2.1.4.5 Amplification of mRNA samples .....	102
2.2.1.4.6 DNase treatment.....	105
2.2.1.4.7 Synthesis of cDNA by reverse transcription .....	105
2.2.1.5 Polymerase Chain Reaction .....	106
2.2.1.6 PCR primer design.....	110
2.2.1.7 Agarose gel electrophoresis of PCR products .....	111
2.2.1.8 Sequencing of PCR products .....	112
2.3 Human hair follicle organ culture .....	114
2.3.1 Skin samples .....	114
2.3.2 Hair follicle isolation .....	114
2.3.3 Hair growth culture conditions.....	115
2.3.4 Measurement of cultured hair follicles.....	116
2.3.5 Statistical analysis .....	116
2.4 Analysis of prostanoid lipid mediators.....	117
2.4.1 Lipidomic analysis.....	119
2.4.2 Skin samples .....	120
2.4.3 Sample preparation.....	120
2.4.4 Preparation of standards and calibration lines .....	121
2.4.5 LC/ESI-MS/MS analysis .....	122

### **3 Results ..... 123**

3.1 Human hair follicle growth in organ culture.....	123
------------------------------------------------------	-----

3.1.1 Effects of PGF <sub>2α</sub> and its analogue, latanoprost, on human hair follicle in organ culture.....	123
3.1.1.1 Scalp hair follicle growth in control conditions . ....	123
3.1.1.2 PGF <sub>2α</sub> stimulated human hair follicle growth <i>in vitro</i> in a dose responsive manner . ....	131
3.1.1.3 A PGF <sub>2α</sub> analogue, latanoprost, also stimulated human hair follicle growth <i>in vitro</i> in a dose responsive manner . ....	137
3.1.1.4 Two PGF <sub>2α</sub> receptor (FP) antagonists AS604872 and AL-8810 blocked PGF <sub>2α</sub> -stimulation of scalp hair growth in organ culture . ....	141
3.2 Histological investigation of deer and human skin . ....	147
3.3 Location of cytokeratins 5 & 6 in human scalp hair follicles . ....	157
3.4 Expression of NK1-beteb in human scalp hair follicles.....	160
3.5 Immunohistochemical localisation of prostaglandin F <sub>2α</sub> receptor (FP) in anagen scalp hair follicles . ....	162
3.6 Investigations to determine whether FP gene is expressed in the human scalp hair follicle using molecular biological methods.....	165
3.6.1 RT-PCR results for β-actin gene expression from human lower hair follicles.....	167
3.6.2 Validation of the RT-PCR for FP gene expression using rat liver tissue	170
3.6.3 Expression of the genes for FP in human hair follicles using RT-PCR ..	170
3.7 Experiments to determine which hair follicle components express the gene for FP . ....	174
3.7.1 Preliminary investigation of scalp hair follicle proportions.....	174
3.7.2 RT-PCR for the FP gene using isolated scalp hair follicle components.	175
3.7.3 RT-PCR results for β-actin gene expression from human hair follicle components.....	179
3.7.4 Expression of FP gene in cDNA extracted from human hair follicle components using RT-PCR . ....	181
3.7.5 The expression of FP gene in amplified RNA from human hair follicle components cells using RT-PCR.....	183
3.7.6 PCR detection of β-actin in amplified hair follicle components . ....	184
3.7.7 Expression of FP gene in amplified RNA from hair follicle components using RT-PCR . ....	190
3.8 Determination of which prostaglandins are present in scalp hair follicles by lipidomic analysis.....	194
3.9 Immunohistochemical localisation of PGE <sub>2</sub> receptor (EP <sub>2</sub> ) in the human scalp hair follicle bulb . ....	201
3.10 The effects of a prostamide F <sub>2α</sub> analogue, bimatoprost, on human scalp hair growth in organ culture . ....	204
3.10.1 Bimatoprost stimulated human hair follicle growth in organ culture in a concentration-dependent manner . ....	204
3.10.2 An FP antagonist, AS604872 (AGN22827), and a prostamide F <sub>2α</sub> receptor antagonist, AGN211336, blocked bimatoprost-stimulation of scalp hair growth in organ culture . ....	210
3.11 Identification of genes for prostamide F <sub>2α</sub> receptors in human scalp hair follicles using molecular biological methods . ....	217
3.11.1 RT-PCR for β-actin gene expression from anagen lower hair follicles	219
3.11.2 Expression of the genes for the prostamide F <sub>2α</sub> receptors (FP splice variants) in human hair follicles using RT-PCR.....	221

3.11.3 Location of gene expression for prostamide F <sub>2α</sub> receptors in amplified RNA from human hair follicle components .....	225
<b>4 Discussion.....</b>	<b>232</b>
<b>5 References .....</b>	<b>266</b>
<b>6 Appendices .....</b>	<b>295</b>
6.1 Sacpic stain.....	295
6.2 Preparation of phosphate buffered saline.....	295
6.3 Lowry method for protein content estimation .....	296
6.4 Representative calibration lines for PGF <sub>2α</sub> , PGD <sub>1</sub> , PGE <sub>1</sub> , PGD <sub>2</sub> , PGE <sub>2</sub> and 13,14-dihydro-15keto PGE <sub>2</sub> .....	298
6.5 Materials presented from this thesis .....	299

# List of figures

## 1. Introduction

Figure 1 Illustrative representation of an anagen hair follicle showing the different component parts.....	19
Figure 2 The structure of the hair follicle.....	21
Figure 3 The hair growth cycle.....	25
Figure 4 The hair follicle embryology.....	29
Figure 5 Mechanism of action of androgens.....	36
Figure 6 Mode of androgens action on the human hair follicle .....	38
Figure 7 Patterns of human hair growth .....	46
Figure 8 The patterns of hair loss in androgenetic alopecia in men .....	46
Figure 9 Prostanoid biosynthesis.....	55
Figure 10 The structures of prostaglandins F and E .....	60
Figure 11 Anandamide conversion pathways.....	67

## 2. Materials and Methods

Figure 12 Deer skin sample .....	77
Figure 13 Human skin sample .....	78
Figure 14 Mounted skin sample on the cryostat machine .....	80
Figure 15 Stage micrometer .....	86
Figure 16 Isolation of hair follicles from human scalp skin .....	91
Figure 17 Micro-dissection of hair follicle components: the dermal papilla, the dermal sheath around the bulb, the bulb matrix, the follicle at the level of the bulge area and the lower follicle between the bulb and the bulge .....	94
Figure 18 mRNA Amplification.....	103

## 3. Results

Figure 19 Sequential photomicrographs of a human hair follicle growing <i>in vitro</i> in control medium .....	125
Figure 20 Scalp hair follicle growth in organ culture under control conditions...	128
Figure 21 Percentage of scalp hair follicles remaining in anagen in organ culture under control conditions .....	129
Figure 22 Total amount of hair produced in organ culture under control conditions.....	130
Figure 23 Sequential photomicrographs of a human hair follicle growing <i>in vitro</i> in media with 100 nM PGF <sub>2α</sub> .....	133
Figure 24 PGF <sub>2α</sub> stimulated human hair follicle growth in organ culture .....	134
Figure 25 PGF <sub>2α</sub> prolongs anagen in scalp hair follicles in organ culture.....	135
Figure 26 PGF <sub>2α</sub> increased total amount of hair produced in organ culture .....	136
Figure 27 Latanoprost stimulated human hair follicle growth in organ culture ..	138
Figure 28 Latanoprost prolongs anagen in scalp hair follicles in organ culture...	139
Figure 29 Latanoprost increased total amount of hair produced in organ culture .....	140
Figure 30 Sequential photomicrographs of a human hair follicle growing in culture with 100 nM PGF <sub>2α</sub> + 1μM PGF <sub>2α</sub> receptor antagonist, AGN222827 .....	142
Figure 31 The PGF <sub>2α</sub> receptor antagonists, AGN222827 and AL-8810, blocked PGF <sub>2α</sub> -stimulation of scalp hair follicle growth rate.....	143
Figure 32 PGF <sub>2α</sub> receptor antagonists, AGN222827 and AL-8810, blocked the PGF <sub>2α</sub> -promoted increase in % of scalp hair follicles in anagen.....	144

Figure 33 The PGF <sub>2α</sub> receptor antagonists AGN222827 and AL-8810 blocked PGF <sub>2α</sub> -stimulated increased total amount of hair production .....	145
Figure 34 Structure of red deer skin .....	149
Figure 35 Structure of human scalp skin .....	152
Figure 36 Location of cytokeratins 5 & 6 in human scalp hair follicle .....	158
Figure 37 Location of NKI-beteb expression in scalp hair follicles .....	161
Figure 38 Immunolocalisation of FP in the human scalp hair follicle bulb .....	163
Figure 39 Gel electrophoresis of RNA from human scalp follicles .....	166
Figure 40 Gel electrophoresis of β-actin RT-PCR products from human scalp lower hair follicles .....	168
Figure 41 Sequencing results for β-actin RT-PCR product amplified from human hair follicle mRNA .....	169
Figure 42 Gel electrophoresis of FP gene RT-PCR product from rat liver cDNA ..	171
Figure 43 Human anagen hair follicles expressed the gene for FP .....	172
Figure 44 Sequencing results for FP RT-PCR product amplified from human hair follicle cDNA, compared to known human sequence .....	173
Figure 45 Agarose gel electrophoresis of total RNA extracted from hair follicle components from three samples .....	178
Figure 46 Gel electrophoresis of β-actin PCR products from human hair follicle components .....	180
Figure 47 PCR detection of FP gene in human hair follicle components .....	182
Figure 48 Agarose gel electrophoresis of total RNA from hair follicle components prior to amplification .....	185
Figure 49 Agarose gel electrophoresis of β-actin PCR products from amplified RNA from human hair follicle components .....	186
Figure 50 Sequencing results for β-actin RT-PCR product from amplified RNA from hair follicle components .....	187
Figure 51 PCR detection of FP gene from amplified RNA from human hair follicle components .....	191
Figure 52 Sequencing results for FP gene PCR product, following amplification from human hair follicle dermal papilla and connective tissue sheath cells .....	192
Figure 53 An example ESI-MS/MS product ion spectrum of PGF <sub>2α</sub> .....	196
Figure 54 Representative LC/ESI-MS/MS chromatograms of the prostanoids, dihydroprostaglandins and isoprostanes produced by human scalp hair follicles .....	198
Figure 55 Profile of the prostanoids naturally present in human scalp anagen hair follicles using LC/ESI-MS/MS .....	200
Figure 56 Immunolocalisation of EP <sub>2</sub> in the human hair follicle bulb .....	202
Figure 57 Sequential photomicrographs of a human scalp hair follicle growing <i>in vitro</i> in media with 100 nM bimatoprost .....	206
Figure 58 Bimatoprost stimulated human scalp hair follicle growth in organ culture .....	207
Figure 59 Bimatoprost prolongs anagen in scalp hair follicles in organ culture ..	208
Figure 60 Bimatoprost increased the total amount of hair produced in organ culture .....	209
Figure 61 Sequential photomicrographs of a human scalp hair follicle growing in culture with 100 nM bimatoprost + 1 μM prostamide F <sub>2α</sub> receptor antagonist, AGN211336 .....	211

Figure 62 AS604872 and AGN211336 blocked bimatoprost-stimulation of scalp hair follicle growth rate .....	212
Figure 63 AS604872 and AGN211336 blocked the bimatoprost-promoted increase in % of scalp hair follicles in anagen .....	213
Figure 64 AS604872 and AGN211336 blocked bimatoprost-stimulated increase in total amount of hair production .....	214
Figure 65 Photomicrographs of scalp hair follicles after growing in different conditions in organ culture for 9 days .....	216
Figure 66 Gel electrophoresis of RNA from human scalp follicles .....	218
Figure 67 $\beta$ -actin gel electrophoresis .....	220
Figure 68 Human scalp anagen hair follicles expressed genes for 2 prostamide $F_{2\alpha}$ receptors .....	222
Figure 69 Sequencing results for FP splice variants RT-PCR products amplified from human scalp hair follicle cDNA, compared to known human sequence .....	224
Figure 70 Dermal papilla and connective tissue sheath cells of human scalp hair follicles expressed genes for 2 prostamide $F_{2\alpha}$ receptors .....	226
Figure 71 Sequence analyses for FP splice variants RT-PCR products amplified from scalp hair follicle components cDNA, DP and CTS .....	228
Figure 72 Summary of the localisation of the gene expression of prostaglandin and prostamide $F_{2\alpha}$ receptors in scalp hair follicle dermal papilla and connective tissue sheath but not in other follicular components .....	230

#### 4. Discussion

Figure 73 Possible mechanisms for the stimulation of hair growth by $PGF_{2\alpha}$ , latanoprost and bimatoprost .....	259
-------------------------------------------------------------------------------------------------------------------------	-----

### List of Tables

Table 1 Different prostaglandin types, their receptors and their functions .....	61
Table 2 Specific forward and reverse primers and optimised conditions used in RT-PCR analysis of $\beta$ -actin, FP and FP splice variant complexes (altFPs) expression .....	108
Table 3 Human scalp skin samples used to prepare lower follicle RNA .....	166
Table 4 Measurements of the distance of the sebaceous gland from both the skin surface and the hair follicle bulb in human scalp skin .....	175
Table 5 Human skin samples used to prepare isolated hair follicle components .....	176
Table 6 Spectrophotometric analysis of human scalp hair follicle components RNA .....	177
Table 7 Human scalp hair follicle samples used to prepare hair follicle components for amplified RNA studies, their RNA concentrations and purities after amplification. ....	183
Table 8 Optimal collision energies and multiple reaction monitoring transitions used for the LC/ESI-MS/MS assay of prostanoids, isoprostane and dihydroprostaglandins (Masoodi and Nicolaou, 2006) .....	195
Table 9 The concentration and purity of RNA from lower follicles from human scalp skin samples used for prostamide receptor detection .....	218
Table 10 Representation of a 96 well plate used to estimate protein content .....	297



## List of Abbreviations

AA	Arachidonic acid
ACTH	Adrenocorticotrophic hormone
AG	Arachidonylglycerol ester
altFP	Prostaglandin F <sub>2α</sub> receptor variant
AMV	Avian Myeloblastosis Virus
ATP	Adenosine triphosphate
B	Follicle bulge area
bp	Base pair
cDNA	Complementary deoxyribonucleic acid
COX	Cyclo-oxygenase
CPA	Cyproterone acetate
CTS	Connective tissue sheath
D	Deer
DEPC	Diethyl pyrocarbonate
DF	Dermal fibroblast
DHA	Docosaheptaenoic acid
DHGLA	Dihomo-γ-linolenic acid
DHT	Dihydrotestosterone
DMSO	Dimethyl sulphoxide
DNA	Deoxyribonucleic acid
dNTP	Deoxynucleotide triphosphates
DP	Dermal papilla
DP	Prostaglandin D <sub>2</sub> receptor
DS	Dermal sheath
EPA	Eicosapentaenoic acid
EP	Prostaglandin E <sub>2</sub> receptor
FAAHs	Fatty acid amide hydrolase
FGF	Fibroblast growth factor
FP	Prostaglandin F <sub>2α</sub> receptor
GPCR <sub>s</sub>	G-protein coupled receptors
H&E	Haematoxylin and eosin

HGF	Hepatocyte growth factor
H-PGDS	Haematopoietic prostaglandin D synthase
IGF	Insulin-like growth factor
IP	Prostaglandin I <sub>2</sub> receptor
IP <sub>3</sub>	Inositol 1, 4, 5-triphosphate
K <sup>+</sup>	Potassium ion
Lef1	lymphoid enhancer-binding factor 1
LF	Lower follicle area between the bulb and sebaceous gland
L-PGDS	Lipocaline prostaglandin D synthase
M	Matrix
MC-1R	Melacortin-1 receptor
mRNA	Messenger ribonucleic acid
MSH	Melanocyte stimulating hormone
NGS	Normal goat serum
NMS	Normal mouse serum
NSAID	Non-steroidal anti-inflammatory drugs
PBS	Phosphate buffered saline
PCR	Polymerase chain reaction
PG	Prostaglandin
PGD11-KR	Prostaglandin D 11-ketoreductase
PGDH	15-hydroxyprostaglandin dehydrogenase
PGDS	Prostaglandin D synthase
PGE9-KR	Prostaglandin E 9-ketoreductase
PGES	Prostaglandin E synthase
PGG <sub>2</sub>	Prostaglandin G <sub>2</sub>
PGH <sub>2</sub>	Prostaglandin H <sub>2</sub>
PGH 9, 11-ER	Prostaglandin H 9, 11-endoperoxide reductase
PGHS	Prostaglandin endoperoxide H synthase
PGI <sub>2</sub>	Prostacyclin
PGIS	Prostacyclin synthase
PLA <sub>2</sub>	Phospholipases A <sub>2</sub>
POMC	Pro-opiomelanocortin
PUFA	Polyunsaturated fatty acids

RNA	Ribonucleic acid
RT-PCR	Reverse transcription-Polymerase chain reaction
SCF	Stem cell factor
SEM	Standard error of the mean
SHBG	Sex-hormone-binding globulin
TAE	Tris-acetate-EDTA
TCF	T cell-specific transcription factor
TGF	Transforming growth factor
TP	Prostaglandin thromboxane A <sub>2</sub> receptor
TXA <sub>2</sub>	Thromboxane A <sub>2</sub>
TXAS	Thromboxane A synthase
VEGF	Vascular endothelial growth factor

## **1. Overall introduction**

## **1.1 The importance of hair**

The skin is the largest organ in the human body comprising about one sixth of the total body weight and it covers about 1.5 - 2 m<sup>2</sup> (Chuong et al., 2002). It contains a number of specialized appendages, developed not only to protect and reinforce the skin but also for social signalling. The most prominent of these appendages is the hair follicle, a special organ found only in mammals which produce the hair fibre. Hair follicles are found all over the body except in the glabrous skin of the lips, palms and soles.

Hair has other many important roles in other mammals, one of the most important role is thermal insulation (Vaughan, 1986). It is an essential mammalian characteristic for warm bloodedness and crucial for their evolutionary success (Young, 1957). In Man the thermoregulatory function is minor because of the reduction in large terminal hairs, probably to enable body cooling by evaporating eccrine sweat (Ebling, 1985), despite the residual display of hair erection in response to cold and seasonal variations in the rate of hair growth (Orentreich, 1969; Randall and Ebling, 1991b; Courtois et al., 1996). Hairs are also involved in camouflage (Cott, 1940), which protects mammals from predation. They are often also specialised as neuroreceptors or sense organs for touch in certain mammals e.g. whiskers (Oliver and Jahoda, 1989b) or for sexual communication e.g. the lion's mane (West and Packer, 2002a).

The hair follicle is also of great interest to scientists; this miniorgan represents an attractive experimental system because of its accessibility, dispensability, and self-renewal capacity. Its complex, but highly organised, structure make it an excellent model for investigating aspects of stem cell biology, cell lineage specification, patterning processes, cell differentiation and cell-cell interactions (Schlake,

2007a). It has the ability to regenerate itself (Dry, 1926b; Kligman, 1959a), recapitulating many steps of embryogenesis, which is of particular interest to cell and developmental biologists (Dry, 1926a; Kligman, 1959c). The human hair follicle is also a paradoxical tissue, where the same hormones, the androgens, can cause stimulation of hair growth in many areas e.g. beard, while inhibiting hair growth on the scalp of genetically predisposed people, causing baldness (Randall, 1994, 2007). This characteristic of the hair follicle is of great interest to endocrinologists.

The reduced hair in human beings has rather different roles to those of many other mammals. The hairs that are obvious in children are mainly protective, the eyelashes and eyebrows stop foreign bodies entering the eyes and scalp hair protects the head and back of the neck from sunlight, physical damage and even from cold since scalp has very little adipose tissue (Goodhart, 1960; Ebling, 1985). The lower incidence of balding among African men (Setty, 1970) suggests the greater importance of scalp hair for the protection of scalp from the hot tropical sun. Abundance of strong, good quality hair signals good health, in contrast to the brittle hair seen during starvation or disease (Bradfield, 1971a). Human hair is also a signalling characteristic in sexual communication; the development of axillary and pubic hair in males and females is an indicator of the onset of puberty and their associated apocrine glands produce secretions yielding odours involved in sexual communication (Ebling, 1976). Growth of greater terminal hair on the face and chest, limbs and upper pubic triangle all indicate sexual maturity in men (Reynolds, 1951; Marshall and Tanner, 1969; Marshall and Tanner, 1970a). Scalp hair also plays important role in many cultures throughout history. Hair removal has strong depersonalising roles e.g. prisoners and ritual shaving of Christian or

Buddhist monks, while long uncut hair has positive connotation such as strength for Samson in the Bible and religion in Sikhs (Randall, 2007). Human hair plays an important role in a person's appearance and in social and sexual communication with other people throughout life (Jansen and van Baalen, 2006). This provides insight into why hair disorders such as alopecia areata, hirsutism and androgenetic alopecia have serious psychological effects on the quality of life, although hair disorders are not life threatening in human beings (Girman et al., 1998; Gulec et al., 2004). Androgenetic alopecia, or male pattern hair loss or common balding (Randall, 2005b), results in anxiety and loss of confidence in affected men even whom never sought any medical help (Girman et al., 1998).

Therefore, understandings of the mechanisms controlling hair growth are of great interest worldwide with the hope that they may lead to the development of new, better treatments for hair disorders.

## **1.2 The structure and function of the hair follicle**

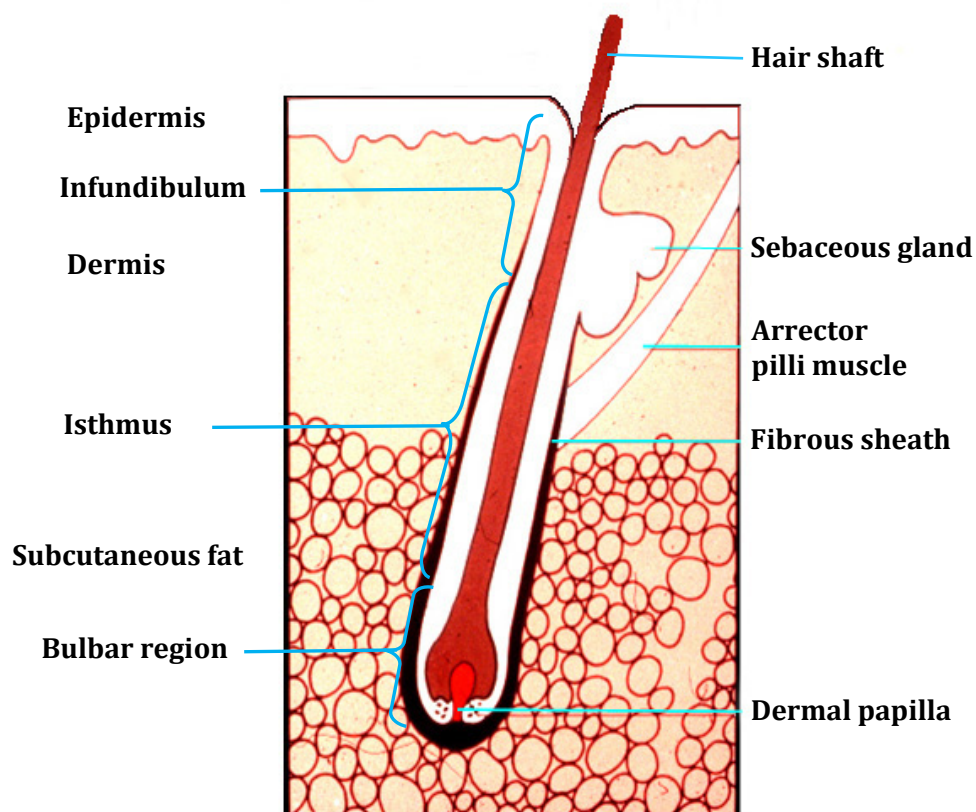
### **1.2.1 Structure of the hair follicle**

The hair follicle has a complex structure which results from epithelial-mesenchymal interactions initiated around the 3rd month of embryonic development (Sengel, 1983; Hardy, 1992; Gorpinich and Nozdrin, 2007). Hair follicles are continuous with the epidermis extending down through the dermis and often project into the subcutaneous adipose layer (Montagna and Van Scott, 1958a); they give rise to the hair, a flexible tube of fully keratinised epithelial cells. At the base, the growing hair follicle enlarges into the hair bulb surrounding the mesenchyme-derived dermal papilla (Auber, 1952; Montagna and Van Scott, 1958c; Oliver and Jahoda, 1989c) (Figure 1). Each anagen hair follicle can be

divided into 3 distinct regions, the infundibulum, isthmus and bulbar regions. The infundibulum includes the area joining the hair follicle to the surface epithelium down to where the sebaceous duct joins the hair follicle. The isthmus starts from below the sebaceous duct down to the bulbar region and contains the bulge area where the arrector pili muscle attaches to the hair follicle and connects it to the dermis. The bulbar region includes the hair bulb and the bulb neck (Montagna and Van Scott, 1958a; Sperling, 1991) (Figure 1).

**Figure 1 Illustrative representation of an anagen hair follicle showing the different component parts**

Reproduced from Randall (2000), with the author's permission.





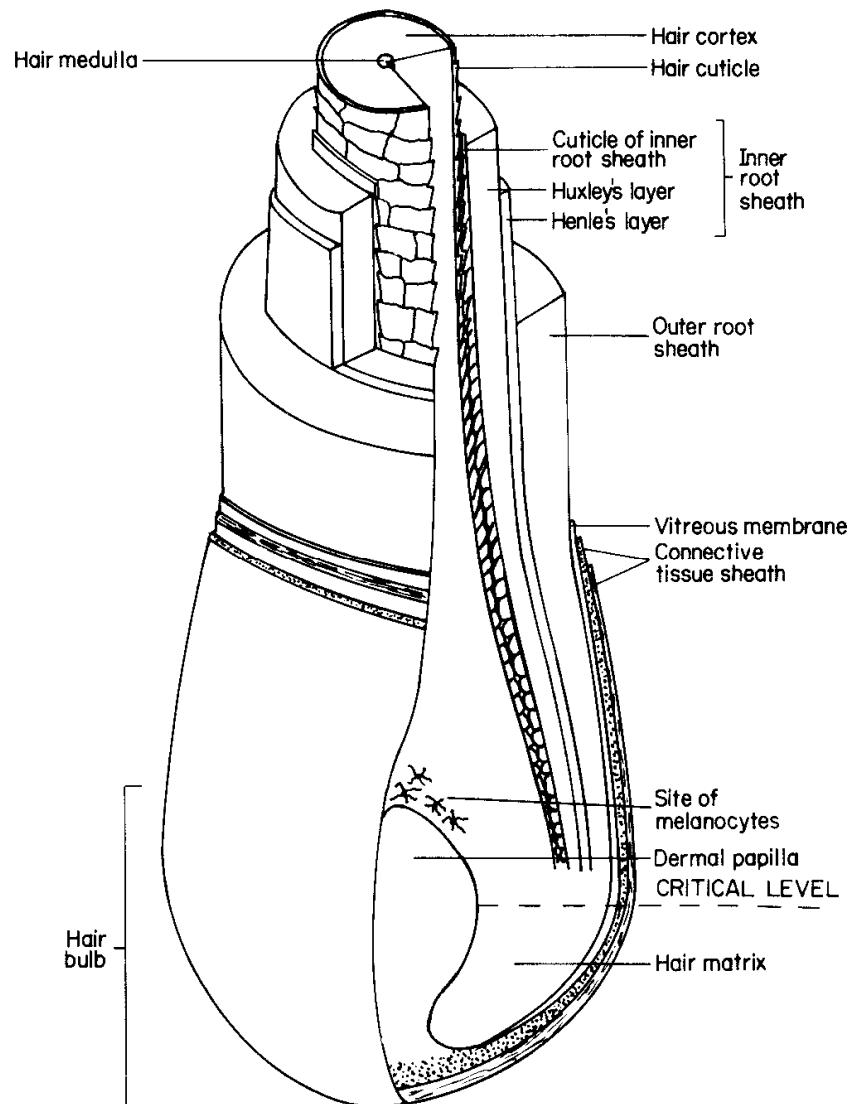
The hair follicle consists of several layers which hold and frame the emerging hair, the inner root sheath, the outer root sheath, the vitreous membrane and the connective tissue sheath (Forslind, 2000). The inner root sheath which surrounds the hair fibre is composed of three distinct cell layers, the outer Henle's layer, the Huxley layers and the inner cuticle; the latter is in direct contact with the cuticle of the hair fibre. The inner root sheath surrounds the hair fibre from the bulb up to the level of the sebaceous gland (Forslind, 2000). The cuticle cells of the hair fibre interconnect/interdigitate with the cuticle cells of the inner root sheath like a zip, consequently fastening the hair fibre to the follicle. The inner sheath is surrounded by the outer root sheath, which is continuous with the epidermis. The vitreous membrane and the connective tissue sheath lie outside the outer root sheath and they surround the whole follicle (Figure 2).

The hair fibre consists of three distinct layers, the outer cuticle, the cortex, and the inner medulla. The cortex is composed of bundles of keratin filaments; the medulla, which is only present in terminal hairs, can be either continuous or discontinuous. Hair fibres with a continuous medulla are stiff in character such as eyelashes (Forslind, 2000).

The types of hair produced are greatly variable in colour, length, diameter and cross-sectional shape (Schlake, 2007b). They can be classified into two main types, vellus hairs and terminal hairs. Vellus hairs are small, fine, unpigmented hairs located in regions of the body described as "hairless", e.g. the cheek, while terminal hairs are longer, thicker, and deeply pigmented hairs located in regions such as the scalp, eyebrows and eyelashes (Blume et al., 1991; Vogt et al., 2007).

## Figure 2 The structure of the hair follicle

An isometric view of the lower part of a human hair follicle cut away to show component parts (drawn by Richard J. Dew). Reproduced from Randall (1994), with the author's permission.



The dermal papilla in the hair bulb has a well developed nerve and blood supply. It contains a relatively small number of specialised fibroblast cells called dermal papilla cells and a large amount of extracellular matrix containing mucopolysaccharides (Montagna et al., 1952) and basement membrane proteins (Messenger et al., 1991; Couchman, 1993). Dermal papilla cells regulate and

control hair follicle growth through the expression and secretion of paracrine factors such as growth factors and cytokines. The dermal papilla plays an important role throughout hair follicle development and its life cycle. The size of dermal papilla is proportional to the size of the hair follicle and therefore the hair fibre produced (Van Scott and Ekel, 1958; Ibrahim and Wright, 1982; Elliott et al., 1999). The hair matrix almost completely encloses the dermal papilla, with the exception of a gap at the base of the follicle bulb, which allows the entrance of blood vessels and nerves into the papilla. The dermal papilla is separated from the epithelial hair matrix by a trilaminar basement membrane (Nutbrown and Randall, 1995). The hair matrix gives rise to all epithelial compartments except the outer root sheath (Schlake, 2007b).

A theoretical line drawn through the widest part of the follicular bulb is called the “critical level”; this separates the undifferentiated, mitotically active lower matrix from the differentiating, less mitotically active upper matrix (Auber, 1952) where cells differentiate into either the inner root sheath or hair fibre cells. Hair production involves rapid cell division of the epithelial keratinocytes in the hair matrix. As the cells move from the bulb into the narrower part of the follicle, the cells become elongated, and keratinisation takes place. The keratinisation process continues as the cells migrate through the follicle, finally becoming fully keratinised when they reach the skin surface. In pigmented hairs, melanocytes situated around the upper part of the dermal papilla incorporate melanin granules into the adjacent keratinocytes in the bulb; melanin is synthesised in a small melanocyte-specific organelle known as a melanosome (Chase, 1958; Castanet and Ortonne, 2000; Slominski et al., 2004; Lin and Fisher, 2007). The amount and type of pigment, melanin, made by the bulb melanocytes and the balance of

brown/black eumelanin and red/yellow pheomelanin in the hair shaft determines the hair colour (Slominski et al., 2004; Rousseau et al., 2007). In most people, hair colour varies according to body site (Wasserman, 1974; Mc Donald, 1991). Eyelashes are usually the darkest and scalp hair is generally lighter than genital hair, which may be due to bleaching of the hair on the scalp as it is exposed to UV light (Rook and Dawber, 1991).

The hair follicle is often referred to as the pilosebaceous unit, due to its association with the sebaceous gland (Wosicka and Cal, 2010). Sebaceous glands secrete a waxy secretion into the follicle through the sebaceous duct, forming a waterproof coating over the hair fibre. Apocrine sweat glands are also present above the sebaceous ducts of follicles in some areas, such as those found in axillae and genital regions (Hurley, 2001). They develop in the embryo, but normally become active at puberty (Cohn, 1994). The apocrine glands release an oily secretion into the superior portion of the hair follicle which is involved in human olfactory communication and is a possible origin of pheromones (Spielman et al., 1995). The arrector pili muscle, a smooth muscle bundle, is also associated with the hair follicle, and attaches to the hair follicle below the bulge region. This muscle allows adjustment of the hair for thermoregulation; for example erection of hairs in response to cold temperatures to trap a layer of air close to the skin to help in insulation. The bulge is a region of outer root sheath below the attachment of the sebaceous gland and is the site of epithelial stem cells (Cotsarelis et al., 1990; Tiede et al., 2007; Yang and Xia, 2007).

### **1.2.2 The hair follicle growth cycle**

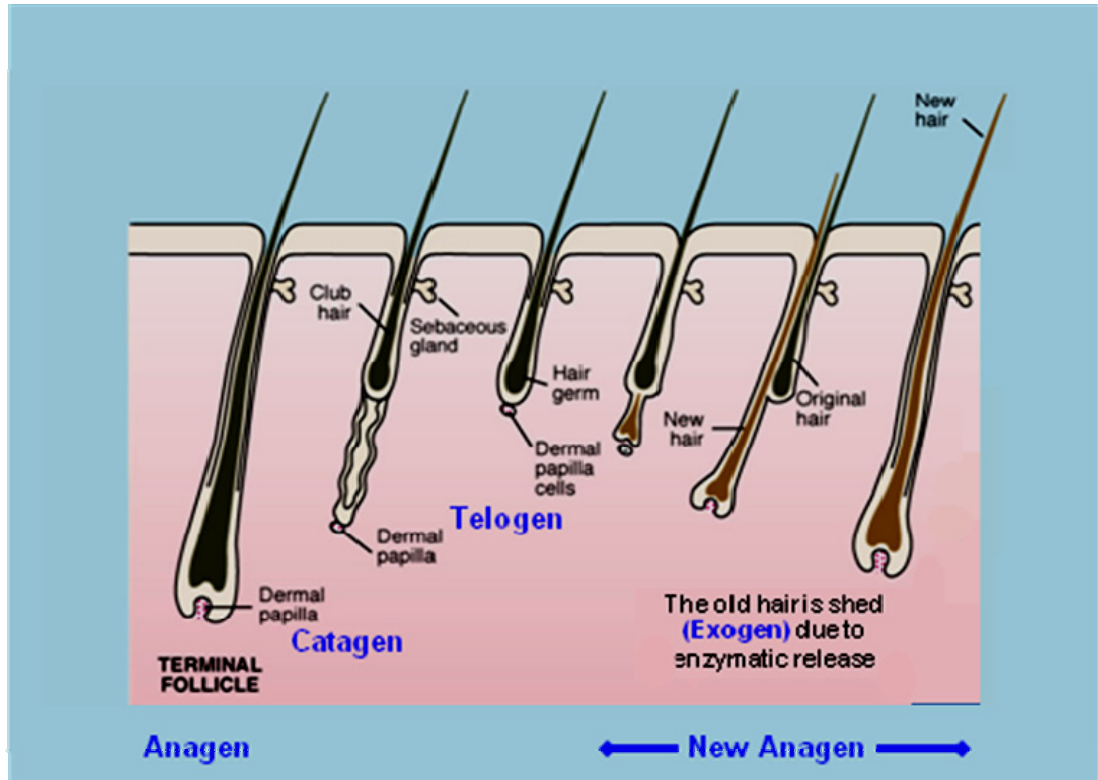
The hair follicle has a very important and unique mechanism of cyclic regeneration in mammals, including human beings, in which hairs are shed and re-grown. The hair follicle growth cycle originally described fully for mouse by Dry (1926) and later for human beings by Kligman (1959). The hair follicle growth cycle includes the destruction of the original lower follicle and its regeneration to form a new follicle which can produce different hairs from the pre-existing one. The role of hairs is different in many mammals through the year and at different stages of their lives. They need a thick winter coat (Young, 1957) and seasonal colour variation for camouflage like the white winter, and brown summer coat of the arctic hare (Cott, 1940). Hair follicle melanin synthesis is cyclical (unlike epidermal melanin synthesis) and confined to the anagen growth phase of the hair cycle (Burnett et al., 1969; Commo and Bernard, 2000; Slominski et al., 2004; Sharov et al., 2005). The mane of the male red deer is also developed only in the breeding season for sexual attraction (Lincoln and Kay, 1971). Therefore the hair produced by a follicle often needs to be changed and the changes happen during the hair growth cycle. During androgenetic alopecia and puberty, the hair growth cycle enables gradual changes to occur in the type of hair produced by various follicles.

The hair growth cycle includes four main stages, the growth phase, anagen, the regression phase, catagen, the resting phase, telogen and the shedding phase, exogen. The hair growth cycle is summarized in figure 3.

How different in size a hair can be to the pre-existing hair is unclear because many changes take place over several years. For example, full beard production takes

### Figure 3 The hair growth cycle

Stages of hair growth cycle. Reproduced with the author's permission, from Randall (2008).



until over 30 years of age (Hamilton, 1958), while ear canal hair continues to develop until the 50's (Hamilton, 1946). The duration of each phase varies between species and varies significantly from site to site on the human body (Trotter, 1924; Saitoh et al., 1970; Messenger, 1993).

The matrix keratinocytes in the hair follicle bulb proliferate rapidly during the anagen phase adding cells to the growing hair fibre; in contrast at the end of anagen, matrix keratinocytes gradually cease proliferating and the follicular melanocytes cease melanin synthesis as the anagen follicle starts the transition into the catagen phase (Kligman, 1959a). During the catagen phase, the follicular melanocytes resorb their dendrites and cease melanin synthesis. Mitosis in the bulb matrix cells also stops; therefore no more cells are added to the hair fibre.

The catagen phase duration is short, lasting for about 2 weeks in human scalp follicles (Kligman, 1959a). The base of the fully keratinised hair become expanded (club hair) and moves toward the skin surface till it reach the level of the sebaceous gland. Condensation of the dermal papilla takes place and become a ball of cells. The involution of the club hair results from apoptosis of the epithelial cells of the hair follicle (Weedon and Strutton, 1981; Lindner et al., 1997; Matsuo et al., 1998; Botchkareva et al., 2006). At the end of catagen, the ball of dermal papilla cells moves with the epithelial cells up in the same direction as the club hair and stops under the bulge; if the dermal papilla fails to reach the bulge level during catagen, the cycle stops and the hair is lost (Paus and Cotsarelis, 1999). The lowermost portion of the bulge collapses around the hair and forms the secondary hair germ at the end of catagen (Ito et al., 2004).

The catagen phase is followed by the telogen phase, the resting phase of the hair cycle. A telogen hair is distinguished by its fully keratinized club hair which is surrounded by a thick epithelial sac. Below this lies the condensed dermal papilla, waiting for the signal to start a new hair growth cycle (Sperling, 1991). The telogen phase lasts around two to three months on the human scalp before the follicle re-enters the anagen phase (Kligman, 1959c; Price and Griffiths, 1985). Plucking of a telogen club hair initiates a premature anagen phase (Ebling, 1976).

The growth phase, anagen, is a period of high proliferation as the lower part of the follicle regenerates and forms a new hair. Anagen has been sub-divided into six stages (Chase et al., 1951; Chase, 1954). Most of the hair growth takes place in anagen stage VI, while stages I-V of anagen are the developmental stages at which point the follicle regenerates. The length of the anagen sub-phases I-V does not differ substantially between follicles from different regions, with the exception of

the last sub-phase, anagen VI, the duration of which dictates the shaft length (Trotter, 1924; Saitoh et al., 1970).

The keratinocytes beneath the bulge region known as the hair germ which play a pivotal role in anagen induction (Cotsarelis et al., 1990; Paus et al., 1999). During anagen I, which is an early anagen stage, the hair germ become active mitotically. This is followed by anagen II, in which the germ starts to grow downward enveloping the ball of dermal papilla cells. The matrix epithelial cells around the dermal papilla form an inverted cone and on top of it a layer of keratinised cells appear which give rise to the inner root sheath. In anagen III, upward growth of the inner root sheath continues, the matrix cells are formed and the hair bulb develops a more characteristic appearance. The matrix melanocytes are activated and start melanin synthesis; the matrix cells divide and generate the hair fibre and the layers of the hair follicle. During anagen IV, the hair fibre reaches the level of the sebaceous gland, but it is still enveloped by an upwardly growing cone of inner root sheath. An inverted cone of pigmented matrix and a narrow and long dermal papilla can be seen in the bulb area. In anagen V, the new shaft breaks through the internal sheath and grows up to the skin surface alongside the telogen hair. The hair fibre also reaches its maximum diameter in this stage. During anagen VI the new hair shaft emerges from the skin surface and proceeds to grow until the follicle re-enters catagen and the cycle starts again. In this stage the follicle is at its greatest depth within the skin. The length of anagen VI determines the length of a hair produced by a follicle which varies with follicle location. For example, eyebrow hair follicles are in anagen for about two to three weeks producing short hairs, while scalp hair follicles are in anagen for two to six years resulting in long hairs (Kligman, 1959c, 1961; Saitoh et al., 1970; Paus and Cotsarelis, 1999).



The last phase within the hair growth cycle is exogen, an active shedding phase, in which specific signals controlling the breakdown of cellular adhesion between the club hair and its surrounding epithelial sac, leading to the release of the old club hair rather than simply being pushed out of the skin (Stenn et al., 1998; Stenn and Paus, 2001; Stenn, 2005; Higgins et al., 2009b).

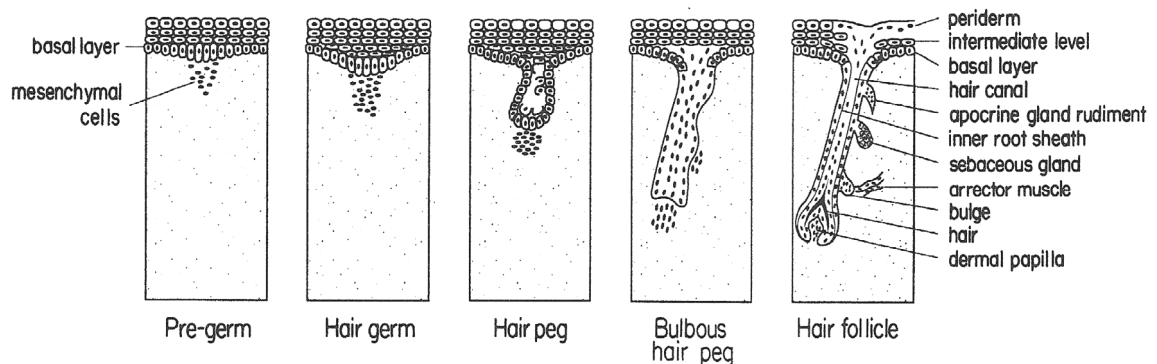
### **1.2.3 Embryogenesis of the hair follicle**

The embryonic development of human hair follicles occurs first in areas of the developing upper lip, chin and eyebrow in the second pregnancy trimester and their development is completed by fetal month 6 (Pinkus, 1958). The developing embryonic epidermis consists of the basal layer, intermediate layer and the periderm. Hair follicle embryonic development is a result of interaction between epithelial and mesenchymal tissues and can be divided into three morphologically distinguishable stages: induction, organogenesis and cytodifferentiation. The spacing, polarity and differentiation patterns of hair follicles are controlled by interactions of inhibitors and activators, which are established jointly by the skin epithelium and mesenchyme (Schmidt-Ullrich and Paus, 2005). Once a mesenchymal condensate of inductive fibroblasts has formed, it takes over control of most subsequent steps of hair follicle organogenesis and of epithelial stem cell differentiation into distinct lineages (Schmidt-Ullrich and Paus, 2005). The hair follicle development initiates with the formation of the pre-germ, which begins as a result of localised thickening of the basal layer of the epidermis and an aggregation of mesenchymal cells at the junction of epidermis and dermis, and these mesenchymal and epidermal cells then continue to grow downward forming the hair germ (Pinkus, 1958; Holbrook and Minami, 1991) (Figure 4). The hair germ

then elongates and grows deeper into the dermis to form a cone of epithelial cells with the cluster of mesenchymal cells at the base forming the hair peg.

#### **Figure 4 The hair follicle embryology**

The different stages of hair follicle embryogenesis. Reproduced from Randall (1994), with the author's permission.



The deepest end of the hair peg flattens, forming a concave-shaped bulbous structure called the bulbous hair peg which finally encloses the mesenchymal cells to form the dermal papilla. The epidermal cells above the primitive dermal papilla become the matrix, which differentiates to form the inner root sheath and hair fibre. The outer root sheath is formed from the epithelial cells connecting the matrix cells to the interfollicular epidermis; the connective tissue sheath is formed from the mesenchymal cells surrounding the epithelial down-growth. On the posterior side of the follicle, two epithelial protrusions develop at about 12-15 weeks estimated gestational age; the uppermost epithelial swelling will develop to form the sebaceous gland and the lower one forms the bulge (the site at which the arrector pili muscle attaches to the follicle). A third protrusion can develop above the sebaceous gland at some regions of the body such as the axilla and groin to form apocrine glands.

At about 15 weeks the middle cells of the bulbous hair peg degenerate to form the hair canal and keratinisation of the canal and the hair fibre begins. At this stage the first sebocytes are seen and the dermal papilla is completely surrounded by epithelial cells. The hair follicle components will continue to differentiate and the hair fibre continue to grow. The follicle will maintain its downward growth into the dermis until it reaches its full depth within the skin. The hair fibre continues growing and at about 19 weeks gestational age; the first lanugo hair emerges from the skin surface. Most of the stages identified above are repeated during the hair growth cycle (Hardy, 1992; Wu-Kuo and Chuong, 2000).

#### **1.2.4 Mesenchymal and epithelial interactions in the hair follicle**

The hair follicle is composed of structures that are derived from both the mesenchyme and the ectoderm as described in section 1.2.3. There is a series of signals between the dermal and epithelial cells of the hair germ during early stages of hair follicle development and these early signals have been shown by several tissue recombination experiments on embryonic skin from several species (Sengel, 1983; Hardy, 1992; Ferraris et al., 2000). The early signal from aggregated dermal cells is transmitted to the overlying epithelial cells to start thickening and form an appendage. The type of the appendage formed depends on the origin of the epidermis.

The epidermis initiates the next signal to instruct the cluster of dermal cells to form a dermal papilla. A second message from the dermal papilla eventually transmits to adjacent epithelial cells and stimulates them to divide rapidly and form a specific appendage. Therefore the embryogenesis of the hair follicle depends on a series of signals between the mesenchyme and epithelia (Mikkola

and Millar, 2006; Fuchs, 2007). The Wnt/beta-catenin activity in the dermal papilla regulates signaling pathways, including IGF and FGF that can mediate the dermal papilla's inductive effects. The inactivation of the Wnt/beta-catenin gene within the dermal papilla of fully developed hair follicles results in dramatically reduced proliferation of the progenitors and their progeny that generate the hair shaft, and then premature induction of the catagen phase of the hair cycle (Enshell-Seijffers et al., 2010).

The dermal papilla is a permanent structure which stays throughout the hair cycle, and controls post-embryonic mesenchymal-epithelial interactions. The important role of the dermal papilla is shown by its removal from anagen vibrissae follicles which results in stopping hair growth (Oliver, 1966; Link et al., 1990). The dermal papilla cells are in direct contact with epithelial cells; the cells of the outer root sheath organise around the dermal papilla to form an epithelial matrix and reform the bulb (Oliver, 1967; Jahoda et al., 1984).

A series of experiments using mainly rat vibrissae follicles has highlighted some of the epithelial-mesenchymal interactions in the adult hair follicle (Oliver and Jahoda, 1989a). When cultured dermal papilla cells from rat vibrissae were implanted in rat ear skin superficially, they induced the formation of new follicles as a result of contact with the epidermis (Jahoda and Oliver, 1984). Vibrissae dermal papilla cells also induced vibrissae follicle formation in rat ear wounds (Jahoda, 1992). So the follicle and the type of hair produced are determined by the origin of the dermal papilla and not by the transplantation site (Reynolds and Jahoda, 1992; Jahoda et al., 1993). This feature of hair growth is a big advantage in hair follicle transplantation surgery, in which hair follicles are relocated from non-balding occipital and parietal sites to cover the balding areas (Orentreich and Durr,

1982; Epstein, 2007). Cultured dermal papilla cells from rat pelage can induce follicle growth when implanted between the dermis and epidermis of a follicular foot-pad skin, which suggests that the dermal papilla has the ability of changing the gene expression of the tissue around it (Reynolds and Jahoda, 1991, 1992). In a recent experiment, the vibrissae dermal papilla of adult rat and mouse revealed the ability to induce new hair follicle structures in rabbit corneal epithelium (Waters et al., 2007). There is evidence that the germinative epithelium and the dermal sheath can also play a role in follicle induction. When germinative epithelium from the hair bulb matrix was cultured alone or with 3T3 feeder cell layers, no growth was observed, but when co-cultured with dermal papilla cells, growth occurred and organoid structures were formed with the dermal papilla cells (Reynolds et al., 1991). When dermal sheath or germinative epithelium cells were implanted into ear skin, they failed to induce follicle formation, but when both were implanted together into the ear wound they induced follicle formation (Reynolds and Jahoda, 1996). This suggests that the dermal sheath cells require signals from the germinative epithelial cells to alter their differentiation state to function as dermal papilla cells and induce follicle formation. In a recent study it was demonstrated that labelled dermal papilla cells made new dermal sheath in induced follicles, suggesting that transformation of dermal sheath cells into dermal papilla cells is not unidirectional (Inamatsu et al., 2006).

Another study demonstrated that cells from dermal sheath cup surrounding the hair bulb had a similar role as dermal papilla cells in inducing hair follicles (McElwee et al., 2003). In this experiment donor mice were used with green fluorescent protein. The cells of the dermal sheath cup were able to form dermal papilla, whilst implantation of non-bulbar dermal sheath cells to induce hair

follicle development was unsuccessful. This suggests that dermal sheath cup cells may be functionally similar to the dermal papilla cells. This was confirmed in another study where dermal sheath cells from scalp hair follicles of a male donor were implanted superficially in the forearm of a female recipient (Reynolds et al., 1999). At the site of implantation new hair follicle was formed producing large and thick hairs; DNA extracted from the dermal papilla cells was found to be of male origin.

These results all suggest that mesenchymal-epithelial interactions are important for both hair follicle development and hair cycling.

### **1.3 Regulation of hair growth**

#### **1.3.1 Hormonal regulation of hair growth**

The hair follicle growth cycle allows the hair produced from the follicle to change during sexual development or to change and be replaced by one more suitable to seasonal variations in climate. In mammals this can be detected in the changing of coat thickness and colour induced by several factors such as temperature, day length (photoperiod) and availability of nutrients (Chase, 1954; Galbraith, 1998). These environmental changes are translated to follicles through the endocrine system, via the pineal and the hypothalamus-pituitary route (Ebling et al., 1991; Randall, 2007). The hormones involved differ according to the species, but generally include gonadal hormones, corticosteroids, thyroid hormones, prolactin and melanocyte stimulating hormone (MSH).

In human beings, a wave of hair shedding occurs a few weeks after birth (Pecoraro, 1968), after this the hair cycle is asynchronous except for the local groups of three follicles called DeMeijère trios (Saitoh and Sakamoto, 1970). The human hair

follicle is also influenced by circulating hormones and by nutrient levels (Bradfield, 1971b; Rushton, 2003; Randall, 2007). Circannual changes in the rate of human hair growth have been reported on the scalp, beard and thigh (Orentreich, 1969; Randall and Ebling, 1991b; Courtois et al., 1996).

Androgens are the major regulating hormones of human hair growth (Randall, 1994, 2008). They have paradoxical effects, stimulating hair growth in many areas such as the face in males after puberty causing transition of vellus follicles into terminal follicles (Hamilton, 1958; Marshall and Tanner, 1969; Marshall and Tanner, 1970b), whilst transforming terminal hair follicles into vellus one on the scalp in genetically predisposed individuals in androgenetic alopecia (Hamilton, 1942, 1960). However, androgens have no effects in other body areas such as the eyelashes, so the response of a hair follicle to androgens depends on the body site; this suggests that the responses of the hair follicles to androgen is intrinsic to the hair follicles itself. This is further illustrated by hair transplantation, where the follicle retains the characteristics of the donor site (Orentreich and Durr, 1982; Orentreich and Orentreich, 1985; Bernstein and Rassman, 1999). These changes are a gradual process, in which several hair growth cycles take place before the type of hair produced is changed (Randall, 1994). The maximal amount of beard growth is achieved around the mid-thirties (Hamilton, 1958) and androgenetic alopecia develops over several years (Kligman, 1959b).

Testosterone is the major circulating androgen; it is derived from cholesterol like all other steroids. In human males, more than 95% of testosterone is produced and secreted by the Leydig cells of the testes and the remaining testosterone is produced by the adrenal cortex. Testosterone also plays a role in hair pigmentation, it had been shown to increase pigmentation in Mallard feathers

(Haase et al., 1995) and deer hair (Bubenik and Bubenik, 1985); high testosterone levels also make lion manes darker (West and Packer, 2002b).

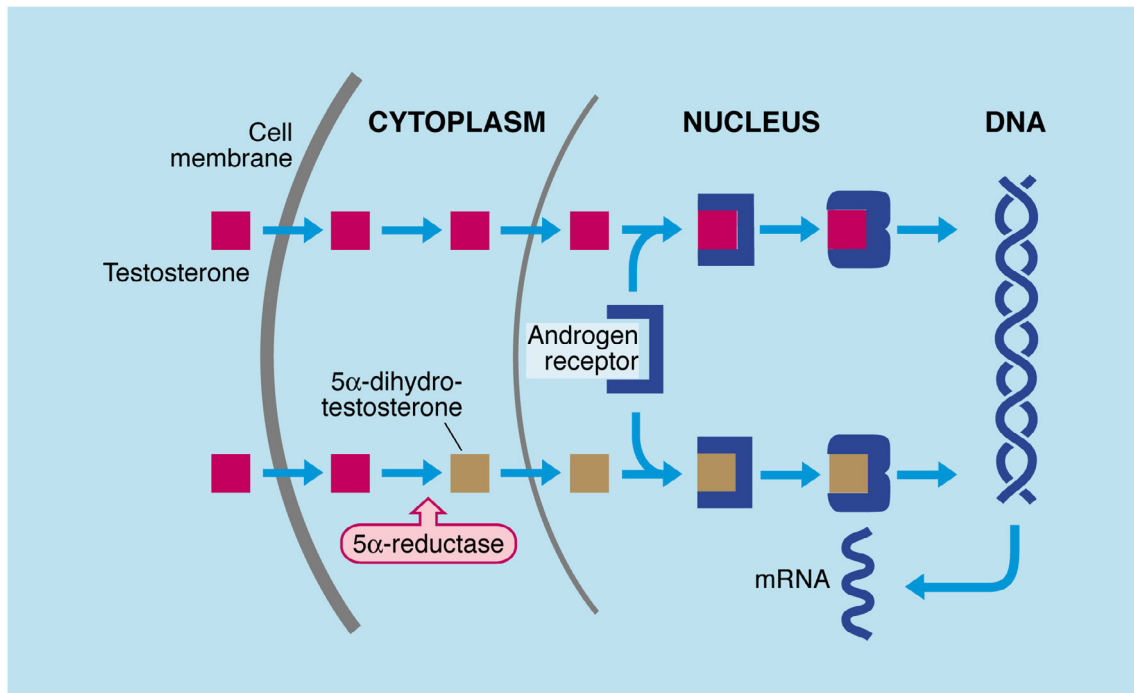
Androgens circulate in the blood either free or bound to proteins such as the sex-hormone-binding globulin (SHBG) and albumin (Rommerts, 2004). Androgens can enter the hair follicle through its blood capillaries into the dermal papilla and the dermal sheath. Androgens diffuse through the cell membrane, passing the cytoplasm and enter the nucleus as androgens are lipophilic molecules; they bind to the androgen receptor leading to the removal of inhibitory proteins such as heat shock protein 90. This induces a conformational change in the receptor exposing the DNA binding domain followed by dimerisation of the androgen-receptor complex; this then binds to a regulatory DNA sequence in or near to the target gene which is known as a hormone response element (Handelsman, 2005). This leads to activation of appropriate genes and transcription of DNA.

The enzyme 5 $\alpha$ -reductase can metabolise testosterone intracellularly to 5 $\alpha$ -dihydrotestosterone (DHT). The 5 $\alpha$ -dihydrotestosterone is a more potent androgen and binds preferentially and more strongly to the androgen receptor to induce gene expression (Randall, 1994). Testosterone metabolism to 5 $\alpha$ -dihydrotestosterone occurs in many tissues including the androgen target organ, prostate. However, testosterone is the active hormone in skeletal muscle (Randall, 2007). The general mechanism of action for both testosterone and 5 $\alpha$ -dihydrotestosterone is shown in figure 5.



### Figure 5 Mechanism of action of androgens

This model demonstrates the mechanism of action of testosterone and 5 $\alpha$ -dihydrotestosterone. Obtained from Randall (2000), with permission by the author.



Two forms of 5 $\alpha$ -reductase have been identified, type 1 and type 2 (Blanchard et al., 2007). The type 1 is mostly found in the liver, but its role is not obvious, whilst lack of 5 $\alpha$ -reductase type 2 leads to the syndrome of 5 $\alpha$ -reductase deficiency, a rare form of male pseudohermaphroditism, in which they are unable to convert testosterone to 5 $\alpha$ -dihydrotestosterone (Andersson et al., 1991). Men with 5 $\alpha$ -reductase deficiency demonstrate female patterns of axillary and pubic hair; although they have high levels of circulating androgens, they grow little or no beard, suggesting that pubic and axillary follicles respond to testosterone, but the male secondary sexual hair growth requires 5 $\alpha$ -dihydrotestosterone (Imperato-McGinley et al., 1974; Wilson et al., 1993; Randall, 2007).

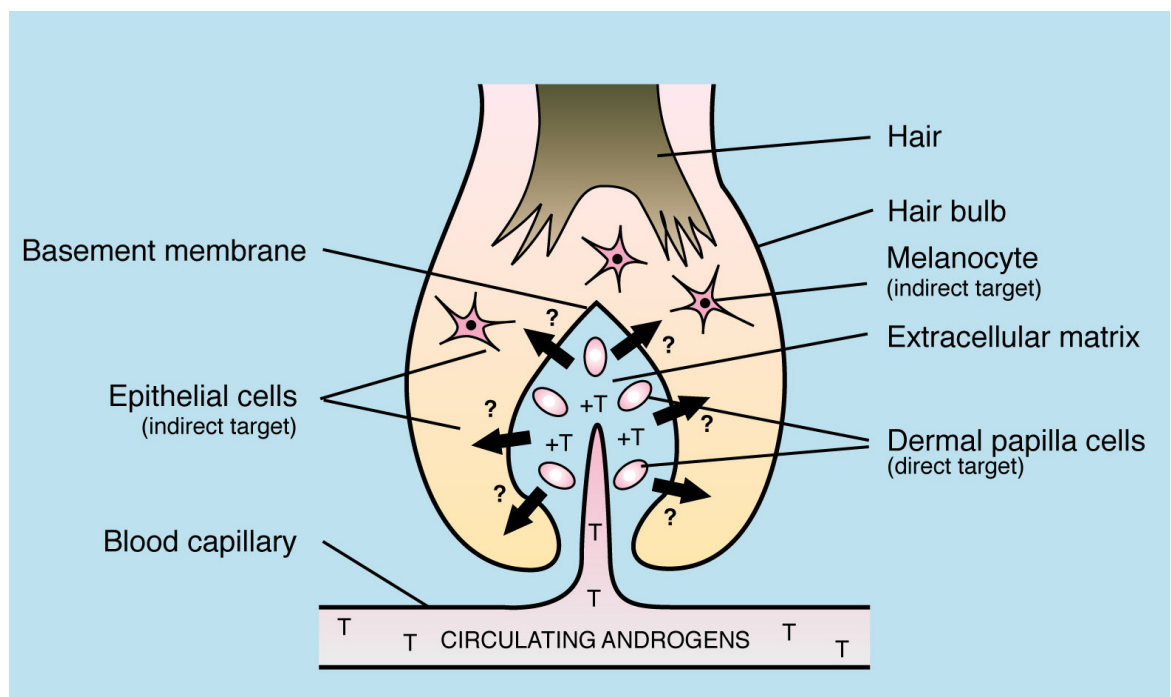
The various forms of androgen insensitivity syndrome explain the mechanism of action of androgens in hair follicles. Individuals with androgen insensitivity syndrome have an XY genotype but without functional androgen receptors, they develop a female phenotype despite normal, or high, circulating androgen levels. However, they do not develop female patterns of pubic or axillary hair and they do not undergo androgen-dependent scalp hair thinning (McPhaul, 2004; Randall, 2007). This suggests that terminal hair growth in these areas is androgen dependant, but growth of follicles located on the scalp, eyelashes and eyebrows are androgen independent.

The current hypothesis of androgen action in hair follicles is that androgens act on the other hair follicle components through the dermal papilla (Randall and Ebling, 1991a; Randall, 2007). Circulating androgens enter the dermal papilla through its blood supply, bind to androgen receptors within dermal papilla cells and then alter the gene expression of the dermal papilla cells in production of regulatory factors, which influence other target cells in a paracrine fashion (Figure 6). These paracrine factors could be soluble mitogenic factors such as growth factors and/or extracellular matrix components. They target the follicular melanocytes, which alter the amount of pigment produced, the keratinocytes, which proliferate to form the hair fibre, various sheaths and the follicle endothelial cells to allow the blood supply (Randall, 2000). The dermal papilla itself is a target of such factors, as a change in hair size can occur through a change in dermal papilla size (Van Scott E], 1958; Elliott et al., 1999). The processes involved in embryonic development in other steroid hormone regulated tissues, the prostate and the mammary gland are also in support of this hypothesis (Oka and Yoshimura, 1986; Cunha et al., 1987).

Recent observations suggest minor modifications to the hypothesis. The dermal sheath and medulla cells are also affected directly by androgen action (Randall, 2007). The dermal sheath cells have the ability to form a new dermal papilla and stimulate new hair follicle development (Reynolds et al., 1999). Expression of the

### **Figure 6 Mode of androgens action on the human hair follicle**

Diagrammatic representation of the current model of androgen action in the hair follicle. In this model androgens enter the follicle via the blood supply in to the dermal papilla where they bind to androgen receptors in the dermal papilla cells, causing changes in their production of regulatory paracrine factors. This would alter the activity of other follicular components. **T**: testosterone; **?**: unknown paracrine factor. Reproduced from Randall (2007), with permission by the author.



genes for 5 $\alpha$ -reductase type 2 was reported in the dermal papilla and dermal sheath of follicles from both balding and non-balding scalp (Asada et al., 2001). The dermal sheath cells may act as a reserve source to replace dermal papilla cells in case of dermal papilla loss (Randall, 2007). Pregnancy hormones also affect hair

growth causing diffuse hair loss shortly after birth. They maintain scalp hair follicles in the anagen phase, 95% anagen during the second and third trimesters of pregnancy and for about a week after birth. Many follicles enter catagen and telogen phases post-partum, this decreasing to about 76% in anagen and remained low for three months (Lynfield, 1960), causing simultaneous partial shedding (Lynfield, 1960). The possible hormones involved in altering hair growth are oestrogen and prolactin, however, the precise hormone involved is not clear. Human hair follicles possess prolactin and  $17\beta$ -oestradiol receptors (Thornton et al., 2003; Foitzik et al., 2006; Thornton et al., 2006) and prolactin decreases human hair growth *in vitro*, supporting its role in hair shedding after birth (Foitzik et al., 2006).

As androgens affect the dermal papilla production of regulatory paracrine factors and they also influence follicular melanocytes resulting in hair colour alterations. One pituitary hormone in particular,  $\alpha$ -melanocyte stimulating hormone ( $\alpha$ -MSH), can affect follicular melanogenesis (Logan and Weatherhead, 1981; Burchill and Thody, 1986; Slominski et al., 2004). Melanocyte-stimulating hormone (MSH) is an important hormone involved in enhancing pigmentation (Lerner and Case, 1959; Lerner, 1960; Lerner and McGuire, 1961). There are three identified types of MSH,  $\alpha$ ,  $\beta$  and  $\gamma$  (Lerner and Case, 1959). These three types of MSH alongside with adrenocorticotrophic hormone (ACTH) are called melanocortins and all derive from a common precursor, pro-opiomelanocortin (POMC), which is secreted from the intermediate lobe of the pituitary gland. These factors, especially the melanocortins and ACTH, can effect epidermal melanocytes through melanocortin-1 receptor (MC-1R) (Rousseau et al., 2007). The human MC-1R gene has been shown to play a crucial role in pigmentation features of eye, hair and skin colour

(Ibarrola-Villava et al., 2010). The level of plasma MSH was found to vary in pathological conditions and in different circumstances depending on the environmental factors such as the amount of UV light exposure. The skin also produces MSH and other POMC-derived peptides (Thody et al., 1983); both melanocytes and keratinocytes were involved in this local production (Slominski et al., 1995; Chakraborty et al., 1996).

Some other local factors such as  $\beta$ -endorphin, endothelin and catecholamines also have an effect on epidermal melanocytes (Slominski et al., 2004; Lin and Fisher, 2007). Factors like POMC, ACTH and  $\alpha$ -MSH, have roles in balancing eumelanin and pheomelanin proportions (Slominski et al., 2004; Tobin and Kauser, 2005; Rousseau et al., 2007). The  $\alpha$ -MSH acts on follicular melanocytes and causes darkening of hair colour (Bolognia and Pawelek, 1988). Quantitative electron microscopy has shown that  $\alpha$ -MSH and its artificial analogue; NDP-MSH stimulate eumelanogenesis rather than pheomelanogenesis in hair bulb melanocytes of C57BL/6J mice (Granholm and van Amerongen 1991) using the stage and shape of melanosomes as a guide to the type of melanin produced. The  $\alpha$ -MSH and ACTH were increased melanogenesis in cultured human melanocytes (Hunt et al., 1994a; Hunt et al., 1994b). Systemic administration of  $\alpha$ -MSH,  $\beta$ -MSH, or ACTH in human beings stimulates skin pigmentation, particularly in the sun-exposed areas. Injection of oestrogen or testosterone to menopausal women or women who had undergone ovariectomy, was increased skin pigmentation (Snell and Bischoff, 1960); increasing pigmentation level occur in the nipples, areola and face of pregnant women (Snell, 1964). In murine, estrogen is an important factor in determining the content of eumelanin and pheomelanin in female hair (Hirobe et al., 2010).

### **1.3.2 Potential paracrine factors produced by hair follicles**

Paracrine factors produced by dermal papilla cells in androgen-regulated follicles have been the focus of much research as they are believed to play an important role in the regulation of the hair follicle (Blume-Peytavi and Mandt, 2000; Paus, 2000; Philpott, 2000; Randall et al., 2000; Hamada and Randall, 2006). A number of growth factors and cytokines have been recognised in androgen action, mainly by investigating cultured dermal papilla cells.

Insulin like growth factor-I (IGF-I) is a potent mitogen which maintains cultured human scalp hair follicles in anagen at physiological concentration (Philpott et al., 1994). Androgens increased gene expression of IGF-I in beard dermal papilla cells *in vitro* (Itami et al., 1995) and androgens also stimulated the proliferation of outer root sheath cells when co-cultured with dermal papilla cells; the stimulatory effect of androgens on the growth of outer root sheath cells was stopped when IGF-I was blocked with antibodies. Abnormal hair growth and differentiation occurred in hair follicles when the action of IGF-I is blocked in the IGF-I receptor deficient mouse (Liu et al., 1993). These results implicate IGF-I involvement in hair growth, including androgen-stimulation

Stem cell factor (SCF), also known as mast cell growth factor, c-kit ligand or steel factor, plays a role in the development of epidermal (Williams et al., 1992; Grichnik et al., 1998) and hair pigmentation (Geissler et al., 1988; Fleischman et al., 1991). Beard dermal papilla cells secrete more SCF than non-balding scalp cells (Hibberts et al., 1996) while cells derived from pale balding scalp follicles secreted less (Randall et al., 2008). Dermal papilla cells secrete SCF and adult scalp hair follicle melanocytes express the receptor for SCF, c-kit, (Randall et al., 2008) suggesting that SCF secreted by the dermal papilla could alter pigmentation by acting on the

hair follicle melanocytes. Interestingly, androgens *in vivo* may alter SCF production by facial or scalp dermal papilla cells resulting in darker facial hair when boys vellus hairs transform to adult beard and paler hairs during the miniaturisation of scalp hair follicles.

Hepatocyte growth factor (HGF) also known as scatter factor, was shown to be a mitogen and morphogen of epithelial cells (Sonnenberg et al., 1993). HGF had a stimulatory effect on follicle length and <sup>3</sup>H-thymidine uptake in both mouse vibrissae (Jindo et al., 1994) and human scalp hair follicles in organ culture (Jindo et al., 1995; Shimaoka et al., 1995). HGF was detected in dermal papilla cells, while the HGF receptor, c-Met, was localised in the hair bulb keratinocytes in anagen mouse follicles using immunohistochemistry (Lindner et al., 2000). HGF mRNA is expressed by cultured human hair follicle dermal papilla cells (Shimaoka et al., 1994; Merrick, 2000). HGF stimulated DNA synthesis in keratinocytes derived from the human hair bulb *in vitro* (Shimaoka et al., 1995) suggesting an active role. Cultured beard dermal papilla cells showed a greater HGF expression than non-balding scalp dermal papilla cells, but balding scalp dermal papilla cells showed very low HGF expression (Merrick, 2000 b). These results suggest that HGF may play a role in maintaining large follicles and androgens may control the level of HGF in androgen-dependent follicles *in vivo* (Randall et al., 2001b).

Another possible paracrine factor is vascular endothelial growth factor (VEGF), a modulator of angiogenesis and vascular permeability. Terminal follicles have a good blood supply, suggesting that microvascular angiogenesis occurs at an early anagen phase (Montagna and Van Scott, 1958b). Cultured dermal papilla cells have been shown to express VEGF (Hibberts, 1996; Lachgar et al., 1996b; Merrick, 1999). Catagen and telogen phase human scalp dermal papilla cells were found to

express decreased levels of VEGF mRNA (Lachgar et al., 1996a). Minoxidil, a treatment for androgenetic alopecia, has been shown to stimulate VEGF mRNA expression in cultured human dermal papilla cells (Lachgar et al., 1998). VEGF expression in a number of cell types is influenced by steroid hormones, such as oestrogen which up-regulates the expression of VEGF in rat ovary (Shweiki et al., 1993) and uterus (Cullinan-Bove and Koos, 1993); and in the human endometrium (Shifren et al., 1996). In a different study, it was reported that patients receiving androgen deprivation therapy for prostate cancer showed decreased levels of VEGF compared to the levels measured before the treatment (Aslan et al., 2005). Therefore, VEGF appears to respond to steroid hormones including androgens making it a likely factor involved in androgen-regulation of hair growth.

Transforming growth factor- $\beta$ 1 (TGF- $\beta$ 1) is another paracrine factor which inhibits hair growth *in vitro* and may be a negative regulator of hair follicle growth (Philpott, 2000). TGF- $\beta$ 1 inhibits human hair growth during organ culture (Philpott et al., 1990). When TGF- $\beta$ 1 was investigated in a co-culture system of balding dermal papilla cells with transfected androgen receptors and keratinocytes (Inui et al., 2002, 2003), there was a significant suppression in keratinocytes growth with the addition of a synthetic androgen to the culture. Androgens also stimulated the expression of TGF- $\beta$ 1 in the cultured balding dermal papilla cells. In addition an antibody against TGF- $\beta$ 1 reversed growth inhibition of the keratinocytes, which suggests that androgens induce the expression of TGF- $\beta$ 1 from balding dermal papilla cells which leads to the suppression of epithelial cell growth. TGF- $\beta$ 1 has also been reported to involve in controlling catagen, in which a suppressor of TGF- $\beta$ 1 delayed progression of catagen in mice *in vivo* (Tsuji et al.,



2003). The injection of TGF- $\beta$ 1 into the back skin of mice induced premature catagen (Foitzik et al., 2000).

In order to reveal further the effect of androgen on the dermal papilla production of paracrine factors, Rutberg *et al* (2006) compared gene expression patterns in cultured human dermal papilla cells isolated from beard (androgen-sensitive) and occipital scalp (androgen-insensitive) hair follicles using DNA microarray methods. Three genes, *sfrp-2*, *mn1* and *atp1 $\beta$ 1*, were expressed at significantly higher levels in the beard dermal papilla cells than non-balding scalp cells (Rutberg et al., 2006) but their significance is not clear.

#### **1.4 Hair disorders**

Hair disorders are not life threatening, however the important role of hair in human social and sexual communication through life, makes any pathological abnormalities in hair growth psychologically distressing in both men (Cash, 1992; Gulec et al., 2004) and women (Cash et al., 1993) (Figure 7). The most common hair disorders are: androgenetic alopecia, hirsutism and alopecia areata.

##### *Androgenetic alopecia*

Androgenetic alopecia, also known as common baldness or male pattern baldness, is the most common type of hair loss disorder in men (Rathnayake and Sinclair, 2010). It occurs on the scalp of both men (Hamilton, 1951) and women (Ludwig, 1977), but more frequently in men. In androgenetic alopecia, thin, short and non-pigmented vellus hairs replace the thick, pigmented terminal hairs on the scalp in slow progression (Figure 7 and 8). The hair loss follows a distinctive pattern of progression, which was first described in men by Hamilton (1951). The degree of hair loss severity was classified to include seven types, with type I being the

normal pre-pubertal scalp hair pattern. The hair loss normally occurs through gradual recession of the bitemporal hairline and thinning of the vertex to type VII in which hair only remains around the back and sides of the head (Norwood, 1975) (Figure 8). Although male pattern balding can occur in women, a different pattern of hair loss is more common, where there is generally a progressive hair loss in the crown, with preservation of the frontal hair line (Ludwig, 1977; Price, 2003).

In androgenetic alopecia, the anagen phase of the hair growth cycle starts to become shorter while the telogen phase remains constant, meaning that the proportion of the telogen follicles increases (Hamilton, 1951; Norwood, 1975; Randall, 2005a). Two main factors play a role in the pathogenesis of androgenetic alopecia: the genetic predisposition and androgen involvement. Androgens are necessary for the progression of the disorder and several studies provided evidence to support this, for example, androgenetic alopecia does not occur in males castrated prior to puberty and progression is stopped if postpubertal males are castrated (Hamilton, 1960); testosterone replacement therapy can also induce hair loss in castrated males (Hamilton, 1958). The role of androgen in androgenetic alopecia is also confirmed by the absence of androgenetic alopecia in people with complete androgen insensitivity syndrome (lack of functional androgen receptors) (McPhaul, 2004). For the onset of alopecia, a genetic predisposition is required alongside androgens (Birch and Messenger, 2001; Ellis and Harrap, 2001).

**Figure 7 Patterns of human hair growth**

Modified from Randall (2000), with the author's permission.

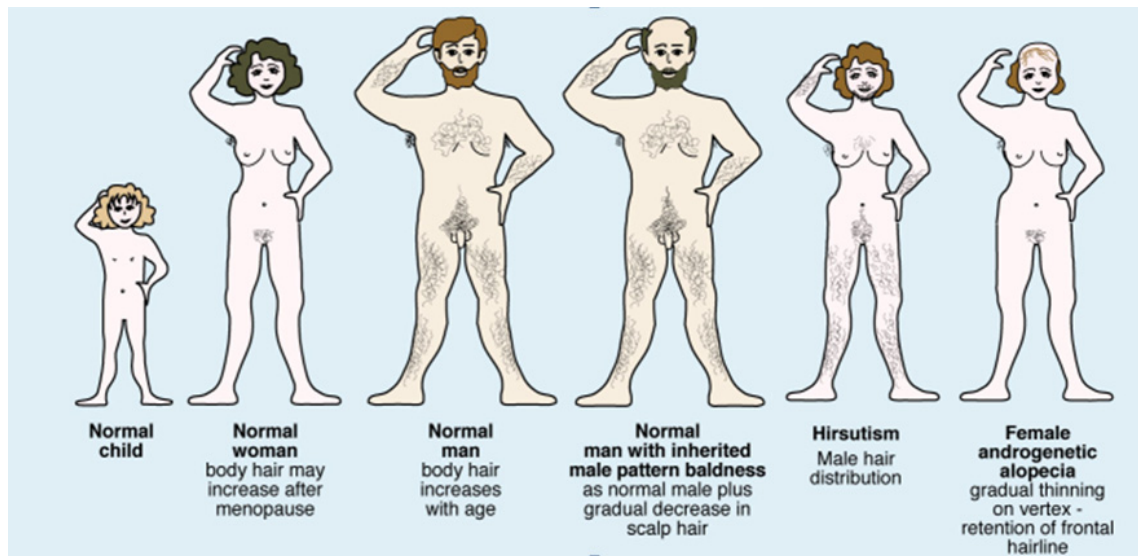


**Figure 8 The patterns of hair loss in androgenetic alopecia in men**

Classification of the common types of baldness in men. Hamilton scale (modified by Norwood). Reproduced from Randall (2000), with the author's permission.



Treatments for androgenetic alopecia include surgery, wigs, hairpieces, hormonal and non-hormonal therapy. The surgical treatment relies on the intrinsic responses of hair follicles to androgens, in which hair follicles from the non-balding areas such as occipital and parietal sites can be relocated on to the bald area to cover it (Orentreich and Durr, 1982). The surgical treatment lasts for a long time, but it also has some disadvantages as it is expensive, painful and may require more surgery as the hair loss develops around the transplanted region.

Hormonal treatments include 5 $\alpha$ -reductase inhibitors and anti-androgens. Anti-androgen treatments act by blocking the androgen binding to the androgen receptor, however, this is not a desirable treatment for men as they also affect male masculinity. The 5 $\alpha$ -reductase inhibitors such as finasteride, a 5 $\alpha$ -reductase type 2 inhibitor, block the conversion of testosterone to its more active metabolite, 5 $\alpha$ -dihydrotestosterone (DHT). Finasteride slows down hair loss progression and also promotes hair growth in men under 42 with stage II to V hair loss (Kaufman et al., 1998). Dutasteride, which is a both type 1 and type 2 5 $\alpha$ -reductase inhibitor, has been shown to have a more rapid effect on scalp hair growth in men with androgenetic alopecia than the finasteride (Olsen et al., 2006). Currently 5 $\alpha$ -reductase inhibitors are the best treatment for androgenetic alopecia in men, but like all other hormonal treatments, must be taken continuously and side-effects are reported (Kaufman et al., 1998; Libecco and Bergfeld, 2004; Finn et al., 2006; Naslund and Miner, 2007; Erdemir et al., 2008).

Minoxidil is the most commonly used non-hormonal treatment for androgenetic alopecia (Lachgar et al., 1998; Li et al., 2001; Messenger and Rundegren, 2004). It is a widely used topical treatment for hair loss in men and women. It was initially developed for the oral treatment of hypertension, but hypertrichosis happened as

a common side effect (Dawber, 2000). Unfortunately hair loss progresses once treatment is stopped (Shapiro and Price, 1998; Dawber, 2000) like all medical approaches as the hormone trigger is being continually produced. It was originally believed to act on the vasculature, increasing the blood supply to the follicle, but a recent study showed its mechanism of action is through the opening of ATP-sensitive potassium  $K_{(ATP)}$  channels in the dermal papilla cell membrane (Shorter et al., 2008).

### *Hirsutism*

Hirsutism is the excessive hair growth on the body of women in the same pattern as a post-pubertal normal male (Brodell and Mercurio, 2010). These areas in normal women are typically covered with fine hair or no hair at all, for example areas on the face like above the upper lip and on the chin, and on other areas of the body like the chest, forearms, back and abdomen (Figure 7). This excessive hair growth can be triggered by excess androgen production above the normal female level which triggers transformation of small, fine vellus hairs to thick, pigmented hairs. This is a paradoxically different effect of androgens compared to their involvement in androgenetic alopecia. There are a number of conditions which can lead to hirsutism; the most common condition is polycystic ovary syndrome (PCOS) which is characterised by over production of androgens (Franks, 1989; Liepa et al., 2008). However a small portion of cases have idiopathic hirsutism, with no hormonal abnormality.

Treatment of hirsutism includes both cosmetic and pharmacological approaches. The cosmetic approach employs various methods which physically remove or lighten the excess hairs, and such treatments include bleaching, shaving, waxing, depilatory creams, electrolysis and laser hair removal. Pharmacological methods

include treatment with anti-androgen drugs, as hirsutism is mediated by androgens. The most commonly used anti-androgen drugs are cyproterone acetate (CPA) and spironolactone (Hammerstein, 1987; Shapiro and Lui, 2005). Anti-androgen drugs also have some disadvantages as the treatment takes a long time before detecting any effect on the hair growth, there may only be partial improvement and there is risk of feminisation of a male foetus (Hughes and Cunliffe, 1988).

### *Alopecia areata*

Alopecia areata is an autoimmune disorder resulting in hair loss, causing patches of baldness particularly on the scalp, but with no scarring of the affected area (Delamere et al., 2008; Alkhalifah et al., 2010); it also occurs in the eyebrows, beard, or other hair-bearing areas of the body (Epstein, 2001). It happens in both male and female adults, children and in all ethnic groups (Muller and Winkelmann, 1963; Sharma et al., 1996). Alopecia areata has two major forms, alopecia universalis which is a more generalised pattern of total body and scalp hair loss, and alopecia totalis, which is less common, and confined to the entire scalp (Delamere et al., 2008)

Although it is believed to be an autoimmune disease the exact cause of alopecia areata is still unknown (Randall, 2001a). The presence of a lymphocytic infiltrate in and around the hair follicles supports the idea that alopecia areata is an autoimmune disease (Wasserman et al., 2007). Several factors have been associated with its pathogenesis, e.g., genetic, neurological factors, possible emotional stress, vaccines, exposure to chemicals and infectious agents (Madani and Shapiro, 2000). It appears to be inherited as an autosomal dominant trait with variable penetrance (Sinclair et al., 1999).

There is no definitive treatment available for alopecia areata yet although, there are some ways to help patients like using wigs and hairpieces (Epstein, 2001). The available treatments include a range of therapies like immune inhibitors, contact sensitizers, immunomodulators, biologic response modifiers, cortico-steroids, minoxidil and non-specific irritants (Gilhar et al., 1998; Wasserman et al., 2007; Delamere et al., 2008). These treatments have varying success rates, but they also have negative side effects and therefore there is no fully satisfactory treatment available for alopecia areata.

Overall, there is a major need for novel approaches to regulate hair growth without androgen-based side effects and preferably useful in both men and women.

## **1.5 Prostanoids and hair growth**

### **1.5.1 Glaucoma treatments stimulate eyelash growth**

A prostaglandin  $F_{2\alpha}$  analogue, latanoprost (Xalatan®), is a common medication in the treatment of open-angle glaucoma, ocular hypertension (Camras, 1996). It lowers intraocular pressure by increasing the natural outflow of fluid from inside the eye into the blood stream (Watson, 1999) and is administered as a single eye-drop once a day into the affected eye or eyes. After its introduction, latanoprost was reported to have a side effect which stimulated the growth of eyelashes and eyebrow hairs (Johnstone, 1997). When 43 patients were unilaterally treated with latanoprost, the eyelashes of the treated eyes showed hypertrichosis. Latanoprost treatment increased the numbers of terminal follicles compared to vellus and intermediate follicles and the pigmentation of the eyelashes was also increased. Curling of the lashes also occurred in several patients. Therefore, increased length, number, thickness, pigmentation and curvature of eyelashes was reported as side effects of latanoprost treatment (Johnstone, 1997).

In Europe and the U.S., latanoprost was first made available in 1996; it is considered to have long term local and systemic safety (Alm et al., 2004).

In another study, hypertrichosis of eyelashes was reported after unilateral topical latanoprost treatment of 89 glaucoma patients; changes to eyelashes including increased number, thickness, length and pigmentation had occurred in 5 of the patients in less than 3 weeks, similar to those patients who had received long term treatment (Johnstone, 1998), suggesting effects on follicles already in anagen. Several other studies have also reported hypertrichosis and darkening of eyelashes in patients following latanoprost treatment (Wand, 1997; Reynolds et al., 1998;



Strober et al., 2001; Sugimoto et al., 2002; Elgin et al., 2006). For example seventeen patients with glaucoma, treated unilaterally with latanoprost, showed a significant increase in eyelash length after 2, 6, and 8 weeks (Sugimoto et al., 2002), with no difference in eyelash measurement in the untreated eyes.

However, in another study, when 7 patients were treated with latanoprost for 5 months eyelash length increased only in one patient (Noecker et al., 1999), though thicker lashes were noticed in 10 of the 14 eyes examined. In a different study, timolol, a beta-receptor antagonist, used for treatment of high intraocular pressure was also examined. Patients (44) were divided into two groups, one treated with timolol and the other with latanoprost. There was an increase in eyelash length in 7% of the patients treated with latanoprost (Stecchi et al., 2002), but no hypertrichosis occurred in any of the patients treated with timolol.

Travoprost (Travatan™), another PGF<sub>2α</sub> analogue, which is structurally similar to latanoprost (Hellberg et al., 2002), was also studied for its effect on eyelash growth; greater increases in eyelash length occurred after treatment with travoprost than latanoprost (Netland et al., 2001; Li et al., 2006). Latanoprost has also been reported to cause re-growth of eyelashes in alopecia areata (Mansberger and Cioffi, 2000; Mehta et al., 2003). In a recent clinical study when they tested the efficacy of latanoprost in eyelash alopecia areata, latanoprost induced acceptable, total and moderate responses in 45% of the patients (Coronel-Perez et al., 2010).

In another study, a murine model (C57BL/6 mice) was used to investigate the effects of prostaglandin F<sub>2α</sub>, and its analogues, latanoprost and isopropyl unoprostone, on hair follicles (Sasaki *et al.*, 2005). In this model system, active melanocytes are confined to the hair follicle, therefore the skin is only pigmented when the follicles are in anagen and during telogen the skin appears pink/white

(Chase *et al.*, 1951; Paus *et al.*, 1994). This model allows observation of the hair cycle stages (section 1.2.2). Mice with dorsal skin in the telogen phase were topically treated with prostaglandin  $F_{2\alpha}$ , latanoprost, isopropyl unoprostone or vehicle control. After 12 days of treatment prostaglandin  $F_{2\alpha}$  and its analogues all caused the development of a grey skin colour indicating the onset of the anagen phase. Overall, these studies showed that  $PGF_{2\alpha}$  and its analogues stimulated anagen hair follicle elongation and caused conversion of the telogen to anagen phase in mice (Sasaki *et al.*, 2005).

### **1.5.2 The Prostanoids**

The prostanoids, which include prostaglandins (PGs), thromboxanes (TXs) and prostacyclins ( $PGI_2$ ) are members of the eicosanoids, a family of oxygenated metabolites of arachidonic acid which includes the prostaglandins, leukotrienes, thromboxanes, lipoxins and other oxygenated derivatives (Haeggstrom *et al.*, 2010). These are potent lipid mediators which are derived from 20 carbon polyunsaturated fatty acids (PUFA). They show a vast number of physiological effects in a wide range of biological systems, such as the brain, eye, cardiovascular system, kidney, skin and lung and are also involved in inflammation (Samad *et al.*, 2002; Wise *et al.*, 2002). Prostanoids act in a paracrine manner, they are produced and inactivated within the same or neighbouring cells before their release as inactive metabolites (15-keto- and 13,14-dihydroketo metabolites) into the circulation (Schuster, 1998; Nomura *et al.*, 2004). The prostanoid signal is ended locally to avoid undesired action at a distance; this metabolic clearance is suggested to happen by two steps, selective uptake across the plasma membrane and oxidation inside the cells (Nomura *et al.*, 2004).

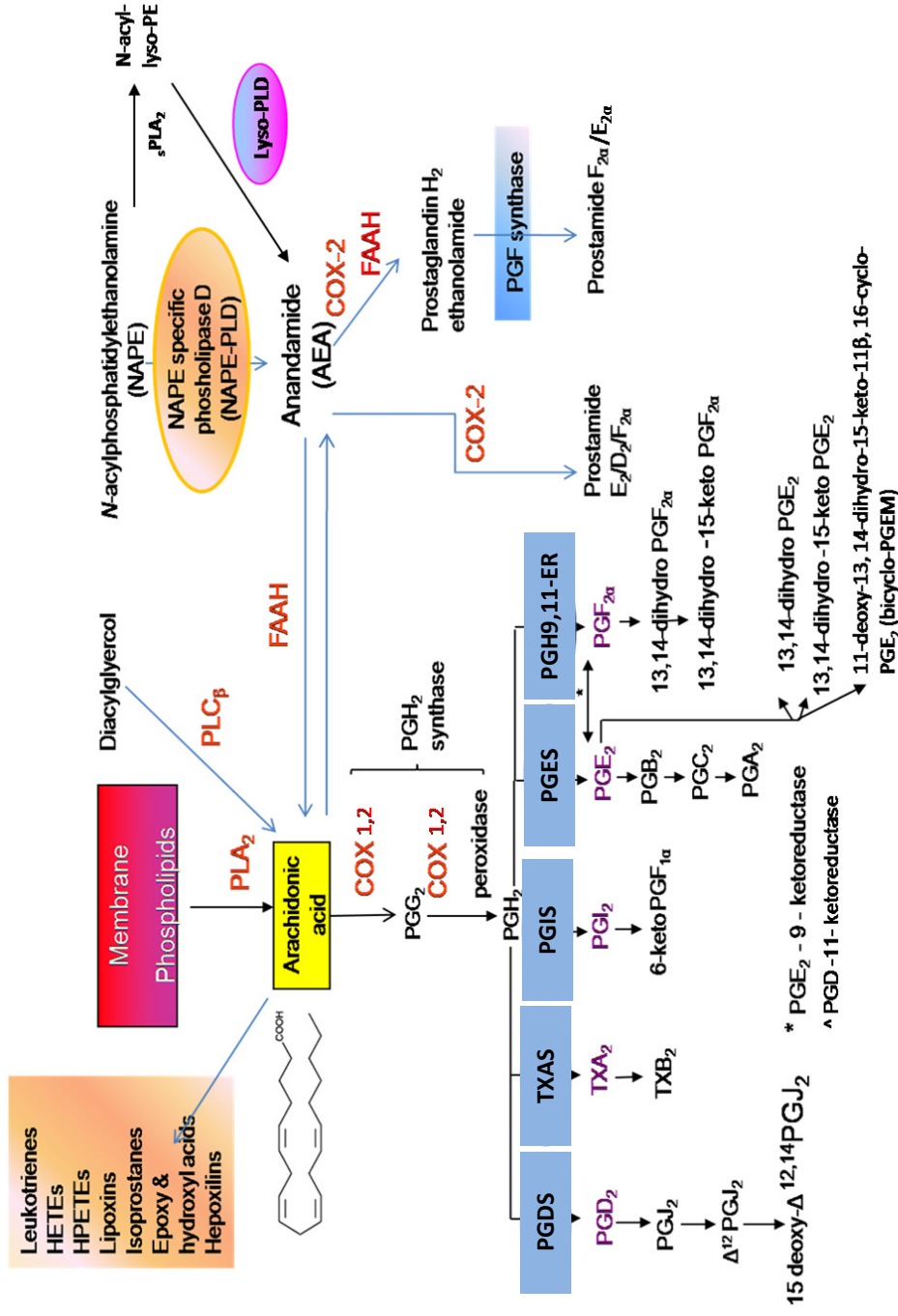
### 1.5.2.1 Prostanoid biosynthesis

Prostanoid biosynthesis involves 3 main steps (Figure 9). Firstly, membrane glycerophospholipids are hydrolysed by phospholipases A<sub>2</sub> (PLA<sub>2</sub>) to generate free fatty acids. The cyclooxygenases, COX-1 and COX-2, catalyse the second step in prostanoid biosynthesis mainly catalysing arachidonic acid (AA) oxidation but also that of docosahexaenoic (DHA) and eicosapentaenoic acid (EPA) (Smith and Song, 2002). COX-1 and COX-2 both have similar active site structures, but the active site of COX-2 is larger than that of COX-1, and COX-2 catalyses more prostanoid synthesis than COX-1 (Smith and Song, 2002). Arachidonic acid is converted by cyclooxygenase to prostaglandin G<sub>2</sub> (PGG<sub>2</sub>) (Figure 9) and PGG<sub>2</sub> is reduced to prostaglandin H<sub>2</sub> (PGH<sub>2</sub>) by a peroxidase reaction; the highly reactive PGH<sub>2</sub> is processed further to individual prostanoids by the action of a series of prostanoid synthases (Smith et al., 2000).

The prostanoid synthases are localised in either the cytoplasm or the microsomes (Ruzicka and Aubeck, 1987). Prostaglandin E synthase (PGES), which has different forms with individual enzymatic properties, catalyses the isomerisation of PGH<sub>2</sub> to PGE<sub>2</sub>. The cytosolic PGES is expressed constitutively in a wide range of cells and tissues, whilst the membrane-associated PGES isozyme is inducible and reacts to a variety of pro-inflammatory stimuli (Jakobsson et al., 1999). The prostaglandin D synthase (PGDS) catalyses the isomerisation of PGH<sub>2</sub> to PGD<sub>2</sub>. There are two types of PGDS: the haematopoietic PGDS (H-PGDS) and the lipocaline PGDS (L-PGDS) (Urade and Eguchi, 2002; Kohno et al., 2006). The synthesis of prostaglandin F<sub>2</sub> occurs through three pathways from PGH<sub>2</sub>, PGE<sub>2</sub> and PGD<sub>2</sub>. PGH<sub>2</sub> is catalysed to

**Figure 9 Prostanoid biosynthesis**

Arachidonic acid conversion to different prostanoids by the cyclooxygenase catalysed pathway. PGDS: prostaglandin D synthase, PGES: prostaglandin E synthase, PGH9,11-ER: prostaglandin H9,11-endoperoxide reductase, TXAS: thromboxane A synthase, COX: cyclooxygenase and PGIS: prostacyclin synthase. Adapted from (Durn, 2008).



PGF<sub>2α</sub> by the enzyme PGH 9,11-endoperoxide reductase (PGH9,11-ER), PGE<sub>2</sub> to PGF<sub>2α</sub> by PGE 9-ketoreductase (PGE9-KR) and PGD<sub>2</sub> to PGF<sub>9α</sub> & 11β-PGF<sub>2α</sub> by PGD 11-ketoreductase (PGD11-KR) (Suzuki-Yamamoto et al., 1999; Komoto et al., 2006). PGH<sub>2</sub> is catalysed to prostacyclin PGI<sub>2</sub> by the enzyme prostacyclin synthase (PGIS) and this unstable PGI<sub>2</sub> is instantly hydrolysed to the inactive 6-keto-F<sub>1α</sub> metabolite. The dehydration within the cyclopentane ring of PGE<sub>1</sub>, PGE<sub>2</sub> and PGD<sub>2</sub> produces the cyclopentanone prostaglandins, PGA<sub>1</sub>, PGA<sub>2</sub> and PGJ<sub>2</sub> respectively (Straus and Glass, 2001). PGH<sub>2</sub> is catalysed to thromboxane A<sub>2</sub> (TXA<sub>2</sub>) by the enzyme thromboxane A synthase (TXAS), and the unstable TXA<sub>2</sub> breaks down to the inactive, but stable TXB<sub>2</sub> (Miyata et al., 1994).

The isoprostanes are prostaglandin-like molecules formed by free radical oxidation of arachidonic acid and other polysaturated fatty acids non-enzymatically (Morrow et al., 1990). The side chains in isoprostanes are *cis* to the cyclopentane ring which are different from that of prostaglandins which are in *trans* orientation. The F-ring compounds (diol substitution on the cyclopentane ring) are isomeric to PGF<sub>2α</sub> and they are known as F<sub>2</sub>-isoprostanes. The 15-series F<sub>2</sub>-isoprostanes are usually referred to as 8-*iso*-PGF<sub>2</sub>. The isoprostanes have been recognised as a marker for lipid peroxidation and oxidative stress *in vivo* (Montuschi et al., 1998; Mehlhorn et al., 2003).

#### **1.5.2.2 The roles of prostanoids**

Prostanoids have a wide range of biological effects such as an involvement in inflammation in which they mediate fever, pain, swelling and erythema; they can act as both proinflammatory and anti-inflammatory mediators depending on the receptors and signalling pathways that they are coupled to (Tilley et al., 2001).

In the vascular system prostanoids are involved in platelet aggregation, haemostasis and thrombosis. Both TXA<sub>2</sub> (mainly synthesised in platelets) and prostacyclin (PGI<sub>2</sub>; mainly produced by endothelial cells) play a vital role in the preservation of vascular homeostasis and control of the blood flow (McAdam et al., 1999). COX-2 is present constitutively in the brain, primarily in neurons and has been shown to play a key role in neuroinflammation and associated disorders such as Alzheimer's disease (Bazan and Flower, 2002). Prostanoids have been reported to be produced in human skin and are involved in the regulation of growth and differentiation of the epidermis (Ikai, 1999); human epidermis expresses both COX-1 and 2 (Goldyne, 2000). Prostanoids also show immunoregulatory and proinflammatory actions in human skin through their effects on blood vessels and inflammatory cells (Ikai, 1999). Both COX-1 and 2 play roles in keratinocyte differentiation and the absence of either isoform can lead to premature differentiation of initiated keratinocytes (Tiano et al., 2002). The main prostaglandins produced in cultured human skin keratinocytes are PGF<sub>2α</sub>, PGE<sub>2</sub> and a small amount of prostacyclin (PGI<sub>2</sub>) (Pentland and Mahoney, 1990). PGD<sub>2</sub> was reported to bind to the DP receptor on Langerhans cells and inhibit their migration (Angeli et al., 2001), however, PGE<sub>2</sub> binds to the EP<sub>4</sub> receptor on Langerhans cells and promotes their maturation and migration; this assists in the initiation of the skin immune response (Kabashima et al., 2003).

Prostanoids are involved in normal renal function by regulating normal blood flow and vascular tone (Agnoli et al., 1999). Prostaglandins are also involved in many reproductive processes from ovulation and fertilisation to parturition and labour. It has been reported that local control of prostaglandin synthesis and degradation occurs in the foetal membranes, myometrium and placenta (Sullivan et al., 1992;

Grigsby et al., 2006); nineteen prostanoids have been identified in human non-labouring and labouring myometrium (Durn *et al.*, 2010b). In the gastrointestinal tract, COX-1 has been shown to be expressed constitutively and COX-1-derived prostanoids especially PGE<sub>2</sub> and PGI<sub>2</sub>, have important cytoprotective effects on the gastrointestinal mucosa (Hansen et al., 1999; Haworth et al., 2005). The involvement of COX-1 in the early stages of tumorigenesis has been reported (Houchen et al., 2000) and an increase in the expression of COX-2 was noted in a wide range of cancers (Bishop-Bailey et al., 2002; Muller-Decker and Furstenberger, 2007). However, some studies indicated that prolonged use of non-steroidal anti-inflammatory drugs (NSAID), such as aspirin, reduced the risk of developing many types of cancer, such as lung, stomach and colon cancer (Anand and Graham, 1999; Khuder et al., 2005); these suggest that specific COX-2 inhibitors may be useful as anticancer treatments. Isoprostanes are indicators of oxidative stress status or free radical lipid peroxidation (Roberts et al., 1998; Cracowski et al., 2002). They have been linked to a number of disorders, such as diabetes, inflammation, cardiovascular disease, atherosclerosis, neurological disorders, reproductive disorders and pulmonary disease (Li et al., 1999; Junger and Sorkin, 2000; Greco and Minghetti, 2004). Both 8-*iso*-PGF<sub>2α</sub> and 8-*iso*-PGE<sub>2</sub> are biologically active in bronchoconstriction and vasoconstriction and these effects were believed to be mediated by isoprostanes through the activation of prostanoid receptors (Daray et al., 2004).

### **1.5.3 Prostaglandins**

Prostaglandins are biologically active acidic lipids that are abundantly distributed in mammalian tissues (Piper, 1973). They were first noticed in 1930 by two American gynaecologists, Kurzork and Lieb, whilst working on female sterility.

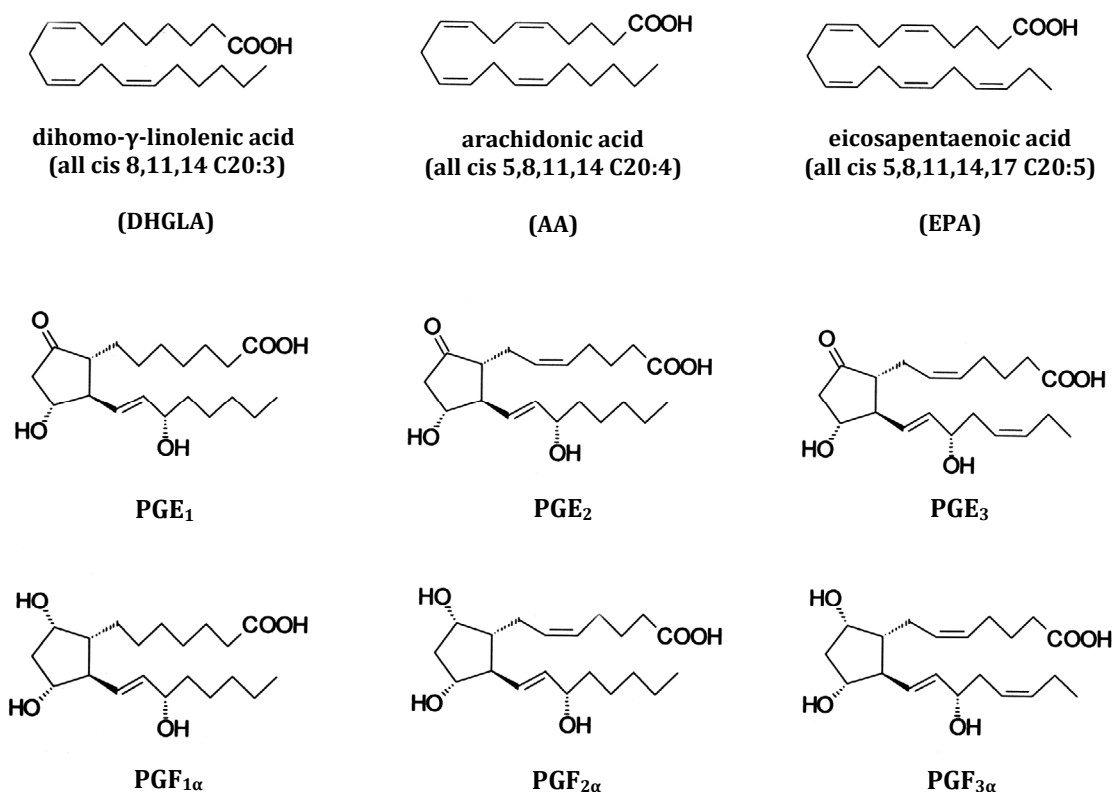
Later, a Swedish physiologist, Ulf von Euler (Von Euler, 1935) isolated lipid soluble acid extracts from seminal fluid and named them prostaglandins (Curtis-Prior, 1976), believing they were part of the prostatic secretions, but afterwards it became clear that many other tissues secrete prostaglandins for various functions. Prostaglandins are oxygenated polyunsaturated 20 carbon carboxylic acids that contain a five-member ring. Thromboxane A (TXA) has an unstable bicyclic oxane-oxetane ring structure, thromboxane B (TXB) is a stable oxane and prostacyclin (PGI) contains an oxygen bridge between C6 and C9 (Slater and McDonald-Gibson, 1987). The number of double bonds in the prostanoid alkyl chain depends on the precursor fatty acid. The prostaglandins of the 1-series with 1 double bond, are derived from dihomo- $\gamma$ -linolenic acid (DHGLA; 20:3 *n*-6), the II-series, with 2 double bonds, are derived from arachidonic acid (AA; 20:4 *n*-6) and the III-series, with 3 double bonds, are derived from eicosapentaenoic acid (EPA; 20:5 *n*-3). Figure 10 shows the structures of prostaglandin F and E of all 3 series and their precursor polyunsaturated fatty acids.

Prostaglandins were originally believed to leave cells via passive diffusion because of their high lipophilicity. The discovery of the prostaglandin transporter (PGT, SLC02A1) which mediates the cellular uptake of prostaglandins, suggests that prostaglandin penetration through the cellular membrane occurs via both simple diffusion and prostaglandin transporters (Chi and Schuster, 2010). Prostaglandins act as autocrine/paracrine local hormones through specific G-protein coupled receptors (GPCRs) (Kobayashi and Narumiya, 2002). The presence of a large number of prostaglandin receptors allows prostaglandins to act on a range of cells, and have a wide variety of actions. The known functions are: constriction or



### Figure 10 The structures of prostaglandins F and E

The structures of series I, II and III prostaglandin F and E; their precursor polyunsaturated fatty acids (Nicolaou, 2005).



dilatation of vascular smooth muscle cells, aggregation or disaggregation of platelets, sensitisation of spinal neurons to pain, constriction of smooth muscle, regulation of inflammatory mediation, regulation of calcium movement, control of hormone regulation and control of cell growth (Bikowski et al., 2010). Prostaglandins, in particular PGF<sub>2 $\alpha$</sub> , are also known to induce labour (Karim et al., 1968). The common functions for each type of prostaglandin are summarised in Table 1.

Prostaglandin receptors belong to the rhodopsin seven transmembrane domains superfamily of receptors, and the five types of prostanoids (PGE<sub>2</sub>, PGF<sub>2 $\alpha$</sub> , PGD<sub>2</sub>, PGI<sub>2</sub> and TXA<sub>2</sub>) bind to their specific receptors (EP<sub>1</sub>, EP<sub>2</sub>, EP<sub>3</sub>, EP<sub>4</sub>; FP; DP<sub>1</sub>, DP<sub>2</sub>; IP; TP

**Table 1 Different prostaglandin types, their receptors and their functions**

Type	Receptor	Function
<b>PGD<sub>2</sub></b>	DP <sub>1</sub>	inhibits vascular permeability
	DP <sub>2</sub>	vasodilatation Inhibition of platelet aggregation
<b>PGE<sub>2</sub></b>	EP <sub>1</sub>	bronchoconstriction GI tract smooth muscle contraction
	EP <sub>2</sub> & EP <sub>4</sub>	bronchodilatation GI tract smooth muscle relaxation vasodilatation
	EP <sub>3</sub>	decrease gastric acid secretion increase gastric mucus secretion uterus contraction GI tract smooth muscle contraction lipolysis inhibition increase autonomic neurotransmitters
<b>PGI<sub>2</sub></b>	IP	nocioception antithrombosis vasodilator actions pulmonary hypotension
<b>PGF<sub>2α</sub></b>	FP	uterus contraction essential for normal birth bronchoconstriction
<b>TXA<sub>2</sub></b>	TP	mediate platelet shape change and aggregation smooth muscle contraction and proliferation

respectively). Despite a high affinity of each prostaglandin binding with its specific receptor, there is significant ligand-binding cross reactivity within the prostaglandin family (Breyer, 2001).

Prostanoid receptors have been classified into three subgroups based upon G protein activity. The first subgroup, FP, EP<sub>1</sub> and TP, trigger G<sub>q</sub> protein-coupled activating Ca<sup>2+</sup> signalling pathways, which lead to inositol 1,4,5-triphosphate turnover and activation of protein kinase C. The second subgroup, IP, EP<sub>2</sub>, EP<sub>4</sub> and DP<sub>1</sub>, trigger G<sub>αs</sub> protein-coupled adenylate cyclase activation which results in protein kinase A activation and cAMP synthesis. The last subgroup, EP<sub>3</sub> and DP<sub>2</sub>, trigger G<sub>i</sub> protein-coupled adenylate cyclase inhibition and decrease intracellular cAMP (Coleman et al., 1994; Breyer et al., 2001). Therefore, prostaglandins act by causing rapid changes in the intracellular levels of secondary mediators cAMP or Ca<sup>2+</sup> generating specific induction of cell regulatory mechanisms.

#### **1.5.4 Prostaglandins and hair growth**

Positive effects of prostaglandin F<sub>2α</sub> analogue, latanoprost, on human eyelash growth have been reported (Johnstone, 1997, 1998; Johnstone and Albert, 2002) (reviewed 1.5.1), but the underlying mechanism of prostaglandin-associated hair growth is poorly understood. Interestingly, minoxidil, a current main treatment for alopecia, was reported to activate purified COX-1 and prostaglandin endoperoxide synthase-1 (PGHS-1) in human hair follicle dermal papilla cells by an oxygen consumption and prostaglandin production assay; this activation was also evidenced by cultured BALB/c3T3 fibroblasts (Michelet et al., 1997).

Various studies have reported that various enzymes involved in prostaglandin synthesis are present in skin tissues. In another study on mice, COX isozymes were shown to be spatiotemporally expressed during morphogenesis of dorsal skin

epithelium of NMRI mice. COX-1 and COX-2 mRNA and protein were detected in embryonic and postnatal epidermal tissue by RT-PCR, northern blot and immunoblot analysis indicating that both isoforms may contribute to prostaglandin production in skin (Muller-Decker *et al.*, 2003). In two different studies, it has also been indicated that the enzymes involved in PGF<sub>2α</sub> and PGE<sub>2</sub> metabolism were present in human scalp skin (Kabashima and Miyachi, 2004), and hair follicle dermal papilla cells (Colombe *et al.*, 2007) using RT-PCR, Western blot and immunohistochemistry.

In order to further investigate the hair growth effects of prostaglandins *in vivo*, several experiments have been performed on animal models. Prostaglandin receptors were investigated in the anagen hair follicle from mouse dorsal skin by RT-PCR and both EP<sub>3</sub> and EP<sub>4</sub> mRNA were shown to be expressed in dermal papilla cells and outer root sheath cells respectively. After 8 weeks, further signals for EP<sub>3</sub> and EP<sub>4</sub> mRNA disappeared when the follicles were in telogen phase. This could suggest that prostaglandin receptors may play a role in mouse hair growth (Torii *et al.*, 2002).

Latanoprost had promoted hair growth in C57/B16 mice compared to control mice (Stjernschantz, 2001). In a further study on stump-tailed macaque (*Macaca arctoides*) (a primate model of androgenetic alopecia), eight monkeys were divided into 2 groups; one group received a daily topical application of 115 nM of latanoprost and the other group had a daily application of vehicle. For an additional 3 months, 2 monkeys from each group were given 1.15 μM latanoprost, while the remaining monkeys continued with the previous treatment. The administration of 115 nM latanoprost caused minimal hair growth, whilst 1.15 μM latanoprost increased hair density and converted vellus hairs to intermediate or

terminal hairs; the vehicle group showed no effect (Uno *et al.*, 2002). Some other drugs such as ibuprofen, aspirin and indometacin, the inhibitors of prostaglandin endoperoxide synthase, were also reported to block prostaglandin synthesis and inhibit hair growth in humans (Meyer, 1979; Pillans and Woods, 1995). These studies all suggest that prostaglandins may be able to regulate hair growth.

### **1.5.5 Prostaglandins and hair growth**

Bimatoprost, a prostamide  $F_{2\alpha}$  analogue, rather than prostaglandin  $F_{2\alpha}$  analogue like latanoprost is the most efficient ocular hypotensive agent currently available for the treatment of glaucoma (Woodward *et al.*, 2008b; Centofanti *et al.*, 2010; Law, 2010). Recently, a paired-eye comparison of medical therapies for glaucoma study was carried out on patients with uncontrolled glaucoma ( $n = 55$ ) (Solish *et al.*, 2010). The patients were treated with bimatoprost 0.03% once daily in one eye and travoprost 0.004% once daily in the fellow eye. Intra ocular pressure (IOP) was evaluated for 4-6 weeks. Bimatoprost significantly reduced mean IOP (from 19.8 mmHg to 17.1 mmHg,  $P < 0.0001$ ) and slightly more than travoprost (from 19.4 mmHg at baseline to 17.7 mmHg at follow-up,  $P = 0.009$ ) (Solish *et al.*, 2010). Following treatment with the antiglaucoma drug, bimatoprost, increases in eyelash growth were also noted (Hart and Shafranov, 2004). Bimatoprost (Latisse®) was licensed for the treatment of hypotrichosis of the eyelashes by the FDA in December 2008 (NDA 022369); it stimulates eyelashes to lengthen, thicken and darken (Easthope and Perry, 2002; Law, 2007, 2010). Latisse was also reported to induce periocular skin hyperpigmentation in some cases as a side-effect (Priluck and Fu, 2010). No other drugs have caused such a dramatic stimulation of hair growth after a local application as these glaucoma treatments have on eyelashes;

minoxidil's effect topically is much less than via the original oral ingestion (Messenger and Rundegren, 2004).

#### **1.5.5.1 Prostamides**

Prostamides (prostaglandin-ethanolamide) are a large series of neutral lipids; they are COX-2 derived oxidation products of the endocannabinoid/endovanilloid anandamide (Woodward et al., 2008b). They were first identified during studies on endocannabinoid oxygenation via COX-2, which resulted in the formation of pharmacologically unique prostamides and PG-glycerol esters (Yu et al., 1997). Anandamide and 2-arachidonylglycerol ester (2-AG) are converted to a range of products that are closely related to those formed by COX-1 and COX-2 from arachidonic acid (Kozak *et al.*, 2002) and prostamides can be produced from anandamide in mice (Weber *et al.*, 2004). The oxidation of anandamide by COX-2 results in a loss of activity at cannabinoid-1 receptors and formation of the prostamides (De Petrocellis et al., 2004). The fatty acid amide hydrolase (FAAHs) hydrolyses anandamide to arachidonic acid, which may supply a substrate source for COX-1 and COX-2 or lipo-oxygenases (Figures 9, 11) (Wei et al., 2006).

It has been reported that prostamide  $F_{2\alpha}$  and its analogue, bimatoprost, show effects independent of prostanoid FP receptor activation; studies involving feline iridial smooth muscle cells had shown that bimatoprost and FP receptor agonists stimulated different cells (Liang et al., 2008).

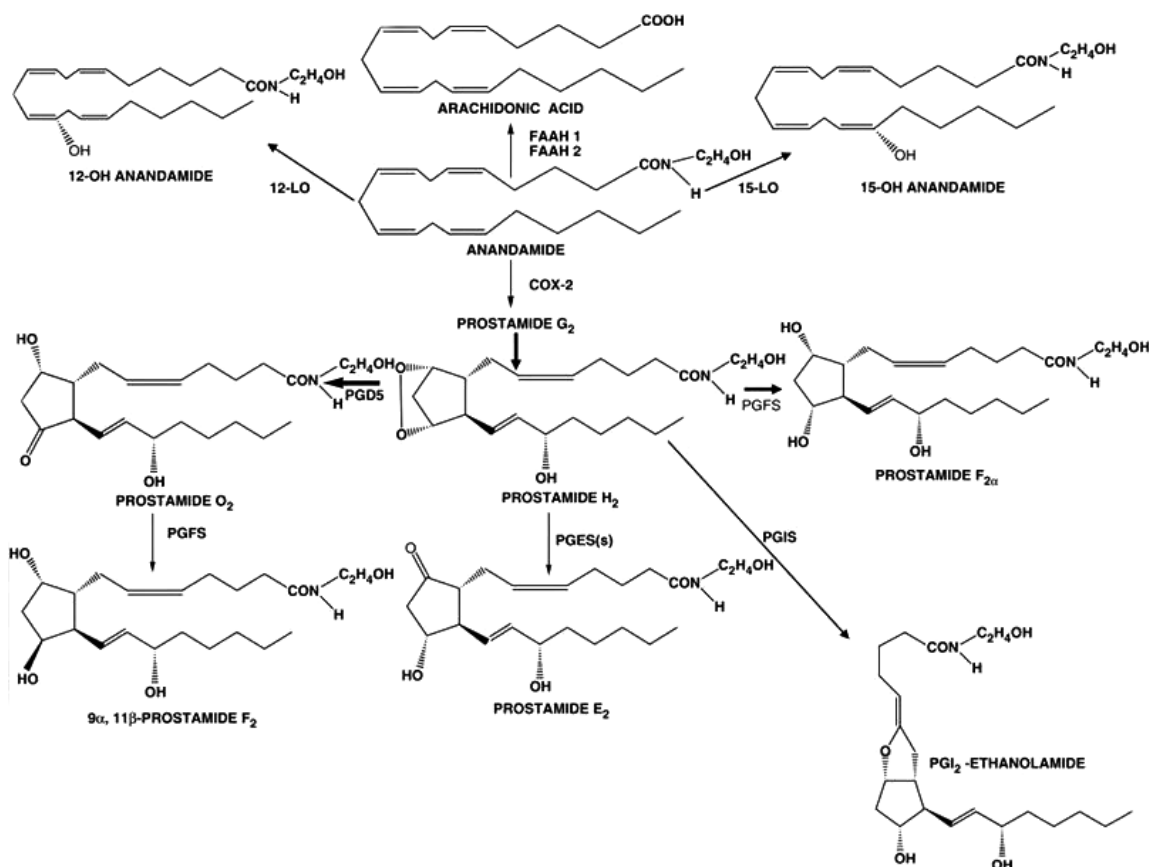
#### **1.5.5.2 Prostamide biosynthesis**

Anandamide is catabolised to arachidonic acid and ethanolamine by the fatty acid amide hydrolase (FAAHs) enzymes (Cravatt et al., 1996; Wei et al., 2006). It is also oxidised by COX-2 and lipo-oxygenase pathways to the endoperoxide

intermediates, prostamide G<sub>2</sub> and prostamide H<sub>2</sub>; they are then converted to the various prostamides by specific prostaglandin synthases (Kozak *et al.*, 2002; Yang *et al.*, 2005). The prostaglandin F synthase catalyses both prostamide H<sub>2</sub> and prostamide D<sub>2</sub> substrates to form prostamide F<sub>2α</sub> and 11β-prostamide F<sub>2α</sub> (Koda *et al.*, 2004; Yang *et al.*, 2005) (Figure 11). The 2-AG is also a substrate for FAAH in addition to anandamide and other fatty acid amides (De Petrocellis *et al.*, 2004). PGE<sub>2</sub>-ethanolamide was recognised as the major product when anandamide was incubated with COX-2 or human foreskin fibroblasts expressing COX-2 (Yu *et al.*, 1997); a later study on mouse leukaemic monocyte macrophage cell line, RAW 264.7 also confirmed the production of prostamide E<sub>2</sub> from anandamide (Burstein *et al.*, 2000).

### Figure 11 Anandamide conversion pathways

The biosynthesis of prostamides from anandamide. Adapted from (Woodward et al., 2008b)



#### 1.5.5.3 Prostamide analogues and their therapeutic roles

The most extensive pharmacological studies with prostanoids have been conducted for prostamide F<sub>2 $\alpha$</sub>  and its analogue, bimatoprost; bimatoprost has been the focus of many studies due to its clinical importance as an intra-ocular pressure lowering agent (Law, 2010). The amide substituent compounds were the most acceptable both pharmacologically and ophthalmologically; the primary amide (CONH<sub>2</sub>) and N-monosubstituted analogues offered potent and selective prostamide agonists. A number of prostamide analogues including bimatoprost



have been made based on the essential PGF<sub>2α</sub> 1-amide structure (Woodward *et al.*, 2004). The unique pharmacology of PGF<sub>2α</sub> amides was originally shown through a FP receptor-mediated event by comparing responses in the isolated feline iris with Ca<sup>2+</sup> signalling (Woodward and Lawrence, 1994). It was shown that only certain isolated tissue preparations distinctively identified prostamide F<sub>2α</sub> receptor, such as feline lung parenchyma (Woodward *et al.*, 2003), feline iris (Matias *et al.*, 2004) and rabbit uterus (Chen *et al.*, 2005).

A number of tissues which were known to constitutively express FP receptors like gerbil colon, mouse uterus, intact rabbit jugular vein, rat uterus and human uterus, were found to be insensitive to prostamide F<sub>2α</sub> and bimatoprost (Woodward *et al.*, 2001; Woodward *et al.*, 2003; Matias *et al.*, 2004; Chen *et al.*, 2005). However, bimatoprost at certain micromolar concentrations acts as a FP receptor agonist (Sharif *et al.*, 2001; Sharif *et al.*, 2003).

Initially it was believed that prostamide activity was species and tissue specific, but when further studies were carried out similar results were obtained when the responses of feline and human recombinant FP receptors were compared (Woodward *et al.*, 2003; Matias *et al.*, 2004). In a different study, the rabbit uterus showed high sensitivity to bimatoprost, but no such activity was observed in the intact rabbit jugular vein (Chen *et al.*, 2005). Further gene regulation studies confirmed that prostamide activity is cell type specific (Liang *et al.*, 2003). In a study when they compared the effects of PGF<sub>2α</sub> and bimatoprost on the expressions of connective tissue growth factor and cysteine-rich angiogenic protein 61 (Cyr 61) in human ciliary smooth muscle cells, PGF<sub>2α</sub> upregulated both connective tissue growth factor and Cyr 61, while bimatoprost only upregulated Cyr 61 (Liang *et al.*, 2003). Similarity in responses of cells and tissues to

prostaglandin  $F_{2\alpha}$  and  $PGF_{2\alpha}$  and their like FP receptor stimulation have made pharmacological analysis extremely difficult (Woodward *et al.*, 2008b). A further study was performed to verify whether the FP receptor subclass equally recognised both  $PGF_{2\alpha}$  and prostaglandin  $F_{2\alpha}$ . When the effects of a series of agonists were investigated on isolated feline iris cells with  $Ca^{2+}$  signalling and monitored by fluorescence confocal microscopy, bimatoprost and the FP receptor agonists ( $PGF_{2\alpha}$ , 17-phenyl  $PGF_{2\alpha}$ ) stimulated entirely different cells (Spada *et al.*, 2005).

Identification of prostaglandin receptor genes was reported in a study on human ocular tissue which recognised the expression of splicing variants of FP receptor genes; bimatoprost actively interacted with FP-altFP4 heterodimer receptor (Liang *et al.*, 2008).

Prostaglandins seem to be involved in disease processes as studies showed upregulation of COX-2 together with anandamide levels at inflammation and infection sites, which could result in the formation of prostaglandins as main products (Glass *et al.*, 2005; Woodward *et al.*, 2008a; Woodward *et al.*, 2008b). Prostaglandins were suggested to work in a different fashion to prostaglandins; clinical studies had shown that glaucoma patients who did not react to latanoprost treatment were found to be susceptible to bimatoprost, which produced a marked lowering of intraocular pressure (Williams, 2002; Gandolfi and Cimino, 2003). The high efficacy of bimatoprost was linked to the dual mechanism of action on aqueous humour outflow that involved both uveoscleral and trabecular meshwork/Schlemm's canal pathways, causing a controlled remodelling of the anterior third of the ciliary body and resulting in new and organized drainage channels that were partially lined with endothelial cells (Richter *et al.*, 2003; Wan *et al.*, 2007). Despite being considered a very safe drug, bimatoprost does have

some side effects, such as periorbital hyperpigmentation, ocular surface hyperaemia and eyelash hypertrichosis (Hollo, 2007; Woodward and Chen, 2007). Bimatoprost causes significantly less iridial hyperpigmentation compared to the latanoprost therapy (Sherwood and Brandt, 2001; Alm *et al.*, 2004).

## **1.6 Aims and experimental design**

Clinical observations of increased eyelash growth as a side-effect of glaucoma treatment by PGF<sub>2α</sub> and prostamide F<sub>2α</sub> analogues (1.5.1) and a range of studies in rodents (1.5.4) (Bikowski *et al.*; Johnstone and Albert, 2002; Namazi, 2003; Wolf *et al.*, 2003; Hart and Shafranov, 2004; Faghihi *et al.*, 2009) suggest that these drugs may be useful for stimulating hair growth in human hair disorders. However, the regulation of human hair growth and pigmentation is complex with their responses varying in different parts of the body. For example, androgens stimulate hair growth in many areas after puberty e.g. the beard and axillary regions, but have no effect on eyelashes. In contrast, the same levels of androgens cause gradual inhibition of hair growth and balding on the scalp in men with the correct genetic background (Randall, 2007). Similarly, loss of pigmentation, hair greying, does not occur in all follicles at the same time; it starts above the ears and progresses across the scalp (Keogh and Walsh, 1965). Eyelashes, while being produced by hair follicles on the eyelid and passing through continuous hair cycles similarly to scalp follicles, spend much less time in the growing phase, anagen (see 1.2.2), than scalp follicles (Thibaut *et al.*, 2009). Eyelashes are specialised hairs designed to protect the eyes and are much shorter, thicker and frequently darker than scalp hairs. The melanocytes in human eyelashes also exhibit tyrosinase-related protein 2 (TRP-2) (Thibaut *et al.*, 2009), unlike human scalp follicles. Therefore, it is important to clarify whether human scalp follicles will also respond

to PGF<sub>2α</sub> and prostamide F<sub>2α</sub> analogues. In addition, there is no understanding of how these drugs actually cause the eyelash stimulation. It is unclear if this is due to direct effects on the eyelash follicles or indirectly via the vasculature by increasing the blood flow. The overall aim of this study was to investigate the hypothesis that PGF<sub>2α</sub> and prostamide F<sub>2α</sub> can affect human scalp hair follicle growth through PGF<sub>2α</sub> and/or prostamide F<sub>2α</sub> receptors located in the hair follicle itself. The initial objectives were to investigate the biological effects of PGF<sub>2α</sub> and a PGF<sub>2α</sub> analogue, latanoprost, on human scalp hair follicle growth in the absence of any blood supply *in vitro* using the hair follicle organ culture model. Isolated scalp hair follicles were grown in organ culture for 9 days in serum-free medium using different concentrations of PGF<sub>2α</sub> and latanoprost (isopropyl-(Z)-7[(1R,2R,3R,5S)3,5-dihydroxy-2-[(3R)-3-hydroxy-5-phenylpentyl]-cyclopentyl]-5-heptenoate). Initially experiments were carried out to determine which concentration would alter hair growth most significantly using PGF<sub>2α</sub> and latanoprost.

This organ culture study of isolated human scalp hair follicles was carried out for 9 days in serum-free medium with or without different concentrations of PGF<sub>2α</sub> and latanoprost using skin samples from 10 donors. Serum was excluded from the culture media, as it has an inhibitory effect on hair growth *in vitro* (Philpott *et al.*, 1996). Daily observation of hair bulb morphology, measurement of length and photography were carried out, a modification of the original technique which enables much more detail to be assessed (Philpot 1990).

Follicles were monitored for changes in morphology, as changes in hair follicle cycle stages are significant to hair growth *in vivo*, recorded as the number of follicles remaining in anagen. The daily increase in hair follicle length and the

overall amount of hair actually produced by all the follicles was also calculated from the final increase in length of each follicle on the final day, day 9, or the last day the follicle maintained a normal anagen morphology. At least 6 follicles were examined per person for each condition.

The next objective of this study was to clarify whether the  $\text{PGF}_{2\alpha}$  and latanoprost-stimulated growth was a receptor-mediated response after the most effective concentration for  $\text{PGF}_{2\alpha}$  and latanoprost was found. Therefore, the effect of two efficient FP antagonists, AS604872 (1  $\mu\text{M}$ ) and AL-8810 (10  $\mu\text{M}$ ) (Woodward *et al.*, 2007) on  $\text{PGF}_{2\alpha}$  and latanoprost-stimulated (100 nM) hair growth was investigated on follicles from 5 further individuals in the same manner. DMSO 0.01% was included in all media for these experiments since the FP antagonists had to be solubilised in DMSO.

Having established that human scalp hair follicles could respond to  $\text{PGF}_{2\alpha}$  and latanoprost by increased growth by a receptor-mediated manner in organ culture, i.e. in the absence of the blood supply, so the next aim was to establish the presence of the receptors in human scalp hair follicles. This stage of the investigation required familiarisation with hair follicle structure and learning the techniques of cryosectioning and staining. Deer skin was used first as it is easily obtainable and easier to work with than human skin due to the large size of the follicles. Later, human skin sections were prepared and stained with the histological stain, Saccpic.

To confirm the presence of FP in scalp hair follicle, the expression of FP proteins were investigated in human scalp anagen hair follicles, using immunohistochemistry.

Initially, the location of cytokeratins 5 & 6, a highly expressed proteins in the hair follicle outer root sheath (Hans-Jürgen *et al.*, 1987), in human skin and hair follicle were investigated by immunohistochemistry to learn the immunohistochemistry techniques with a highly expressed antigen.

Since the glaucoma drugs also darkened eyelashes (Reynolds *et al.*, 1998), the location of melanocytes was also determined in human scalp hair follicles by immunohistochemistry using a monoclonal primary antibody to NKI-beteb, melanoma associated antigen. The NKI-beteb antibody detects all melanocytes in the hair follicle (Staricco, 1963; Hayashibe *et al.*, 1986; Randall *et al.*, 2008).

To investigate the location of FP protein within the hair follicle, immunohistochemistry was performed using two polyclonal primary antibodies for human FP.

The next objective was to investigate the expression of genes for FP in human anagen scalp hair follicles using the molecular biological approach: reverse transcription-polymerase chain reaction (RT-PCR). This required designing specific forward and reverse primers for FP from the human FP gene sequence and synthesising cDNAs from 5 samples of microdissected anagen hair follicles; amplifying the gene for FP and confirming gene identity by the size of product bands on gel electrophoresis and gene product sequence analysis, using the NCBI BLAST programme to align the homology of the sequenced PCR products against the known human FP gene sequence. Three samples were used for the hair follicle components to localise the FP gene expression in hair follicle components, the dermal papilla, connective tissue sheath around the bulb, epithelial matrix, hair follicle “bulge” area and the follicle area between the “bulge” and the bulb; these were microdissected individually for the RT-PCR analysis. To increase the yield

from the isolated components 3 further sets of isolated hair follicle component's RNA was amplified prior to analysis.

A third aim of this study was to investigate the *in vivo* relevance of these *in vitro* experiments, therefore, the presence of prostanoid lipid mediators in scalp anagen hair follicles from 3 individuals was analysed, using quantitative lipidomic approaches. Electrospray tandem mass spectrometry coupled to liquid chromatography (LC/ESI-MS/MS) was used to investigate the presence of prostaglandins, dihydroprostaglandins and isoprostanes. These lipid mediators were selected as they had been reported previously expressed in other human tissues including myometrium (Masoodi and Nicolaou, 2006). A range of multiple reaction monitoring (MRM) transitions and optimum collision energies were used for each compound to detect and quantify the most abundant product ions from scalp anagen hair follicles.

Since PGE<sub>2</sub> was the most prevalent prostaglandin detected (with PGF<sub>2α</sub> next) and PGE<sub>2</sub> has been reported to cause re-growth of hair in mice (Torii *et al.*, 2002) and is produced by cultured rat vibrissae dermal papilla (Lachgar *et al.*, 1996a) and human dermal papilla cells (Michelet *et al.*, 1997); the presence of one of its receptors, EP<sub>2</sub>, was localised in the dermal papilla using immunohistochemistry. Therefore, to investigate the location of PGE<sub>2</sub> receptor (EP<sub>2</sub>) protein within the human hair follicles, immunohistochemistry was performed using a polyclonal primary antibody for human EP<sub>2</sub>.

The final aim of this study was to investigate whether bimatoprost itself can effect scalp hair follicle growth in organ culture. The bimatoprost (Z-7-[(1R,2R,3R,5S)-3,5-dihydroxy-2-[1E,3S)-3-hydroxy-5-phenyl-1-pentenyl]cyclopentyl]-5-N-ethylheptenamide) was donated by Dr Woodward of Allergan, California as a

personal favour to Professor V A Randall. The effects of this drug at different concentrations (10, 100, 1000 nM) on isolated hair follicles in organ culture was also investigated as described previously to determine which, if any, concentration would alter hair growth most significantly. These concentrations were selected to concur with the saturation of a receptor-mediated effect as reported in other tissues (Sharif *et al.*, 1999; Liang *et al.*, 2003; Woodward *et al.*, 2003).

To clarify whether the bimatoprost-stimulated growth was a receptor-mediated response after the most effective concentration for bimatoprost (100 nM) was found, the effect of a prostamide  $F_{2\alpha}$  receptor antagonist, AGN211336, and an FP antagonist, AS604872, on bimatoprost-stimulated hair growth in organ culture was also investigated on follicles from 5 further individuals.

To confirm and localise the expression of prostamide  $F_{2\alpha}$  receptors in scalp hair follicles, the expression of prostamide  $F_{2\alpha}$  receptor genes in isolated scalp hair follicle and hair follicle components was investigated by molecular biological methods as described for FP. Prostamide  $F_{2\alpha}$  receptor genes are alternative splicing variants of the FP gene such as FP variant 4 which appears to heterodimerise with FP to create a bimatoprost-sensitive receptor (Liang *et al.*, 2008). The detection of prostamide  $F_{2\alpha}$  receptor genes was carried out using specific primers for FP splice variants including one which detected FP, all 5 known splice variants and 5 pairs for the 5 different FP splice variants. Primers for FP variant4 (altFP4) and FP variant1 (altFP1) were newly designed from human gene sequence; the others were from Liang *et al* (2008).



## **2 Materials and Methods**

### **2.1 Histological and immunohistological staining of human and red deer hair follicles**

#### **2.1.1 Tissue samples**

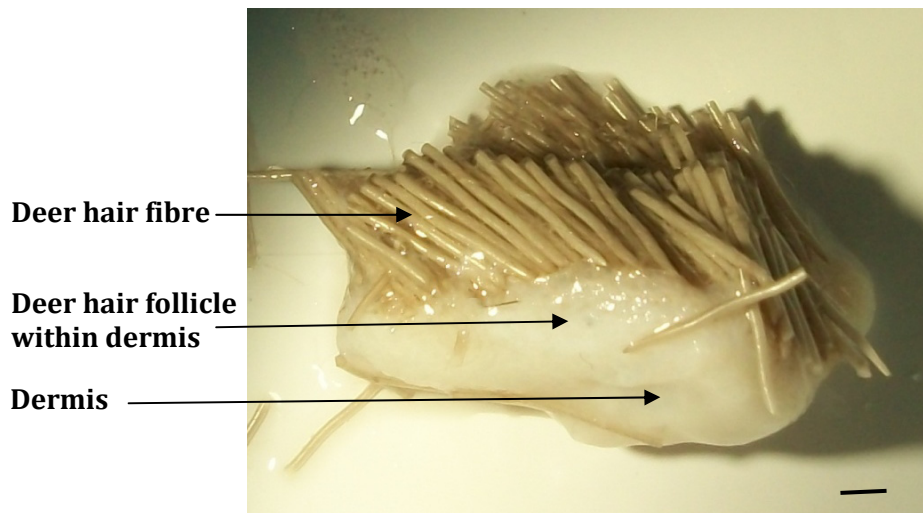
##### **2.1.1.1 Deer skin**

Red deer skin samples were collected as waste products from healthy animals routinely bred and harvested for food in Yorkshire. They were collected during October when the hair follicles were in anagen from the neck/mane region of young male adults, ranging from 12 to 18 months old. Collection medium was prepared prior to the abattoir visit. It consisted of RPMI 1640 supplemented with: 10% fetal calf serum, 10 units/ml penicillin, 100µg/ml streptomycin, 100 ng/ml fungizone (amphotericin B), and 2mM L-glutamate (Gibco, Paisley, UK); the collection medium was aliquoted into 50ml Falcon tubes (Greiner Bio-One Ltd, Gloucestershire, UK) and pre-cooled on ice (4°C).

Skin samples were collected shortly after death, dissected into strips, cleaned of extra fat tissue and the long hairs trimmed using a sterile blade before transfer to labelled tubes of collection medium. The tubes were stored on ice for the duration of transportation, and once at the university the samples were washed thoroughly in sterile PBS to remove all traces of cell debris and blood. Samples for histology were dissected into 1cm<sup>2</sup> pieces (Figure 12), washed thoroughly in sterile phosphate buffered saline (PBS; appendix 6.2) and placed individually into 1.5 ml sterile plastic vials (Sarstedt, Nümbrecht, Germany) containing the cryoprotectant Sakura Tissue-Tek O.C.T™ (Raymond A Lamb Ltd, Sussex, UK) and stored at -80°C until used.

### **Figure 12 Deer skin sample**

A piece of deer neck skin sample of approximately 1cm<sup>2</sup>, showing the hair fibre, dermis and hair follicle inside dermis. Photographed on a dissecting microscope (Leica MZ8, Leica, Germany) using a Nikon Coolpix4500 (Nikon E4500) digital camera (Scale bar=1mm).

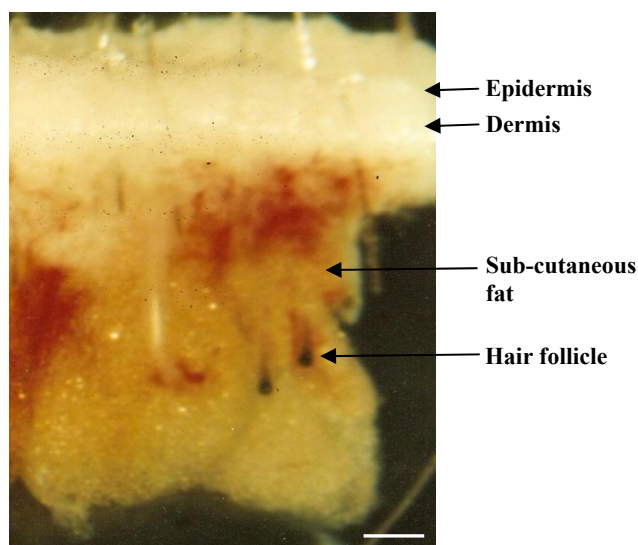


#### **2.1.1.2 Human skin**

Human scalp skin samples were obtained from non-balding areas (occipital and temporal regions) of healthy donors (26-48 years) undergoing elective cosmetic surgery with ethical approval and written donor consent. Samples were placed in collection medium RPMI as described earlier (2.1.1.1) and kept on ice until return to the university and then dissected into 1cm<sup>2</sup> pieces (Figure 13), washed thoroughly in sterile PBS and stored in O.C.T<sup>TM</sup> at -80°C until further use.

### Figure 13 Human skin sample

A human temporal region skin piece of approximately 1cm<sup>2</sup> photographed on light dissecting microscope (Leica MZ8, Leica, Germany) using a Nikon Coolpix4500 (Nikon E4500) digital camera (Scale bar=0.5mm).



#### 2.1.2 Preparation of poly-l-lysine coated slides

To help sections to adhere to twin-frost glass slides (76 x 26 x 1 mm; BDH, Lutterworth, UK), the slides were cleaned and coated in poly-l-lysine (Sigma-Aldrich Ltd, Dorset, UK). The slides were placed individually into a plastic slide carrier, before cleaning in pyrogen detergent (Diversey Lever Ltd, Northampton, UK) and distilled water for 20 minutes. To wash out traces of detergent the slides were rinsed thoroughly in distilled water then immersed in absolute ethanol (Sigma-Aldrich Ltd, Dorset, UK) for 5 minutes. The slides were allowed to dry in the drying cabinet at 60 °C, before being immersed in 10% (v/v) poly-l-lysine in distilled water for 5 minutes. Once dry, the slides were stored in the original box and kept at room temperature until required.

### **2.1.3 Tissue sectioning**

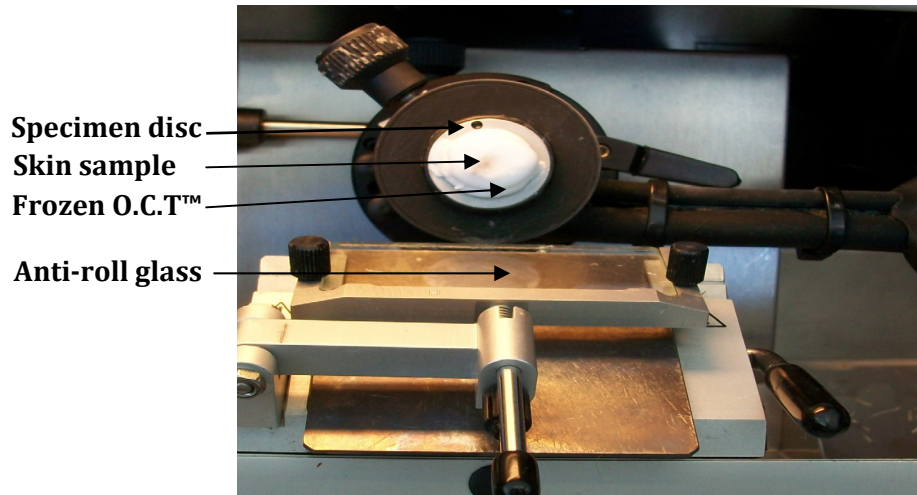
The skin samples were removed from -80°C and sections were prepared using the Leica CM 1800 Cryostat (Leica, Germany). O.C.T™ was applied to the small, round, specimen disc to form an even disc, ensuring all bubbles were removed and placed in the cryostat set at -27°C to freeze solid. The frozen O.C.T™ disc was then placed into the sample holder of the cryostat and sliced until level. A small cubic piece of the skin sample (~0.5cm<sup>2</sup>) was placed onto the O.C.T™ disc on its side to ensure the blade cut through the dermis and fat simultaneously and therefore cut smoothly; it was orientated so that longitudinal hair follicle sections could be obtained (Figure 14). Then O.C.T™ was gradually applied all around the sample until it was no longer visible, and allowed to freeze solid. Sections (5µm) were cut at -23 °C and mounted on to labelled poly-l-lysine coated slides at room temperature, then checked under the light microscope, placed into labelled slide carrier wrapped with foil and kept at -20°C until use for histological or immunohistological analysis.

### **2.1.4 Histological study of skin and hair follicle structure using Sacpic staining**

Frozen deer and human skin sections were stained with the Sacpic staining technique, which is a histochemical staining procedure employing different dyes to distinguish the different components of the hair follicle and skin. The method used was adapted from Nutbrown and Randall (1996) and Nixon (1993). The preparation of the stains is given in appendix 6.1. Frozen skin sections were left at room temperature for about 30 minutes to defrost gradually to prevent the tissue getting temperature shock, before being placed into ice cold acetone (Fisher Scientific, Loughborough, UK) for 15 minutes to fix the proteins; this was followed

#### **Figure 14 Mounted skin sample on the cryostat machine**

Mounted skin sample on the Leica CM 1800 cryostat (Leica) photographed using a Nikon Coolpix4500 (Nikon E4500) digital camera.



by two rinses in distilled water. The sections were immersed in celestine blue staining solution for 5 minutes then rinsed in tap water before placing in Gill's haematoxylin for 5 minutes and a further rinse in tap water. The sections were blued in Scott's tap water for 2 minutes and rinsed in tap water before staining in 2% safranin for 5 minutes. The sections were then immersed for 1 minute in each of the following: tap water, 70% ethanol and 95% ethanol to become dehydrated. The slides were differentiated in absolute picric acid/ethanol for 3 minutes before placing in 95% ethanol, 70% ethanol and tap water for 1 minute each, to rehydrate the sections. After staining in picro-indigo carmine for 1 minute and rinsing in tap water, the sections were dehydrated in ascending ethanol solutions 70%, 95% and absolute ethanol for 5 minutes each. The sections were cleared by placing in histoclear:ethanol (50:50 v/v), and absolute histoclear (National Diagnostics, Hull, UK) for 4 minutes at a time before mounting using coverslips (VWR International, Leicester, UK) and histomount (VWR International).

### **2.1.5 Immunohistochemical studies**

Immunohistochemistry was carried out to study expression and localisation of protein to a number of markers of skin and hair follicles. The technique was carried out several times to establish the optimum concentrations of the primary antibodies which needed to be high enough to produce sufficient staining, and low enough to reduce background staining and cost. The concentration of the blocking and diluting solutions of mouse and goat serum (Sigma-Aldrich Ltd) were also optimised. All the incubations were carried out in a histology wet box to prevent evaporation, at room temperature (25°C) apart from the primary antibodies which were incubated at 4°C for 18 hours.

#### **2.1.5.1 Immunohistochemical localisation of cytokeratins 5 & 6**

Human skin sections were immunostained with cytokeratins 5 & 6 which is a marker for the outer root sheath of the hair follicle. Longitudinal (5µm) sections of human hair follicle (as described in section 2.1.3) which were mounted to poly-l-lysine coated slides (as described in section 2.1.2) were air dried at room temperature for 30 min. The sections were then fixed in ice cold (4°C) acetone for 10 minutes to fix the proteins, followed by 3 washes in sterile PBS. The sections were circled with a Vector ImmEdge Pen (Vector Laboratories, Peterborough, UK) to produce a hydrophobic ring around the sections and therefore reduce the volume of antibody needing to be applied. The sections were incubated with 0.3% (v/v) hydrogen peroxide (Sigma-Aldrich Ltd, Dorset, UK) in methanol (Fisher Scientific, Loughborough, UK) for 30 minutes to block endogenous peroxidase activity and rinsed in PBS for 5 minutes. Incubation with normal mouse serum (5% v/v) (Sigma-Aldridge Ltd) in PBS for 20 minutes blocked potential non-

specific binding (Serum must be from the host of the secondary antibody) (Ramos-Vara, 2005); excess serum was blotted away from the sections and followed by 2 washes in sterile PBS. The sections were incubated with the primary antibody, goat polyclonal anti-cytokeratins 5 & 6 antibody (SantaCruz Biotechnology, INC, California, USA) for 18 hours at 4°C. The antibody was diluted 1:50 with 1.5% (v/v) mouse serum in PBS (Sigma-Aldrich Ltd). The sections were washed in PBS twice for 10 minutes to remove excess primary antibody. Goat ExtrAvidin® Peroxidase Staining Kit (Sigma-Aldrich Ltd) was used to detect the primary antibody. The sections were incubated with mouse monoclonal anti-goat IgG biotin conjugate secondary antibody (from Goat ExtrAvidin® Peroxidase Staining Kit-Product code EXTRA-1, Sigma-Aldrich Ltd) to detect the goat antigens, for 30 minutes then washed in PBS twice for 10 minutes. The sections were incubated with ExtrAvidin-Peroxidase (from kit) for 30 minutes, followed by two 10 minute washes in PBS.

The peroxidase substrate 3-amino-9-ethylcarbazole (AEC; Vector Laboratories, Peterborough, UK) visualised antibody binding. The reaction of AEC substrate with the peroxidase enzyme produces a red-brown chromogen; this reaction was monitored under the light microscope and when sufficient colour had developed the reaction was halted by placing the slides in distilled water. To enable the clear definition of tissue structure, the sections were counter stained with Harris's haematoxylin for 30 seconds and rinsed in tap water for 3 minutes. The sections were then blued in Scott's tap water for 5 minutes and finally rinsed in tap water for 3 minutes before being mounted with aqueous mountant, Aquamount (VWR International, Leicester, UK); they were left to dry overnight before clear nail

varnish (Laval, UK) was applied around the edges of the coverslips to prevent evaporation of the aquamount.

To ensure no non-specific binding was occurring, each time the procedure was carried out negative controls were also conducted. The negative controls were:

1. 1.5% NMS + secondary antibody + Chromogen system

Initially, the primary antibody was excluded and replaced with 1.5% normal mouse serum to check that the secondary antibody was not binding non-specifically to the tissue without the presence of the primary antibody. The AEC solution was added to detect any non-specifically bound secondary antibody.

2. Primary antibody + PBS + Chromogen system

In this control the secondary antibody was excluded and replaced with PBS; this checked that the primary antibody was not activating the AEC solution without the existence of the secondary antibody.

3. 1.5% NMS + PBS + Chromogen system

In the third control, both the primary and secondary antibodies were also replaced with 1.5% normal mouse serum and PBS respectively. This checked that the blocking procedure had been successful and there was no endogenous peroxidase activity left in the tissue which could activate the AEC.

#### **2.1.5.2 Localisation of melanoma-associated antigen, NKI-beteb, in human hair follicles**

Melanocytes were localised in the human hair follicle bulb by immunohistochemistry using an antibody to human melanoma associated antigen, NKI-beteb. Immunostaining of human hair follicles with NKI-beteb was carried out using the procedure described in section 2.1.5.1. However, a mouse monoclonal anti-human NKI-beteb primary antibody (Hycult biotechnology, Uden, Netherland)



was incubated with sections at a dilution of 1:10 and 1:30 with 1% (v/v) normal goat serum in PBS at 4°C for 18 hours. To block non-specific binding the sections were incubated with 10% goat serum for 1 hour at room temperature prior to antibody application and a goat anti-mouse IgG secondary antibody kit was used to detect the primary antibody (Dako LSAB2® system kit, Dako, Cambridge, UK).

#### **2.1.5.3 Localisation of PGF<sub>2α</sub> receptor (FP) in human hair follicles by immunohistochemistry**

In order to investigate whether FP protein was present in human hair follicles, immunostaining of scalp hair follicle sections from five individuals (3 men and 2 women aged between 38-55) was performed using two polyclonal primary antibodies to the FP; these were called PGF<sub>2α</sub>R (N-18; sc-33363) and (T-15; sc-46449) (Santa Cruz Biotechnology, INC). The immunohistochemistry technique used to detect the FP was other wise as described in section 2.1.5.1. These polyclonal antibodies against the FP were the only types commercially available and had not previously been used for immunostaining of human tissues and therefore had to be optimised. The goat polyclonal anti-human FP antibodies were incubated with human hair follicle sections at a dilution of 1:75 with 1.5% (v/v) normal mouse serum which considered optimal; at 4°C for 18 hours.

#### **2.1.5.4 Localisation of PGE<sub>2</sub> receptor (EP<sub>2</sub>) expression in human hair follicles**

To investigate the expression of EP<sub>2</sub> protein in human hair follicles immunohistochemistry carried out on scalp hair follicle sections from five individuals (same samples used in section 2.1.5.3). Immunostaining was performed using a polyclonal primary antibody to the EP<sub>2</sub> (Santa Cruz Biotechnology, INC); the technique was other wise the same as that for

cytokeratins 5 & 6 as described in section 2.1.5.1. The antibody for the EP<sub>2</sub> was also optimised as it had not previously been used for immunostaining human tissues. The goat polyclonal anti-human EP<sub>2</sub> antibody was incubated with human hair follicle sections at a dilution of 1:100 with 1.5% (v/v) normal mouse serum which considered optimal; at 4°C for 18 hours.

### **2.1.6 Visualising the staining**

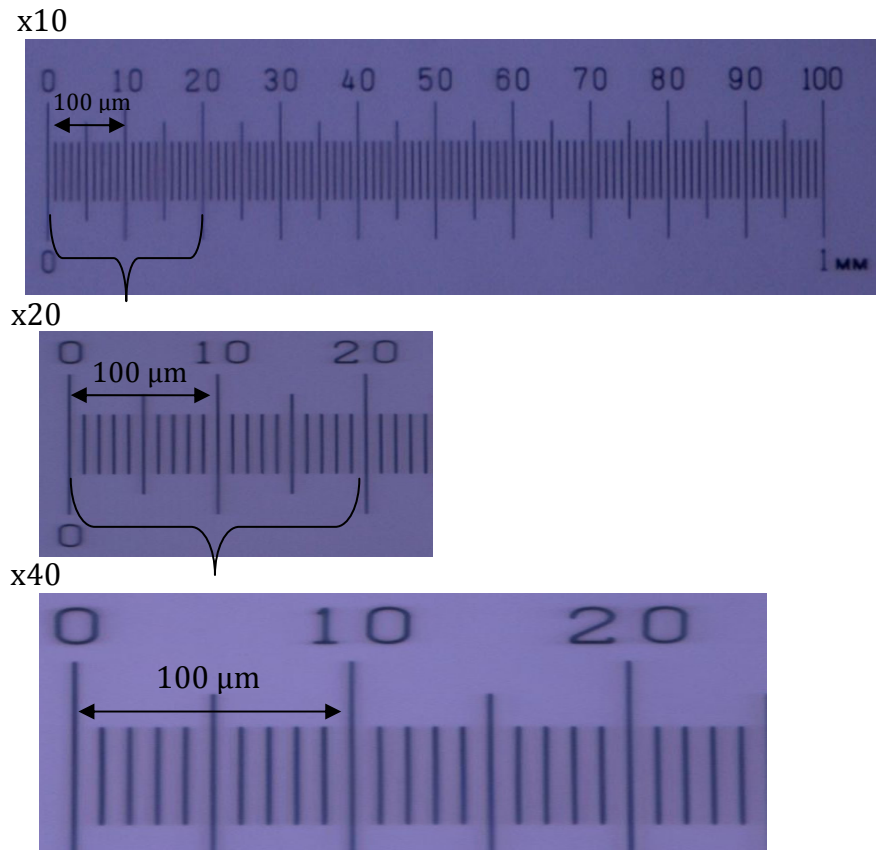
The immunohistochemistry stained sections were examined and photographs were captured using an Nikon Eclipse 80i microscope with a Nikon ACT-2U photographic system (Nikon, Surrey, UK). The Saccpic stained sections were photographed using a Nikon Coolpix4500 (Nikon E4500) digital camera fixed on an Ortholux II light microscope (Leitz, Germany) and the images were downloaded using Nikon View 5 software. The pictures were measured and measurements were converted to mm using a stage micrometer (Figure 15).

## **2.2 Detection of gene expression in human hair follicles by reverse transcription - polymerase chain reaction (RT-PCR)**

Amplification of a specific region of template DNA can be achieved by PCR. The template can include genomic, plasmid and phage DNA or RNA converted to complementary DNA (cDNA) (Cha and Thilly, 1995). Investigating mRNA expression has great advantage as it indicates the genes expressed in the cell or tissue from which RNA was extracted. cDNA can be synthesised from mRNA by the enzyme reverse transcriptase which is used alongside oligo (dT) primers that bind to the poly (A) tail of mRNA. To identify specific DNA sequences, the cDNA is then

### Figure 15 Stage micrometer

A stage micrometer, photographed on the Orthodox II light microscope (Leitz, Germany) using a Nikon Coolpix4500 (Nikon E4500) digital camera.



applied in the PCR reaction, indicating whether genes are actively expressed in the cell or tissue at the time of RNA extraction (Kawasaki, 1990).

Amplification of a target DNA sequence by PCR requires specific forward and reverse primers which should be carefully designed to be complementary to the regions bordering the target DNA sequence. The specific forward and reverse primers anneal to either end of the target DNA sequence and they run in opposite directions to each other, spanning the entire target DNA region for amplification. Thermostable Taq DNA polymerase, buffers and a mixture of deoxynucleotide triphosphates (dNTPs), which contain the four bases, are required for synthesis of

new DNA strands in a PCR reaction alongside with the template DNA and specific forward and reverse primers.

To allow DNA amplification to occur, the PCR reaction mixture is exposed to cycles of specific set temperatures using PCR thermocycler. Firstly, a high temperature is used to denature the DNA template, and if double stranded, separates them. In order to allow the oligonucleotide primers to anneal to the complementary single-stranded target DNA sequence after denaturation, the temperature is then lowered and this annealing temperature is critical and depends on the primer set used. Generally it is a few degrees below the average melting temperature of the primers, determined from the base composition of the oligonucleotides. The annealing temperature must be perfectly adjusted and must not be too high to allow efficient annealing of the primer, or too low to minimise non-specific binding. Eventually the temperature is raised to allow Taq DNA polymerase to extend the annealed oligonucleotide primers at 72-74°C, which is the optimal temperature for the enzyme. As a result of the PCR cycles a new strand of DNA will be produced, if cDNA is used as a template, or it will produce two new strands of DNA when double stranded DNA is used as a template. This cycle of temperatures is repeated between 25-40 times and the amplified products from each PCR cycle act as a template for the next cycle, so that there is a significant rise in the number of target DNA sequences (McPherson and Moller, 2000).

The concentration of  $MgCl_2$  salt is critical in the PCR reaction mix and can affect the activity of DNA polymerase, which in turn can affect yield and primer annealing, which can affect specificity (Cha and Thilly, 1995). Mismatches in primer hybridisation may occur resulting in undesired amplicons when the  $MgCl_2$

concentration is too high, however, if it is too low a lower yield of amplification occurs.

### **2.2.1 Investigations into whether human hair follicles express the genes for prostaglandin and prostamide F<sub>2α</sub> receptors using RT-PCR**

In order to investigate the expression of PGF<sub>2α</sub> receptor (FP) and prostamide F<sub>2α</sub> receptor (FP-variant complexes (altFPs)) genes in human hair follicles, RT-PCR was performed. The gene expression for specific molecules can be identified using PCR, which amplifies a specific region of template DNA that can include genomic, plasmid and phage DNA or can be from RNA transformed to complementary DNA (cDNA) using reverse transcriptase (RT). Investigating mRNA expression reveals the genes expressed in the cell or tissue from which the RNA was extracted (Cha and Thilly, 1995).

Specific forward and reverse primers for the PGF<sub>2α</sub> receptor (FP) and prostamide F<sub>2α</sub> receptors, altFP1 and altFP4, were carefully designed from the human FP gene sequence (Section 2.2.1.6); all other primers used were obtained from published sources (Liang *et al* 2008, Shorter *et al* 2008). Taq DNA polymerase, buffers, MgCl<sub>2</sub> and a mixture of deoxynucleotide triphosphates (dNTPs) containing the four bases as well as the template DNA and specific forward and reverse primers were required for synthesis of new DNA strands in a PCR reaction. The PCR thermocycler was used to amplify the DNA sequence. A control gene, β-actin, was first used to check the quality of the cDNA samples and the PCR system. The gene expression of the FP and FP splice variants (altFPs) was investigated in samples of isolated hair follicles from 10 men (33-46 years). To localise the gene expression in the scalp hair follicle, the process was repeated using cDNA from isolated hair follicle components: the dermal papilla, the dermal sheath around the bulb, the

bulb matrix, the follicle at the level of the bulge area and the lower follicle between the bulb and the bulge. These were isolated separately from follicles from 2 men aged 39, 42 and a woman aged 48. For detection of gene expression in amplified RNA from scalp hair follicle components due to the limited sample size, the same components were microdissected from scalp hair follicles from a further 3 men, aged 30, 41 and 45, and their mRNAs were amplified before cDNA synthesis.

To prevent genomic contamination, all work areas were cleaned thoroughly with 70% ethanol and RNase Zap solution (Sigma-Aldrich Ltd) prior to undertaking any procedure, and gloves were worn and changed frequently.

#### **2.2.1.1 Tissue collection**

Human skin samples from occipital regions of scalp (non-balding) were gathered as described in section 2.1.1.2, with the exception that the skin samples were placed into 50ml falcon tubes that contained 30ml RNA stabilisation solution, *RNAlater*<sup>TM</sup>, to preserve the tissue by inhibiting RNases (Sigma-Aldrich Ltd). The tubes were labelled with the patient's age and gender and accompanied by an information sheet including the date of sample collection, sample site, gender and age of donor. The tubes were kept on ice until brought to the university and then transferred to the fridge (4°C) overnight to allow the *RNAlater*<sup>TM</sup> to penetrate the tissue. After 24 hours the tubes were stored in the freezer (-80°C) until needed.

#### **2.2.1.2 Hair follicle microdissection**

A Leica MZ8 (Leica, Germany) dissecting microscope was used at x20-30 magnification to dissect individual hair follicles from the skin samples using autoclaved dissection tools and sterile plastic-ware. Initially the frozen skin samples in *RNAlater*<sup>TM</sup> were defrosted on ice then transferred to a petri dish

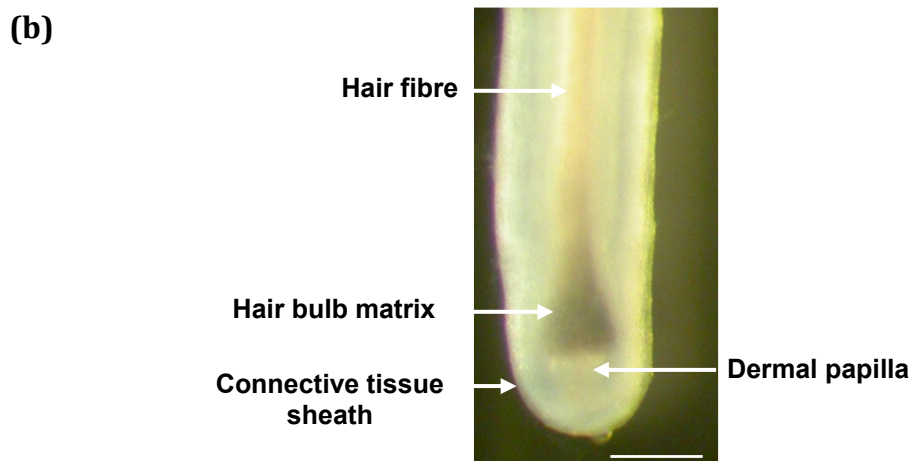
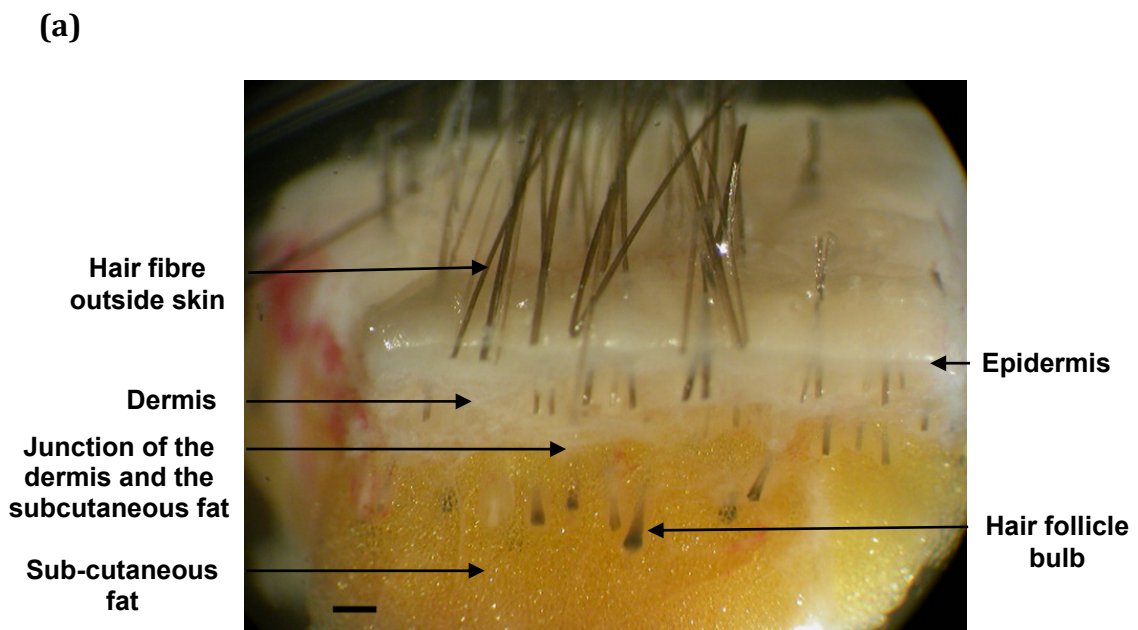
(35x10mm) containing cold (4°C) *RNAlater*<sup>TM</sup> to ensure the skin remained at a low temperature. Then the skin sample inside the petri dish was placed under the dissecting microscope and the skin was cut at the junction of dermis and subcutaneous fat (Figure 16a) using a sterile scalpel blade. Fine forceps (size 5 and 7) were used to pluck the follicles out from the skin by gently grasping the outer root sheath and then the dissected follicle was transferred to a fresh dish of *RNAlater*<sup>TM</sup> on ice. Under a higher magnification (x50) the freshly isolated follicles were cleaned of any dermis or fat debris (Figure 16b) using syringe needles (27G1/2 tuberculin syringe; Sigma) before transfer to a 1.5ml Eppendorf containing 150 µl *RNAlater*<sup>TM</sup> placed on ice. A total of 65 hair follicles were isolated from each donor for hair follicle total RNA isolation.

### Figure 16 Isolation of hair follicles from human scalp skin

The skin samples which were collected in *RNAlater* and kept at 4°C overnight were cut into small sections (a) to promote conspicuousness of hair follicles and individual lower follicles were microdissected (b), which were then cleaned to remove any dermis and subcutaneous fat using syringe needles. Photographed on a dissecting microscope (Leica MZ8, Leica, Germany) using a Nikon Coolpix4500 (Nikon E4500) digital camera.

**(a)** Human scalp skin showing hair follicle and skin layers, epidermis, dermis and subcutaneous fat. Scale bar = 400  $\mu$ m

**(b)** Isolated hair follicle, demonstrating lower follicle parts including hair fibre, hair matrix, dermal papilla and connective tissue sheath. Scale bar = 200  $\mu$ m





### **2.2.1.3 Microdissection of human hair follicle components**

To localise the FP and FP-variant complexes (altFPs) gene expression in the scalp hair follicle, hair follicle components: the dermal papilla, the dermal sheath around the bulb, the bulb matrix, the follicle at the level of the bulge area and the lower follicle between the bulb and the bulge, were microdissected from isolated whole follicles under the Leica MZ8 (Leica) dissecting microscope (x40-60 magnification). The follicles were harder to dissect than fresh tissue because they had been kept in the preservative solution, *RNAlater*<sup>TM</sup>.

#### **2.2.1.3.1 Experiment to determine follicle area including the bulge**

The sebaceous gland cannot be seen in tissues which had been kept in *RNAlater*<sup>TM</sup>, therefore, a small experiment was carried out to detect the sebaceous gland and then the area including the follicle bulge. The distance of the top of sebaceous gland from the skin surface and the bottom of sebaceous gland from the bottom of the follicle bulb were measured in 10 follicles from a fresh human scalp skin sample using a dissecting microscope (Leica MZ8) fitted with an eyepiece graticule. The measurement values were converted to mm using a stage micrometer and the average measurements worked out.

The skin samples which were in *RNAlater* (Figure 16a) were first measured under the dissecting microscope using the data obtained from the experiment mentioned earlier. The hair follicle was cut at both the upper and lower level of sebaceous gland and this follicle area was microdissected out from the skin using fine tweezers (size 5) and collected in an Eppendorf tube containing cold *RNAlater*<sup>TM</sup>. This was then used as the hair follicle bulge area, as the bulge area is located in the follicle outer root sheath below the sebaceous gland level (Ohyama, 2007; Waters

et al., 2007). The remaining hair follicle was microdissected further to isolate the other hair follicle components.

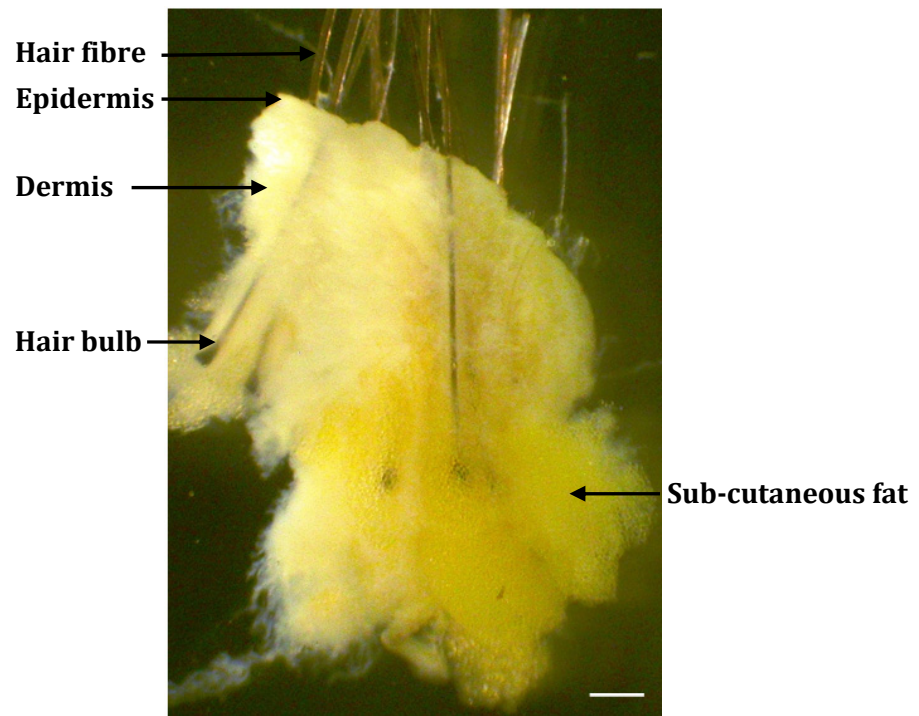
#### **2.2.1.3.2 Microdissection procedure to isolate human follicle components**

The skin piece which contained follicles below the sebaceous gland level was cut at the junction of the dermis and the subcutaneous fat to get the hair follicle bulb and the lower follicle area (Figure 17a). The follicles were plucked out from the skin by gently grasping the outer root sheath using fine forceps (size 5 and 7) and the isolated follicles were transferred to a fresh dish of *RNAlater*<sup>TM</sup> for further microdissections. Under a higher magnification (X50) the isolated hair follicles were dissected to separate the individual follicle's "bulge" region and lower follicle part (Figure 17b, c) from the bulb (Figure 17d); the isolated follicle bulbs were transferred to a fresh dish of *RNAlater*<sup>TM</sup> for further microdissections of follicle bulb components using sterile syringe needles (27G<sup>1</sup>/2 tuberculin syringe). The side of the connective tissue sheath was cut to avoid damaging the dermal papilla, and then the connective tissue sheath inverted to expose the matrix with dermal papilla. The matrix was gently pushed out (Figure 17e) and separated from the dermal papilla and the connective tissue sheath (Figure 17f) before collecting in an Eppendorf tube containing 150µl *RNAlater*<sup>TM</sup> left on ice. The dermal papillae were separated from the connective tissue sheath (Figure 17g) by cutting through the dermal papilla stalk and they were cleaned from any remains of connective tissue sheath then both dermal papilla (Figure 17h) and connective tissue sheath were collected in different Eppendorf tubes containing 150µl *RNAlater*<sup>TM</sup>. The microdissection continued until a total of 125 of each hair follicle component was obtained.

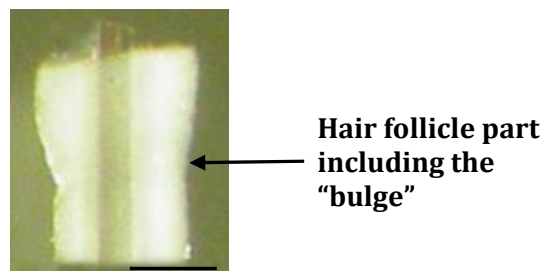
**Figure 17 Micro-dissection of hair follicle components: the dermal papilla, the dermal sheath around the bulb, the bulb matrix, the follicle at the level of the bulge area and the lower follicle between the bulb and the bulge**

- (a)** Human scalp skin showing hair follicle and skin layers, epidermis, dermis and subcutaneous fat. Scale bar = 400µm
- (b)** The hair follicle part including the bulge.  
Scale bar = 100µm
- (c)** Lower hair follicle part between sebaceous gland and hair bulb.  
Scale bar = 500µm
- (d)** Isolated hair follicle bulb, demonstrating hair follicle matrix, dermal papilla and connective tissue sheath. Scale bar = 200µm
- (e)** Isolated hair matrix. Scale bar = 200µm
- (f)** Connective tissue sheath of hair bulb and dermal papilla is still inside the sheath. Scale bar = 200µm
- (g)** The dermal papilla and the connective tissue sheath were separated. A small part of connective tissue sheath was left over on the dermal papilla which had to be removed. Scale bar = 200µm
- (h)** Isolated and cleaned dermal papilla. Scale bar = 100µm

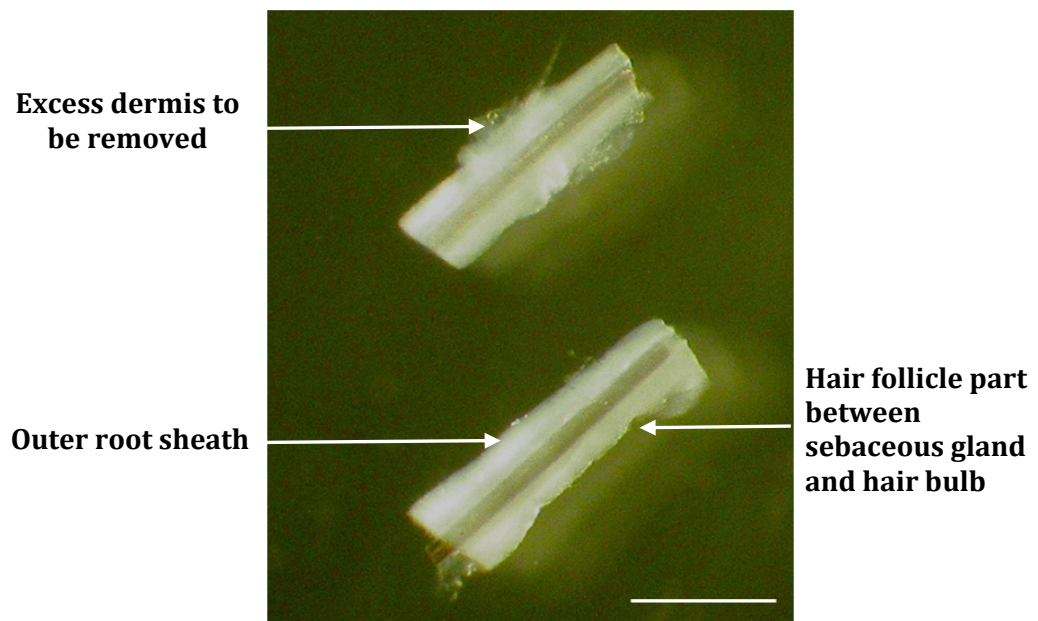
**(a)**



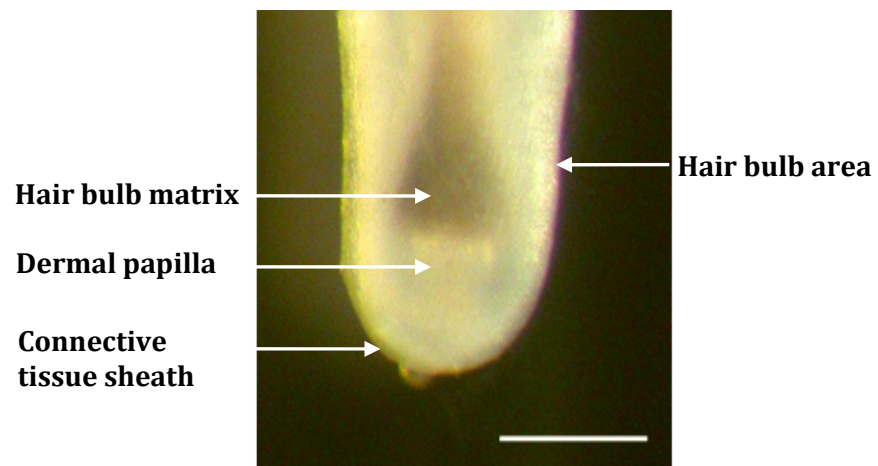
**(b)**



**(c)**

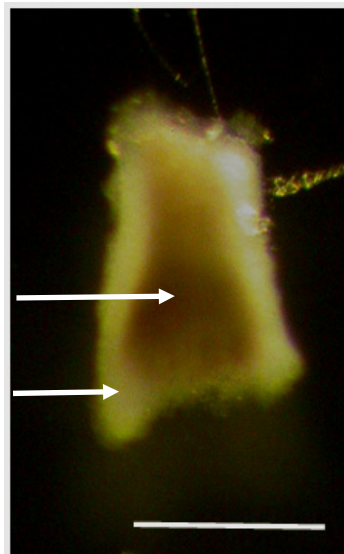


**(d)**



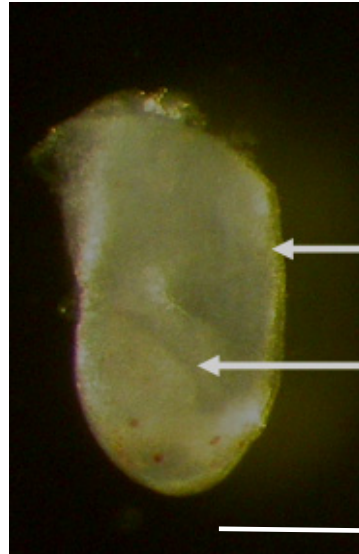
**(e)**

**Pigmented  
hair matrix**  
**Unpigment-  
ed hair  
matrix**



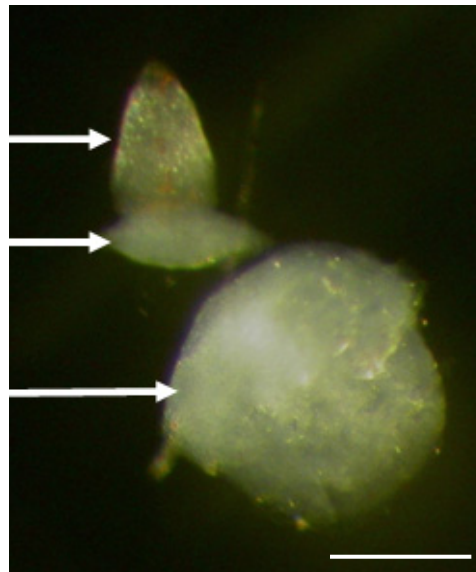
**(f)**

**Connective  
tissue sheath**  
**Dermal papilla  
inside the  
sheath**

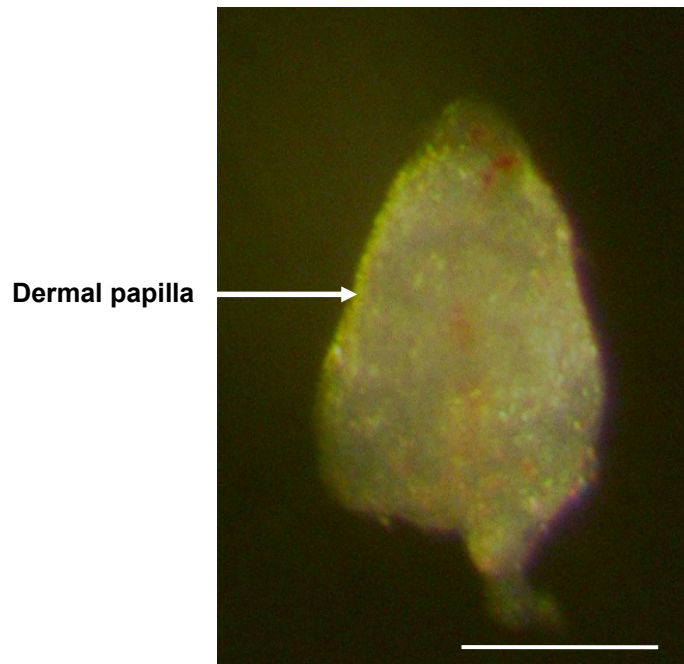


**(g)**

**Dermal papilla**  
**Excess connective  
tissue sheath  
to be removed**  
**Connective  
tissue sheath**



**(h)**



#### **2.2.1.4 RNA isolation, DNase treatment and cDNA synthesis**

When dissection of the required number of hair follicles was completed, total RNA was isolated, checked for quality, purity and concentration using agarose gel-electrophoresis and spectrophotometry respectively. Further purification was carried out to isolate poly(A)<sup>+</sup>RNA followed by DNase treatment to remove any contaminating DNA from isolated poly(A)<sup>+</sup>RNA samples; then they were converted to single stranded cDNA using the Avian Myeloblastosis Virus (AMV) reverse transcription system ready for PCR amplification.

##### **2.2.1.4.1 Total RNA extraction**

Total RNA was extracted using a GenElute Mammalian Total RNA kit (Sigma-Aldrich Ltd) in accordance with the manufacturer's instructions provided with the kit. The microdissected hair follicles and hair follicle components from each individual were transferred separately into glass homogenisers with 500µl lysis

solution and 5µl 2-mercaptoethanol solution. Each sample was homogenised for about 10 minutes until no visible pieces remained and the homogenate was then transferred to a GenElute filtration column and centrifuged (Eppendorf 5415 R) at 13000x g for 2 minutes to remove all cellular debris and to shear the DNA. After centrifugation, the filtration column was discarded, and an equal volume of 70% ethanol (made using 0.05% (v/v) DEPC treated water) was added to the filtered lysate and mixed thoroughly by vortexing.

The lysate/ethanol mixture (700 µl) was then transferred to a clear GenElute binding column and centrifuged for 15 seconds at 13000x g to bind RNA to the column. The flow through was then discarded, and the binding column with the bound total RNA moved back to the collection tube. The remaining sample was added to the binding column, and the same procedure repeated. The binding column was then transferred to a new collection tube.

To wash the binding column, 500 µl of wash solution 1 was added to the binding column and centrifuged for 15 seconds. The column was transferred to a new collection tube and a second wash carried out by adding 500 µl of wash solution 2 to the binding column and centrifuging for 15 seconds, the flow-through was discarded. The binding column was placed back into the collection tube. To remove ethanol and dry the column, a third wash was carried out by the addition of a second 500 µl of wash solution 2, centrifuged for 2 minutes and the column was transferred to a new collection tube. To elute the RNA from the binding column, 50 µl of Elution Solution was added to the centre of the binding column and centrifuged for 1 minute. To elute all RNA bound to the column, a second 50 µl of Elution Solution was added to the centre of the column and centrifuged for 1 minute. The flow through containing the purified total RNA was collected, and



could be used immediately for quality, purity and concentration checking and then poly(A)<sup>+</sup>RNA extraction, or stored at -80°C until used.

#### **2.2.1.4.2 Agarose gel electrophoresis**

To check the quality of the extracted total RNA samples, agarose gel electrophoresis were carried out using 1.5% (w/v) agarose gel. Agarose (1.5 g; Invitrogen Ltd) was dissolved in 100 ml of 1X tris-acetate-EDTA (TAE) buffer by using a 950 W microwave (Proline Microchef ST44) with sporadic swirling of the mixture until the boiling point (~135 sec). The molten agarose was left at room temperature to cool down to approximately 50-55°C before the addition of 25µl ethidium bromide (1 mg/ml; Sigma-Aldrich Ltd). The gel was immediately poured into plastic gel trays containing gel combs to form wells, and left for approximately 45 minutes to set. After the gel set, the gel combs were removed gently and the gel, which was still in the tray, was placed in the electrophoresis tank containing 300 µl 1X TAE buffer with 75 µl 0.5 µg/ml ethidium bromide. A 10 µl aliquot from the total RNA was mixed with 2 µl of blue/orange 6X loading dye in a ratio of 5:1 (Promega, Southampton, UK) to assist loading and monitor the progression of the total RNA through the gel during electrophoresis; then carefully loaded into the gel. The tank was set to run at 100 volts for approximately 30 minutes. The UVitec gel documentation system (UVItec Limited, Cambridge, UK) was used to visualise total RNA at 312nm wavelength and the images were captured and stored on the computer.

#### **2.2.1.4.3 Spectrophotometric analysis**

The concentrations of the total RNA samples were checked spectrophotometrically. The spectrophotometer (Ultrospec II, Cambridge, UK) was

calibrated first using 400µl nuclease free water in a quartz cuvette. The RNA sample, 20µl was mixed with 380µl of nuclease free water in another quartz cuvette by pipetting up and down, placed in the spectrophotometer and the absorbance reading recorded both at 260 nm and 280 nm wavelengths. The blank cuvette was used to calibrate the spectrophotometer to zero between the readings.

The concentration of RNA in µg/ml was calculated as follows:

Concentration of RNA =  $X \times Y \times 40$  µg/ml (X: absorbance value at 260 or 280 nm and Y: dilution factor). The ratio of absorbance at 260 to 280 nm values for total RNA should fall between 1.8 to 2.2 and any total RNA sample quantity with less than 1.8 value indicates that the RNA quality is not good enough and will result in poor cDNA (Farrell, 1998).

#### **2.2.1.4.4 Poly (A)+RNA isolation**

Poly (A)+RNA was isolated from the total RNA samples using a GenElute mRNA Miniprep kit (Sigma-Aldrich Ltd) in accordance with the manufacturer's instructions provided. The volume of each total RNA samples was brought up to 250µl using RNase-free water, then mixed with 250µl of 2X Binding solution and 15µl of oligo (dT) beads, and vortexed thoroughly. The samples were incubated at 70°C for 3 minutes to denature RNA and were then left at room temperature for 10 minutes. The samples were then centrifuged for 2 minutes at 13000 g to pellet the beads: poly(A)+RNA complexes. The supernatants were discarded and the pellets resuspended in 500 µl of wash solution by vortexing. Each sample suspension was then transferred to a spin filter/collection tube and centrifuged for 2 minutes at 13000 g, before the flow through was discarded and the column containing the beads: poly(A)+RNA complex was washed again with a second 500 µl of wash solution followed by centrifugation for 2 minutes. The column was transferred into

a fresh collection tube and 50 µl Elution solution (preheated to 70°C) was added to the centre of the filter and incubated for 5 minutes at 70°C, before centrifuging for 1 minute. This elution procedure was repeated with an additional 50 µl elution solution. The isolated poly(A)<sup>+</sup>RNA was then stored at -80°C until further use or kept on ice for immediate DNase treatment and cDNA synthesis.

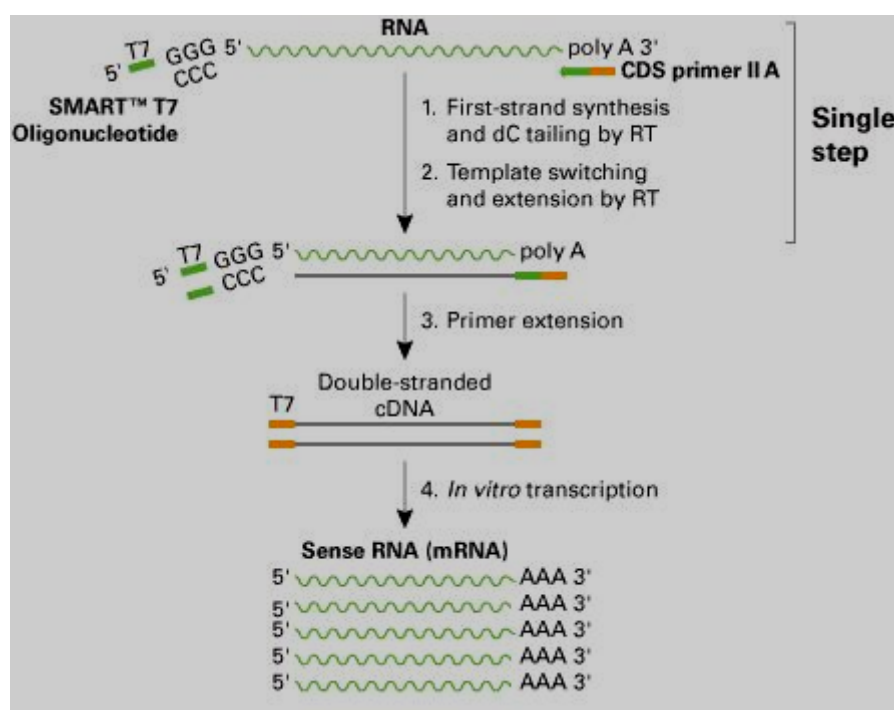
#### **2.2.1.4.5 Amplification of mRNA samples**

Due to the limited amounts of tissue after microdissection into components (the dermal papilla, connective tissue sheath around the bulb, hair bulb matrix, follicle bulge region and the lower follicle area between the bulge and the bulb), the components mRNA was amplified before cDNA synthesis using the SMART™ mRNA Amplification Kit (Clontech Laboratories, Inc. CA, USA) according to the manufacturer's instructions. Initially first-strand cDNA was synthesised by adding 1 µl of CDS primer II A (12 µM; 5'-AAGCAGTGGTATCAACGCAGAGTACTVN-3') (Figure 18) and 1.25 µl deionised water to 3 µl of mRNA sample (0.1-5 µg) in a 0.5 ml eppendorf tube (Alpha Laboratories); this was mixed thoroughly and incubated for 3 minutes at 70°C, followed by 42°C for 2 minutes in a PCR Sprint thermal cycler (Thermo Hybaid, Ashford, UK). A master mix was prepared for each reaction tube in a 0.5 ml eppendorf tube containing 2 µl 5X first-strand buffer, 0.5 µl DTT (100 mM), 0.25 µl RNase inhibitor, 1 µl SMART™ T7 oligonucleotide (10 µM; 5'-ACTCTAATA CGACTCACTATAGGGAGAGGGCGGG-3'), 1 µl 50X dNTP mix (10 nM each dATP, dGTP, dCTP and dTTP) and 1 µl MMLV reverse transcriptase; this was mixed well by vortexing and spinning briefly in a microcentrifuge. The master mix (5.75 µl) was added to the mRNA (4.25 µl) tube and mixed thoroughly before incubating at 42°C for 1.5 hour. The reaction was terminated by heating at 68°C for 10 minutes.

Second-strand cDNA was synthesised by preparing a master mix for each reaction containing 73 µl deionised water, 10 µl 10X advantage® 2 PCR buffer, 2 µl 50X dNTP mix (10 nM each), 2 µl T7 extension primer (10 µM; 5'-GCTCTAATACG ACTCACTATAGG-3'), 1 µl RNase H (10U/µl) and 2 µl 50X advantage® 2 polymerase mix. The master mix was mixed well by vortexing and spinning briefly in a microcentrifuge, then added to the first-strand cDNA tube, mixed well and placed in the PCR Sprint thermal cycler (Thermo Hybaid); the thermocycling programme ran was: 37°C for 15 minutes, 95°C for 2 minutes, 60°C for 1 minutes and 68°C for 10 minutes. The double-stranded cDNA was purified prior to performing *in vitro*

### Figure 18 mRNA Amplification

A diagram shows SMART™ mRNA Amplification protocol (Chenchik and al, 1998).



transcription using the Atlas Nucleospin® Extract II kit following the manufacturer's instructions. Buffer NT (2 volumes) was added to 1 volume of sample (200 µl buffer NT and 100 µl double-stranded cDNA), then loaded in to a

Nucleospin® Extract II column in a 2 ml collection tube and centrifuged for 1 minute at 11000g. The flow-through was discarded and the column with the bound double-stranded cDNA moved back to the collection tube. Buffer NT3 (600 µl) was added to the column and centrifuged for 1 minute at 11000g; the flow-through was discarded and the column placed back in to the collection tube. The column was centrifuged for an additional 2 minutes at 11000g to remove any residual buffer NT3 and the column transferred to a new 1.5 ml microcentrifuge tube. To elute the cDNA, 50 µl buffer NE was added to the column, incubated at room temperature for 1 min and centrifuged at 13000 g for 1 minute. To ensure complete elution, this process was repeated. The eluted cDNA was centrifuged at 13000 g for 3 minutes and the supernatant transferred to a new collection tube. Linear acrylamide (3 µl), 10 µl sodium acetate (3 M) and 250 µl 100% ethanol were added to the supernatant and mixed thoroughly. The tube was placed on dry ice for 15 minutes to precipitate the cDNA, centrifuged for 20 minutes at 13000 g and the supernatant carefully removed. The pellet was washed in 100 µl of 70% ethanol for 10 minutes and then dissolved in 9 µl deionised water.

Finally T7 transcription was carried out by preparing a master mix of 10X T7 transcription buffer (2 µl), 3X rNTP mix (7 µl), RNase inhibitor (1 µl) and T7 RNA polymerase (1 µl) (1000U/ µl), mixed well and added in to the tube containing the resuspended cDNA. The reaction mix was mixed well and incubated at 37°C for 12 hours. After sense RNA was transcribed, reinitiated and elongated, this resulted in a successful linear amplification of mRNA *in vitro*; cDNA was synthesised from the amplified mRNA samples of scalp hair follicle components after they were DNase treated.

#### **2.2.1.4.6 DNase treatment**

The mRNA samples were treated with the enzyme dideoxynuclease I (DNase I) to remove any contaminating genomic DNA prior to cDNA synthesis by reverse transcription. A 0.5 ml eppendorf tube (Alpha Laboratories, Ltd, Eastleigh, UK) was used to make each reaction mix. This consisted of 8µl of poly (A)<sup>+</sup>RNA, 1µl DNase I amplification grade and 1µl 10X reaction buffer (Invitrogen Ltd); mixed thoroughly before incubating for 15 minutes at room temperature. To inactivate the DNase enzyme, 1µl EDTA (25mM; Invitrogen Ltd) was added and incubated at 65°C for 10 minutes. The DNase treated poly (A)<sup>+</sup>RNA samples were either placed on ice to be used immediately for cDNA synthesis or stored at -80°C until further use.

#### **2.2.1.4.7 Synthesis of cDNA by reverse transcription**

The DNase treated poly (A)<sup>+</sup>RNA samples were converted to cDNA using the Avian Myeloblastosis Virus (AMV) reverse transcription system (Promega). All reaction mixes were prepared in 0.5 ml eppendorf tubes (Alpha Laboratories) on ice, containing 1µl oligo (dT)<sup>15</sup> primer (0.5 µg/µl; Promega), 2µl dNTP mix (10mM; Promega), 2µl 10X reaction buffer (Promega), 0.5µl recombinant RNasin<sup>®</sup> ribonuclease inhibitor (40 units/µl; Promega) and 0.75µl AMV reverse transcriptase (high concentration: 25 units/µl, Promega). The reaction mix was brought to a final volume of 10µl by the addition of 3.75µl nuclease free water and mixed thoroughly. This reaction mix was added to a 0.5 ml eppendorf tube containing 10µl of DNase treated poly (A)<sup>+</sup>RNA, and mixed using a vortex mixer. The eppendorf tubes were then placed in the PCR Sprint thermal cycler (Thermo Hybaid) and set to run the reverse transcription programme which was: incubation for 1 hour at 42°C to allow cDNA synthesis from mRNA by reverse

transcription, followed by 5 minutes incubation at 99°C to inhibit the reverse transcriptase and finally 5 minutes at 4°C to let the tubes cool down. To ensure that all cDNA was collected at the base of the eppendorf tubes, the tubes were centrifuged at 13000 g for 10 seconds, and then the cDNA was aliquoted into 10µl sample per tube, labelled and kept at -20°C until required.

#### **2.2.1.5 Polymerase Chain Reaction**

All PCR reaction mixes were prepared on ice in 0.5 ml eppendorf tubes (Alpha Laboratories) containing 2.5µl of forward and reverse positive control primers (10µM) or 3µl of forward and reverse FP and FP-variant complexes (altFP) primers (5µM); 5µl of 10X reaction buffer (Invitrogen Ltd); 1µl of nucleotide mix containing equal volumes of ATP, CTP, GTP and TTP (10 mM each; Promega); 1.5–2.5 µl MgCl<sub>2</sub> (50 mM; Invitrogen Ltd) and 3–10 µl cDNA depending on the target primer set; 0.5µl recombinant Taq DNA polymerase (5 units/µl; Invitrogen Ltd). Nuclease free water was used to bring up the final volume of the mixture to 50µl, and then mixed thoroughly. By replacing the cDNA with nuclease free water, a negative control was prepared for every PCR reaction. To prevent evaporation of reaction components during PCR thermocycling, one drop of mineral oil (Sigma-Aldrich Ltd) was added on to the top of each reaction mixture, except when the PCR was done to prepare the DNA product to be sent for sequencing.

In order to get the best amplification during PCR, each target primer set required optimisation of primer concentrations, annealing temperatures and MgCl<sub>2</sub> concentrations. Details for each target primer set optimisation are shown in table 2. For the β-actin primer set, the PCR thermocycling programme was: initial denaturation at 94°C for 5 minutes followed by 35 cycles of: PCR amplification at 94°C, optimum annealing temperature at 56°C for 1 minute, extension at 72°C for 1

minute, followed by a final extension of 11 minutes at 72°C. After the thermocycling finished the tubes were cooled at 4°C. The PCR products were placed on ice to be analysed immediately by agarose gel electrophoresis or could be stored at -20°C for later analysis.



**Table 2 Specific forward and reverse primers and optimised conditions used in RT-PCR analysis of  $\beta$ -actin, FP and FP splice variant complexes (altFPs) expression**

For each cDNA target sequence, specific forward (F) and reverse (R) primers were used to perform RT-PCR. The primer sequences, their optimised RT-PCR conditions, their expected amplicon size and optimal  $MgCl_2$  concentration are showed below. Those for  $\beta$ -actin were obtained from Shorter *et al* (2008) and altFPs, altFP5, altFP3, altFP2 from Liang *et al* (2008); FP, altFP4 & altFP1 were newly designed and PCR conditions required extensive optimisation.

Primer name	Primer sequence	Optimal thermocycling conditions	Expected amplicon size	Optimal $MgCl_2$ conc.
$\beta$ -actin	<b>F:</b> 5' ATCTGGCACCACACCTTCTACAATGAGCTGCG 3' <b>R:</b> 5' CTCATACTCCTGCTTGTGCTGATCCACATCTGCG 3' Shorter <i>et al</i> 2008	94°C for 5 min 94°C for 1 min 56°C for 1 min 72°C for 1 min 72°C for 10 min 4°C $\infty$ 35 cycles	838 bp	2.5 mM
PGF <sub>2<math>\alpha</math></sub> receptor (FP)	<b>F:</b> 5' ATGTCCATGAACAATTCCAA 3' <b>R:</b> 5' CTAGGTGCTTGTGCTGATTTCT 3' newly designed (GenBank accession number NC_ 000001.10)	95°C for 7 min 95°C for 1 min 53°C for 1 min 72°C for 1 min 72°C for 7 min 4°C $\infty$ 36 cycles	1080 bp	2 mM
All splice variants of FP (altFPs)	<b>F:</b> 5' TGCAATGCAATCACAGGAAT 3' <b>R:</b> 5' CACTCCACAGCATTGACTGG 3' Liang <i>et al</i> 2008	95°C for 7 min 95°C for 30 sec 53°C for 30 sec 72°C for 30 sec 72°C for 10 min 4°C $\infty$ 36 cycles	Bands >321 bp	2 mM

Primer name	Primer sequence	Optimal thermocycling conditions	Expected amplicon size	Optimal MgCl <sub>2</sub> conc.
FP-V1 (altFP1)	<b>F:</b> 5' GTGGTGTGTGCTTGCTTGTGCTG 3' <b>R:</b> 5' GCTAGGTGCTTGCTGATTCTCTGCG 3' newly designed (GenBank accession number NC_ 000001.10)	95°C for 7 min 95°C for 30 sec } 36 cycles 53°C for 30 sec } 72°C for 30 sec } 72°C for 10 min 4°C∞	392 bp	2 mM
FP-V2 & 3 (altFP2 & altFP3)	<b>F:</b> 5'GAGCCCATTTCTGGGATACA 3' <b>R:</b> 5'-AGTGCCTCTCTTCACCCCTCA 3' <i>Liang et al 2008</i>	95°C for 7 min 95°C for 30 sec } 36 cycles 53°C for 30 sec } 72°C for 30 sec } 72°C for 10 min 4°C∞	463 bp & 534 bp	2 mM
FP-V4 (altFP4)	<b>F:</b> 5' AGCCC ATTTCTGCGATAAGA 3' <b>R:</b> 5' GTTCTGGAGCCTCAGGTGTC 3' newly designed (GenBank accession number NC_ 000001.10)	95°C for 7 min 95°C for 30 sec } 36 cycles 53°C for 30 sec } 72°C for 30 sec } 72°C for 10 min 4°C∞	141 bp	2 mM
FP-V5 (altFP5)	<b>F:</b> 5'AGCTCCTGGCGATAATGTGT-3' <b>R:</b> 5'CCYYCHCAAYAHYCCYCCAA 3' <i>Liang et al 2008</i>	95°C for 7 min 95°C for 30 sec } 36 cycles 53°C for 30 sec } 72°C for 30 sec } 72°C for 10 min 4°C∞	460 bp	2 mM

#### 2.2.1.6 PCR primer design

The  $\beta$ -actin primer set, which was used for positive control gene expression, has been used previously for human hair follicle cDNA (Shorter *et al.*, 2008); this was slightly modified from an existing established primer set (Merrick, 2000). Although there are few published primer sets for prostaglandin  $F_{2\alpha}$  receptor (FP) used for mouse, when they were checked on the human prostanoid receptor gene sequence using NCBI BLAST, none of them matched. Therefore, the primer sets used for detection of prostaglandin  $F_{2\alpha}$  receptor (FP) and FP splice variants 1 & 4 (altFP1 & altFP4) gene expression were newly designed from the human FP gene sequence. The ensemble genome browser was used to find the human prostanoid receptor genomic sequence, and the exon information was used for primer design. Primers were selected from exon numbers three and four: forward primers from exon 3 and reverse from exon 4. This primer combination using two different exons, crossing an intron, was selected to ensure that the correct sized product would only be obtained from cDNA and not from any contaminating genomic DNA sequence which might be present in the PCR mixture and to pick up any splice variants expressed in areas between these two functional exons. The designed primer sets were then checked with the human gene sequence using the NCBI BLAST programme (<http://www.ncbi.nlm.nih.gov/blast/bl2seq/wblast2.cgi>) to confirm that they were appropriate for use in human samples. Ensemble blast was also used to check the chromosomal location of each primer, the length of matching area on the chromosome and the length of the gap between the end of forward primer matching area and the start of reverse primer matching area, all done against the human genome. The primers were synthesised by Sigma Genosys Biotechnologies Ltd (Pampisford, UK). The designed FP primer set was first

checked on a positive control tissue, rat liver, cDNA which is known to express FP gene (Arend *et al.*, 2005; Koukoui *et al.*, 2006), it was available and easy to prepare compared to human hair follicle cDNA which is very valuable due to the limited sample availability and the time consuming process involved in isolating hair follicles.

#### **2.2.1.7 Agarose gel electrophoresis of PCR products**

RT-PCR products were analysed using agarose gel electrophoresis by separating the products on a 1.5% (w/v) agarose gel prepared as in section 2.2.1.4.2. Aliquots from all PCR products were mixed with agarose blue/orange 6X loading dye (Promega) in a ratio of 5:1 to assist loading and monitor the progression of the product through the gel during electrophoresis. The mixture and the negative controls were loaded into the wells, and their positions noted. In order to estimate the product size, 10 µl of standard DNA fragments was mixed with 2 µl of loading dye, and then loaded onto the gel to provide a DNA ladder (The ladder consisted of eleven fragments that ranged in size from 100–1,500 bp; Promega). The tank was set to run at 100 volts for approximately 40 minutes until the orange dye reached the other side of the gel. The Uvitec gel documentation system (UVItec Limited) was used to visualise the PCR products at a wavelength of 312nm and the image captured and recorded on a computer. In order to get rid of any white shadows on the pictures which were due to ethidium bromide over staining, some of the PCR products were analysed on 1.5% (w/v) agarose gel made without ethidium bromide and the electrophoresis tank contained only 1 X TAE buffer. Ethidium bromide staining was carried out after electrophoresis by placing the gel in a light protected container with ethidium bromide solution (100µl ethidium bromide in 1 L distilled water) for 20 minutes. To wash out extra ethidium bromide on the gel,

the gel was placed in distilled water for 20 minutes, then visualised by Uvitec gel documentation system (UVItec Limited).

#### **2.2.1.8 Sequencing of PCR products**

The identities of PCR products were verified by sending the expected amplicon size products to a commercial company (Geneblitz, Sunderland, UK) for sequencing. The PCR products were prepared for this as described in section 2.2.1.5 except that small, thin walled PCR tubes (VWR International Ltd, Poole, UK) and the hot lid were used in the thermocycler instead of adding mineral oil, as the oil may interfere with the sequencing. Low-melting point agarose gel (Invitrogen Ltd) was used to separate the PCR products in order to allow using a lower temperature to dissolve the gel during the purification of the PCR products to prevent the DNA from degradation. Approximately 50 ng/ $\mu$ l of DNA was required by the commercial sequencing service, therefore 30 $\mu$ l of weaker PCR products were loaded onto the gel to allow sufficient product for sequencing. The MinElute Gel Extraction kit (Qiagen, Crawley, UK) was used, according to manufacturer's instructions to purify the PCR products prior to sending them for sequencing. Using a UV-light source (UVitec) to visualise the separated product bands inside the gel, the target DNA fragment was excised from the gel using a scalpel blade, and transferred to an empty pre-weighted 1.5ml Eppendorf tube. The tube with the gel containing the DNA fragment was weighed to obtain the net weight of the gel. To dissolve the gel slice, buffer QC was added in the proportion of 3 volumes of buffer to 1 mg of gel (e.g. 300  $\mu$ l of Buffer QC to 100 mg of gel) and the tube was incubated at 50°C for 10 minutes and vortex mixed every 3 minutes during this incubation. After the gel was fully dissolved, one volume of isopropanol (Sigma-Aldrich Ltd) was added, and mixed by inversion. The sample was added to a MinElute column

and centrifuged (13000 g) for 1 minute to bind the DNA to the column, then the flow-through from the column was discarded. Further buffer QC 500µl was added to the column and the process repeated as mentioned earlier. The column was placed back in the collection tube, and washed by adding 750µl of buffer PE to the column and incubated for 5 minutes at room temperature before centrifuging for 1 minute at 13000 g and discarding the flow-through. The column was centrifuged (13000 g) for another minute and the flow-through discarded to remove any residual ethanol from buffer PE. The MinElute column was placed into a clean 1.5 ml Eppendorf tube, followed by addition of 10 µl of buffer EB to the centre of the column and incubated at room temperature for 1 minute before centrifuging at 13000 g for 1 minute to elute the purified DNA from the column. The purified PCR product was sent with 20 µl of appropriate forward and reverse primers (10 µM) for sequencing at Geneblitz (Sunderland, UK).

To compare the homology of the sequencing result to the known published sequences, the NCBI BLAST programme (<http://www.ncbi.nlm.nih.gov/blast/bl2seq/wblast2.cgi>) was used. The chromatogram of the sequencing data was produced using the Chromas Lite software (version 2.0) available from <http://www.technelysium.com.au/>. The chromatogram was used to analyse any non-matching nucleotides between the sequenced and known data. In the chromatogram, each base is allocated a different colour, and the sequence determined by the highest peak. If more than one peak is of a similar height, without significant distance, then the base was recorded as 'n' in the sequence.

## **2.3 Human hair follicle organ culture**

### **2.3.1 Skin samples**

Human scalp skin samples were obtained from healthy donors, 1 woman and 14 men aged between 22-48 years undergoing elective cosmetic surgery; donors provided written consent, and appropriate ethical committee approval was obtained. The samples were collected as whole skin specimens or as individual follicles into 50 ml falcon tubes containing 30 ml transport medium: William's E medium (Sigma-Aldrich Ltd) supplemented with 100ng/ml hydrocortisone (Sigma-Aldrich Ltd), 10µg/ml insulin (Sigma-Aldrich Ltd), 10 units/ml penicillin (Sigma-Aldrich Ltd) and 2mM L-glutamine (Gibco, Paisley, UK). The tubes were labelled with the patient's age, gender, date of sample collection and sample site. Throughout the transportation, the samples were kept on ice and when arrived at the University they were stored at 4°C until micro-dissection, which was performed within 10 hours of removal.

### **2.3.2 Hair follicle isolation**

A Leica MZ8 dissecting microscope was used to dissect anagen hair follicles from the scalp skin samples in a sterile condition; all plasticware used was sterile and sterile cold PBS was used as a dissecting medium. Special care was taken throughout the dissection process to ensure the follicles were intact as undamaged follicles are essential for successful culture (Philpott *et al.*, 1990). A scalpel blade was used to cut the skin (Figure 16a) at the level of the dermal-subcutaneous fat interface and then intact anagen hair follicles were pulled out from the subcutaneous fat gently with fine forceps (sizes 5 and 7). The isolated undamaged follicles were transferred into fresh cold PBS and gently cleaned of any attached

subcutaneous fat or dermis by using 27<sup>1/2</sup> gauge sterile syringe needles (Tyco health care Ltd, Gosport, UK). The isolated clean and undamaged follicles were transferred to the culture medium immediately after isolation was completed (Figure 16b).

### **2.3.3 Hair growth culture conditions**

William's E medium (containing 10µg/ml phenol red) (sigma) was prepared supplemented with 2mM L-glutamine (Gibco), 10 µg/ml insulin, 10units/ml penicillin (Sigma) and 100ng/ml hydrocortisone (Sigma). This culture medium was further supplemented depending on which experiment was being conducted, with one of the following: PGF<sub>2α</sub> (10, 100 & 1000 nM; dissolved in a stock solution of William's E medium; Sigma), latanoprost (10, 100 & 1000 nM; dissolved in a stock solution of William's E medium), bimatoprost (10, 100 & 1000 nM; dissolved in a stock solution of dimethyl sulfoxide (DMSO); Sigma), prostaglandin F<sub>2α</sub> receptor (FP) antagonist AS604872 (1 µM; dissolved in a stock solution of DMSO), FP antagonist AL-8810 (10 µM; dissolved in a stock solution of DMSO), prostamide F<sub>2α</sub> receptor antagonist AGN211336 (1µM; dissolved in a stock solution of DMSO), both PGF<sub>2α</sub> (100 nM) and AS604872 (1 µM), both PGF<sub>2α</sub> (100 nM) and AL-8810 (10 µM), both latanoprost (100 nM) and AS604872 (1µM), both latanoprost (100 nM) and AL-8810 (10 µM), both bimatoprost (100 nM) and AS604872 (1 µM), both bimatoprost (100 nM) and AGN211336 (1 µM). Stock solutions of all compounds were dissolved using a sonicating water bath (Dawe Instruments Ltd., Middlesex, UK). Control medium was prepared without supplements, but for bimatoprost and antagonists experiments contained the vehicle (0.001% DMSO). The media were prepared in advance and were sterile-filtered using a 0.2 µm pore filter (Sarstedt, Nümbrecht, Germany).



Each isolated and cleaned human anagen hair follicle was transferred carefully to an individual well of a 24-well plate (Corning Glassworks, Corning, NY, USA) containing 1 ml of William's E medium supplemented as described above. Follicles were incubated and maintained free-floating at 37°C in an atmosphere of 5% CO<sub>2</sub> and 95% air in a humidified incubator over a period of nine days. To feed the cultured follicles, fresh & pre-warmed media was introduced at three day intervals, taking care not to damage or lose the follicles.

#### **2.3.4 Measurement of cultured hair follicles**

Hair follicles were assessed for morphology of the follicle bulb, photographed using a Nikon Coolpix 4500 digital camera (Nikon, Tokyo, Japan) and measured every 24 hours for 9 days, using a Leitz Labovert inverted microscope (Leitz Labovert FS, Wetzlar, Germany) fitted with an eyepiece graticule. All measurements were taken at X 50 magnification (eyepiece 12.5 × objective lens 4X) and then converted to mm by comparison with a stage micrometer. To work out variation in growth rate of the follicles, the initial length of each follicle was deducted from the measurement obtained at each time point, so results were recorded as increase in hair follicle length over time. Hair follicles that had not grown after 3 days in culture were classed as nonviable and excluded from further study. Any changes in follicle morphology were also recorded within these nine days.

#### **2.3.5 Statistical analysis**

The mean value per person for each parameter for each treatment was determined before calculation of the sample mean. The elongation of hair follicles in each individual treatment group was expressed as the mean increase in length (mm) ± SEM of the number of individuals used. Data from each experimental group were

analyzed for normal distribution using the Kolmogorov-Smirnov test. The effect of the different treatments with time on the daily rate of growth, percentage of follicles remaining in anagen and total amount of hair follicle produced in culture was analyzed by a two-factor, within-subjects analysis of variance using the SPSS statistical analysis program (SPSS Inc., Chicago, IL, USA). If the sample means of the different experimental groups differed significantly ( $P < 0.05$ ), selected experimental group means were compared using a Student's paired  $t$  test with Sidak's correction for multiple comparisons.

## **2.4 Analysis of prostanoid lipid mediators**

Prostanoid profiles are tissue- and stimuli-dependent and their metabolites have low concentrations, short half-lives and structural similarities, therefore, all quantitative methodologies require high selectivity and sensitivity (Yue *et al.*, 2007). A variety of methodologies for the analysis of prostanoids have been developed such as gas chromatography/mass spectrometry (GC/MS), high pressure liquid chromatography (HPLC) with fluorescence or UV detection, chromatography/tandem mass spectrometry (GC/MS/MS), enzyme immunoassays and radioimmunoassay (Hoch *et al.*, 2000; Waddington *et al.*, 2001; Wiswedel *et al.*, 2002; Yue *et al.*, 2007). Immunoassays are very common even though they do not allow simultaneous analysis of more than one metabolite. GC/MS offers more sensitivity compared to immunoassays, but requires extensive sample preparation. Most prostanoids do not absorb UV except at low wavelengths, therefore, using radiolabelled fatty acid precursors is essential in HPLC-based methods (Terragno *et al.*, 1981). Electrospray ionisation (ESI) is a very suitable ionisation method for the analysis of eicosanoids (Murphy *et al.*, 2005). ESI is commonly used in the negative ionisation mode as prostanoid and other fatty acid derivatives are readily

ionised to form carboxylate anions (Yue *et al.*, 2007). The liquid chromatography electrospray tandem mass spectrometry (LC/ESI-MS/MS) method allows the analysis of wide range of lipids from biological samples quickly and with high sensitivity. Mass spectrometry identifies the chemical composition of compounds on the basis of the mass/charge ( $m/z$ ) ratio of ions and their relative abundances (Bruins, 1991). The mass spectrometers comprise three main parts, the ionisation source, the analyser and the detector. The first step involves using electron ionisation to generate gas-phase ions of the compound of interest (Hoffmann and Stroobant, 1999). The common ionisation methods are ESI, Fast Atom Bombardment (FAB), Matrix-Assisted Laser Desorption Ionisation (MALDI) and Atmospheric Pressure Chemical Ionisation (APCI). After ionisation of the compound of interest, the ions pass through a mass analyser and they are separated according to their  $m/z$  ratio. The analyser's main characteristics are the transmission, the upper mass limit and the resolution. The transmission is the ratio between the number of ions reaching the detector and the number of ions produced by the source, and mass limit determines the highest value of  $m/z$  ratio that could be measured; resolution is the ability of the instrument to yield different signals for two ions with small mass difference (Hoffmann and Stroobant, 1999). The common types of mass analysers are: Quadrupoles, Time of Flight (ToF), Ion Traps and magnetic & electromagnetic analysers with Fourier transform. The main types of detectors are the photographic plate and the Faraday cage that permit direct measurement of the charge that reaches the detector and the electron or photon multiplier detectors and array detectors that allow enhancement of the intensity of the signal (Hoffmann and Stroobant, 1999).

In the electrospray ionisation method, the samples are dissolved in a volatile solvent, ionised at atmospheric pressure and passed through a high voltage (2000-5000 v) capillary tube to create an electric field gradient; the solvent evaporates rapidly as the charged droplets travel through the electric field. The large droplets then divide into smaller droplets and eventually into individual charged molecules which enter the mass spectrometer (Watson, 2006).

Tandem mass spectrometry (MS/MS) involves two stages of analysis, the first analyser isolates the precursor ion followed by fragmentation to yield product ions; the second stage involves fragmentation of the precursor ions selected by first analyser to allow the second analyser to analyse the product ions by the spectrophotometer. A collision cell is placed between the two mass analysers in the MS/MS instrument in order to obtain optimal collision activation (Hoffmann and Stroobant, 1999).

#### **2.4.1 Lipidomic analysis**

Lipid mediator extraction from isolated scalp anagen hair follicles from 3 men (aged 34-42) was undertaken using the method adapted from Masoodi and Nicolaou (2006) and the lipid extracts were investigated using a targeted approach for identification and quantification of prostanoids, dihydroprostaglandins and isoprostanes using electrospray tandem mass spectrometry coupled to liquid chromatography (LC/ESI-MS/MS). A range of multiple reaction monitoring (MRM) transitions and optimum collision energy for each compound were used to generate the most abundant product ions (Kempen *et al.*, 2001; Yang *et al.*, 2002; Masoodi and Nicolaou, 2006; Taylor *et al.*, 2006) (see Table 8).

### **2.4.2 Skin samples**

Occipital scalp skin samples were obtained from 3 healthy male donors (aged 34, 39, 42) with written consent. The samples were immediately placed in to 50ml falcon tubes that contained either 30ml *RNAlater*<sup>TM</sup> (Sigma-Aldrich Ltd) or normal saline solution; the tubes were kept on ice until brought to the University, cut into small pieces (approximately 1 cm<sup>2</sup>) and then stored at -80°C until analysed.

### **2.4.3 Sample preparation**

The prostanoids, dihydroprostaglandins and isoprostane were from Cayman Chemicals (Michigan, USA). HPLC-grade ethanol, methanol, hexane, hydrochloric acid and acetonitrile were from Fisher Chemicals, UK. HPLC-grade glacial-acetic acid and methyl formate were from Sigma-Aldrich).

Anagen lower hair follicles (60) were microdissected from each individual's scalp skin sample as described in section 2.2.1.2. Isolated hair follicles were disrupted in 3 ml ice-cold Milli-Q water using a sonicator (Dawe Instruments Ltd., Middlesex, UK) at 60 Hz for 3 two minute intervals with 1 minute cooling down on ice in between. The homogenate was then transferred to a glass tube with glass Pasteur pipette and methanol (HPLC grade) was added to adjust the solution to 15% methanol (v/v), followed by 40 µl of internal standard (IS) (PGB<sub>2</sub>-d<sub>4</sub>) (Cayman Chemical); the resulting solutions were vortexed and centrifuged at 3000 rpm (849 g) for 5 min at 4 °C to remove any precipitating proteins. The clear supernatant was collected, acidified to pH 3.0 using 0.1 M hydrochloric acid (5-10 drops); a pH indicator paper (pH range 2.5-4.5) was used to test the pH of the solutions. To extract the lipid mediators, the acidified samples were immediately applied to solid phase extraction (SPE) cartridges (C18-E, 500 mg, 6 ml,

Phenomenex, Macclesfield, UK). The SPE cartridges were attached to a vacuum manifold (Phenomenex) and they were pre-conditioned with methanol (20 ml) followed by water (20 ml) and then washed with 15% (v/v) methanol (20 ml), water (20 ml), and hexane (10 ml) in series. The vacuum pressure of the manifold used was adjusted to ~5 mmHg so that individual drops could be eluted from each cartridge. The lipid mediators were then eluted in 15 ml methyl formate and gathered in clean glass tubes. The organic solvent, methyl formate, was evaporated under a fine stream of nitrogen and the residue was re-constituted in 100  $\mu$ l ethanol (HPLC grade), transferred to a small glass vial using a glass syringe, which was sealed with a screw cap and Teflon septa and then stored at -20°C for up to 1 week until further analysed on LC/MS/MS.

#### **2.4.4 Preparation of standards and calibration lines**

For all prostanoids, dihydroprostaglandins and isoprostane, stock standard solutions were prepared in ethanol (400 pg/ $\mu$ l) and stored at -20°C under nitrogen. Suitable stock solution dilutions of 100, 50, 20, 10 and 1 pg/ $\mu$ l were prepared to be used as composite standard solutions. The internal standard, PGB<sub>2</sub>-*d*4, was prepared in ethanol (1 ng/ $\mu$ l) and added to all composite standards at a final concentration of 400 pg/ $\mu$ l. Peak-area ratios of every compound to PGB<sub>2</sub>-*d*4 were calculated and plotted against the concentration of the calibration standards; calibration lines were calculated by the least-squares linear regression method. To calculate the concentration of any given analyte the peak-area ratio to PGB<sub>2</sub>-*d*4 was calculated and read off the corresponding calibration line. Peak integrations and signal-to-noise (S/N) ratio calculations were performed using the MassLynx™ V4.0 software (Waters, Elstree, UK).

#### **2.4.5 LC/ESI-MS/MS analysis**

The LC/MS/MS analysis was carried out using a Waters Alliance 2695 HPLC pump coupled to an electrospray ionisation (ESI) triple quadrupole Quattro Ultima mass spectrometer (Waters, Elstree, Hertsfordshire, UK). Instrument control and data acquisition were performed using the MassLynx™ V4.0 software. The instrument was operated in the negative ion mode. For optimisation of MS and MS/MS conditions, standards at a concentration of 10 ng/μl were individually introduced into the spectrometer by direct infusion through a syringe pump (flow rate of 10 μl/min) into the HPLC solvent flow (flow rate 0.2 ml/min). Sample injections were performed with a Waters 2690 autosampler and the sample chamber temperature was set at 8°C. The sample injection volume was 10 μl and the flow rate 0.2 ml/min. The column was maintained at ambient temperature. The capillary voltage was set at 3.00 KV, source temperature 120°C, desolvation temperature 360°C, and cone voltage 35 eV. The optimum collision energy was applied for each compound and argon was used as the collision gas; the reside times were 0.2 second.

Chromatographic analysis was carried out using a gradient system comprising (45:55:0.02) (v/v/v) and (90:10:0.02) (v/v/v) of acetonitrile: water: glacial acetic acid at a flow rate of 0.2 ml/min as described previously (Masoodi and Nicolaou, 2006).

The identified prostanoids were quantified using calibration lines of commercially available standards (Cayman Chemicals). The amount of protein in each sample was estimated with a BioRad protein assay kit using the Lowry method (appendix 6.3) (BioRad laboratories, Herts, UK); BSA at a range of 0-1.5 dilutions in NaOH (0.5M) was used as standard. Results are expressed as pg/mg protein.

## 3 Results

### 3.1 Human hair follicle growth in organ culture

#### 3.1.1 Effects of PGF<sub>2α</sub> and its analogue, latanoprost, on human hair follicles in organ culture

##### 3.1.1.1 Scalp hair follicle growth in control conditions

To investigate the effects of PGF<sub>2α</sub> on scalp hair follicle growth in the absence of any blood supply *in vitro*, isolated hair follicles (Figure 19a) were grown in organ culture for 9 days. Carefully micro-dissected hair follicles were maintained in serum-free culture medium with daily observation of their morphology, measurement and photography as detailed in section 2.3.4, a modification of the original technique (Philpott *et al.*, 1990) which enables much more detail to be assessed. Follicles which showed no increase over 3 days were assumed to be damaged and removed from the experiment. Most of the hair follicles in normal culture medium (approximately 70%) increased in length regularly during the nine day culture period (Figures 19a, 20, 21). Sequential photographs taken every 24 hours showed that this hair follicle elongation was due to the production of a new hair fibre with associated inner and outer root sheath, but the connective tissue sheath did not grow and remained at the initial length over the culture period (Figure 19a). Daily observation of the hair follicle bulb morphology was carried out to monitor if the follicle remained in anagen. Some hair follicles developed catagen-like changes in their bulb morphology, but most follicles maintained their anagen bulb morphology during the nine days of culture (Figure 19c, 21). Those follicles which were designated as undergoing catagen-like changes in their hair bulb morphology showed that pigmentation had ceased and the base of the hair fibre moved upward, losing contact with the regulatory



mesenchyme-derived dermal papilla, which became rounded up into a ball of cells (Figure 19c, d). After 2 days there was a gradual increase in the number of follicles showing catagen-like changes in the hair bulb region (Figure 21). The overall amount of hair actually produced by all the follicles in the organ culture was also calculated from the final increase in length of each follicle on the final day, day 9, or the last day the follicle maintained a normal anagen morphology (Figure 22).

**Figure 19 Sequential photomicrographs of a human hair follicle growing *in vitro* in control medium**

**(a)** Photographs taken every 24 h for 9 days of a typical scalp anagen hair follicle in organ culture under control conditions using an inverted microscope (Leica MZ8, Leica) with a Nikon Coolpix4500 (Nikon E4500) digital camera, show growth of hair fibre and the inner and outer root sheaths, but not the connective tissue sheath (CTS). Hair follicles synthesised new hair fibre increasing in length over 9 days, and most maintained the follicle bulb anagen morphology.

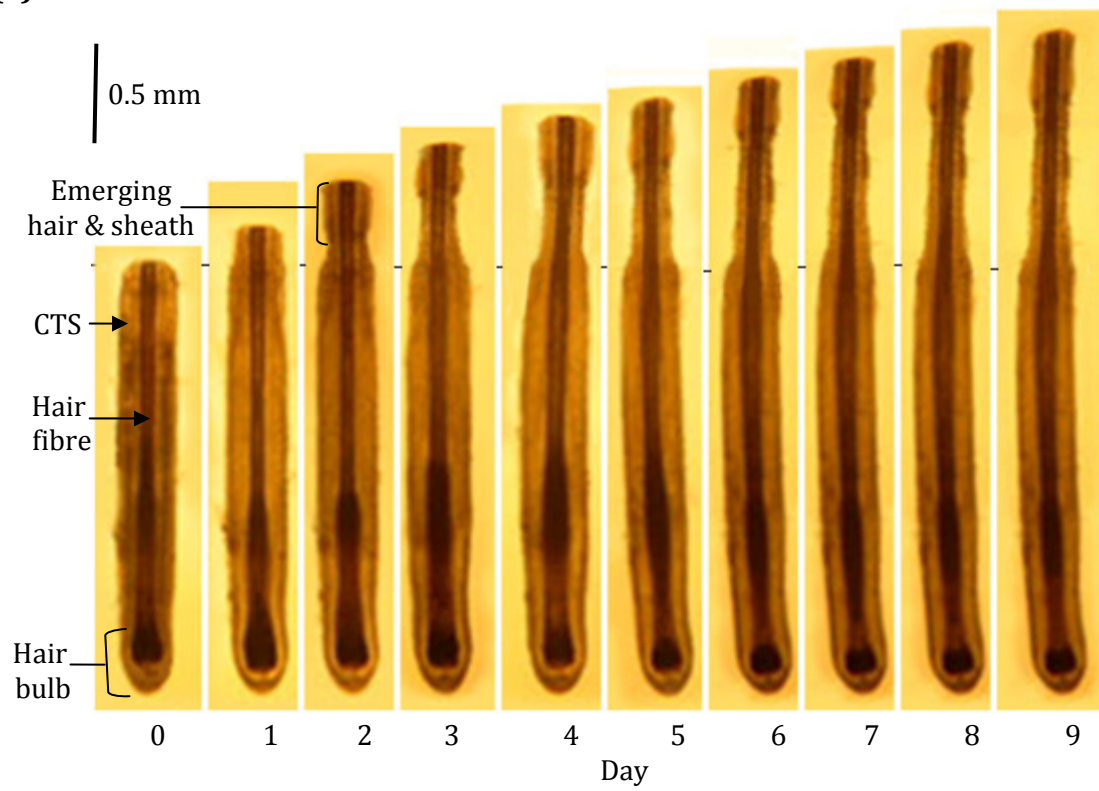
Scale bar = 0.5 mm

**(b)** Enlarged photomicrographs of the hair follicle bulb (pictured in a), showing anagen morphology during 9 days in culture. Scale bar = 0.2 mm

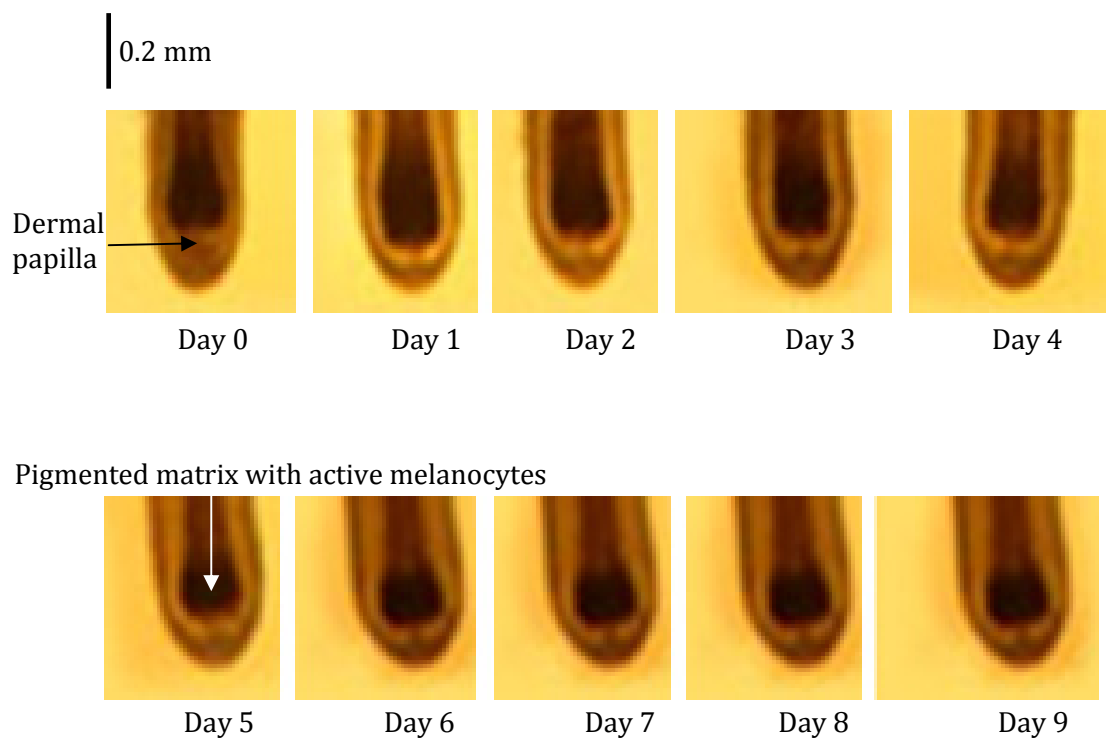
**(c)** Sequential photomicrographs of a hair follicle entering a catagen-like state, showing catagen-like changes in hair bulb morphology. By day 5, pigmentation had ceased; the base of the hair fibre appeared to be retracting up the follicle, leaving behind a ball of dermal papilla (DP) cells. Scale bar = 0.5 mm

**(d)** Enlarged photomicrographs of the hair follicle bulb in (c), Initial changes in hair bulb morphology were clearly visible by day 4. Scale bar = 0.2 mm

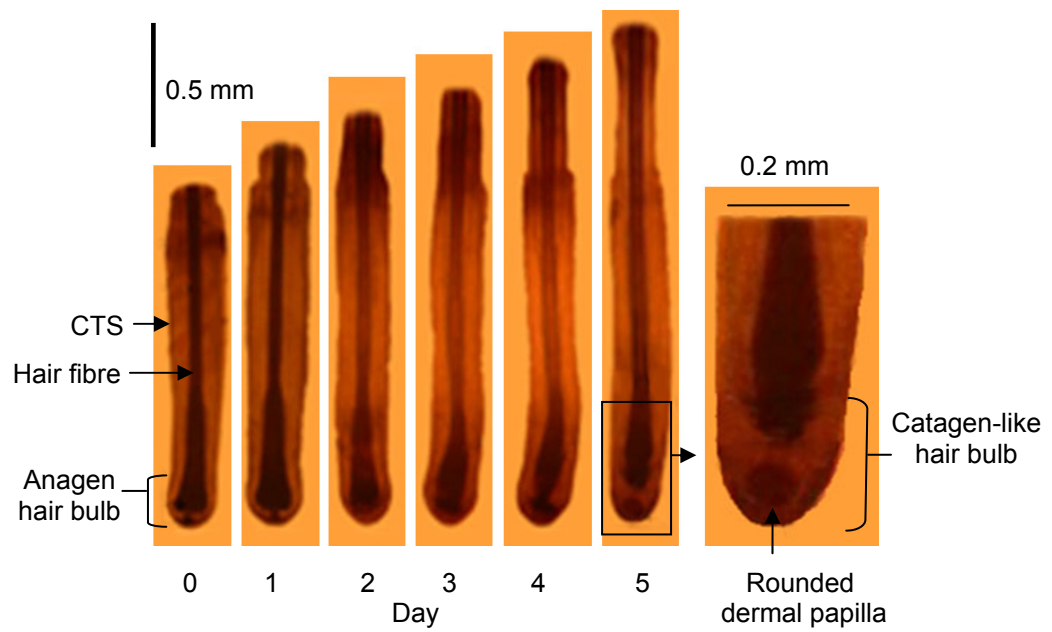
**(a)**



**(b)**



(c)



(d)

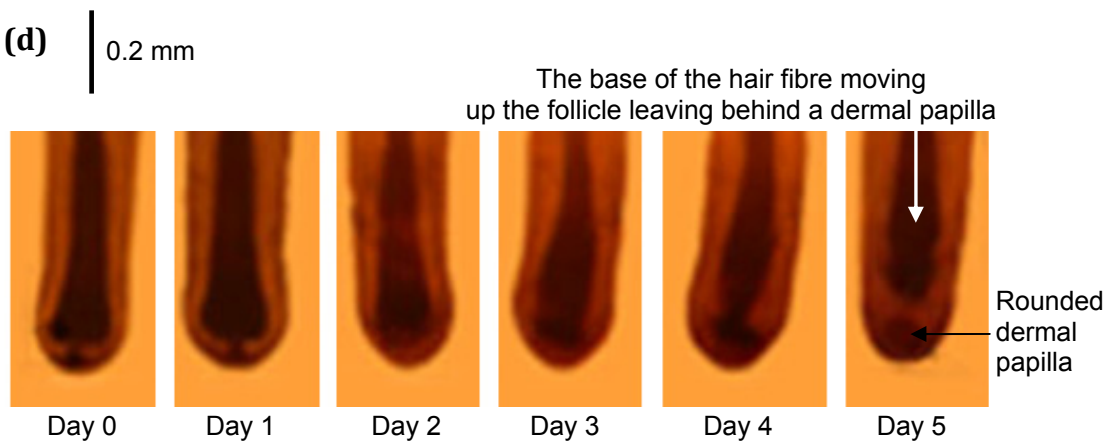


**Figure 20 Scalp hair follicle growth in organ culture under control conditions**

Anagen follicles were assessed daily for changes in morphology and measured while cultured in basic culture medium using an inverted microscope fitted with an eyepiece graticule. The increase in follicle length occurred regularly throughout the culture period at a rate of approximately 100  $\mu\text{m}/\text{day}$ . Values are the mean  $\pm$  SEM of 5 individuals; at least 6 follicles were examined per person.

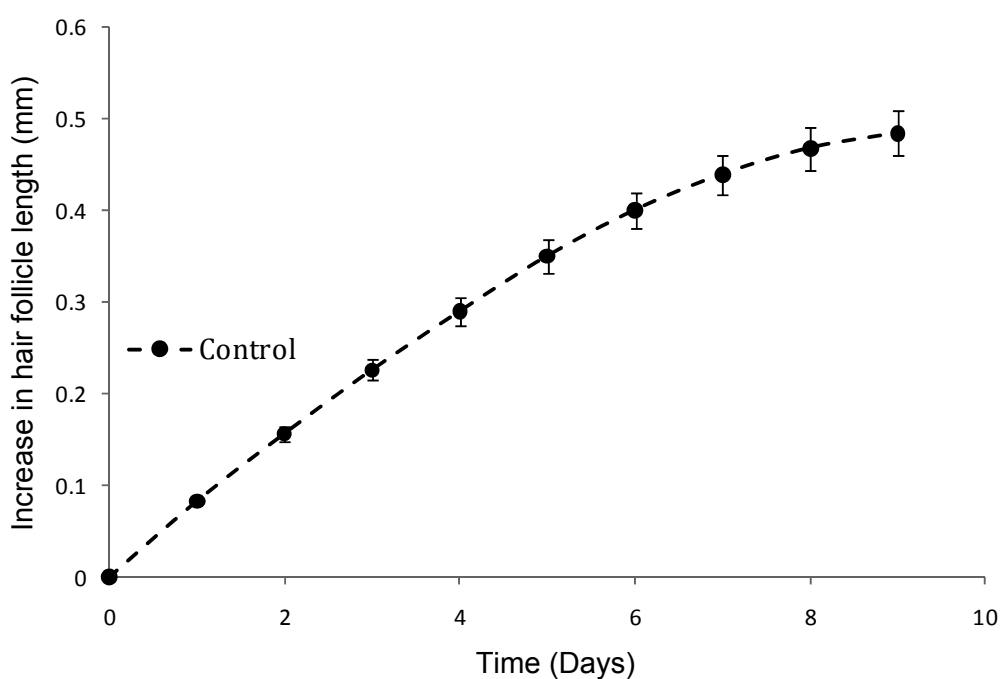


**Figure 21 Percentage of scalp hair follicles remaining in anagen in organ culture under control conditions**

The proportion of hair follicles remaining in anagen throughout nine days of culture was calculated and any follicles which developed catagen-like changes in their bulb morphology were not counted as anagen hair follicles. The number of anagen follicles gradually decreased after two days in culture. Values are the mean  $\pm$  SEM of 5 individuals; at least 6 follicles were examined per person.

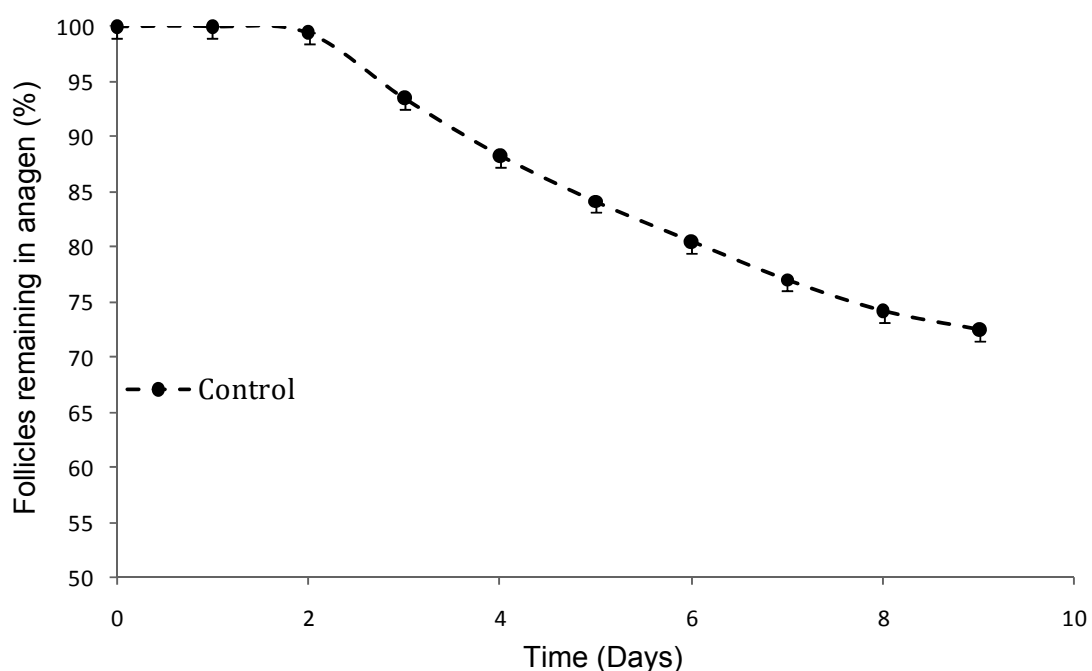
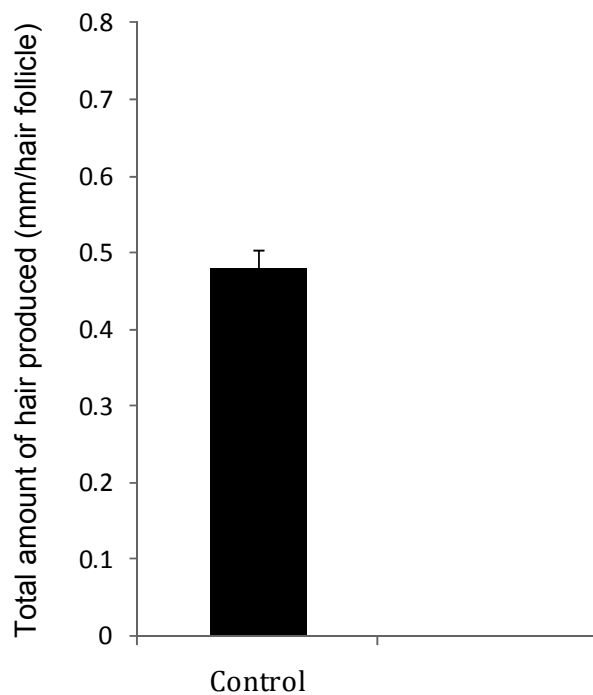


**Figure 22 Total amount of hair produced in organ culture under control conditions**

Anagen follicles were measured while cultured in basic culture medium under control conditions. The overall amount of hair produced *in vitro* was  $0.477 \pm 0.023$  mm/follicle (mean  $\pm$  SEM). Values are the mean  $\pm$  SEM of 5 individuals; at least 6 follicles were examined per person for each condition.



### 3.1.1.2 PGF<sub>2α</sub> stimulated human hair follicle growth *in vitro* in a dose responsive manner

To investigate the biological effects of PGF<sub>2α</sub> on human scalp hair follicles *in vitro*, isolated human scalp hair follicles were cultured in the presence of either the vehicle control or three concentrations of PGF<sub>2α</sub> (10, 100 and 1000 nM). Scalp hair follicles grew well in normal control and PGF<sub>2α</sub>-supplemented culture media showing synthesis of new hair fibre, inner and outer root sheaths, but not the connective tissue sheath (Figure 23).

All 3 concentrations of PGF<sub>2α</sub> stimulated human scalp hair follicles to grow faster *in vitro* (Figure 24); 10 nM increased growth significantly by approximately 16% ( $P < 0.01^{**}$ ) while 100 & 1000 nM had a similar and greater effect of approximately 25% ( $P < 0.001^{***}$ ) (mean  $\pm$  SEM of 5 individuals; at least 6 follicles were examined per person per condition) (Figure 24).

The effect of PGF<sub>2α</sub> on the proportion of follicles exhibiting changes in morphology during culture was also examined. All 3 different concentrations of PGF<sub>2α</sub> slightly raised the number of follicles remaining in anagen, with 10 nM increasing % anagen by day 9 by about 6% ( $P < 0.05^{*}$ ) and 100 & 1000 nM by about 10% ( $P < 0.01^{**}$ ) (Figure 25).

The overall amount of hair actually produced by all the follicles in the organ culture was calculated by recording the final length of each follicle on the last day of the experiment, day 9, or the last day the follicle maintained a normal anagen morphology. PGF<sub>2α</sub> at all 3 concentrations increased the overall amount of hair follicle synthesised in organ culture (Figure 26), from  $0.477 \pm 0.023$  mm/follicle (mean  $\pm$  SEM) by about 20% to  $0.567 \pm 0.023$  mm/follicle with 10 nM PGF<sub>2α</sub> ( $P < 0.05^{*}$ ), by about 32% to  $0.626 \pm 0.025$  mm/follicle with 100 nM PGF<sub>2α</sub>



( $P < 0.01^{**}$ ) and by about 30% to  $0.616 \pm 0.024$  mm/follicle with 1000 nM  $\text{PGF}_{2\alpha}$  ( $P < 0.01^{**}$ ) (Figure 26a, b).

**Figure 23 Sequential photomicrographs of a human hair follicle growing *in vitro* in media with 100 nM  $\text{PGF}_{2\alpha}$**

Light micrographs taken under an inverted microscope every 24 hours for 9 days of typical scalp hair follicles growing in organ culture with 100 nM  $\text{PGF}_{2\alpha}$  showing growth of hair fibre and the inner and outer root sheaths, but not the connective tissue sheath (CTS). Hair follicles synthesised new hair fibre increasing in length (at a faster rate compared to the vehicle) over 9 days, and most maintained the follicle bulb anagen morphology. Scale bars = 0.5 mm.

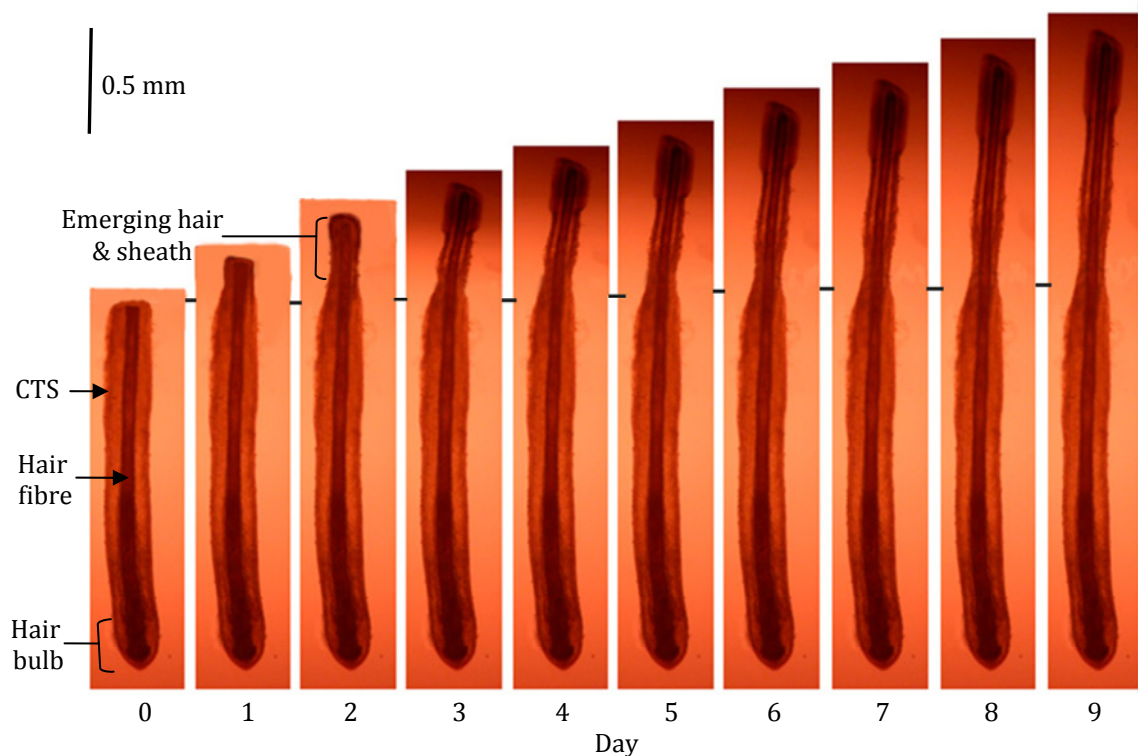


### Figure 24 PGF<sub>2α</sub> stimulated human hair follicle growth in organ culture

Anagen follicles were assessed daily for changes in morphology and measured while cultured in basic culture medium under different conditions: vehicle alone (control) and PGF<sub>2α</sub> (10, 100 & 1000 nM) using an inverted microscope fitted with an eyepiece graticule. PGF<sub>2α</sub> increased scalp follicle growth rate *in vitro*, 10 nM ( $P < 0.01^{**}$ ) and 100 & 1000 nM ( $P < 0.001^{***}$ ). Values are the mean  $\pm$  SEM of 5 individuals; at least 6 follicles were examined per person for each condition. Statistical analysis was performed using a two-factor within-subjects ANOVA using SPSS, after confirming normal distribution, using the Kolmogorov-Smirnov test (KS-test).

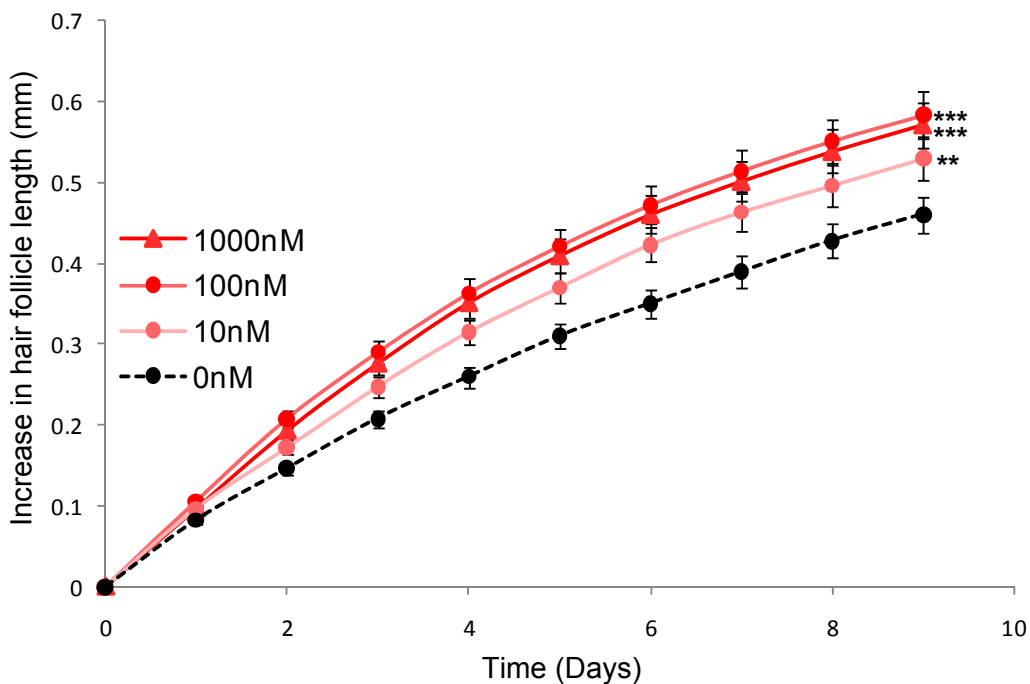


### Figure 25 $\text{PGF}_{2\alpha}$ prolongs anagen in scalp hair follicles in organ culture

The proportion of hair follicles remaining in anagen throughout nine days of culture was calculated excluding any follicles which developed catagen-like changes. The number of anagen follicles gradually decreased after one day in culture.  $\text{PGF}_{2\alpha}$  prolonged anagen on day 9 by about 6% with 10 nM ( $P<0.05^*$ ) and by about 10% with 100 & 1000 nM ( $P<0.01^{**}$ ). Values are the mean  $\pm$  SEM of 5 individuals for each experiment; at least 6 follicles were examined per person for each condition. Statistical analysis was performed using a two-factor within-subjects ANOVA using SPSS, after confirming normal distribution, using the KS-test.

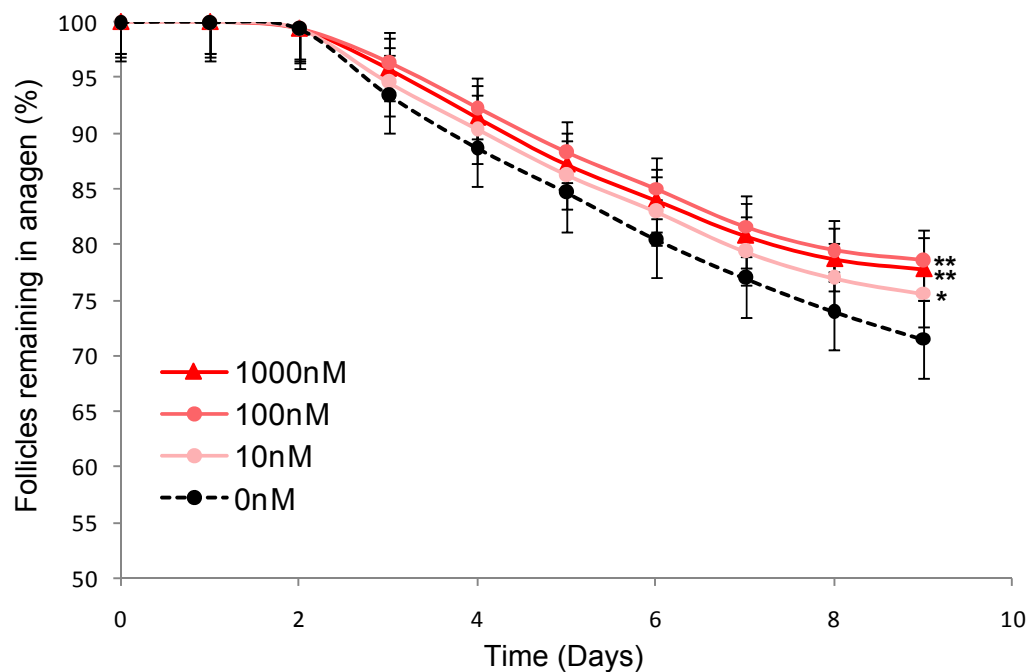
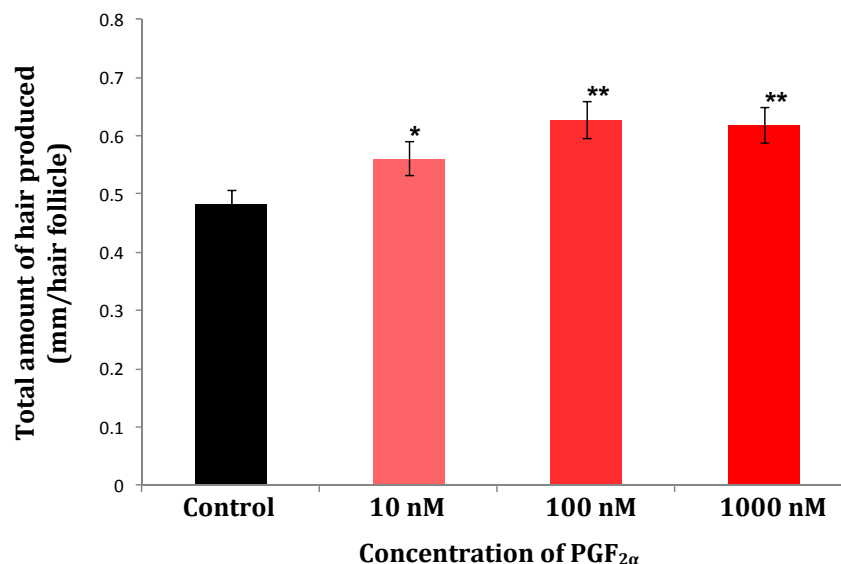


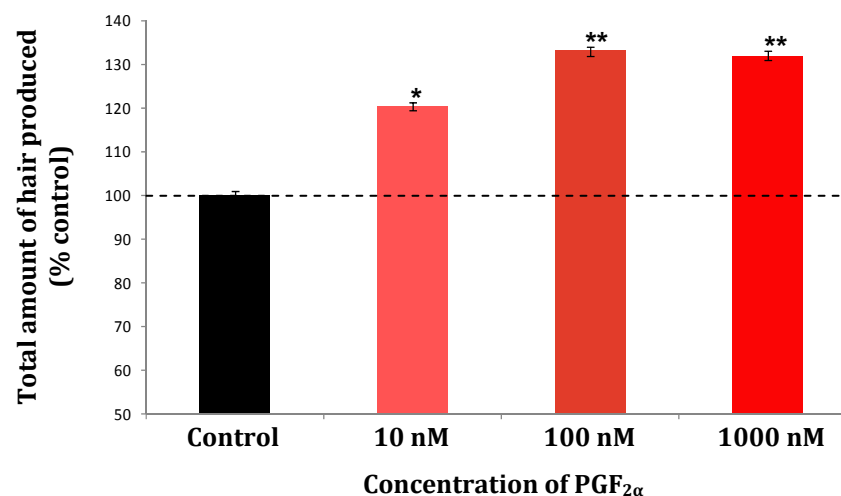
### Figure 26 PGF<sub>2α</sub> increased total amount of hair produced in organ culture

Anagen follicles were measured while cultured under different conditions: vehicle alone (control) and PGF<sub>2α</sub> (10, 100 & 1000 nM). PGF<sub>2α</sub> at all 3 concentrations increased the overall amount of hair produced *in vitro*. Expressed as mean actual values (a) or as a % of their own control follicles (b); by about 20% with 10 nM PGF<sub>2α</sub> (P<0.05\*), by about 32% with 100 nM PGF<sub>2α</sub> (P<0.01\*\*) and by about 30% with 1000 nM PGF<sub>2α</sub> (P<0.01\*\*). Values are the mean ± SEM of 5 individuals; at least 6 follicles were examined per person for each condition. Statistical analysis was performed using a two-factor within-subjects ANOVA using SPSS after confirming normal distribution, using the KS-test.

(a)



(b)



### **3.1.1.3 A PGF<sub>2α</sub> analogue, latanoprost, also stimulated human hair follicle growth *in vitro* in a dose responsive manner**

To investigate the biological effects of latanoprost, a PGF<sub>2α</sub> analogue, on human scalp hair follicles *in vitro*, isolated human scalp hair follicles were cultured in the presence of either the vehicle control or three concentrations of latanoprost (10, 100 and 1000 nM). Scalp hair follicles grew well in normal control and latanoprost-supplemented culture media.

Latanoprost stimulated human scalp hair follicles to grow faster *in vitro* (Figure 27); 10 nM increased growth significantly by approximately 18% ( $P < 0.01^{**}$ ) while 100 & 1000 nM had a similar and greater effect of approximately 26% ( $P < 0.001^{***}$ ) (mean  $\pm$  SEM of 5 individuals; at least 6 follicles were examined per person per condition) (Figure 27).

When the effect of latanoprost on the proportion of follicles experiencing changes in morphology during culture was examined, all 3 different concentrations of latanoprost slightly raised the number of follicles remaining in anagen, with 10 nM increasing % anagen by day 9 by about 6% ( $P < 0.05^{*}$ ) and 100 & 1000 nM by about 10% ( $P < 0.01^{**}$ ) (Figure 28).

Latanoprost at all 3 concentrations also increased the overall amount of hair follicle synthesised in organ culture (Figure 29), from  $0.477 \pm 0.022$  mm/follicle (mean  $\pm$  SEM) by about 22% to  $0.579 \pm 0.023$  mm/follicle with 10 nM latanoprost ( $P < 0.05^{*}$ ), by about 33% to  $0.6318 \pm 0.026$  mm/follicle with 100 nM latanoprost ( $P < 0.01^{**}$ ) and by about 31% to  $0.6208 \pm 0.025$  mm/follicle with 1000 nM latanoprost ( $P < 0.01^{**}$ ) (Figure 29).

### Figure 27 Latanoprost stimulated human hair follicle growth in organ culture

Anagen follicles were assessed daily for changes in morphology and measured while cultured under different conditions: vehicle alone (control) and latanoprost (10, 100 & 1000 nM) using an inverted microscope fitted with an eyepiece graticule. Latanoprost increased scalp follicle growth rate *in vitro*, 10 nM ( $P < 0.01^{**}$ ) and 100 & 1000 nM ( $P < 0.001^{***}$ ). Values are the mean  $\pm$  SEM of 5 individuals; at least 6 follicles were examined per person for each condition. Statistical analysis was performed using a two-factor within-subjects ANOVA using SPSS, after confirming normal distribution, using the Kolmogorov-Smirnov test (KS-test).

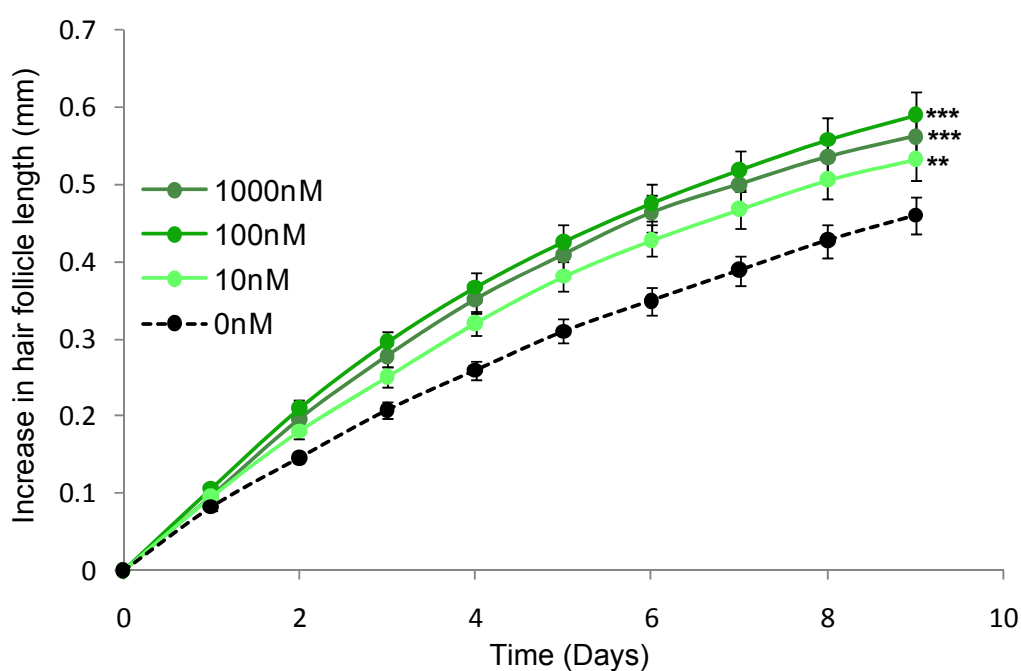


**Figure 28 Latanoprost prolongs anagen in scalp hair follicles in organ culture**

The proportion of hair follicles remaining in anagen throughout nine days of culture was calculated and any follicles which developed catagen-like changes in their bulb morphology were not counted as anagen hair follicles. The number of anagen follicles gradually decreased after two days in culture. Latanoprost prolonged anagen on day 9 by about 6% with 10 nM ( $P<0.05^*$ ) and by about 10% with 100 & 1000 nM ( $P<0.01^{**}$ ). Values are the mean  $\pm$  SEM of 5 individuals; at least 6 follicles were examined per person for each condition. Statistical analysis was performed using a two-factor within-subjects ANOVA using SPSS, after confirming normal distribution, using the KS-test.

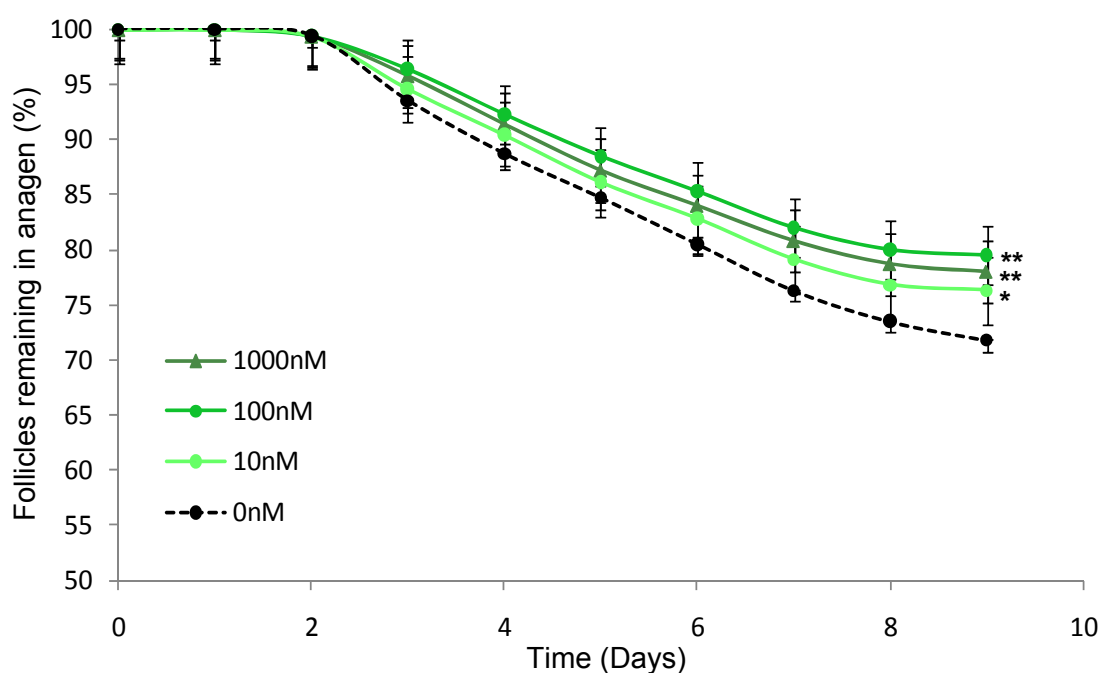
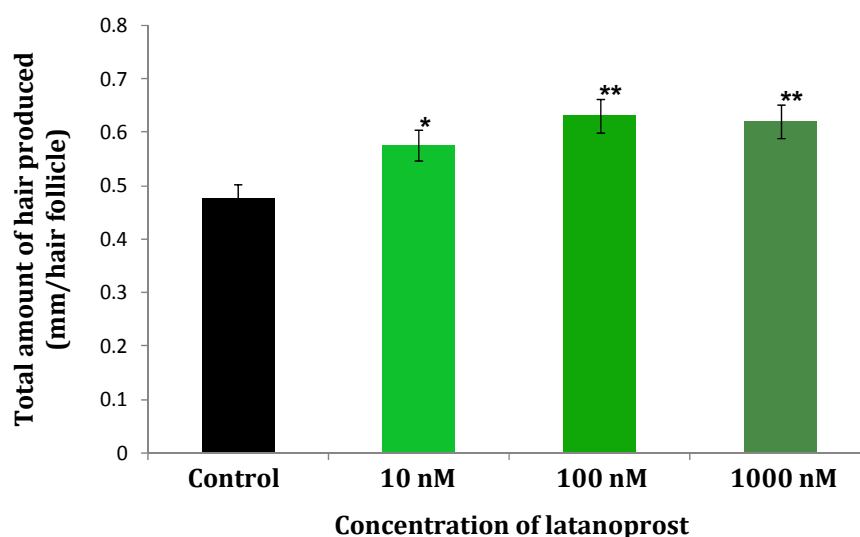




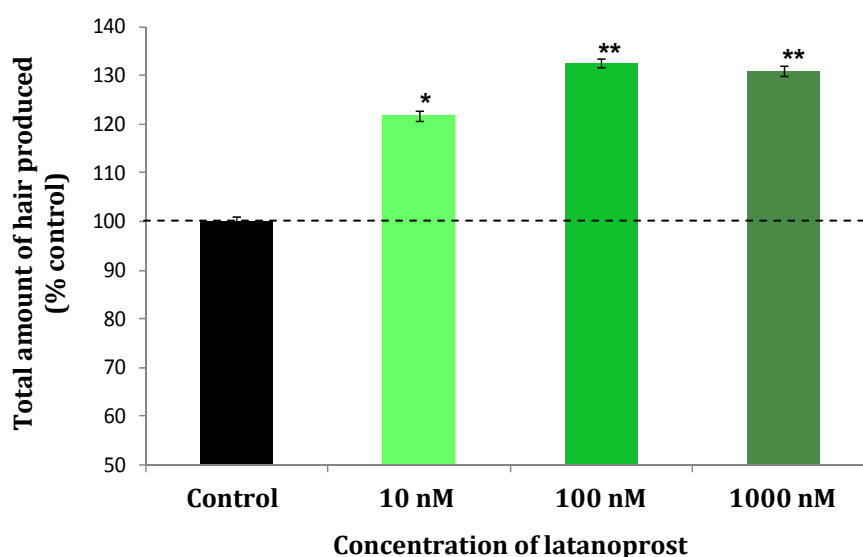
**Figure 29 Latanoprost increased total amount of hair produced in organ culture**

Latanoprost at all 3 concentrations increased the overall amount of hair produced *in vitro*. Results are expressed as mean actual values (a) or as a % of their own control follicles (b), by about 22% with 10 nM ( $P<0.05^*$ ), by about 33% with 100 nM ( $P<0.01^{**}$ ) and by about 31% with 1000 nM ( $P<0.01^{**}$ ). Values are the mean  $\pm$  SEM of 5 individuals; at least 6 follicles were examined per person for each condition. Statistical analysis was performed using a two-factor within-subjects ANOVA using SPSS after confirming normal distribution, using the KS-test.

**(a)**



**(b)**



#### **3.1.1.4 Two PGF<sub>2α</sub> receptor (FP) antagonists AS604872 (AGN222827) and AL-8810 blocked PGF<sub>2α</sub>-stimulation of scalp hair growth in organ culture**

To determine whether the PGF<sub>2α</sub> stimulation was a receptor-mediated response, the effect of two PGF<sub>2α</sub> receptor antagonists AGN222827 and AL-8810 on PGF<sub>2α</sub>-stimulated hair growth was investigated on follicles from 5 further individuals; at least 6 follicles were examined per person per condition. The addition of 0.01% DMSO to the control media, necessary to solubilise the PGF<sub>2α</sub> receptor antagonists (AGN222827 and AL-8810), caused no significant differences in growth rate ( $P=0.107$ ), percentage of follicles remaining in anagen at day 9 ( $P=0.216$ ) nor the overall amount of hair synthesised ( $P=0.142$ ) compared to the original control media (compare Figures 24-26 with 31-33). Similarly, the presence of 0.01% DMSO did not significantly alter any of responses to 100nM PGF<sub>2α</sub> ( $P=0.086-0.207$ ) (compare Figures 24-26 with 31-33). PGF<sub>2α</sub> alone (100 nM) again significantly increased all parameters compared to the vehicle alone: hair growth rate ( $P < 0.001^{***}$ ) (Figure 31), the % of follicles remaining in anagen ( $P < 0.001^{**}$ ) (Figure 32) and the overall amount of hair follicle synthesised by about 32% ( $P<0.01^{**}$ ) (Figure 33). The stimulatory effect of the PGF<sub>2α</sub> on all parameters was blocked when it was combined either with the PGF<sub>2α</sub> receptor antagonist AGN222827 at 1μM or AL-8810 at 10μM ( $P < 0.05^{*}- 0.001^{***}$ ) (Figures 30-33). Both PGF<sub>2α</sub> receptor antagonist, AGN222827 at 1μM and AL-8810 at 10μM alone slightly, but not significantly, inhibited all parameters of scalp hair growth compared to those in the control conditions ( $P= 0.076- 0.1$ ) (Figures 30-33).

**Figure 30 Sequential photomicrographs of a human hair follicle growing in culture with 100 nM  $\text{PGF}_{2\alpha}$  + 1 $\mu\text{M}$   $\text{PGF}_{2\alpha}$  receptor antagonist, AGN222827**

Photographs of the same human hair follicle were taken under an inverted microscope every 24 hours for nine days growing in organ culture in 100 nM  $\text{PGF}_{2\alpha}$  and 1 $\mu\text{M}$   $\text{PGF}_{2\alpha}$  receptor antagonist (AGN222827), showing growth of hair fibre, the inner and outer root sheaths, but not the connective tissue sheath (CTS). Hair follicles synthesised new hair fibre regularly increasing in length (similarly to the vehicle but at a slower rate compared to 100 nM  $\text{PGF}_{2\alpha}$  alone) over 9 days, and most maintained the follicle bulb anagen morphology. Scale bar = 0.3 mm

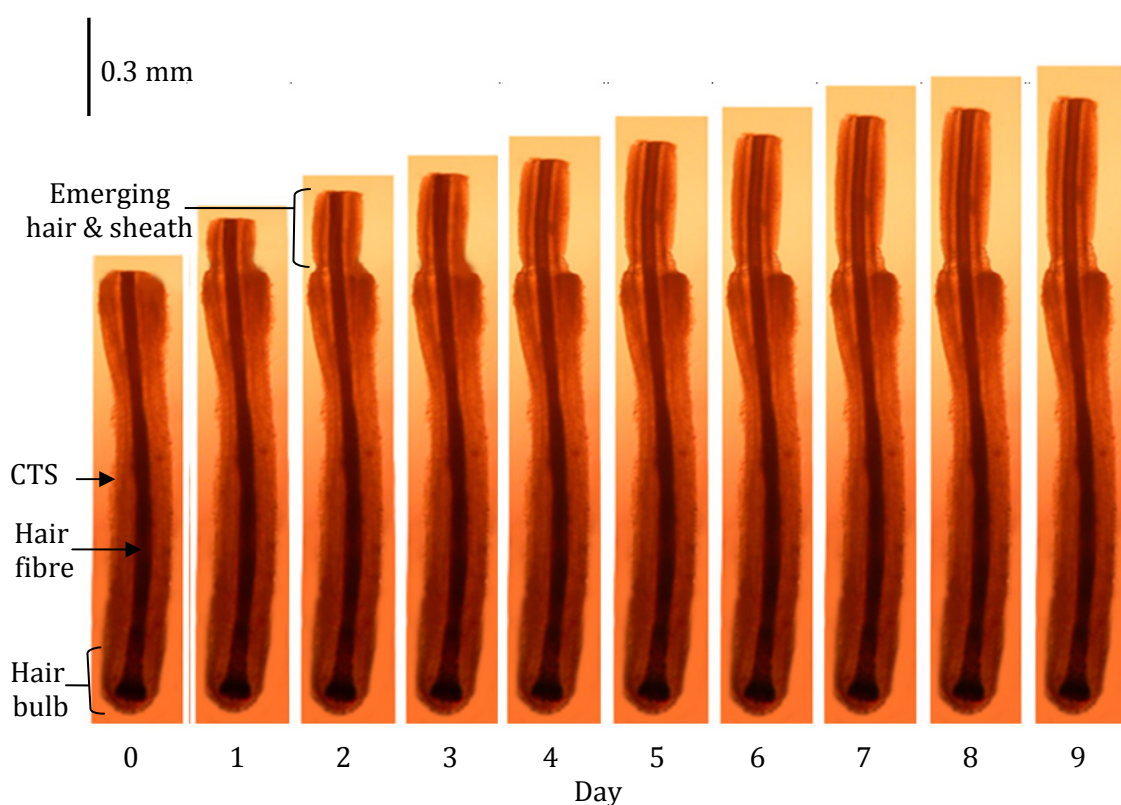
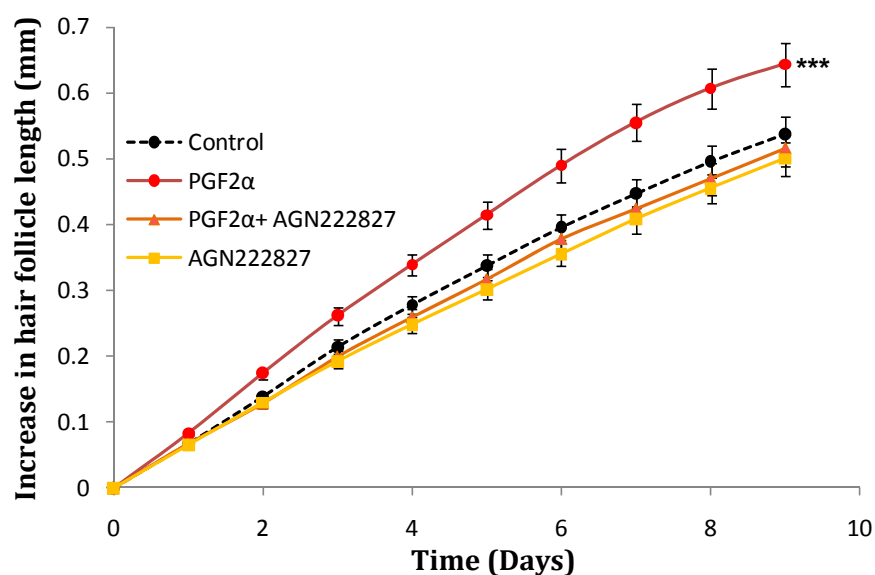


**Figure 31 The  $\text{PGF}_{2\alpha}$  receptor antagonists, AGN222827 and AL-8810, blocked  $\text{PGF}_{2\alpha}$ -stimulation of scalp hair follicle growth rate**

$\text{PGF}_{2\alpha}$  (100 nM) alone significantly increased the hair growth rate ( $P < 0.001^{***}$ ) in organ culture. This growth-stimulating effect of  $\text{PGF}_{2\alpha}$  (100 nM) was abolished when it was combined with the  $\text{PGF}_{2\alpha}$  receptor antagonists AGN222827 (1 $\mu\text{M}$ ) (a) and AL-8810 (10 $\mu\text{M}$ ) (b) ( $P < 0.001^{***}$ ). Results are the mean  $\pm$  SEM of 5 individuals; at least 6 follicles were examined per person per condition. Statistical analysis was performed using a two-factor within-subjects ANOVA using SPSS after confirming normal distribution, using KS-test.

**(a) AGN222827**



**(b) AL-8810**

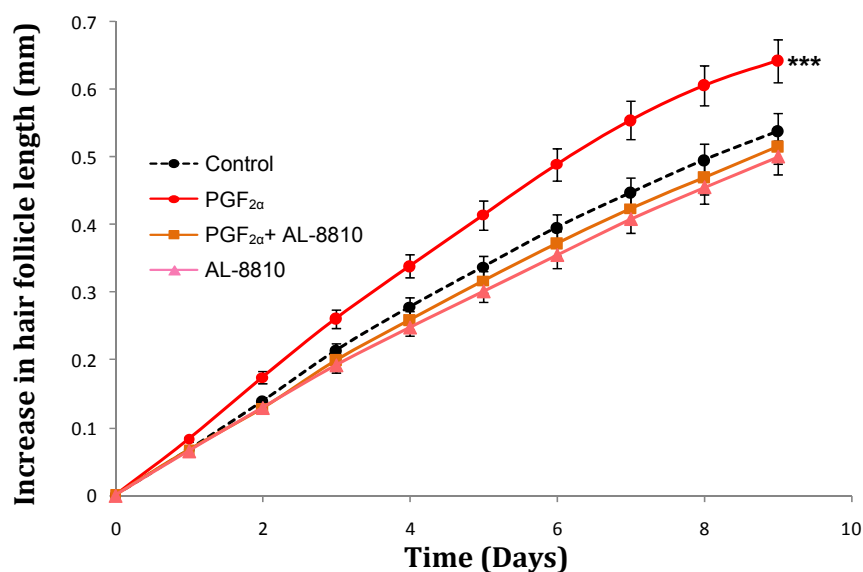
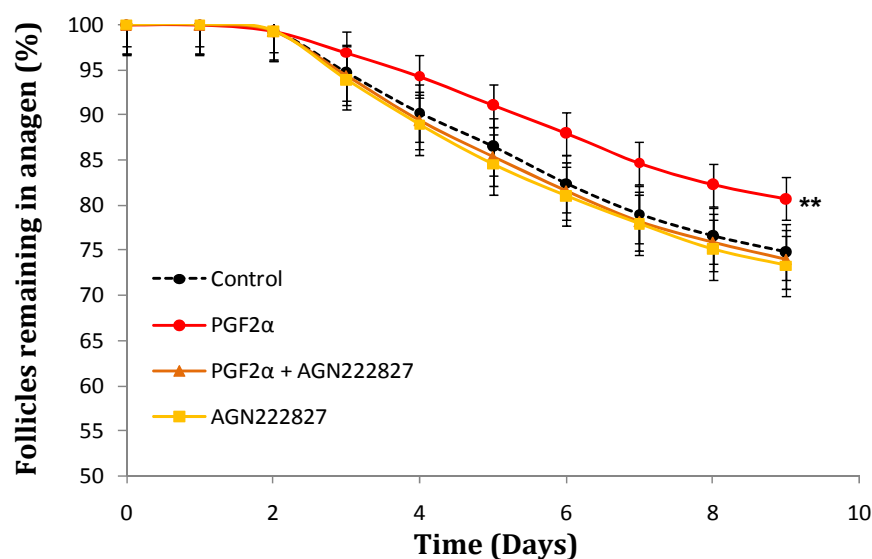


**Figure 32 PGF<sub>2α</sub> receptor antagonists, AGN222827 and AL-8810, blocked the PGF<sub>2α</sub>-promoted increase in % of scalp hair follicles in anagen**

PGF<sub>2α</sub> (100 nM) alone significantly increased the the percentage of follicles in anagen (P< 0.01\*\*), but this effect was abolished when it was combined with the FP antagonists AGN222827 (1μM) (a) and AL-8810 (10μM) (b) (P< 0.01\*\*). Values are the mean ± SEM of 5 individuals; at least 6 follicles were examined per person for each condition. Statistical analysis was performed using a two-factor within-subjects ANOVA using SPSS after confirming normal distribution, using KS-test.

**(a) AGN222827**



**(b) AL-8810**

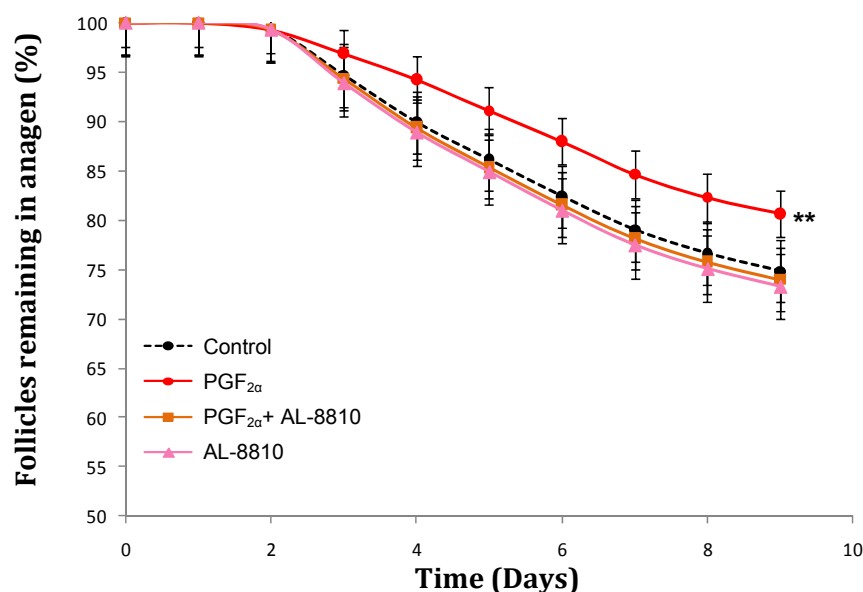
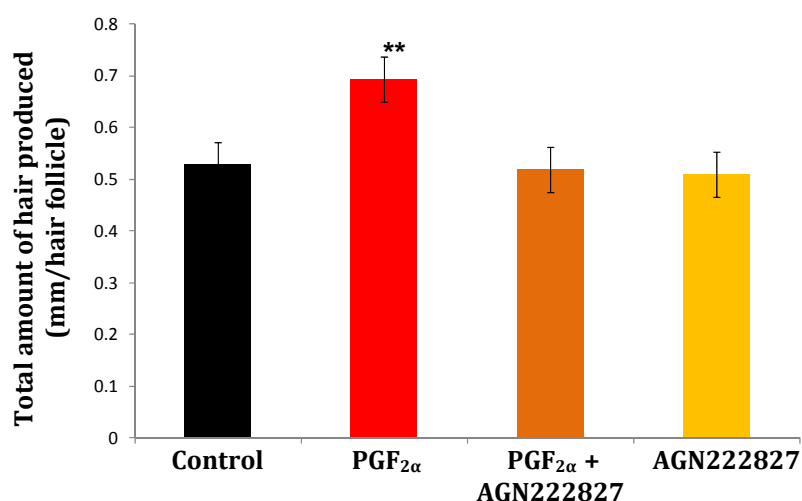


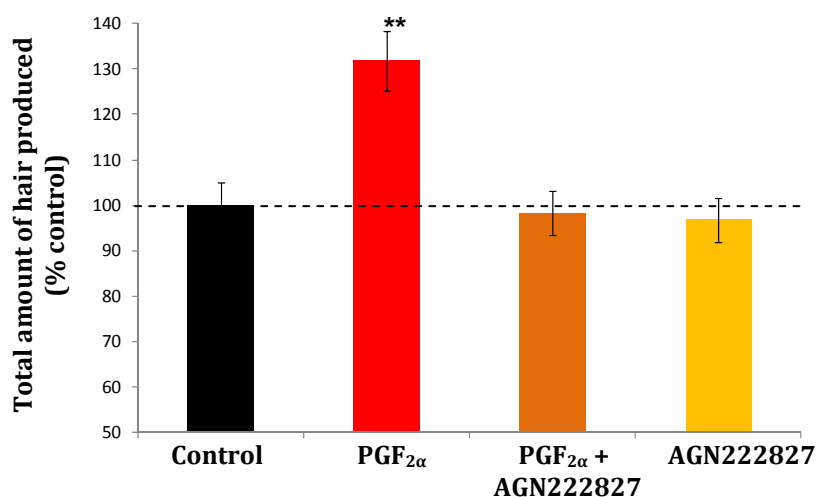
**Figure 33 The PGF<sub>2α</sub> receptor antagonists AGN222827 and AL-8810 blocked PGF<sub>2α</sub>-stimulated increased total amount of hair production**

PGF<sub>2α</sub> (100 nM) increased the overall amount of hair synthesised in organ culture by about 32% ( $P < 0.01^{**}$ ), but the FP antagonists AGN222827 at 1μM (**a, b**) and AL-8810 at 10μM (**c, d**) both abolished this response ( $P < 0.01^{**}$ ). Results are expressed as mean actual values (a, c) or as a % of their own control follicles (b, d). Values are the mean  $\pm$  SEM of 5 individuals; at least 6 follicles were examined per person for each condition. Statistical analysis was performed using a two-factor within-subjects ANOVA using SPSS after confirming normal distribution, using KS-test.

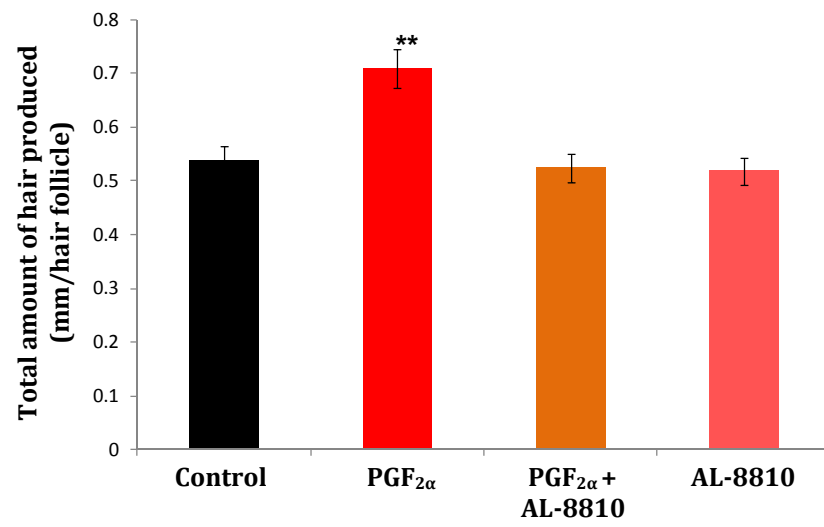
**(a) AGN222827**



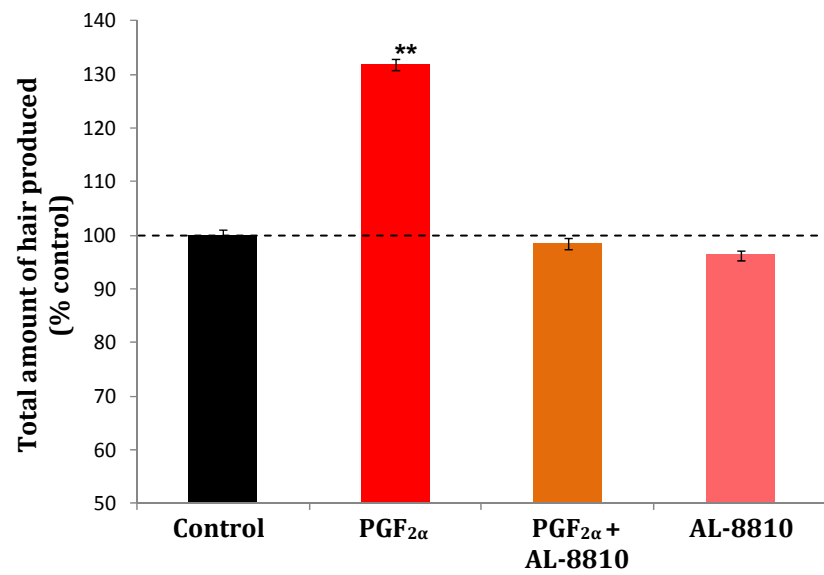
**(b) AGN222827**



**(c) AL-8810**



**(d) AL-8810**



### **3.2 Histological investigation of deer and human skin**

To become familiar with the structure of the skin and hair follicle, Saccpic staining was carried out on horizontal and vertical frozen skin sections from deer and human skin (as described in section 2.1.4). Deer skin was used first to learn the techniques of cryosectioning and histology because the skin is readily available without ethical difficulties and contains large hair follicles which are less difficult to orientate to obtain appropriate vertical sections than the smaller human follicles. Saccpic is a histochemical stain in which a number of different dyes are involved to differentiate hair follicle components (Nixon, 1993; Nutbrown & Randall 1996). The general structure of the anagen follicles showed a thin epidermis in both species and the stained hair follicles were prominent within obvious blue/green stained dermis (Figure 34 & 35). In the hair bulb, the dermal papilla was surrounded by the hair matrix and the hair fibre was surrounded by the inner and outer root sheaths. The connective/dermal sheath encapsulated the entire follicle separating it from the dermis. These hair follicle layers were differentiated by Saccpic staining, with the inner root sheath staining bright red, the outer root sheath blue and the connective tissue sheath dark blue with black/blue nuclei. Also, fully keratinised parts of hair and epidermis were stained yellow.

The histological staining of human scalp hair and red deer neck hair follicles indicated that the overall structure of the follicles were similar. However, there were a few differences between them; human hair follicles were visibly much smaller than the deer hair follicles, but lacked an obvious medulla like that present within the deer hair which could be seen in both vertical (Figure 34c) and midway cross sections (Figure 34d). Deer skin also had a thicker dermis while human skin



had a thicker fat layer. Cross-sections of human skin (Figure 35e) also revealed additional grouping of follicles in trios.

### Figure 34 Structure of red deer skin

**(a) Photograph of red deer skin.** This side view shows the general skin structure with intact anagen follicles penetrating into the dermis. (Scale bar = 500 $\mu$ m)

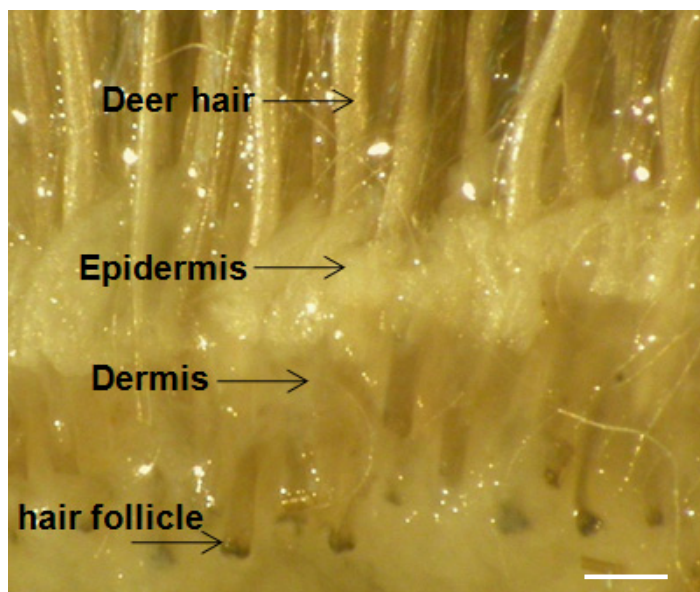
#### **(b) Photomicrograph of vertical cryosection of red deer skin**

This shows a thin epidermis (E) with longitudinal hair follicles extending into the thick dermal layer (D). The structure of hair follicle components are highlighted by the Saccpic stain including the red inner root sheath (IRS) and the hair fibre (H). (Scale bar = 200 $\mu$ m)

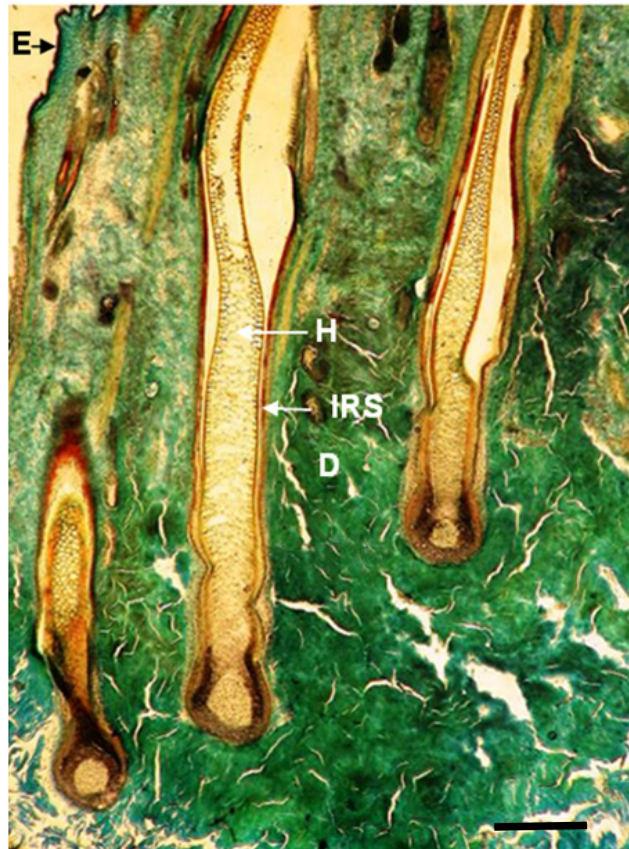
**(c) The structure of an anagen hair bulb and lower follicle.** This vertical cryosection stained with Saccpic shows the dermal papilla (DP), hair matrix (M), connective tissue sheath (CTS), which encapsulates the entire follicle separating it from the dermis, hair medulla (MD), inner root sheath (IRS) and the outer root sheath (ORS). (Scale bar = 100 $\mu$ m)

**(d) A cross section through an anagen hair follicle about half way up the follicle.** The Saccpic staining shows the hair cortex (C), medulla (M), the red inner root sheath (IRS), the outer root sheath (ORS) and the connective tissue sheath (CTS). (Scale bar= 100 $\mu$ m).

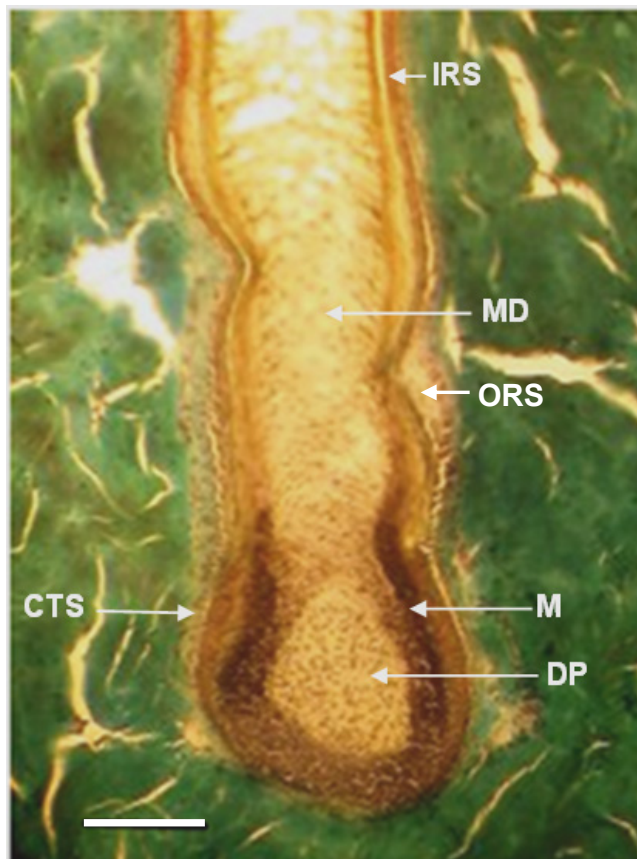
**(a)**



(b)



(c)



(d)

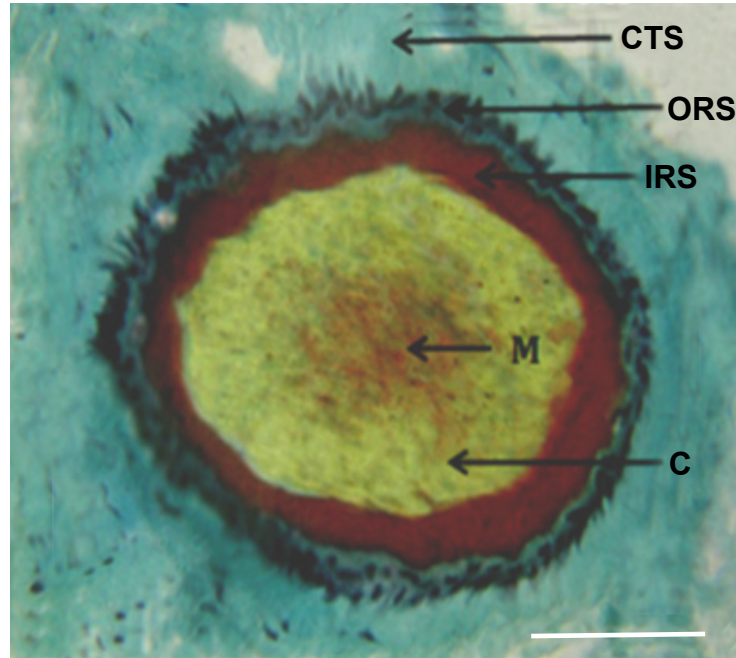


### **Figure 35 Structure of human scalp skin**

**(a) Photograph of intact human scalp skin.** This shows the general skin structure with longitudinal hair follicles (HF) which extend into subcutaneous fat layer (SF), a thin epidermis (E), and a thick dermis (D) composed of collagen. (Scale bar = 350µm)

Right is a higher magnification of an isolated hair follicle displaying the connective tissue sheath (CTS), pigmented matrix (M) in the hair bulb and the dark pigmented hair fibre (HF). (Scale bar = 150µm)

**(b) Saccpic stained cryosection of human scalp skin.** Histology highlights a longitudinal hair follicle which extends into the subcutaneous fat layer (SF) with its attachment to the sebaceous gland (SG); a thin epidermis (E), a thick dermis below with bright blue stained collagen (C) and also some of the components of the hair follicle including the outer root sheath (ORS), inner root sheath (IRS), connective tissue sheath (CTS) and the hair fibre (H). (Scale bar = 200µm).

**(c) The structure of an anagen hair bulb.** The dermal papilla (DP) is connected to the connective tissue sheath (CTS) at its base and surrounded by the matrix (M). The hair bulb is deep within the skin located in the subcutaneous fat (SF). (Scale bar = 150µm)

**(d) Higher magnification photomicrograph of an anagen mid follicle.** The Saccpic staining clearly highlights the structures of the yellow keratinised hair fibre (KHF), the dark hair medulla (MD), the red inner root sheath (IRS), the green outer root sheath (ORS) and the sebaceous glands (SG). (Scale bar = 150µm)

**(e) Horizontal section of mid human scalp skin stained with Saccpic.**

Bundles of hair follicles can be seen in cross-sections of the follicles demonstrate the dermis, yellow keratinised hair fibre surrounded by the red stained inner layer of the inner root sheath (IRS), blue outer root sheath (ORS) and darker blue connective tissue sheath (CTS). (Scale bar = 150µm)

**(f) Higher magnification of a follicle horizontal section located in the mid part of the hair follicle.**

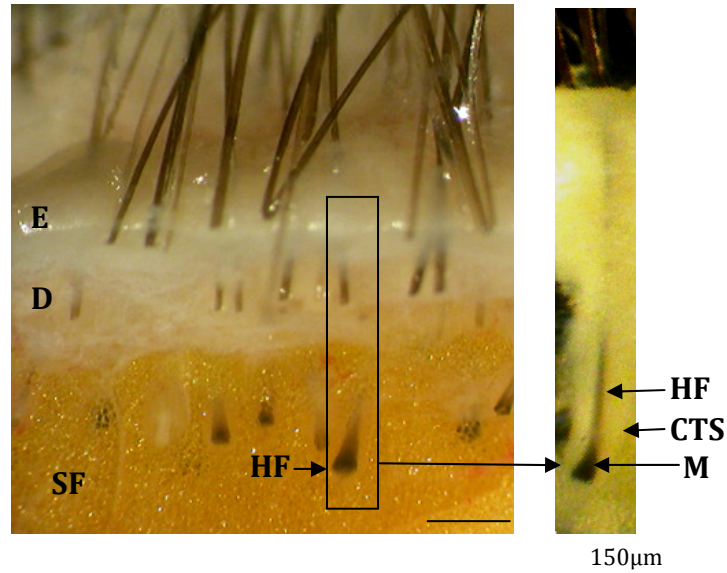
This shows a fully keratinised yellow hair fibre, the hair shaft medulla and cortex, hair shaft cuticle, inner root sheath (IRS) cuticle, Huxley's and Henle's layers of the

inner root sheath, the outer root sheath (ORS) and connective tissue sheath (CTS) which surrounded the follicle and separated it from the dermis. (Scale bar = 100 $\mu$ M)

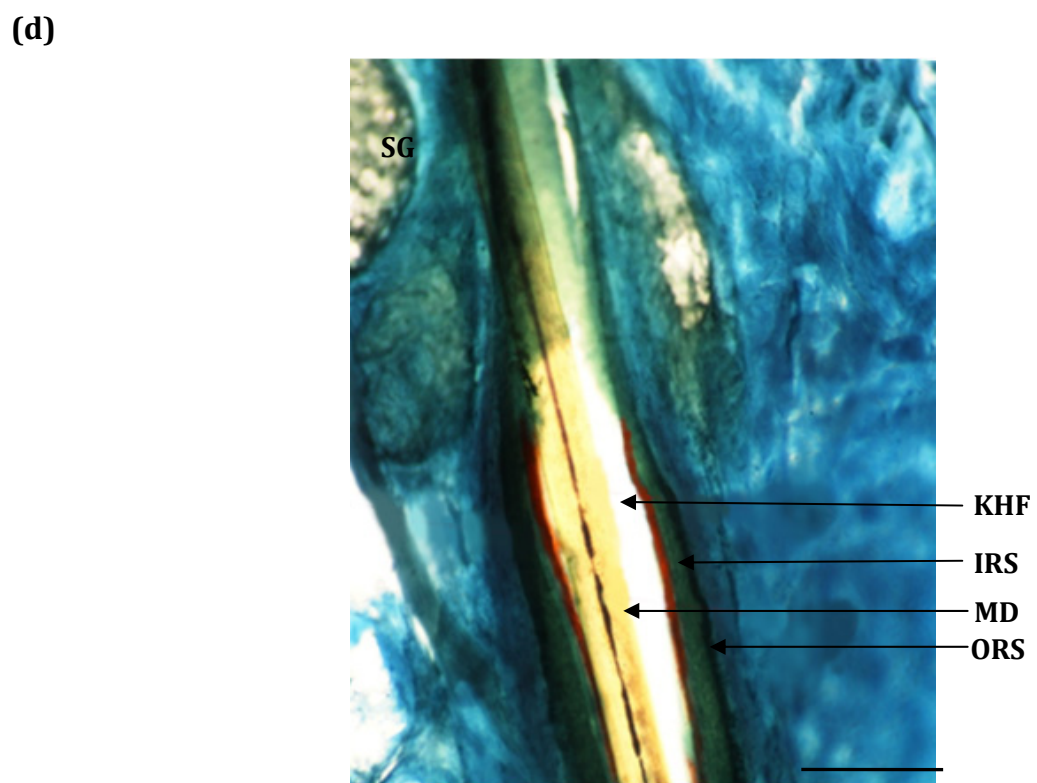
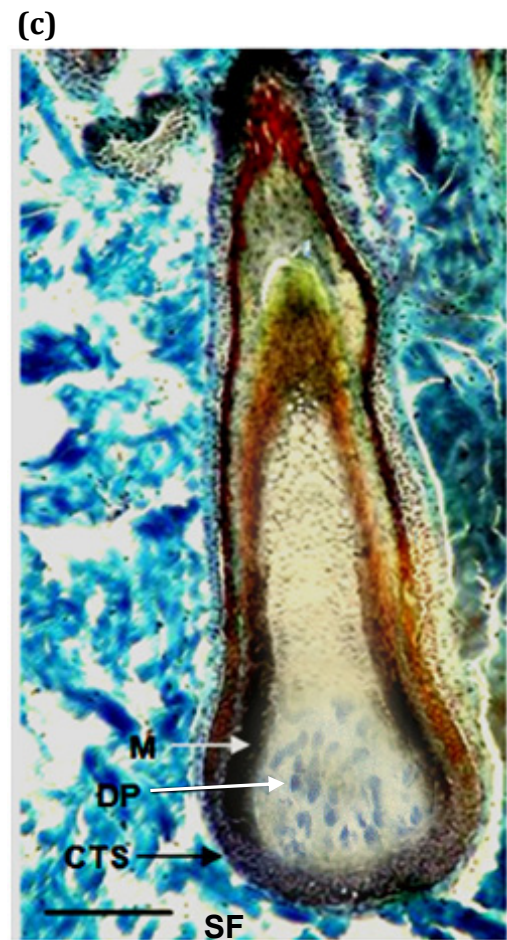
**(g) Compilation of longitudinal human hair follicles with the relevant cross sections at different levels.**

The upper part of the follicles just below the sebaceous gland duct showed the connective tissue sheath (CTS), the outer root sheath (ORS), the inner root sheath (IRS) and the keratinised hair fibre (KHF). The hair bulb region showed the dermal papilla (DP) which was located in the centre surrounded by the epithelial matrix (M) cells; both are encapsulated by the connective tissue sheath (CTS). The connective tissue sheath was present in all cross and longitudinal sections, separating the hair follicle components from the dermis and the subcutaneous fat. (Scale bar = 200 $\mu$ M)

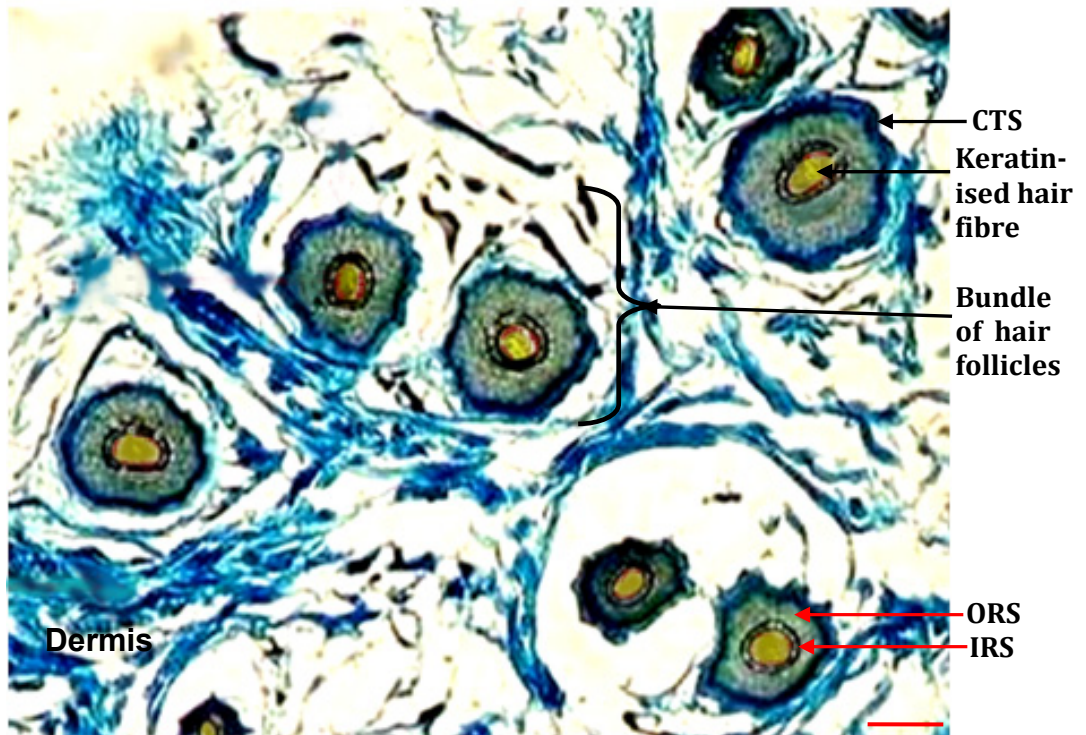
**(a)**



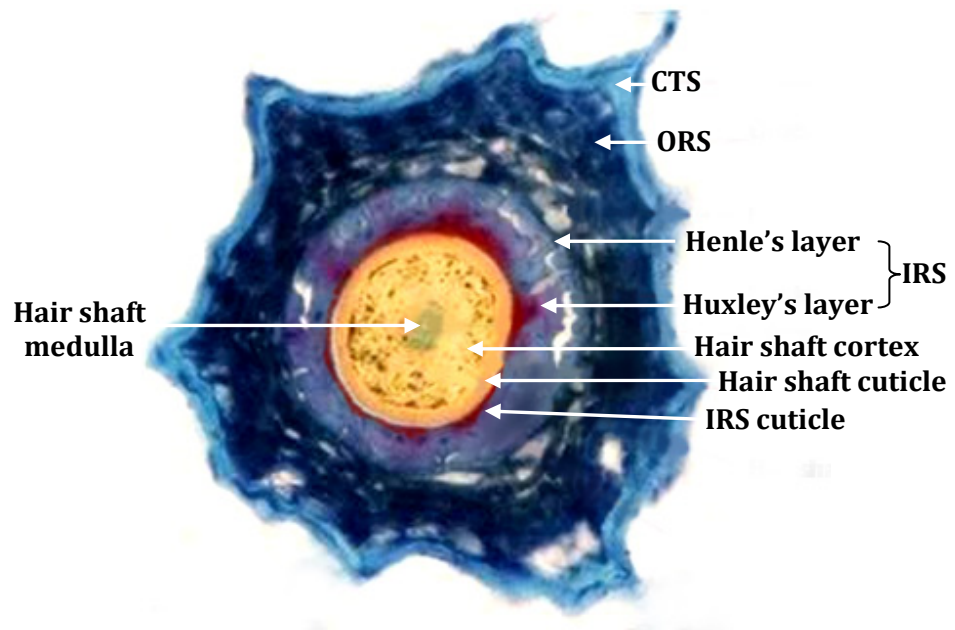




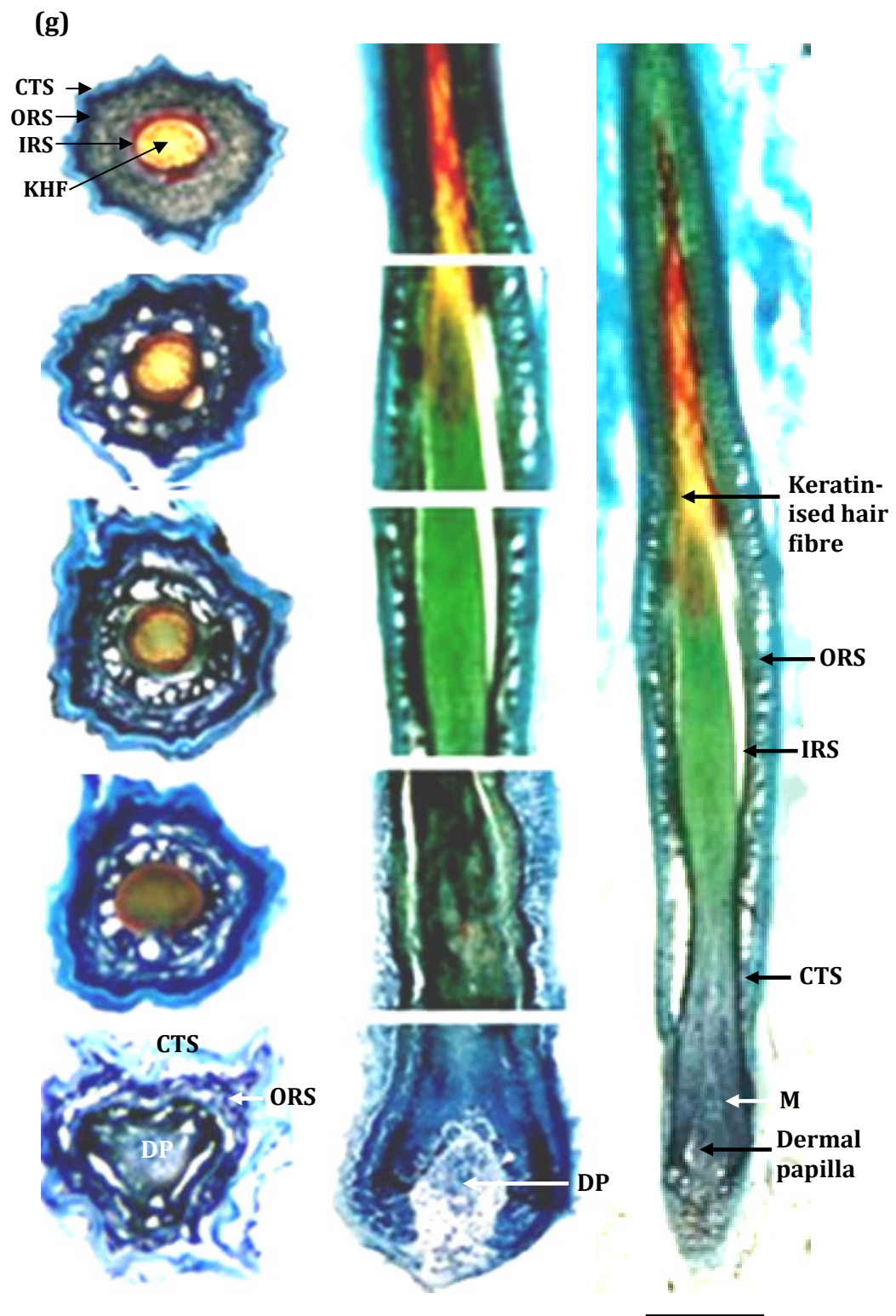
(e)



(f)







### **3.3 Location of cytokeratins 5 & 6 in human scalp hair follicles**

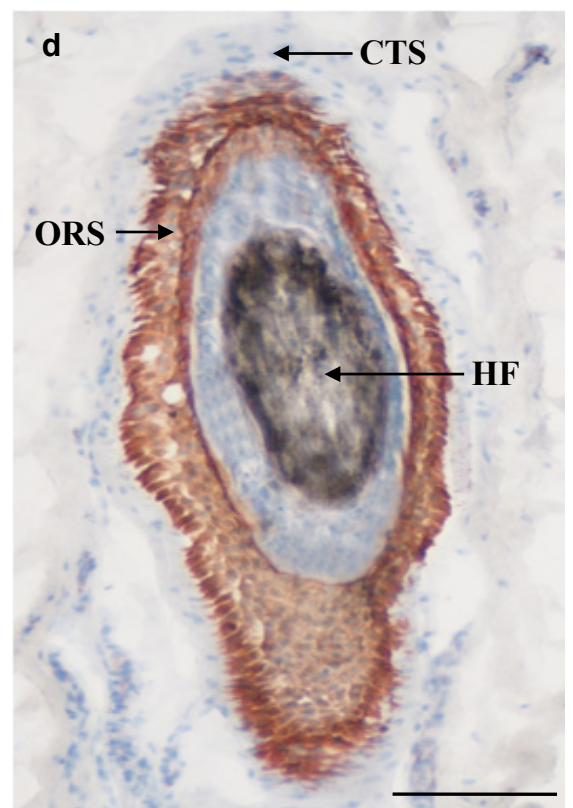
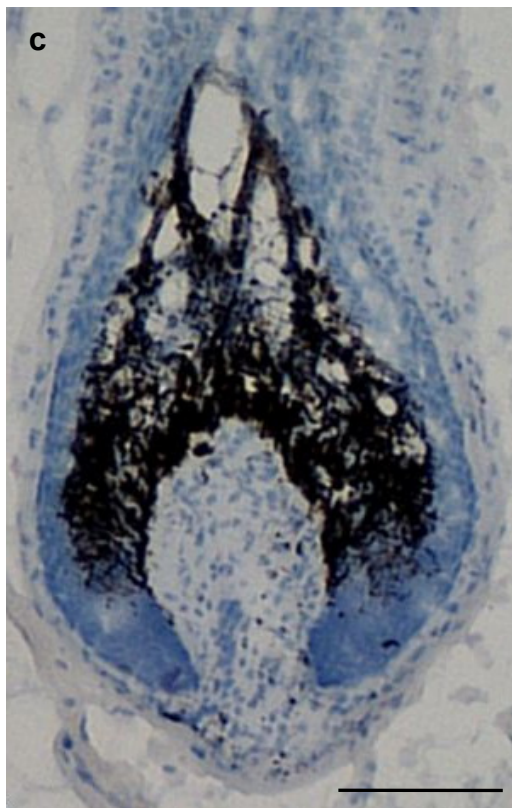
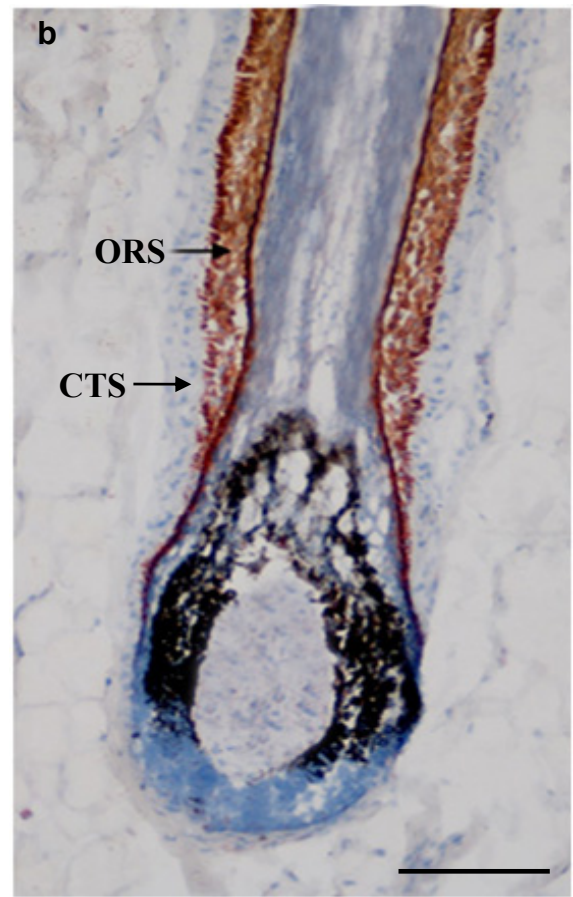
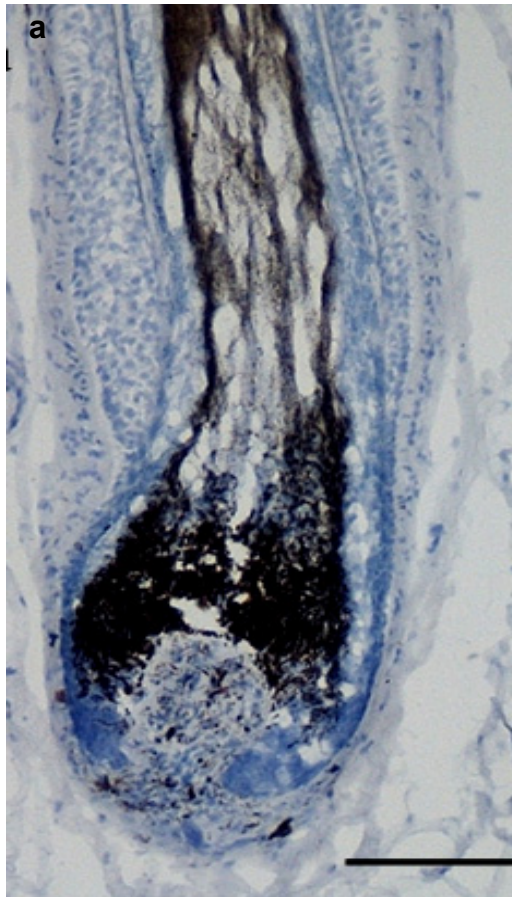
Immunohistochemical analysis of human scalp hair follicle cryosections were used to investigate the location of cytokeratins 5 & 6. An antibody for these highly expressed antigens was used to master the immunohistochemistry techniques. A goat polyclonal anti-cytokeratins 5 & 6 antibody was optimised for use at a 1:50 dilution. As described in section 2.1.5.1, three negative controls were carried out. The first two were to determine whether either the primary antibody alone or the AEC colour system caused colour development, but neither showed any non-specific staining. There was also no non-specific staining in the third negative control (Figure 36a, c) in which 1.5% NMS/PBS was used instead of the primary antibody to determine whether the secondary antibody was causing non-specific binding.

Cytokeratin 5/6 was strongly expressed in the outer root sheath of the hair follicle (Figure 36b, d).

### **Figure 36 Location of cytokeratins 5 & 6 in human scalp hair follicle**

Expression of cytokeratin 5/6 was detected by immunohistochemistry using a goat polyclonal anti-cytokeratins 5 & 6 antibody diluted 1:50. Before application of the antibody, the tissue's non specific binding sites were first blocked with 5% (v/v) normal mouse serum in PBS. Sections were counterstained with Harris's haematoxylin and blued in Scott's tap water.

- (a)** Absence of staining in the negative control where 1.5% normal mouse serum/PBS replaced the primary antibody. (Scale bar = 150µm)
- (b)** Cytokeratin 5/6 expression in human scalp skin. Positive red staining present only in the outer root sheath (ORS) of the hair follicle. (Scale bar = 150µm)
- (c)** Negative control. (Scale bar = 100µm)
- (d)** Horizontal section of mid human scalp hair follicle shows location of cytokeratin 5 & 6 in outer root sheath (ORS). CTS: connective tissue sheath, HF: hair fibre (Scale bar = 150µm).



### **3.4 Expression of NKI-beteb in human scalp hair follicles**

To determine the location of hair follicle melanocytes, as these are potential targets for prostaglandin regulation, the expression of NKI-beteb was investigated in human scalp skin by immunohistochemistry using a mouse monoclonal primary antibody to human melanoma associated antigen, NKI-beteb at 1:10 dilution, after extensive optimisation. Prior to antibody application the sections were blocked with 1% normal goat serum in PBS.

Three negative controls were carried out as described in section 2.1.5.1. There was some non-specific staining when 1% normal goat serum/PBS replaced the primary antibody, therefore the concentration of the blocking serum was increased to 10% to reduce background staining.

NKI-beteb was expressed in melanocytes in the hair bulb matrix above and around the upper portion of the dermal papilla (Figure 37b). No staining was observed in other parts of the skin. There was also no non-specific staining in the negative control (Figure 37a) when the primary antibody was replaced with 1% normal goat serum/PBS.



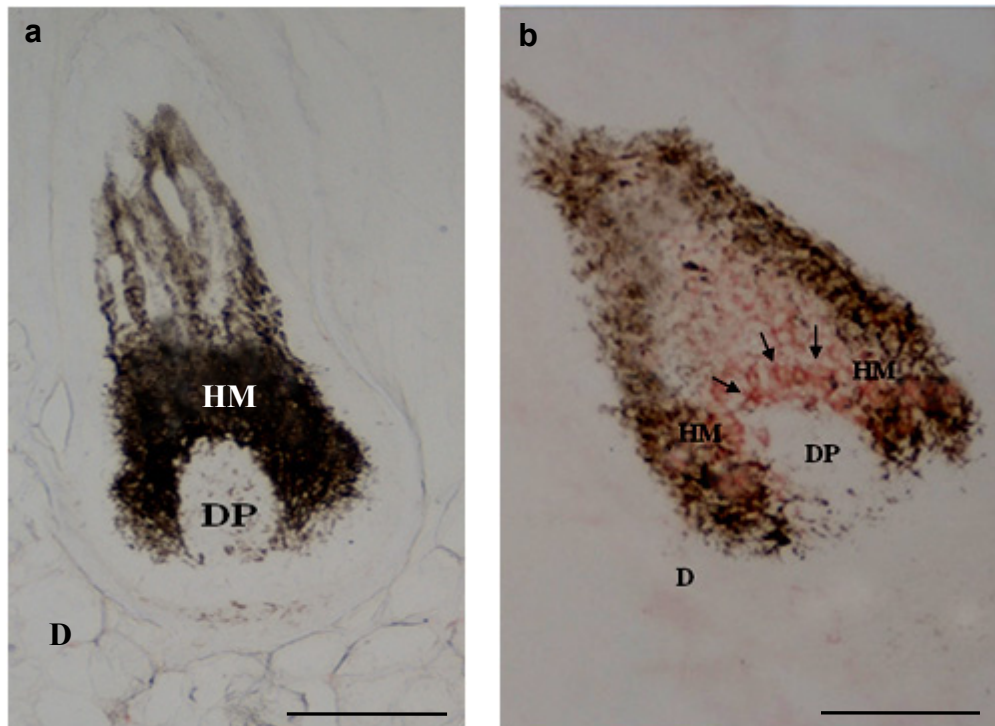
### Figure 37 Location of NKI-beteb expression in scalp hair follicles

Immunohistochemistry was performed using a mouse monoclonal primary antibody to human melanoma associated antigen; NKI-beteb (1:10 dilution).

**(a)** Absence of staining in the negative control in the hair bulb when the primary antibody was replaced with 1% normal goat serum. (Scale bar = 150µm)

**(b)** Red stain indicating expression of NKI-beteb in the hair bulb, staining was predominantly seen in the matrix above, and around, the upper portion of the dermal papilla as indicated by the arrows.

**D:** dermis, **DP:** dermal papilla and **HM:** hair matrix. (Scale bar = 150µm)



### **3.5 Immunohistochemical localisation of prostaglandin F<sub>2α</sub> receptor (FP) in anagen scalp hair follicles**

The expression of the protein for FP was investigated in lower human hair follicles by immunohistochemistry using two polyclonal antibodies (goat polyclonal anti-human PGF<sub>2α</sub>R (N-18 & T-15) antibodies). Both of these antibodies had to be optimised since they had not previously been used for this technique. A range of dilutions between 1:10 to 1:100 was investigated and 1:75 in 1.5% normal mouse serum was considered optimal for both antibodies.

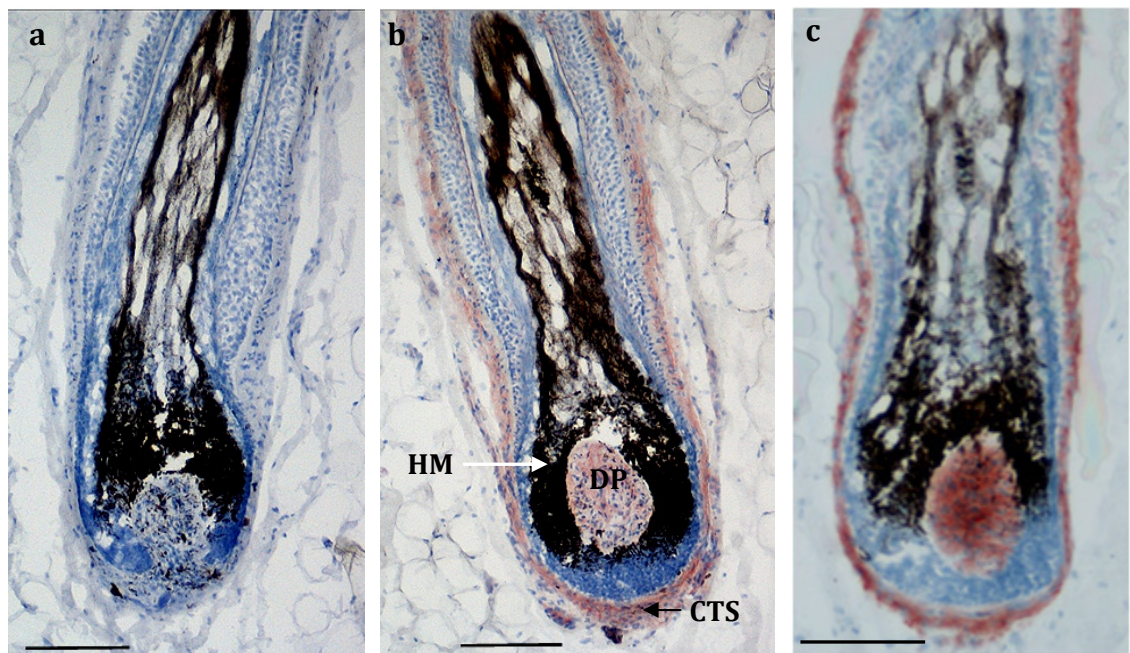
Immunostaining was detected in the cells of the dermal papilla and in the connective tissue sheath surrounding the hair bulb and lower follicle, but not in the epithelial cells or melanocytes of the hair bulb matrix in cryosections of scalp skin from 5 individuals with both antibodies (Figure 38b, c, e, f); no similar staining was seen when the primary antibodies were excluded (Figure 38a, d).

### Figure 38 Immunolocalisation of FP in the human scalp hair follicle bulb

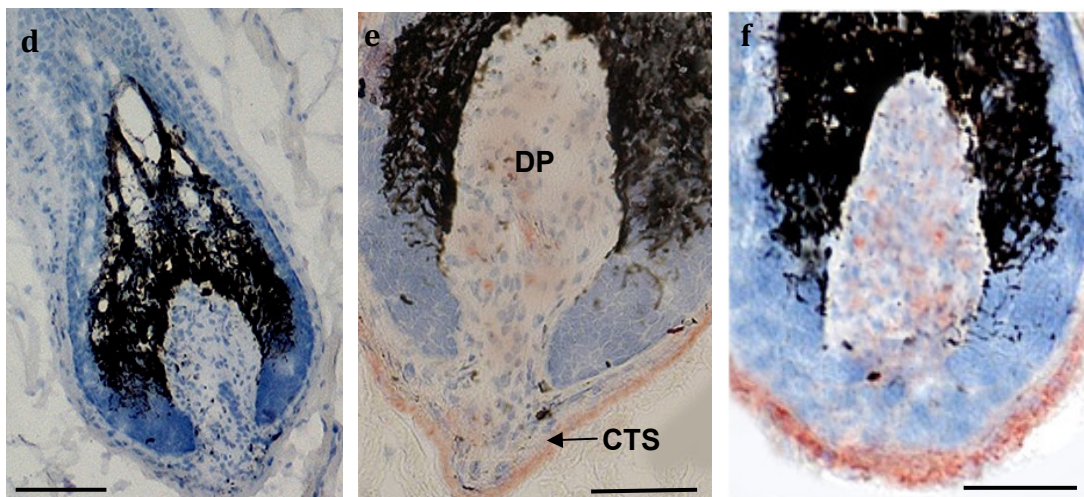
Immunohistochemical analysis of normal scalp cryosections localised FP protein in the hair bulb in the cells of the dermal papilla and connective tissue sheath (b, c, e, f) using two goat polyclonal anti-human FP antibodies diluted 1:75 in normal mouse serum. Sections were counter stained with Harris's haematoxylin and blued in Scott's tap water. Normal dark pigment (melanin) is visible in the hair bulb. Bulb components are labeled as follows: DP, dermal papilla; CTS, connective tissue sheath; HM, hair matrix. Red: positive staining; blue: haematoxylin counterstain.

No staining occurred in the hair bulb in the negative control when the primary antibodies were omitted (a, d). FP protein was localised in the hair bulb in the cells of the dermal papilla (DP) and connective tissue sheath (CTS) with PGF<sub>2α</sub>R (N-18) antibody (b, e) and with PGF<sub>2α</sub>R (T-15) antibody (c, f).

Scale bars a, b, c = 150 μm; d, e, f = 100 μm







### **3.6 Investigations to determine whether FP gene is expressed in the human scalp hair follicle using molecular biological methods**

RT-PCR was used to investigate the expression of FP genes in occipital scalp anagen hair follicles from 5 different adult male individuals. Non balding scalp hair follicles were isolated, poly(A<sup>+</sup>)RNA extracted and cDNA was prepared separately from each individual's sample. Each cDNA was prepared from 65 lower hair follicles per donor and each individual's hair follicles were investigated separately (Table 3). Anagen hair follicle microdissection as detailed in section 2.2.1.2, proved to be extremely difficult and time consuming, especially when the skin sample had been stored in *RNAlater* as the tissue becomes hard. Generally about ten clean, undamaged follicles were obtained in an hour, thus approximately a day had to be dedicated for each sample.

The quality of each RNA sample was checked by gel electrophoresis on a 1.5% agarose gel. The total RNA from each sample had sharp 28S and 18S rRNA bands and the 28S rRNA band was approximately twice as intense as the 18S rRNA band (Figure 39). This indicated that the RNA samples were of good quality as intact RNA has sharp bands and can be detected by this 2:1 ratio (28S:18S), while degraded RNA will not exhibit a 2:1 ratio, and a completely degraded RNA will appear as a very low molecular weight smear (Skrypina et al., 2003).

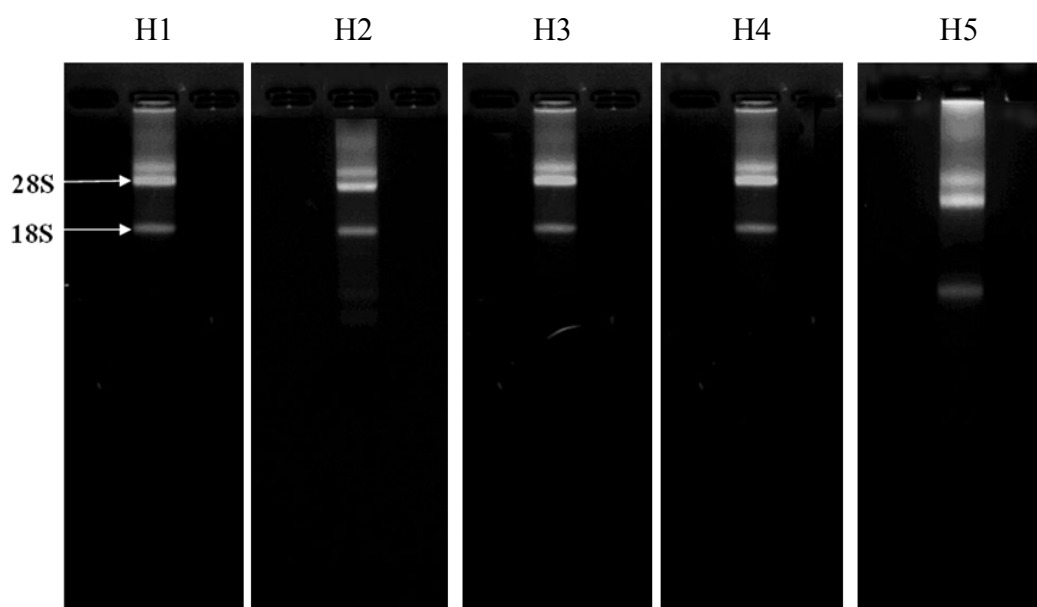
The concentration and purity of each total RNA sample was also checked spectrophotometrically (Table 3) before further purification was carried out to isolate poly(A<sup>+</sup>)RNA. To remove any contaminating genomic DNA the poly(A<sup>+</sup>)RNA samples were treated with DNase I and cDNAs were synthesised immediately using the avian myeloblastosis virus (AMV) reverse transcription system.

**Table 3 Human scalp skin samples used to prepare lower follicle RNA**

Human sample number	Gender	Age (Years)	Total RNA purity ( $A_{260}/A_{280}$ )	Total RNA concentration ( $\mu\text{g/ml}$ )
H1	Male	41	1.35	165
H2	Male	38	1.7	102
H3	Male	46	1.8	136
H4	Male	45	1.5	149
H5	Male	37	1.85	122

**Figure 39 Gel electrophoresis of RNA from human scalp follicles**

The success of the extractions were checked by gel electrophoresis of RNA, loading 10 $\mu\text{l}$  from each total RNA sample into a 1.5% agarose gel; 18S and 28S ribosomal RNA bands were obvious in the total RNA samples, exhibiting a 2:1 ratio.



### **3.6.1 RT-PCR results for $\beta$ -actin gene expression from human lower hair follicles**

Amplification of a positive control gene,  $\beta$ -actin, was carried out to investigate the cDNA quality of all the samples prior to investigating the expression of the FP gene. Human  $\beta$ -actin is a highly expressed housekeeping gene with 3432 bp length and 11 exons on chromosome 22 ([www.Ensemble.org](http://www.Ensemble.org)). Established  $\beta$ -actin primers that amplified 838 bp DNA molecules of exon 11 were used (Shorter et al., 2008). Successful  $\beta$ -actin gene expression would indicate that the isolated RNA was of sufficient quality and the cDNA suitable for further analysis.

Agarose gel electrophoresis of the PCR products (30  $\mu$ l) of hair follicle cDNAs prepared from isolated scalp hair follicles from each of 5 different individuals showed appropriately sized bands corresponding to  $\beta$ -actin (838 bp) (Figure 40). No bands were observed in the negative control in which the template cDNA was omitted from the PCR reaction mix. This indicated that the product bands resulted from the direct amplification of cDNA synthesised from the mRNA samples, and also showed that the reagents used in the PCR reaction mix were free from any DNA contamination.

To confirm the identity of the  $\beta$ -actin PCR products, sequence analysis of the PCR product was carried out. The  $\beta$ -actin PCR products showed 98% homology with the known human sequence (Figure 41). Using the chromatogram programme, each base is represented by a colour and the colour of the highest peak at each interval determines the base in the sequence. When two or more peaks happen at once and neither is significantly higher than the other, then the result is recorded as 'n' in the sequencing data. Therefore 'n' does not necessarily mean that an incorrect base is present.

**Figure 40 Gel electrophoresis of  $\beta$ -actin RT-PCR products from human scalp lower hair follicles**

$\beta$ -actin gene expression in cDNA from 5 human scalp lower hair follicle samples were investigated by RT-PCR using specific primers for  $\beta$ -actin, and 5 $\mu$ l of cDNA from each sample. The resulting PCR products were separated by agarose gel (1.5% w/v) electrophoresis and visualised with ethidium bromide staining. 10 $\mu$ l of molecular weight markers (100bp DNA ladder; 11 fragments ranging from 100–1,500bp) (lane 1) and 30  $\mu$ l of each person's PCR product (lanes 2-6) were loaded on to the gel. A negative control where cDNA was excluded from the PCR reaction mix was loaded on to lane 7. All PCR products showed appropriately sized bands (838 bp) corresponding to  $\beta$ -actin gene.

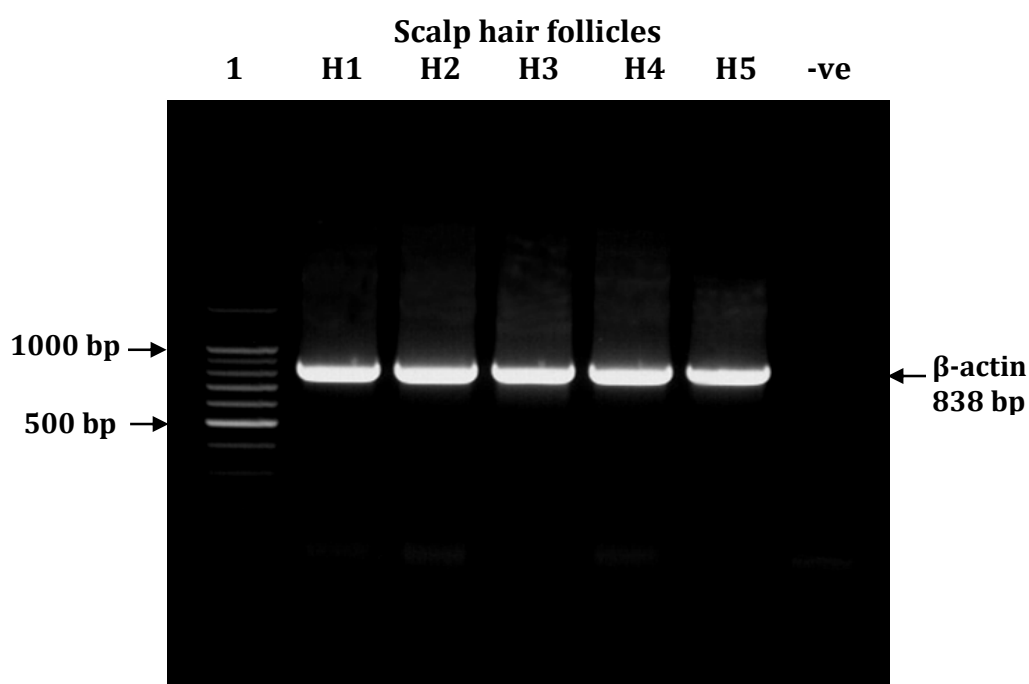


## Figure 41 Sequencing results for $\beta$ -actin RT-PCR product amplified from human hair follicle mRNA

The PCR products of  $\beta$ -actin gene amplification using human hair follicle cDNA were separated by gel electrophoresis and a band of the expected amplification size (838 bp) was cut out from the gel; the DNA was purified and sent for sequencing to check its identity. The NCBI BLAST program was then used to align the sequenced product (query: red) against the known human  $\beta$ -actin sequence (subject: black). The matching bases between the two sequences are indicated by a bar. The homology of the sequenced PCR product to the known human  $\beta$ -actin sequence is 98%.

```

Query: 2   tgtggccccgaggagcaccgcgtgctgctgaccgaggccccctgaacccaaggccaa 61
          |||||  |||||  |||||  |||||  |||||  |||||  |||||  |||||  |||||  |||||
Sbjct: 33  tgtggctcccgaggagcaccgcgtgctgctgaccgaggccccctgaacccaaggccaa 92

Query: 62   ccgagagaagatgacncagattatgtttgagaccttcaacaccccagccatgtacgtngc 121
          |||||  |||||  |||||  |||||  |||||  |||||  |||||  |||||  |||||  |||||
Sbjct: 93   ccgcgagaagatgaccagatcatgtttgagaccttcaacaccccagccatgtacgttgc 152

Query: 122  tatccaggctgtgctatccctgtacgcctctggccgtaccactggcattgtgatggactc 181
          |||||  |||||  |||||  |||||  |||||  |||||  |||||  |||||  |||||  |||||
Sbjct: 153  tatccaggctgtgctatccctgtacgcctctggccgtaccactggcatcgtgatggactc 212

Query: 182  nggtgacggggtcaccacactgtgcccattctacgaggggtatgcctcccccatgccat 241
          |||||  |||||  |||||  |||||  |||||  |||||  |||||  |||||  |||||  |||||
Sbjct: 213  cggtgacggggtcaccacactgtgcccattctacgaggggtatgcctcccccatgccat 272

Query: 242  cctgcgctctggacctggctggcgggacctgactgactacctcatgaagatcctcaccga 301
          |||||  |||||  |||||  |||||  |||||  |||||  |||||  |||||  |||||  |||||
Sbjct: 273  cctgcgctctggacctggctggcgggacctgactgactacctcatgaagatcctcaccga 332

Query: 302  gcgcggctacagcttcaccaccacggccgagcgggaaatcgtgcgtagacattaaggagaa 361
          |||||  |||||  |||||  |||||  |||||  |||||  |||||  |||||  |||||  |||||
Sbjct: 333  gcgcggctacagcttcaccaccacggccgagcgggaaatcgtgcgtagacattaaggagaa 392

Query: 362  gctgtgctacgtcgccctggacttcgagcaagagatggccaengctgcttcengctcttc 421
          |||||  |||||  |||||  |||||  |||||  |||||  |||||  |||||  |||||  |||||
Sbjct: 393  gctgtgctacgtcgccctggacttcgagcaagagatggccaengctgcttcengctcttc 452

Query: 422  tctggagaagagct 435
          |||||  |||||  |||||  |||||  |||||  |||||  |||||  |||||  |||||  |||||
Sbjct: 453  cctggagaagagct 466

```

### **3.6.2 Validation of the RT-PCR for FP gene expression using rat liver tissue**

A new specific set of forward and reverse primers for FP genes were designed as described in section (2.2.1.6). The designed primers to detect the FP gene were first checked on rat liver tissue cDNA which is known to express the FP gene (Arend *et al.*, 2005; Koukoui *et al.*, 2006). Rat liver was used first as a positive control tissue as it was available and easy to prepare compared to human hair follicle cDNA. An amplified band of the expected size for FP gene (1100bp in rat) was obtained after agarose gel electrophoresis (Figure 42). No bands were observed in the negative control in which the template cDNA was excluded from the PCR reaction mix.

### **3.6.3 Expression of the genes for FP in human hair follicles using RT-PCR**

Following successful detection of gene expression in rat liver, FP gene expression was investigated in human scalp hair follicles. Extensive optimisation of the RT-PCR experimental conditions were carried out which are described in section 2.2.1.5 and the resulting PCR products were separated by 1.5% agarose gel electrophoresis. All 5 human scalp lower hair follicle cDNA samples produced PCR products which corresponded to the expected amplification size (1080 bp) in human tissue (Figure 43). There were no bands in the negative control in which the cDNA was replaced with nuclease-free water.

The identities of the FP gene PCR products were checked by sequence analysis. The comparison with the known expected human FP gene sequence using NCBI BLAST program showed that the human hair follicle FP gene PCR product had 99% homology to the known human FP gene sequence after adjusting the similar peaks with the chromatogram programme as described in 3.7.1 (Figure 44).

**Figure 42 Gel electrophoresis of FP gene RT-PCR product from rat liver cDNA**

FP gene expression in mRNA from rat liver tissue sample was investigated using RT-PCR. Specific primers for the FP gene were used with 5  $\mu$ l cDNA. The PCR products were analysed using 1.5% agarose gel electrophoresis and visualised with ethidium bromide staining. **Lane 1** – 100-1500 bp molecular weight marker (10  $\mu$ l), **lane 2** – blank, **lane 3** – rat liver tissue FP gene PCR product (30  $\mu$ l). **Lane 4** – negative control (30  $\mu$ l) in which cDNA was excluded from the PCR reaction mix. The expected amplicon size is 1100 bp.

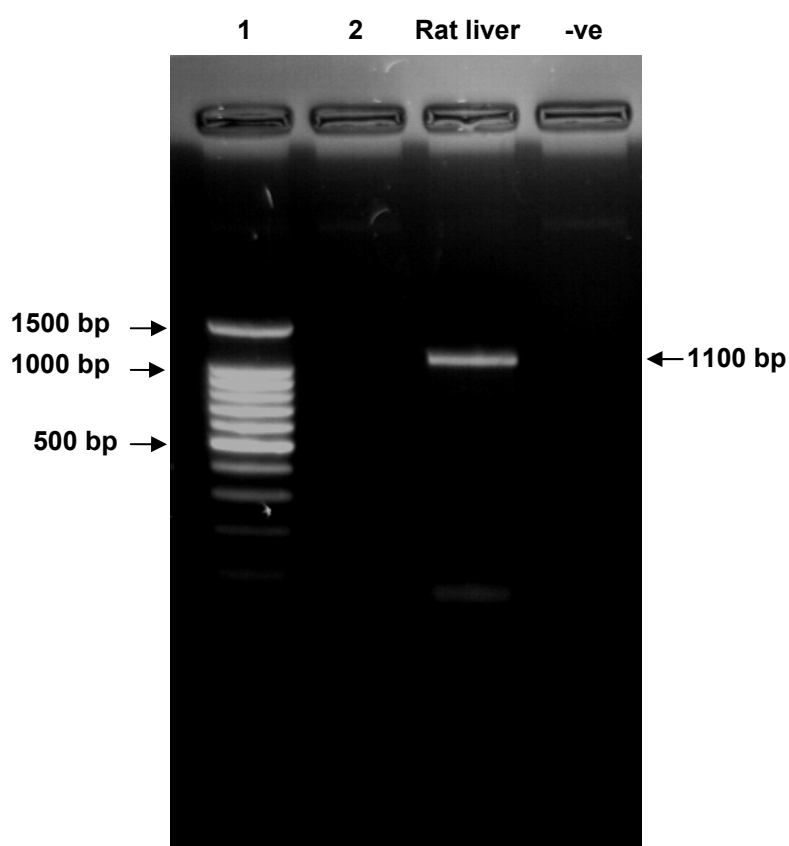




**Figure 43 Human anagen hair follicles expressed the gene for FP**

FP gene expression in mRNA from 5 human anagen lower hair follicle samples was investigated using RT-PCR. Specific primers for FP gene were used with 10  $\mu$ l cDNA. The PCR products were analysed using 1.5% agarose gel electrophoresis. 10  $\mu$ l of DNA ladder 100-1500 bp (lanes 1 & 8) and 30  $\mu$ l of each person's PCR product (lanes 2-6) were loaded on to the gel. A negative control where cDNA was excluded from the PCR reaction mix was loaded on to lane 7. All PCR products showed appropriately sized bands (1080 bp) corresponding to FP gene.

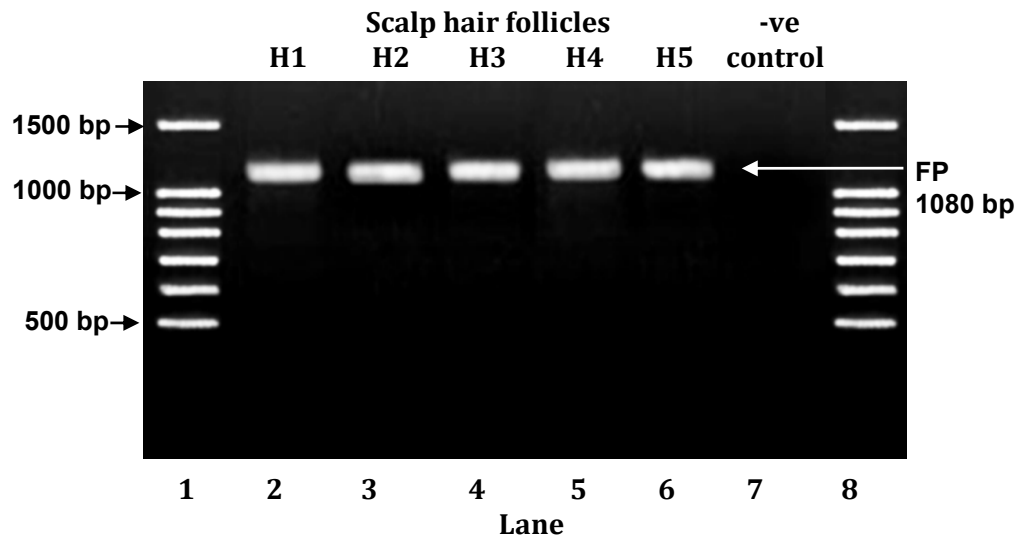


**Figure 44 Sequencing results for FP RT-PCR product amplified from human hair follicle cDNA, compared to known human sequence**

To confirm the identity of the PCR products, the products were separated by agarose gel electrophoresis and the band of expected amplicon size (1080 bp) was excised from the gel, DNA extracted and purified and sent for sequence analysis for identification. The NCBI BLAST programme was used to align the sequenced product (query: red) against the known human FP gene sequence (subject: black). The bases that match in the two sequences are shown by a vertical line. The FP PCR product of the human hair follicle exhibited 99% homology to the known human FP gene sequence.

Query	1	GCGCTTCTTTCAAACACAACCTGCCAGACGGAAACCGGCTTTCGGTATTTTTTTCAGTA	60
Sbjct	43	GCGCTTCTTTCAAACACAACCTGCCAGACGGAAACCGGCTTTCGGTATTTTTTTCAGTA	102
Query	61	ATCTTCATGACAGTGGGAATCTTGTCAAACAGCCTTGCCATCGCCATTCTCATGAAGGCA	120
Sbjct	103	ATCTTCATGACAGTGGGAATCTTGTCAAACAGCCTTGCCATCGCCATTCTCATGAAGGCA	162
Query	121	TATCAGAGATTTAGACAGAAGTCCAAGGCATCGTTTCTGCTTTTGGCCAGTGGCCTGGTA	180
Sbjct	163	TATCAGAGATTTAGACAGAAGTCCAAGGCATCGTTTCTGCTTTTGGCCAGTGGCCTGGTA	222
Query	181	ATCACTGATTTCCTTGGCCATCTCATCAATGGAGCCATAGCAGTATTTGTATATGCTTCT	240
Sbjct	223	ATCACTGATTTCCTTGGCCATCTCATCAATGGAGCCATAGCAGTATTTGTATATGCTTCT	282
Query	241	GATAAAGAATGGATCCGCTTTGACCAATCAAATGTCCTTTGCAGTATTTTGGTATCTGC	300
Sbjct	283	GATAAAGAATGGATCCGCTTTGACCAATCAAATGTCCTTTGCAGTATTTTGGTATCTGC	342
Query	301	ATGGTGTTTTCTGGTCTGTGCCACTTCTTCTAGGCAGTGTGATGGCCATTGAGCGGTGT	360
Sbjct	343	ATGGTGTTTTCTGGTCTGTGCCACTTCTTCTAGGCAGTGTGATGGCCATTGAGCGGTGT	402
Query	361	ATTGGAGTCACAAAACCAATATTTCACTTCTACNAAAATTACATCCAAACA	410
Sbjct	403	ATTGGAGTCACAAAACCAATATTTCACTTCTACGAAAATTACATCCAAACA	452

### **3.7 Experiments to determine which hair follicle components express the gene for FP**

#### **3.7.1 Preliminary investigation of scalp hair follicle proportions**

Initially a small experiment was carried out to measure some areas of isolated anagen scalp hair follicle to ensure that the whole of the potential bulge region was collected (detailed in section 2.2.1.3.1). When 10 follicles from a fresh occipital scalp skin sample from a 37 year old male were measured using a dissecting microscope. The mean distance of the upper level of the sebaceous gland from the skin surface was  $0.92 \pm 0.1$  mm, the lower level of the sebaceous gland from the bottom of the hair follicle was  $1.99 \pm 0.1$  mm and the mean length of the follicles was  $3.445 \pm 0.1$  mm (Table 4). These data from the fresh skin sample were used to guide the “bulge region” in microdissection of the follicle area below the sebaceous gland from the skin samples which were kept in *RNAlater* as the sebaceous gland could not be seen easily in tissues which had been kept in this preservative solution.

**Table 4 Measurements of the distance of the sebaceous gland from both the skin surface and the hair follicle bulb in human scalp skin**

<b>Follicle number</b>	<b>Distance of the top of sebaceous gland from the skin surface (mm)</b>	<b>The distance of the bottom of sebaceous gland from the bottom of the hair follicle (mm)</b>	<b>Length of follicle surface to bottom of bulb(mm)</b>
1	0.71	1.84	3.15
2	1.09	2.07	3.6
3	0.98	2.10	3.55
4	0.93	1.96	3.4
5	0.87	1.90	3.3
6	1.03	2.0	3.6
7	0.90	2.02	3.5
8	0.84	2.15	3.55
9	1.0	2.03	3.5
10	0.85	1.92	3.3
<b>Mean ± SD</b>	<b>0.92 ±0.1</b>	<b>1.99 ±0.1</b>	<b>3.445 ±0.1</b>

### **3.7.2 RT-PCR for the FP gene using isolated scalp hair follicle components**

To detect the location of FP gene expression in human hair follicles, RT-PCR was performed on isolated follicular components from 125 follicles from each of three different human scalp skin samples (Table 5) and each individual's hair follicles components were investigated separately. Anagen hair follicles were carefully microdissected to isolate the dermal papilla, connective tissue sheath, matrix, follicle "bulge area" and the follicle area between the bulge and the bulb as detailed in section 2.2.1.3.2. This further microdissection was very difficult and time consuming and approximately three days were required to get individual components from 125 follicles. Each microdissected hair follicle component from the follicles from each individual were pooled immediately after microdissection and measured as described previously (2.2.1.4). The quantity and quality of the

total RNA samples were checked; when the total RNA from each hair follicle component was tested by gel electrophoresis, that from matrix and lower follicle area between the bulge and the bulb showed sharp 28S and 18S rRNA bands and the 28S rRNA bands were approximately twice as intense as the 18S rRNA bands (Figure 45), indicating good quality. The total RNA from other three hair follicle components (dermal papilla, connective tissue sheath and the follicle in bulge region) had only weak 28S and 18S rRNA bands which did not show a 2:1 ratio indicating that these RNA samples were of poor quality.

Spectrophotometric analysis of the concentration and purity of the total RNA from the three hair follicle components samples shows very low concentrations, especially for dermal papilla (DP), connective tissue sheath (CTS) and the follicle in the “bulge region”. The hair matrix (HM) and lower follicle (LF) below the bulge had more concentrated RNA (Table 6).

**Table 5 Human skin samples used to prepare isolated hair follicle components**

Follicles used to prepare components, including dermal papilla, connective tissue sheath, matrix, follicle “bulge region” and the lower follicle area between the bulge and the bulb

Sample number	Gender	Age (Years)	Source
H6	Male	39	Occipital scalp
H7	Female	48	Facelift
H8	Male	42	Occipital scalp

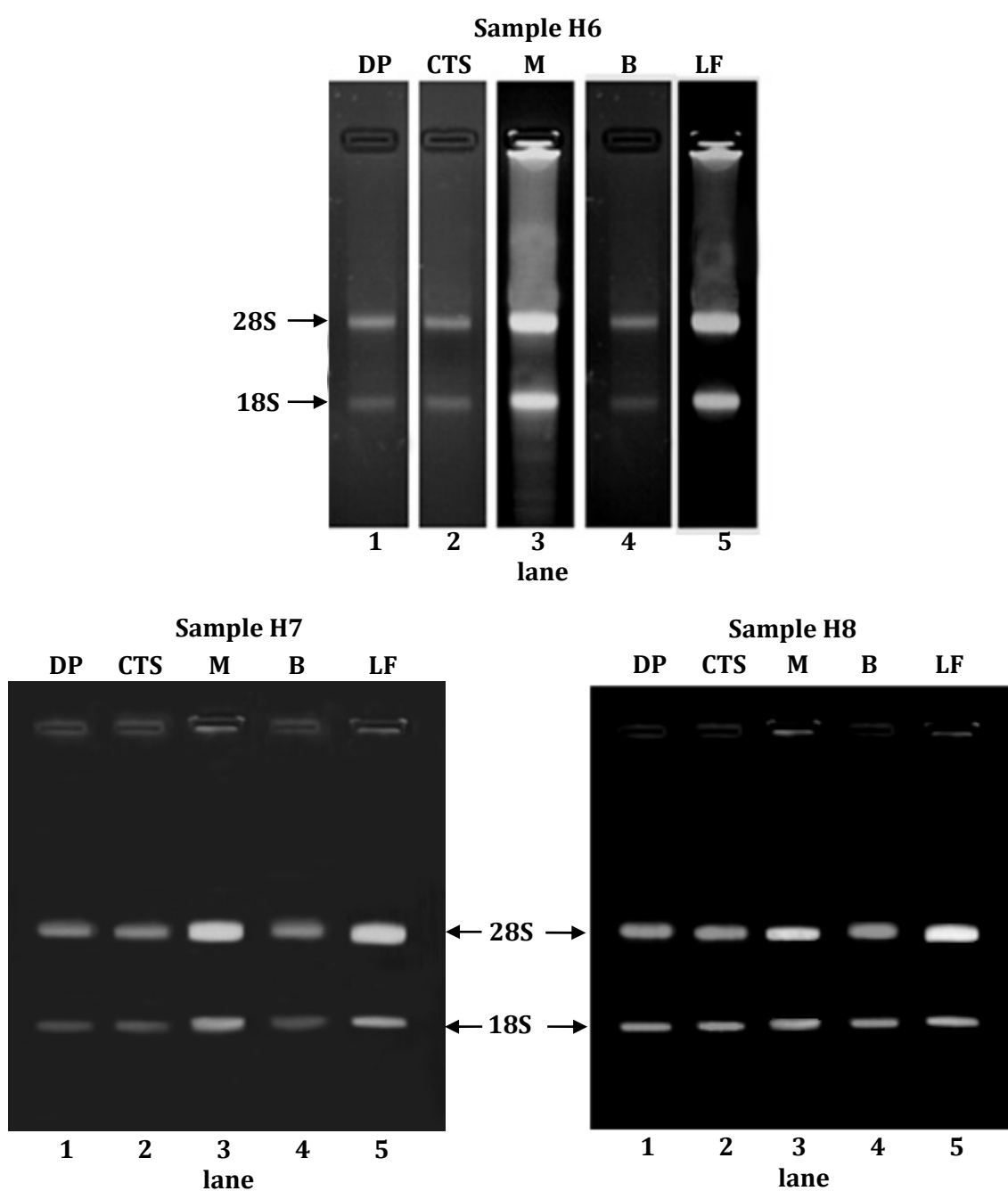
**Table 6 Spectrophotometric analysis of human scalp hair follicle components RNA**

DP: dermal papilla, CTS: connective tissue sheath around the bulb, HM: hair matrix and LF: lower follicle area below the bulge region.

Total RNA sample		Purity ( $A_{260}/A_{280}$ )	Concentration (ng/ml)
<b>H6</b>	DP	1.15	33
	CTS	1.08	29
	HM	1.7	72
	Bulge	1.2	40
	LF	1.55	78
<b>H7</b>	DP	1.1	25
	CTS	1	22
	HM	1.55	65
	Bulge	1.18	39
	LF	1.45	74
<b>H8</b>	DP	1.4	41
	CTS	1.25	34
	HM	1.8	81
	Bulge	1.3	47
	LF	1.7	86

**Figure 45 Agarose gel electrophoresis of total RNA extracted from hair follicle components from three samples**

The agarose gel electrophoresis of the total RNA from hair follicle components from 3 individuals. 10µl from each sample was loaded on to a 1.5% agarose gel. **Lane 1** - dermal papilla (DP), **lane 2** - connective tissue sheath (CTS), **lane 3** - matrix (M), **lane 4** - follicle in bulge region (B) and **lane 5** - lower follicle region between the bulge and the bulb (LF). The 18S and 28S ribosomal RNA bands were strong in the bulb matrix and the lower follicle but weak in the other three.



### **3.7.3 RT-PCR results for $\beta$ -actin gene expression from human hair follicle components**

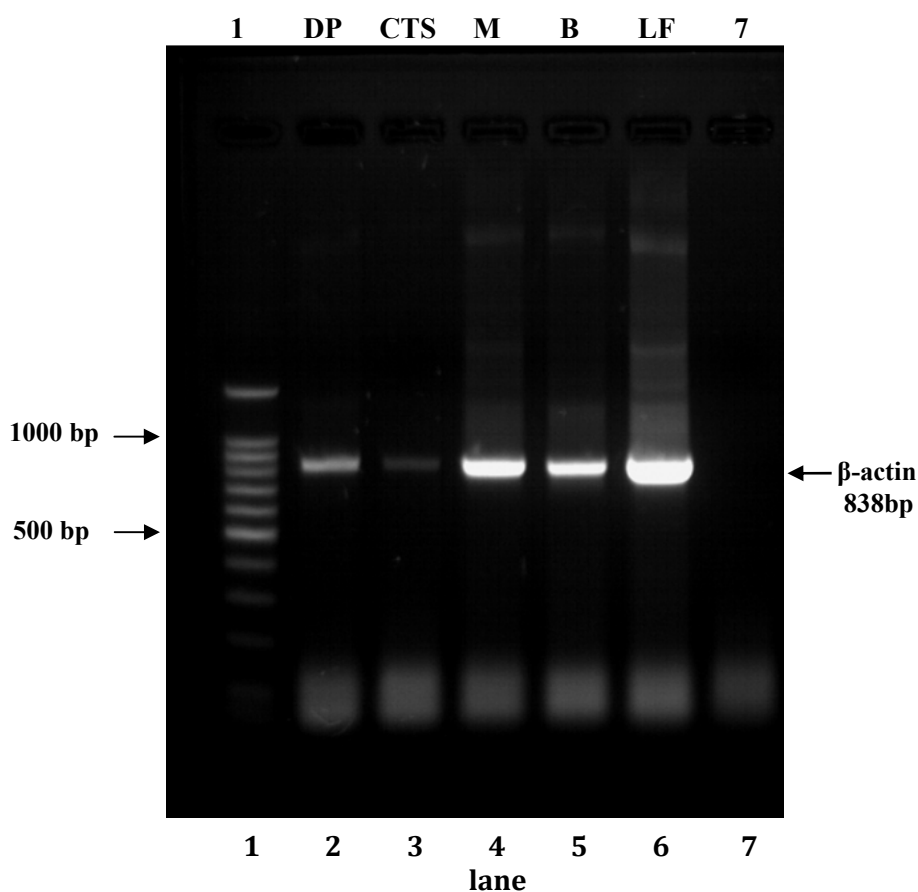
cDNAs prepared from each of the components from three individuals were checked for their quality by RT-PCR using primers for the positive control gene  $\beta$ -actin. When the PCR products were separated by agarose gel electrophoresis, all 3 samples amplified bands for each individual component, corresponding to the expected amplicon size for  $\beta$ -actin (838 bp) (Figure 46). The PCR products from matrix, the follicle in the “bulge region” and the lower follicle region below the “bulge” showed stronger bands which indicated that those cDNA quantities were sufficient to be used for FP gene amplification, but PCR products from dermal papilla and the connective tissue sheath showed weak bands indicating that the cDNA was of poor quantity and more cDNA must be used for FP gene amplification. No bands were observed in the negative control in which the template cDNA was omitted from the PCR reaction mix.

The identities of the PCR products were checked by sequence analysis. The homology of the sequenced PCR product to the known human  $\beta$ -actin gene sequence for the dermal papilla was 93%, the connective tissue sheath was 91%, the matrix was 94%, the follicle in bulge region was 90% and the lower follicle between the bulge and the bulb was 96% (Data not shown).



**Figure 46 Gel electrophoresis of  $\beta$ -actin PCR products from human hair follicle components**

A typical agarose gel electrophoresis (1.5% w/v) after RT-PCR of human hair follicle components using primers for  $\beta$ -actin and 10 $\mu$ l of cDNA. **Lane 1**–10 $\mu$ l molecular weight markers (DNA ladder; eleven fragments ranging from 100–1,500bp), **lane 2-6** – human hair follicle components  $\beta$ -actin PCR products (30  $\mu$ l): lane 2, dermal papilla (DP); lane 3: connective tissue sheath (CTS), lane 4: matrix (M), lane 5: follicle in bulge region (B) and lane 6: lower follicle between the bulge and the bulb (LF), **lane 7** – negative control in which cDNA was omitted from the PCR reaction mix (30  $\mu$ l). The expected amplicon size for  $\beta$ -actin is 838 bp.

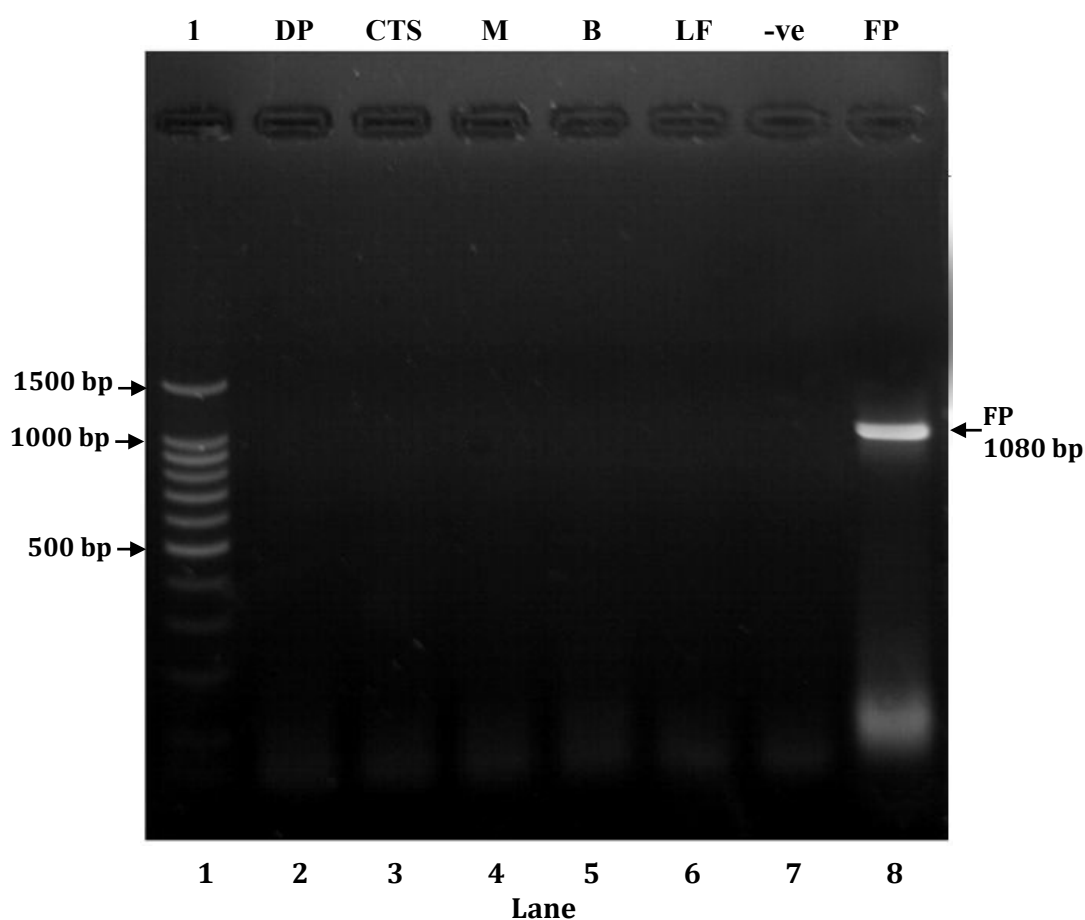


#### **3.7.4 Expression of FP gene in cDNA extracted from human hair follicle components using RT-PCR**

When FP gene expression was investigated in the human hair follicle components cDNA samples (15 $\mu$ l) from the dermal papilla, connective tissue sheath, matrix, follicle from the “bulge area” and the area between the bulge and the bulb, none of the cDNA samples from any of the 3 different individuals produced detectable PCR products (Figure 47). However, the expression of FP gene in whole lower hair follicles (Figure 47 lane 8) and the detection of good  $\beta$ -actin expression in the matrix, follicle from the “bulge” area and the lower follicle between the “bulge” and the bulb (Figure 46) suggested that this was not due to problems with the FP PCR or the amount of cDNA available for the three mainly epithelial components.

### Figure 47 PCR detection of FP gene in human hair follicle components

Expression of FP gene in human hair follicle components was investigated by RT-PCR using 15 $\mu$ l of cDNA. **Lane 1** – 10 $\mu$ l molecular weight markers (100bp DNA ladder), **lane 2-6** – FP gene PCR products from human hair follicle components (30 $\mu$ l loaded). DP: dermal papilla, CTS: connective tissue sheath, M: matrix, B: follicle from bulge area and LF: lower follicle area between the bulge and the bulb, **lane 7** – negative control (-ve) in which cDNA was excluded (30 $\mu$ l). **Lane 8** – (30 $\mu$ l) positive control, FP gene expression from human hair follicle cDNA (H1, 10 $\mu$ l). The expected amplicon size for FP gene is 1080 bp. The PCR products (lanes 2-6) did not show any bands indicating that the cDNA from hair follicle components were not of sufficient quantity to yield FP gene amplification. There was a band of expected amplicon size (1080 bp) for the positive control in lane 8.



### 3.7.5 The expression of FP gene in amplified RNA from human hair follicle components cells using RT-PCR

To determine whether the lack of detection of FP gene expression (Figure 47) was simply due to insufficient cDNA, the experiment described in 3.7.2 was repeated using a further three human male scalp skin samples (Table 7), but the RNA from each hair follicle component was amplified before cDNA synthesis as described in section 2.2.1.4.5.

**Table 7 Human scalp hair follicle samples used to prepare hair follicle components for amplified RNA studies, their RNA concentrations and purities after amplification.**

Human sample	Age (year)	Component parts	Purity ( $A_{260}/A_{280}$ )	Concentration ( $\mu\text{g/ml}$ )
<b>H9</b>	30	DP	1.8	22.3
		CTS	1.75	18.5
		HM	1.95	26.2
		Bulge	1.7	20.8
		LF	1.85	28.4
<b>H10</b>	45	DP	2	16.6
		CTS	1.75	13.7
		HM	1.8	19.5
		Bulge	1.9	14.7
		LF	1.85	17.9
<b>H11</b>	41	DP	1.85	18.2
		CTS	1.8	14.8
		HM	1.9	20.4
		Bulge	1.8	16.2
		LF	1.85	21.1

The quality of each extracted RNA sample was checked before amplification by gel electrophoresis on a 1.5% agarose gel (Figure 48). The total RNA from each sample showed sharp 28S and 18S rRNA bands and the 28S rRNA bands were approximately twice as intense as the 18S rRNA bands (Figure 48), indicating that the RNA samples were of appropriate quality. The RNA samples were amplified using the SMART™ mRNA Amplification Kit; the concentration and purity were checked spectrophotometrically (Table 7). All three samples after amplification showed much higher concentrations for all the hair follicle components compared to the earlier non-amplified RNAs (see Table 6 & 7). The amplified RNA samples were treated with DNase I and cDNAs were synthesised immediately.

### **3.7.6 PCR detection of $\beta$ -actin in amplified hair follicle components**

The cDNAs prepared from all three samples were checked for their quality by RT-PCR using primers for the positive control gene,  $\beta$ -actin. All amplified hair follicle components from each individual produced bands corresponding to the expected amplicon size for  $\beta$ -actin (838 bp) when separated by agarose gel electrophoresis (Figure 49). No bands were observed in the negative control when the template cDNA was omitted.

The identities of the PCR products were checked by sequence analysis. The sequenced dermal papilla, connective tissue sheath, hair matrix, the follicle in the “bulge” region and lower follicle PCR products were aligned with the known human  $\beta$ -actin sequence using NCBI BLAST program and showed 97%, 92%, 94%, 90% & 95% respectively (Figure 50).

**Figure 48 Agarose gel electrophoresis of total RNA from hair follicle components prior to amplification**

Agarose gel electrophoresis showed obvious 28S and 18S ribosomal RNA bands exhibiting 2:1 ratio in all components RNA when 10 $\mu$ l from each sample was loaded into a 1.5% agarose gel. DP: dermal papilla, CTS: connective tissue sheath, M: hair matrix, the follicle in bulge region and LF: lower follicle below the bulge region.

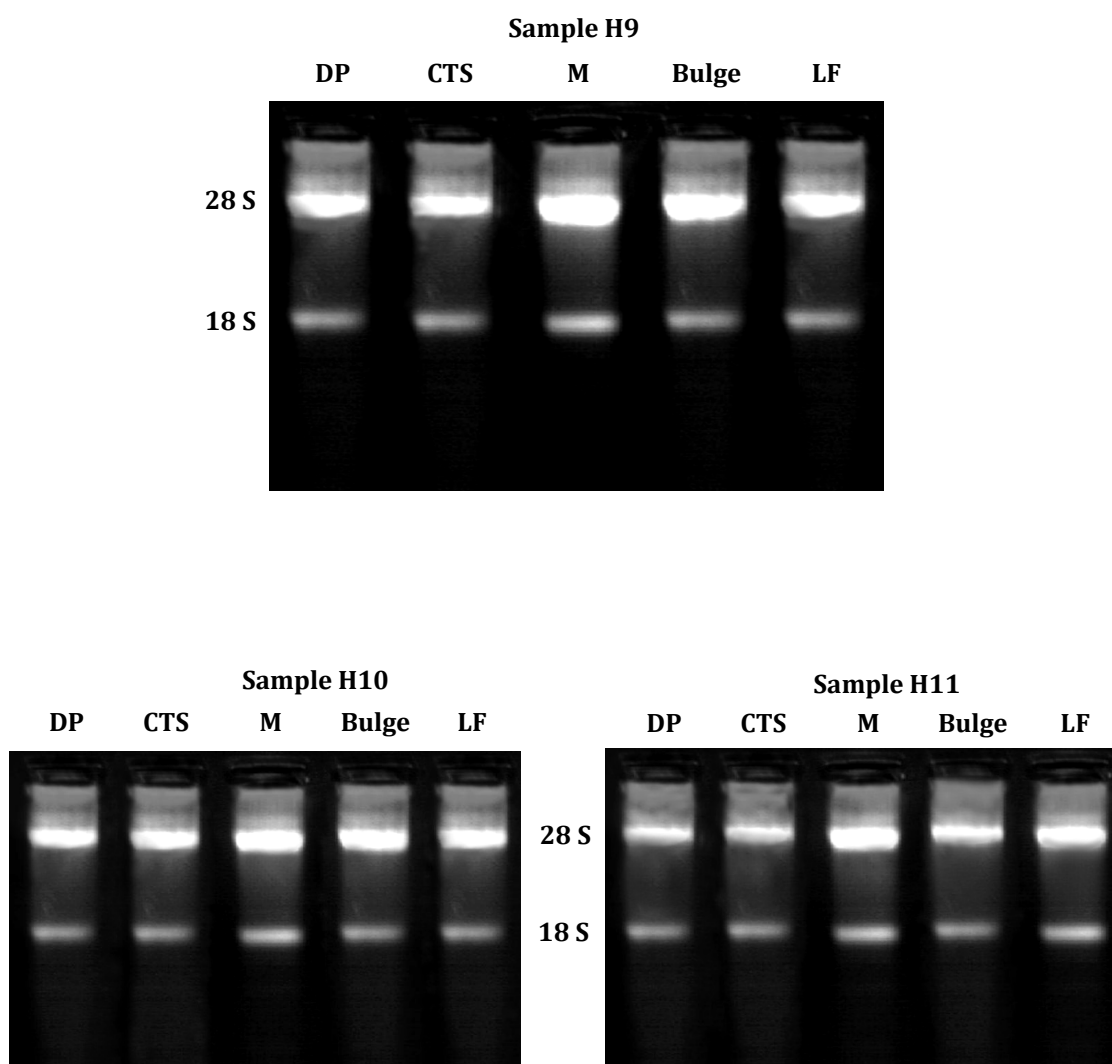


**Figure 49 Agarose gel electrophoresis of  $\beta$ -actin PCR products from amplified RNA from human hair follicle components**

A typical agarose gel electrophoresis (1.5% w/v) after RT-PCR of amplified RNA from human hair follicle components using primers for  $\beta$ -actin and 10  $\mu$ l of cDNA. **Lanes 1 & 8** – 10  $\mu$ l molecular weight markers (DNA ladder 100-1500 bp), **lane 2-6** – hair follicle components  $\beta$ -actin PCR products (30  $\mu$ l): lane 2: dermal papilla (DP); lane 3: connective tissue sheath (CTS), lane 4: matrix (M), lane 5: follicle in bulge region (B); lane 6: lower follicle between the bulge and the bulb (LF) and **lane 7** – negative control in which cDNA was omitted from the PCR reaction mix (30  $\mu$ l). The expected amplicon size for  $\beta$ -actin is 838 bp. All hair follicle components showed a strong band indicating that those cDNA were of good quality and they were suitable to be used for FP gene amplification.

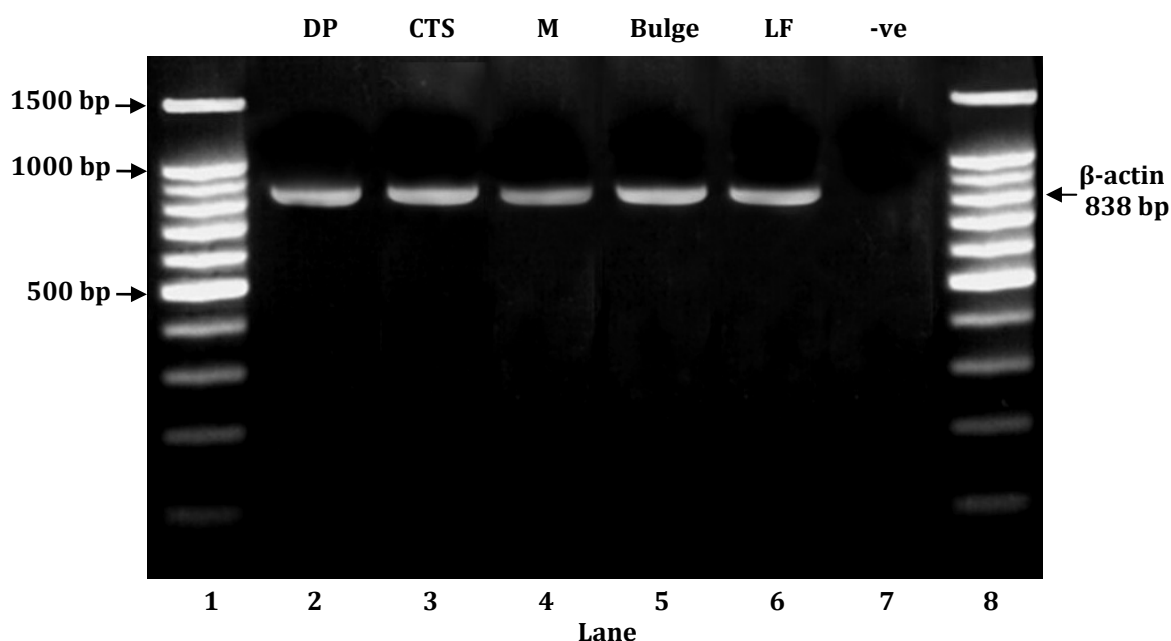


**Figure 50 Sequencing results for  $\beta$ -actin RT-PCR product from amplified RNA from hair follicle components**

The identity of a  $\beta$ -actin PCR product was checked by sequence analysis using the NCBI BLAST program to align the homology of the sequenced product (query: red) against the known human  $\beta$ -actin gene sequence (subject: black). The matching bases between the two sequences are indicated by a bar. The homology of the sequenced PCR product to the known human  $\beta$ -actin sequence for the dermal papilla was 97% (a), connective tissue sheath was 92% (b), matrix was 94% (c), the follicle in bulge region was 90% (d) and lower follicle between the bulge and the bulb was 95% (e).

**(a) Dermal papilla**

Query: 2 tgtggccccgaggagcaccgcgtgctgacccgagccccctgaacccaaggccaa 61  
Sbjct: 33 tgtggctcccgaggagcaccgcgtgctgacccgagccccctgaacccaaggccaa 92

Query: 62 ccgagagaagatgacncagatcatgtttgagaccttcaacaccccagccatgtacgtngc 121  
Sbjct: 93 ccgcgagaagatgaccagatcatgtttgagaccttcaacaccccagccatgtacgttgc 152

Query: 122 tatccaggctgtgctatccctgtacgcctctggncgnaccactggcatttgtgatggactc 181  
Sbjct: 153 tatccaggctgtgctatccctgtacgcctctggccgtaccactggcatcgtgatggactc 212

Query: 182 nggtgacggggtcaccacactgtgccatctacgaggggtatgccctccccatgccat 241  
Sbjct: 213 cgggtgacggggtcaccacactgtgccatctacgaggggtatgccctccccatgccat 272

Query: 242 cctgcgtctggacctggctggccgggacctgactgactacctcatgaagatcctcacnga 301  
Sbjct: 273 cctgcgtctggacctggctggccgggacctgactgactacctcatgaagatcctcaccga 332

Query: 302 gcgcgggtacagcttcaccaccacggccgagcgggaaatcgctgcgtgacattaaggagaa 361  
Sbjct: 333 gcgcgggtacagcttcaccaccacggccgagcgggaaatcgctgcgtgacattaaggagaa 392

Query: 362 gctgtgctacgtcgccctggacttcgagcaagagatggccaengctgcttcennctcttc 421  
Sbjct: 393 gctgtgctacgtcgccctggacttcgagcaagagatggccaengctgcttcagctcctc 452

Query: 422 tctgggnaanagct 435  
Sbjct: 453 cctqqaqaagact 466



(b) Connective tissue sheath

Query: 2	tgtggcccccaggagcaccocgtgctgtgacccaggcccccctgaaccccaaggccaa	61
Sbjct: 33	tgtggctcccaggagcaccocgtgctgtgacccaggcccccctgaaccccaaggccaa	92
Query: 62	ccgagagaagatgacncagatcatgtttgagacattcaaacacccagcccatgtacgttgc	121
Sbjct: 93	ccgcgagaagatgacccagatcatgtttgagacattcaaacacccagcccatgtacgttgc	152
Query: 122	tatccaggctgtgtatccctgtacggmtctggnacacactggccattgtgatggactc	181
Sbjct: 153	tatccaggctgtgtatccctgtacggmtctggnacacactggccattgtgatggactc	212
Query: 182	nggtgacggggtcacccacactgtgcccatctacgaggggtatgcccctccccatgccat	241
Sbjct: 213	cggtgacggggtcacccacactgtgcccatctacgaggggtatgcccctccccatgccat	272
Query: 242	cctnagttctgacctggctggccgggacctgactgactaactcatgaagatcctcacnga	301
Sbjct: 273	cctggtctgacctggctggccgggacctgactgactaactcatgaagatcctcacnga	332
Query: 302	gcgcggctacagcttcacaccacacggccgagcggggaaatcgtgcgtgacattaggagaa	361
Sbjct: 333	gcgcggctacagcttcacaccacacggccgagcggggaaatcgtgcgtgacattaggagaa	392
Query: 362	gctgtgctacgtgcgcctggacttcgagcaagagatccccacngctgcttccnnccttc	421
Sbjct: 393	gctgtgctacgtgcgcctggacttcgagcaagagatggccacngctgcttccagctcttc	452
Query: 422	tctggmaanaagct	435
Sbjct: 453	cctggagaagagct	466

(c) Matrix

Query: 2	tgtggcccccaggagcaccocgtgctgtgacccaggcccccctgaaccccaaggccaa	61
Sbjct: 33	tgtggctcccaggagcaccocgtgctgtgacccaggcccccctgaaccccaaggccaa	92
Query: 62	ccgagagaagatgacncagatcatgtttgagacattcaaacacccagcccatgtacgttgc	121
Sbjct: 93	ccgcgagaagatgacccagatcatgtttgagacattcaaacacccagcccatgtacgttgc	152
Query: 122	tatccaggctgtgtatccctgtacggmtctggnacacactggccattgtgatggactc	181
Sbjct: 153	tatccaggctgtgtatccctgtacggmtctggnacacactggccattgtgatggactc	212
Query: 182	nggtgacggggtcacccacactgtgcccatctacgaggggtatgcccctccccatgccat	241
Sbjct: 213	cggtgacggggtcacccacactgtgcccatctacgaggggtatgcccctccccatgccat	272
Query: 242	cctnagttctgacctggctggccgggacctgactgactaactcatgaagatcctcacnga	301
Sbjct: 273	cctggtctgacctggctggccgggacctgactgactaactcatgaagatcctcacnga	332
Query: 302	gcgcggctacagcttcacaccacacggccgagcggggaaatcgtgcgtgacattaggagaa	361
Sbjct: 333	gcgcggctacagcttcacaccacacggccgagcggggaaatcgtgcgtgacattaggagaa	392
Query: 362	gctgtgctacgtgcgcctggacttcgagcaagagatccccacngctgcttccnnccttc	421
Sbjct: 393	gctgtgctacgtgcgcctggacttcgagcaagagatggccacngctgcttccagctcttc	452
Query: 422	tctggmaanaagct	435
Sbjct: 453	cctggagaagagct	466



### **3.7.7 Expression of FP gene in amplified RNA from hair follicle components using RT-PCR**

The expression of the FP gene was investigated in the human scalp hair follicle components using 10 µl of amplified cDNA. Dermal papilla and connective tissue sheath cDNA samples from three different individuals all showed appropriate bands corresponding to the FP gene (1080 bp) (Figure 51); none of the other three components, the matrix, the follicle from the “bulge” area and the area between the “bulge” and the bulb, showed any detectable bands.

The identities of the dermal papilla (DP) and connective tissue sheath (CTS) PCR products were confirmed by sequence analysis. When the DP and CTS PCR products sequences were aligned with the known human FP gene sequence using the NCBI BLAST program, they showed 98% & 95% homology respectively (Figure 52).

### Figure 51 PCR detection of FP gene from amplified RNA from human hair follicle components

The FP gene expression using amplified RNA from hair follicle components was investigated by RT-PCR. **Lane 1 & 8** – 10µl molecular weight markers (100-1500 bp DNA ladder), **lane 2-6** – FP gene PCR products from human hair follicle components (30µl loaded); DP: dermal papilla, CTS: connective tissue sheath, M: matrix, B: follicle from bulge area and LF: lower follicle area between the bulge and the bulb; **lane 7** – negative control (-ve) in which cDNA was omitted (30µl). The expected amplicon size for FP gene is 1080 bp. Only the dermal papilla (DP) and the connective tissue sheath (CTS) (lane 2, 3) showed bands indicating FP gene amplification but none of the other components, M, bulge and LF (lane 4-6) showed any bands.

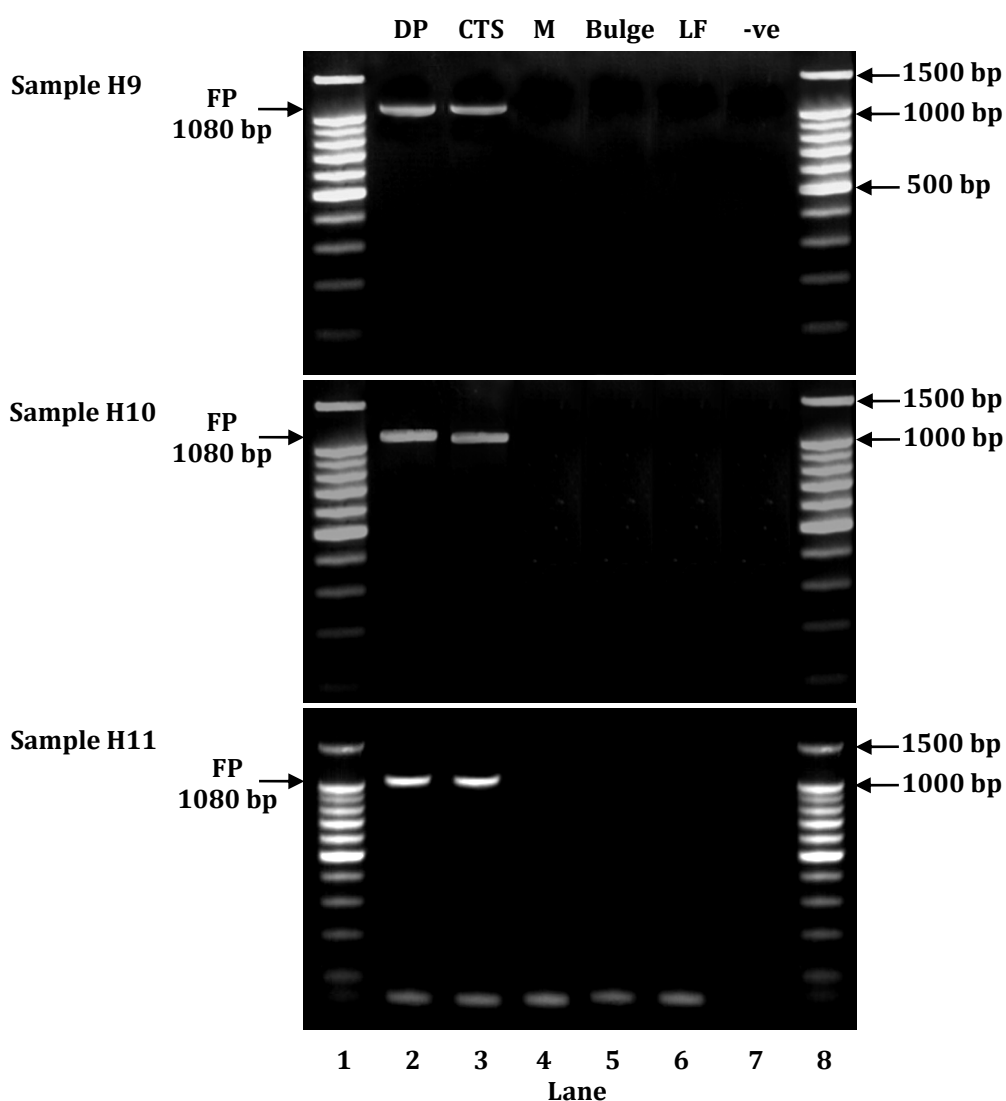


**Figure 52 Sequencing results for FP gene PCR product, following amplification from human hair follicle dermal papilla and connective tissue sheath cells**

To ascertain the identity of the dermal papilla and connective tissue sheath PCR products of FP gene expression from amplified RNA from human hair follicle components, sequence analysis was carried out. The NCBI BLAST programme was used to align the sequenced products (red; query) against the known human FP gene sequence (black; subject). The FP gene PCR product sequence of the human hair follicle dermal papillae (a) and connective tissue sheath (b) exhibited 98% & 95% homology respectively to the known human FP gene sequence.

**(a) Dermal papilla**

Query	1	GCGCTTCTTTCAAACACAACCTGCCAGACGGAAAACCGGCTTCCGTATTTTTTTCAGTA	60
Sbjct	43	GCGCTTCTTTCAAACACAACCTGCCAGACGGAAAACCGGCTTCCGTATTTTTTTCAGTA	102
Query	61	ATCTTCATGACAGTGGGAATCTTGTCAAACAGCCTTGCCATCGCCATTCTCATGAAGGCA	120
Sbjct	103	ATCTTCATGACAGTGGGAATCTTGTCAAACAGCCTTGCCATCGCCATTCTCATGAAGGCA	162
Query	121	TATCAGAGATTTAGACAGAAGTCCAAGGCATCGTTTCTGCTTTTGGCCAGTGGCCTGGTA	180
Sbjct	163	TATCAGAGATTTAGACAGAAGTCCAAGGCATCGTTTCTGCTTTTGGCCAGTGGCCTGGTA	222
Query	181	ATCACTGATTTCTTTGGCCATCTCATCAATGGAGCCATAGCAGTATTTGTATATGCTTCT	240
Sbjct	223	ATCACTGATTTCTTTGGCCATCTCATCAATGGAGCCATAGCAGTATTTGTATATGCTTCT	282
Query	241	GATAAAGAATGGATCCGCTTTGACCAATCAAATGTCCTTTGCAGTATTTTGGTATCTGC	300
Sbjct	283	GATAAAGAATGGATCCGCTTTGACCAATCAAATGTCCTTTGCAGTATTTTGGTATCTGC	342
Query	301	ATGGTGTTTCTGGTCTGTGNCCACTTCTTCTAGGCAGTGTGATGGCCATTGAGCGGTGT	360
Sbjct	343	ATGGTGTTTCTGGTCTGTGCCACTTCTTCTAGGCAGTGTGATGGCCATTGAGCGGTGT	402
Query	361	ATTGGAGTCACAAAACCNATATTTTCATTCTACNAAAATTACATCCAAACA	410
Sbjct	403	ATTGGAGTCACAAAACCAATATTTTCATTCTACGAAAATTACATCCAAACA	452

**(b) Connective tissue sheath**

Query	1	GCGCTTCTTTCAAACACAACCTGCCAGACGGAAACCGGCTTTCGGTATTTTTTTCAGTA	60
Sbjct	43	GCGCTTCTTTCAAACACAACCTGCCAGACGGAAACCGGCTTTCGGTATTTTTTTCAGTA	102
Query	61	ATCTTCATGACAGTGGGAATCTTGTCAAACAGCCTTGCCATCGCCATTCTCATGAAGGCA	120
Sbjct	103	ATCTTCATGACAGTGGGAATCTTGTCAAACAGCCTTGCCATCGCCATTCTCATGAAGGCA	162
Query	121	TATCAGAGATTTAGACAGAAGTCCAAGNCATCGTTTCTGCTTTTGGCCAGTGGCCTGGTA	180
Sbjct	163	TATCAGAGATTTAGACAGAAGTCCAAGGCATCGTTTCTGCTTTTGGCCAGTGGCCTGGTA	222
Query	181	ATCACTGATTTCCTTTGGCCATCTCATCAATGGAGCCATAGCAGTATTTGTATATGCTTCT	240
Sbjct	223	ATCACTGATTTCCTTTGGCCATCTCATCAATGGAGCCATAGCAGTATTTGTATATGCTTCT	282
Query	241	GATAAAGAATGGATCCGCTTTGACCAATCAAATGTCCTTTGCAGTATTTTGGTATCTGC	300
Sbjct	283	GATAAAGAATGGATCCGCTTTGACCAATCAAATGTCCTTTGCAGTATTTTGGTATCTGC	342
Query	301	ATGGTGTCTTCTGGTCTGTGNCCACTTCTTCTAGGCAGTGTGATGGCCATTGAGCGGTGT	360
Sbjct	343	ATGGTGTTTTTCTGGTCTGTGCCACTTCTTCTAGGCAGTGTGATGGCCATTGAGCGGTGT	402
Query	361	ATTGGAGTCACAAAACCNATATTTTATTCTACNAAAATTACATCCAAACA	410
Sbjct	403	ATTGGAGTCACAAAACCAATATTTTATTCTACGAAAATTACATCCAAACA	452

### 3.8 Determination of which prostaglandins are present in scalp hair follicles by lipidomic analysis

To determine which prostaglandins occur naturally in human scalp hair follicles in anagen, the types of prostanoid, dihydroprostaglandin and isoprostane lipid mediators were investigated in isolated anagen scalp hair follicles using electrospray tandem mass spectrometry coupled to liquid chromatography (LC/ESI-MS/MS), a method adapted from Masoodi and Nicolaou (2006). Prostanoid profiles are tissue-dependent and quantitative methodologies need a high sensitivity and selectivity because of the short half-lives, low concentrations and structural similarities of these compounds. The LC/ESI-MS/MS is a sensitive and quick assay appropriate to lipidomic analyses. Electrospray ionisation (ESI) was used in this analysis as prostanoids have free carboxylic acid groups and ESI results in a copious [M-H] carboxylate ion that allows for relatively low concentrations to be detected.

The LC/ESI-MS/MS analysis identified 7 prostanoids, 1 isoprostane and 1 dihydroprostaglandin in scalp hair follicle samples from 3 individuals using a range of multiple reaction monitoring (MRM) transitions and optimum collision energy for each compound (Table 8) to generate the most abundant product ions (Kempen et al., 2001; Yang et al., 2002; Masoodi and Nicolaou, 2006; Taylor et al., 2006). The limits of detection were in the range of 0.1-10 pg/μl and the limits of quantification were in the range of 0.5-20 pg/μl depending on the compounds. The ESI-MS/MS product ion spectra revealed 7 prostanoids: PGF<sub>2α</sub> (Figure 53), PGE<sub>1</sub>, PGD<sub>1</sub>, PGE<sub>2</sub>, PGD<sub>2</sub>, TXB<sub>2</sub> and 6-keto PGF<sub>1α</sub>; a dihydroprostaglandin: 13,14 dihydro-15-keto PGE<sub>2</sub>; an isoprostane: 8-*iso*-PGE<sub>2</sub>. The LC/ESI-MS/MS chromatographic separation of the compounds on a C18 column using a gradient of two acetonitrile-

**Table 8 Optimal collision energies and multiple reaction monitoring transitions used for the LC/ESI-MS/MS assay of prostanoids, isoprostane and dihydroprostaglandins (Masoodi and Nicolaou, 2006).**

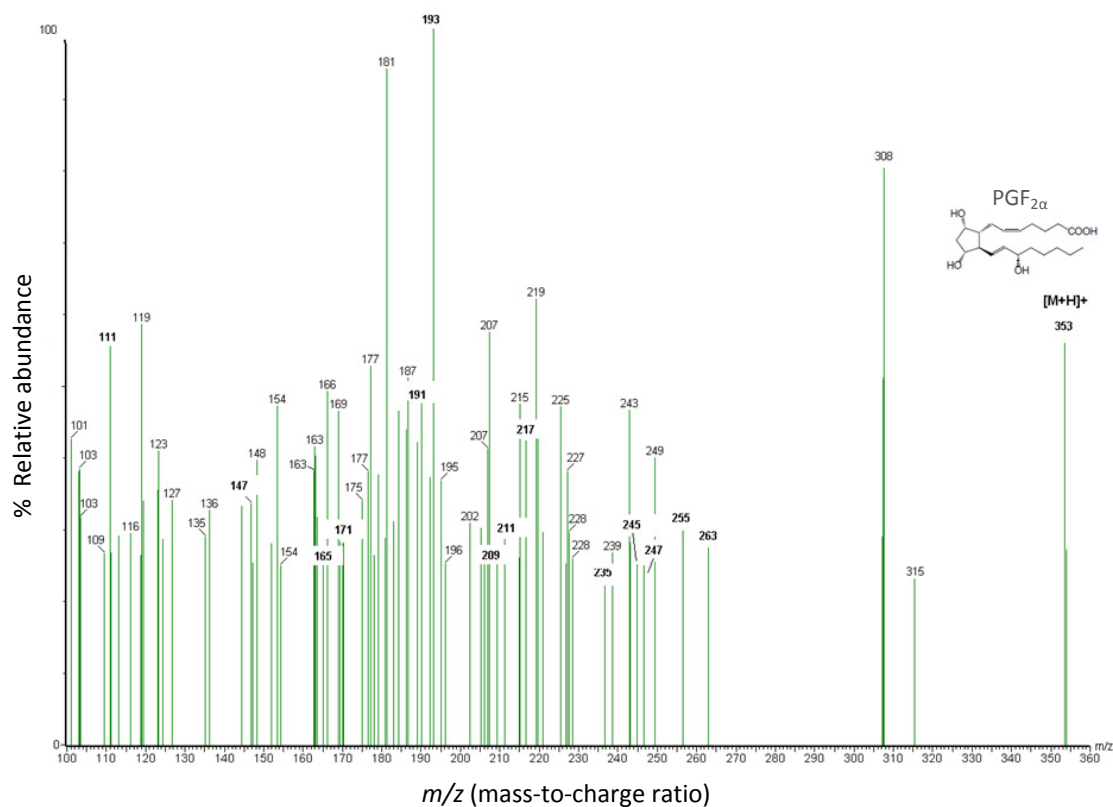
Multiple reaction monitoring (MRM) transitions and optimum collision energy to generate the most abundant product ions for each compound. PGB<sub>2</sub>-d<sub>4</sub>: internal standard.

Compound	MRM (m/z)	Collision energy (eV)
PGD <sub>1</sub>	353>317	15
PGE <sub>2</sub>	351>271	17
PGB <sub>2</sub> -d <sub>4</sub>	337>179	20
PGE <sub>1</sub>	353>317	15
PGF <sub>2α</sub>	353>193	25
TXB <sub>2</sub>	369>169	17
6-keto PGF <sub>1α</sub>	369>163	23
13,14-dihydro PGF <sub>2α</sub>	355>311	30
13,14-dihydro-15-keto PGF <sub>1α</sub>	355>193	32
13,14-dihydro-15-keto PGE <sub>1</sub>	353>335	12
13,14-dihydro-15-keto PGE <sub>2</sub>	351>333	12
8- <i>iso</i> -PGE <sub>2</sub>	351>315	15
PGD <sub>2</sub>	351>271	17



**Figure 53 An example ESI-MS/MS product ion spectrum of PGF<sub>2α</sub>**

ESI-MS/MS analysis identified PGF<sub>2α</sub>, PGE<sub>1</sub>, PGD<sub>1</sub>, PGE<sub>2</sub>, PGD<sub>2</sub>, TXB<sub>2</sub>, 6-keto PGF<sub>1α</sub>, 13,14 dihydro-15-keto PGE<sub>2</sub> and 8-*iso*-PGE<sub>2</sub> in scalp hair follicles from 3 individuals. The spectra were recorded at the optimum collision energy for each compound (Table 8). This typical graph shows the ESI-MS/MS spectrum of PGF<sub>2α</sub> detected. The molecular ion [M-H]<sup>-</sup> is *m/z* 353, using a collision energy of 25 eV.



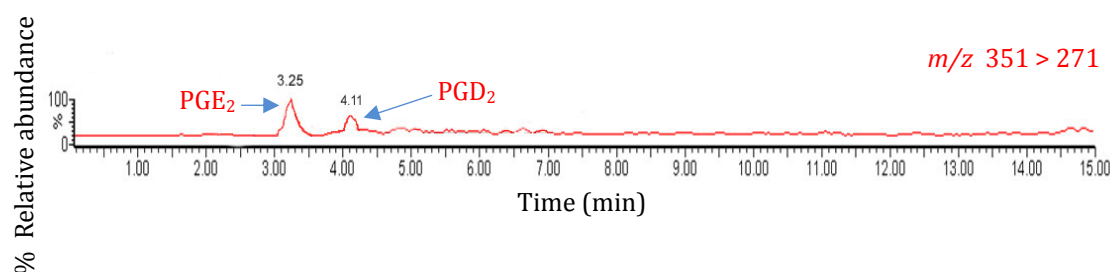
based solvents identified prostaglandins PGF<sub>2α</sub>, PGE<sub>1</sub>, PGD<sub>1</sub>, PGE<sub>2</sub>, PGD<sub>2</sub>, TXB<sub>2</sub>, 6-keto PGF<sub>1α</sub>, 13,14 dihydro-15-keto PGE<sub>2</sub> and 8-*iso*-PGE<sub>2</sub> (Figure 54). The isobaric compounds PGE<sub>2</sub> and PGD<sub>2</sub> were detected through the same MRM transition, but were separated chromatographically ( $m/z$  351→271; retention times: 3.25 and 4.11 min, respectively) (Figure 54a). Similarly PGE<sub>1</sub> and PGD<sub>1</sub> were separated chromatographically ( $m/z$  353→317; retention times were 2.38 and 4.43 min, respectively) (Figure 54b). Calibration lines for the various prostaglandins were produced by analysing an 6 point standard curve from 1-100 pg/μl for each compound (appendix 6.4).

The quantities of the identified prostanoids were worked out as concentration per mg of protein in the sample as the mean ± SEM from three different experiments each analysed in duplicate. The most predominant prostanoid lipid mediators identified were PGE<sub>2</sub> (17.1920±2.2 pg/mg protein) and PGF<sub>2α</sub> (13.39±1.8 pg/mg of follicle protein) (Figure 55). The concentration of the other prostanoids identified were: PGD<sub>2</sub>: 8.5843±3.5, PGE<sub>1</sub>: 5.2710±0.2, PGD<sub>1</sub>: 3.8817±5.7, 15-k-PGE<sub>2</sub>: 3.5317±8.9, 8-*iso*-PGE<sub>2</sub>: 4.3589±3.6, TXB<sub>2</sub>: 4.0145±1.1, 6-keto PGF<sub>1α</sub>: 3.2861±4.5 pg/mg of follicle protein (Figure 55).

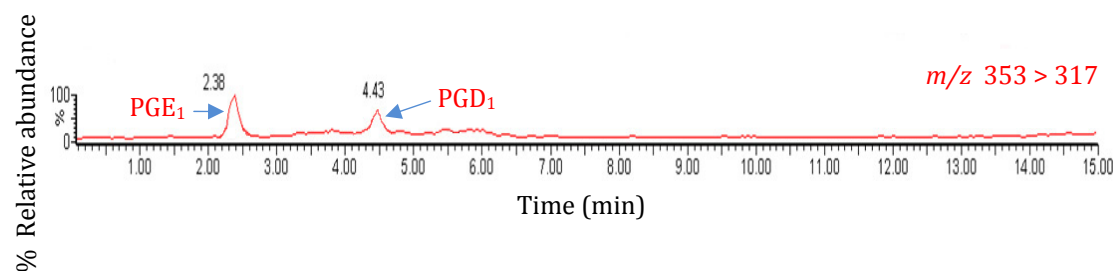
**Figure 54 Representative LC/ESI-MS/MS chromatograms of the prostanoids, dihydroprostaglandins and isoprostanes produced by human scalp hair follicles**

The compounds were chromatographically determined on a C18 column using a gradient of two acetonitrile-based solvents. This demonstrated the chromatograms of these lipid mediators: PGF<sub>2α</sub>, PGE<sub>1</sub>, PGD<sub>1</sub>, PGE<sub>2</sub>, PGD<sub>2</sub>, TXB<sub>2</sub>, 6-keto PGF<sub>1α</sub>, 13,14 dihydro-15-keto PGE<sub>2</sub> and 8-*iso*-PGE<sub>2</sub> (a-g). The run time of the assay was 30 min including a 10 min wash cycle programmed to run before the next injection.

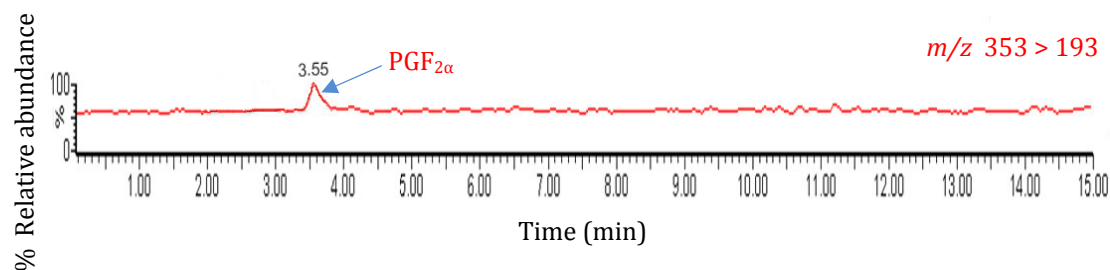
**(a)** Chromatogram showing LC/ESI-MS/MS analysis of PGE<sub>2</sub> & PGD<sub>2</sub>



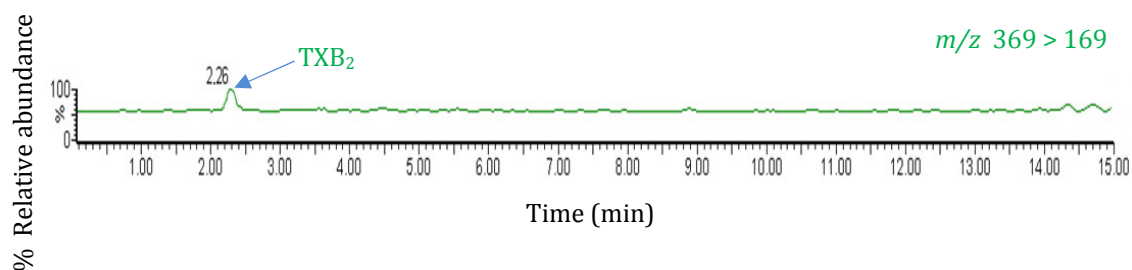
**(b)** Chromatogram showing LC/ESI-MS/MS analysis of PGE<sub>1</sub> & PGD<sub>1</sub>



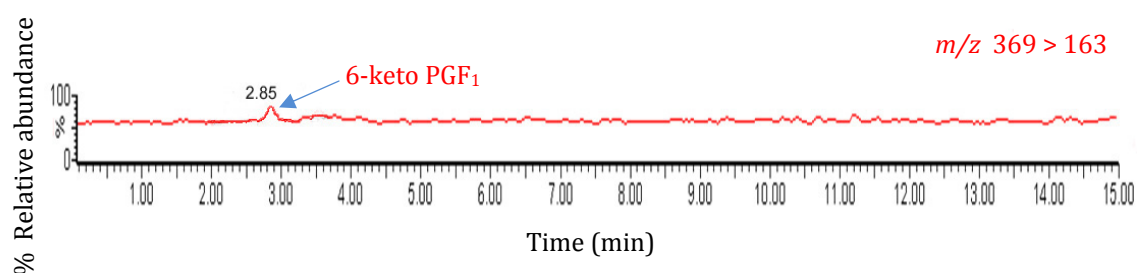
**(c)** Chromatogram showing LC/ESI-MS/MS analysis of PGF<sub>2α</sub>



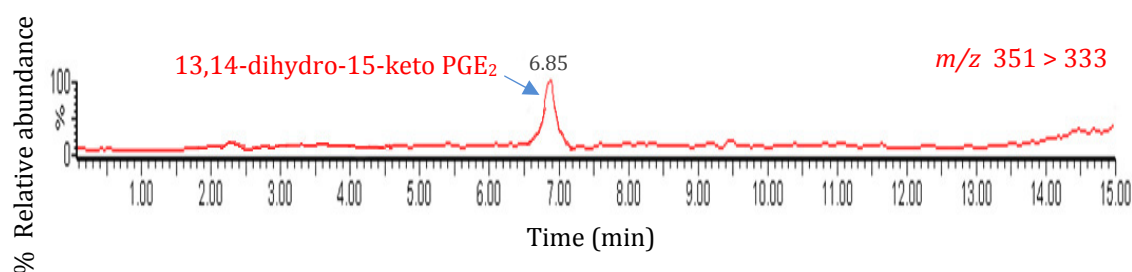
**(d)** Chromatogram showing LC/ESI-MS/MS analysis of TXB<sub>2</sub>



**(e)** Chromatogram showing LC/ESI-MS/MS analysis of 6-keto PGF<sub>1</sub>



**(f)** Chromatogram showing LC/ESI-MS/MS analysis of 13,14-dihydro-15-keto PGE<sub>2</sub>



**(g)** Chromatogram showing LC/ESI-MS/MS analysis of 8-*iso*-15-PGE<sub>2</sub>

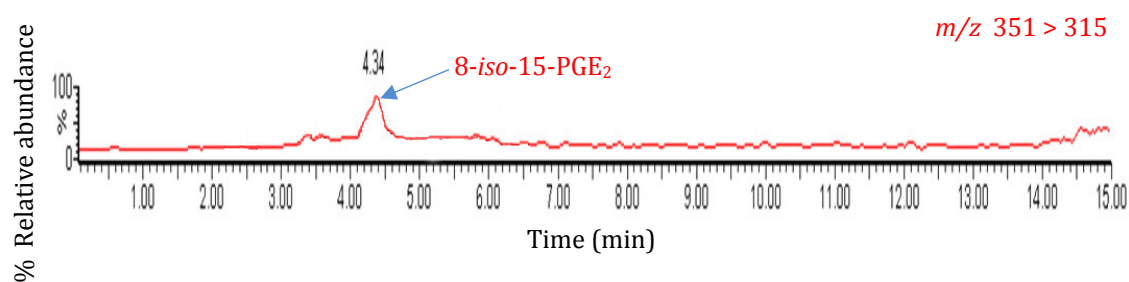
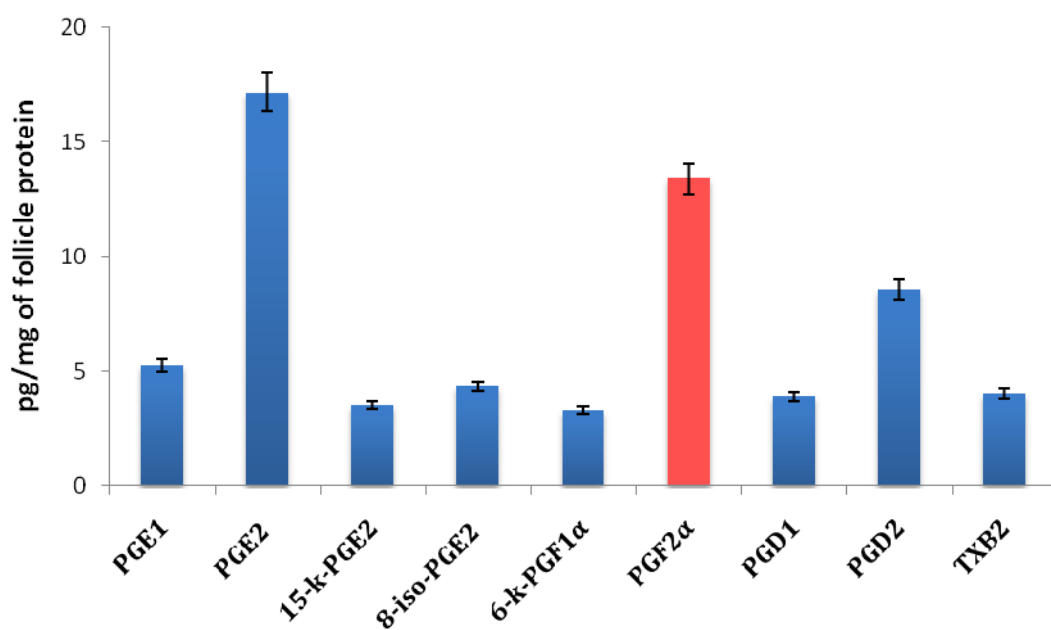


**Figure 55 Profile of the prostanoids naturally present in human scalp anagen hair follicles using LC/ESI-MS/MS**

Values are the mean  $\pm$  SEM of 3 samples of human scalp hair follicles from adult men; each sample was analysed in duplicate.



### **3.9 Immunohistochemical localisation of PGE<sub>2</sub> receptor (EP<sub>2</sub>) in the human scalp hair follicle bulb**

Following the identification of large amount of PGE<sub>2</sub> in the human scalp anagen hair follicles using LC/ESI-MS/MS (Figure 54a, 55), the expression of PGE<sub>2</sub> receptor (EP<sub>2</sub>) protein was investigated in the human scalp hair follicle from 5 men (26-48 years) by immunohistochemistry using a goat polyclonal anti-human EP<sub>2</sub> antibody. This antibody had to be optimised, a range of antibody dilutions between 1:50 to 1:200 was investigated and 1:100 in 1.5% normal mouse serum was considered optimal.

No non-specific staining occurred in the negative controls when the primary antibody was absent (Figure 56a, c). EP<sub>2</sub> was expressed in the cells of the human hair follicle dermal papilla and connective tissue sheath surrounding the hair bulb and lower follicle (Figure 56b, d).

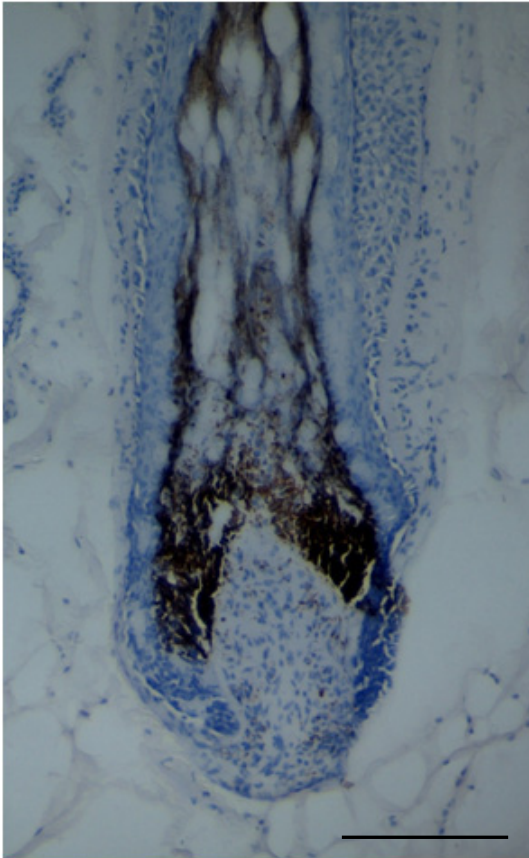
**Figure 56 Immunolocalisation of EP<sub>2</sub> in the human hair follicle bulb**

Immunohistochemistry was performed using a goat polyclonal antibody to EP<sub>2</sub> (1:100 dilution). DP: dermal papilla, CTS: connective tissue sheath; HM: hair matrix. Red: positive staining; blue: hematoxylin counterstain.

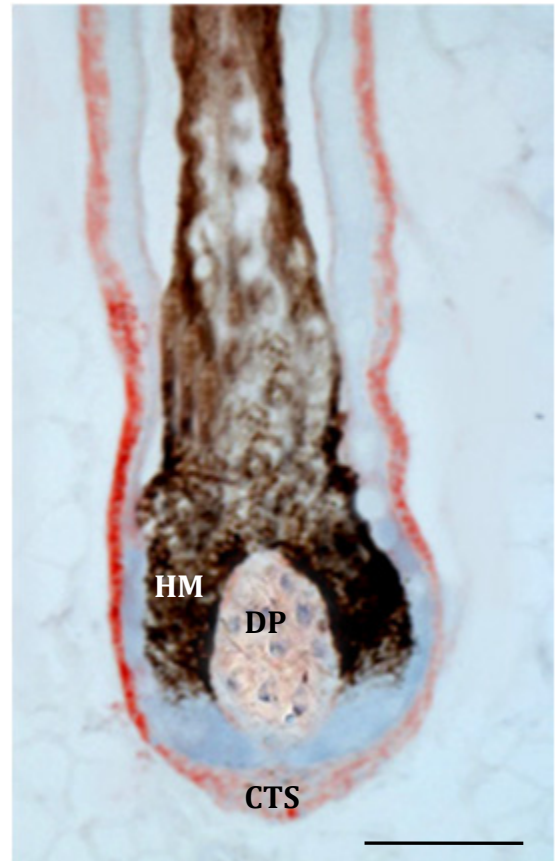
Absence of staining in the negative control where the primary antibody was replaced with 1.5% normal mouse serum (a, c). EP<sub>2</sub> protein was localised in the cells of the dermal papilla (DP) and connective tissue sheath (CTS) surrounding the hair bulb and lower follicle but not in the epithelial cells or melanocytes of the hair bulb matrix (b, d).

Scale bars a,b = 150µm; c,d = 100µm

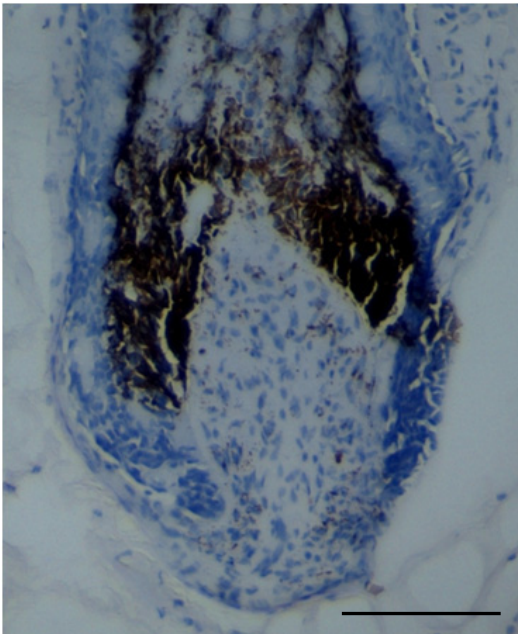
**(a)**



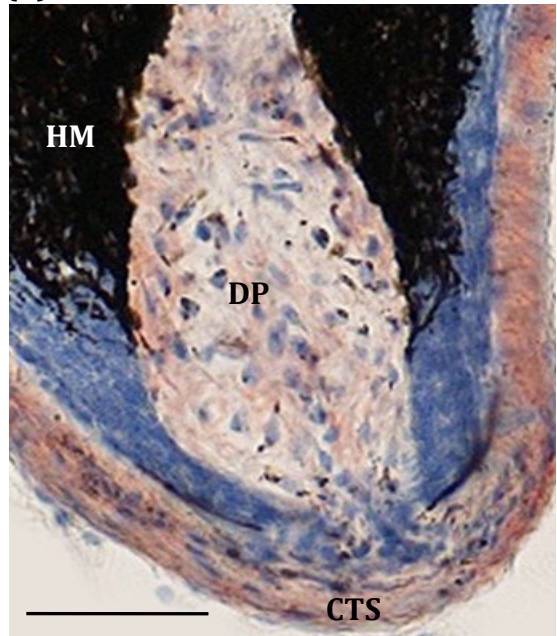
**(b)**



**(c)**



**(d)**





### **3.10 The effects of a prostamide F<sub>2α</sub> analogue, bimatoprost, on human scalp hair growth in organ culture**

#### **3.10.1 Bimatoprost stimulated human hair follicle growth in organ culture in a concentration-dependent manner**

Bimatoprost, a treatment for glaucoma (ocular hypertension) has been shown to have potent ocular hypotensive activity and stimulate eyelash growth as a side effect. To investigate the effects of different concentrations of bimatoprost on scalp hair follicle growth in the absence of any blood supply *in vitro*, hair follicle organ culture was carried out. Carefully microdissected hair follicles were maintained in serum-free culture medium for 9 days (Figure 57) with daily observation of their morphology, measurement and photography.

Since bimatoprost needed to be solubilised in DMSO, 0.01% DMSO was added to all control conditions used for these experiments using scalp hair follicle samples from a further 5 individuals. Most of the hair follicles (>70%) increased in length regularly during the nine day culture period in all conditions (Figures 57, 58, 59). Follicles which showed no increase in length over 3 days were assumed to be damaged and removed from the experiment. Sequential photographs taken every 24 hours showed that this hair follicle elongation was due to the production of a new hair fibre alongside with associated inner and outer root sheath, but the connective tissue sheath did not grow and remained at the initial length throughout the culture period (Figure 57). Daily observation of the hair follicle bulb morphology was carried out to monitor each follicle's anagen status (Figure 59). Some hair follicles developed catagen-like changes in their bulb morphology with pigmentation ceasing and the base of the hair fibre retracting up the follicle, leaving behind a rounded up ball of dermal papilla cells (see Figure 19c,d). After 2

days there was a gradual increase in the number of follicles showing catagen-like changes in the hair bulb region (Figure 59). The overall amount of hair actually produced by all the follicles in the organ culture was also calculated from the final increase in length of each follicle on the final day, day 9, or the last day the follicle maintained a normal anagen morphology (Figure 60). All 3 concentrations of bimatoprost stimulated human scalp hair follicle growth rate in organ culture, 10 nM promoted growth significantly by about 16% ( $P<0.01^{**}$ ), while 100 & 1000 nM had a greater effect of about 27% ( $P<0.001^{***}$ ; mean  $\pm$  SEM) (Figure 58).

Bimatoprost also prolonged anagen increasing the number of hairs remaining in anagen on day 9 by about 7% with 10 nM ( $P<0.05^{*}$ ) and about 11% with 100 & 1000 nM ( $P<0.01^{**}$ ) (Figure 59). Bimatoprost also stimulated the overall amount of hair synthesised in organ culture, expressed as actual values (Figure 60a) and as a % of their control follicles (Figure 60b). These were from  $0.482 \pm 0.021$  mm/follicle (mean  $\pm$  SEM) by about 20% to  $0.575 \pm 0.024$  mm/follicle with 10 nM ( $P<0.05^{*}$ ), by about 35% to  $0.648 \pm 0.024$  mm/follicle with 100 nM ( $P<0.01^{**}$ ) and by about 33% to  $0.639 \pm 0.024$  mm/follicle with 1000 nM ( $P<0.01^{**}$ ).

**Figure 57 Sequential photomicrographs of a human scalp hair follicle growing *in vitro* in media with 100 nM bimatoprost**

**(a)** Sequential photomicrographs of typical scalp hair follicles were taken every 24 hours for 9 days in organ culture with 100 nM bimatoprost, demonstrating growth of new hair fibre and the root sheaths but not the connective tissue sheath (CTS). Scale bar = 500 $\mu$ m.

**(b)** Enlarged photomicrographs of the hair follicle bulb (pictured in a), showing anagen morphology during 9 days in culture. Scale bar = 200 $\mu$ m.

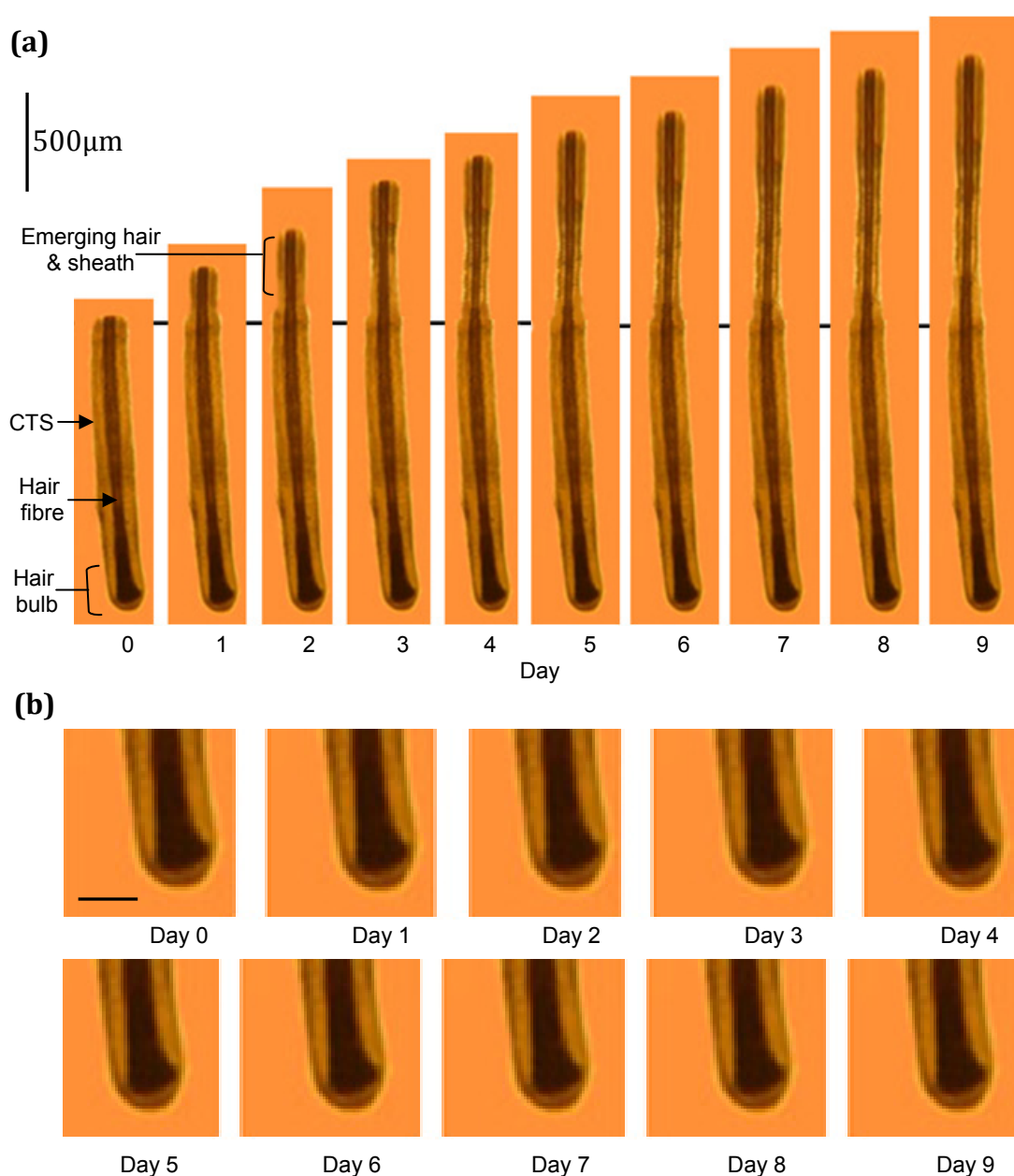


**Figure 58 Bimatoprost stimulated human scalp hair follicle growth in organ culture**

Anagen follicles were measured while cultured in basic culture medium either vehicle alone (control), or bimatoprost (10, 100 & 1000 nM) using an inverted microscope fitted with an eyepiece graticule. Hair follicles increased in length regularly and bimatoprost increased scalp hair follicle growth rate: with 10 nM ( $P < 0.01^{**}$ ) and with 100 & 1000 nM ( $P < 0.001^{***}$ ). Values are the mean  $\pm$  SEM of 5 individuals for each experiment; at least 6 follicles were examined per person for each condition. Statistical analysis was performed using a two-factor within-subjects ANOVA using SPSS, after confirming normal distribution, using KS-test.

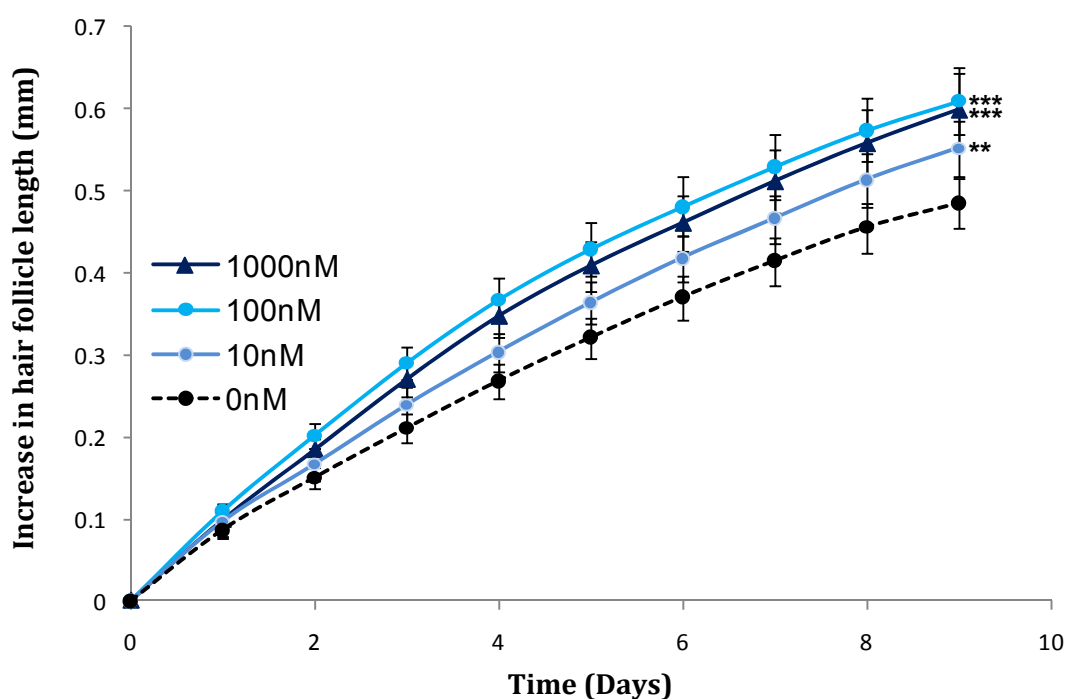


**Figure 59 Bimatoprost prolongs anagen in scalp hair follicles in organ culture**

Anagen follicles were assessed daily for changes in morphology while cultured in basic culture medium containing either the vehicle alone (control), or bimatoprost (10, 100 & 1000 nM). The proportion of hair follicles remaining in anagen throughout the culture was calculated and any follicles which developed catagen-like changes in their bulb morphology were not counted as anagen. The proportion of anagen follicles gradually decreased after one day in culture. Bimatoprost prolonged anagen on day 9 by about 7% with 10 nM ( $P<0.05^*$ ) and by about 11% with 100 & 1000 nM ( $P<0.01^{**}$ ). Values are the mean  $\pm$  SEM of 5 individuals; at least 6 follicles were examined per person for each condition. Statistical analysis was performed using a two-factor within-subjects ANOVA using SPSS, after confirming normal distribution, using the KS-test.

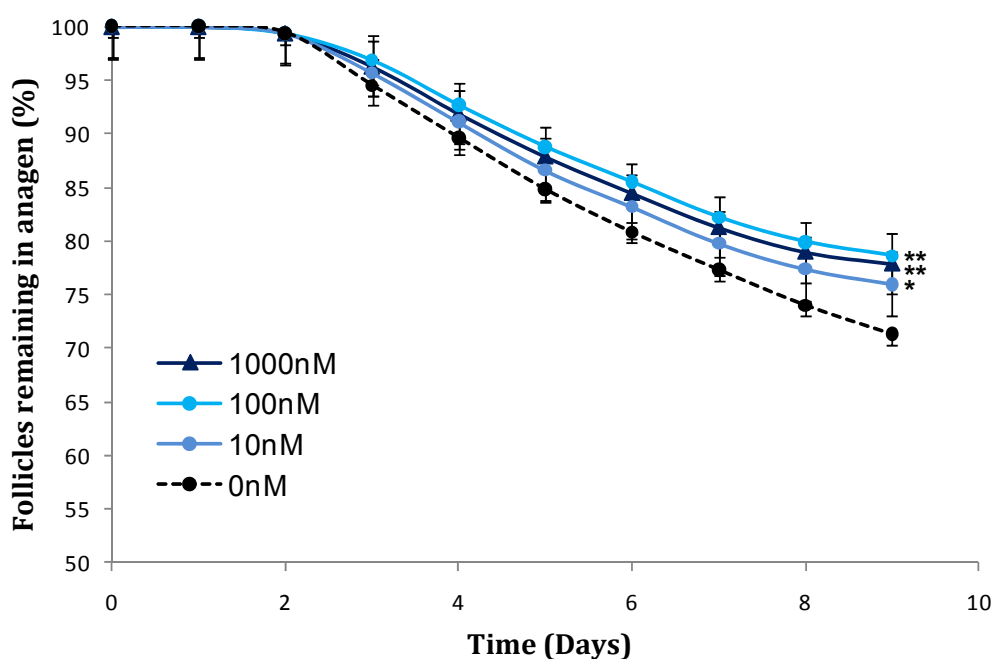
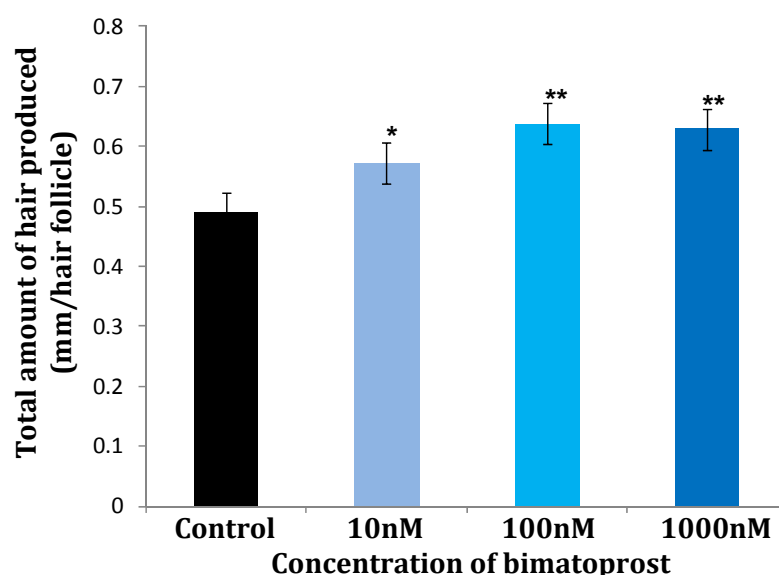


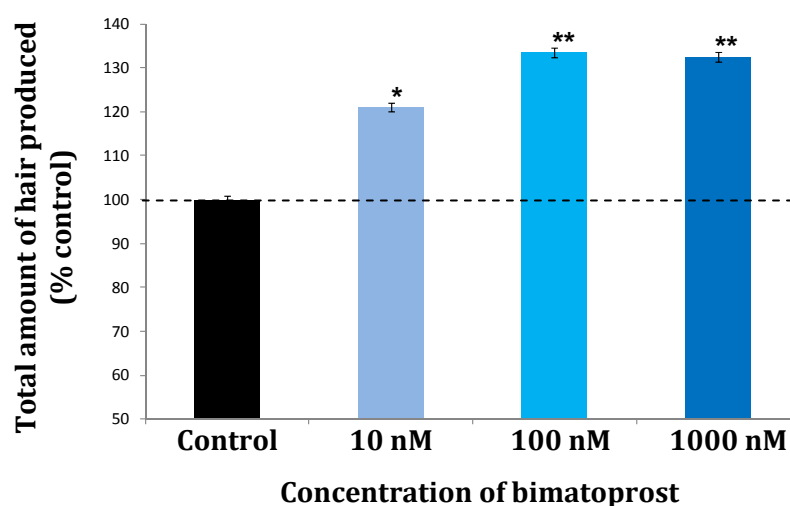
# **Figure 60 Bimatoprost increased the total amount of hair produced in organ culture**

Anagen follicles were measured while cultured in basic culture medium either vehicle or bimatoprost (10, 100 & 1000 nM). Bimatoprost stimulated the overall amount of hair synthesised in organ culture, results are expressed as mean actual values (a) or as a % of their own control follicles (b), by about 20% with 10 nM ( $P<0.05^*$ ), by about 35% with 100 nM ( $P<0.01^{**}$ ) and by about 33% with 1000 nM ( $P<0.01^{**}$ ). Values are the mean  $\pm$  SEM of 5 individuals; at least 6 follicles were examined per person for each condition. Statistical analysis was performed using a two-factor within-subjects ANOVA using SPSS, after confirming normal distribution, using KS-test.

(a)



(b)



### **3.10.2 An FP antagonist, AS604872 (AGN22827), and a prostamide F<sub>2α</sub> receptor antagonist, AGN211336, blocked bimatoprost-stimulation of scalp hair growth in organ culture**

To determine whether the bimatoprost stimulation was through FP and/or prostamide F<sub>2α</sub> receptor, the effect of an FP antagonist, AS604872, and a prostamide F<sub>2α</sub> receptor antagonist, AGN211336, on bimatoprost-stimulated hair growth was investigated on follicles from 5 further individuals; at least 6 follicles were examined per person per condition. Bimatoprost (100 nM) alone significantly increased the hair growth rate by about 27% ( $P < 0.001^{***}$ ) (Figure 62), the % of follicles remaining in anagen by about 11% ( $P < 0.01^{**}$ ) (Figure 63) and the total increase in follicle length by about 35% ( $P < 0.01^{**}$ ) (Figure 64). This stimulatory action of bimatoprost on all parameters was abolished when it was combined either with AS604872 or AGN211336 at 1μM ( $P < 0.05^{*}$ -  $0.001^{***}$ ) (Figures 61-64). The combination of bimatoprost and either of the antagonists were not significantly different from the control for all the parameters: growth rate ( $P=0.098$ ), percentage of follicles remaining in anagen at day 9 ( $P=0.104$ ) nor the overall amount of hair follicle synthesised ( $P=0.086$ ) (mean  $\pm$  SEM) (Figures 62-64).

**Figure 61 Sequential photomicrographs of a human scalp hair follicle growing in culture with 100 nM bimatoprost + 1 $\mu$ M prostamide F<sub>2 $\alpha$</sub>  receptor antagonist, AGN211336**

**(a)** Photographs of the same human hair follicle were taken every 24 hours for nine days growing in culture under combination of the 100nM bimatoprost and 1 $\mu$ M AGN211336 condition. Hair follicles synthesised new hair fibre regularly, increasing in length (similar to the vehicle but at much slower rate compared to 100nM bimatoprost alone). Scale bar = 0.5mm

**(b)** Enlarged photomicrographs of the hair follicle bulb (pictured in a), showing that the follicle maintained the anagen bulb morphology during the 9 days in culture. Scale bar = 0.2mm

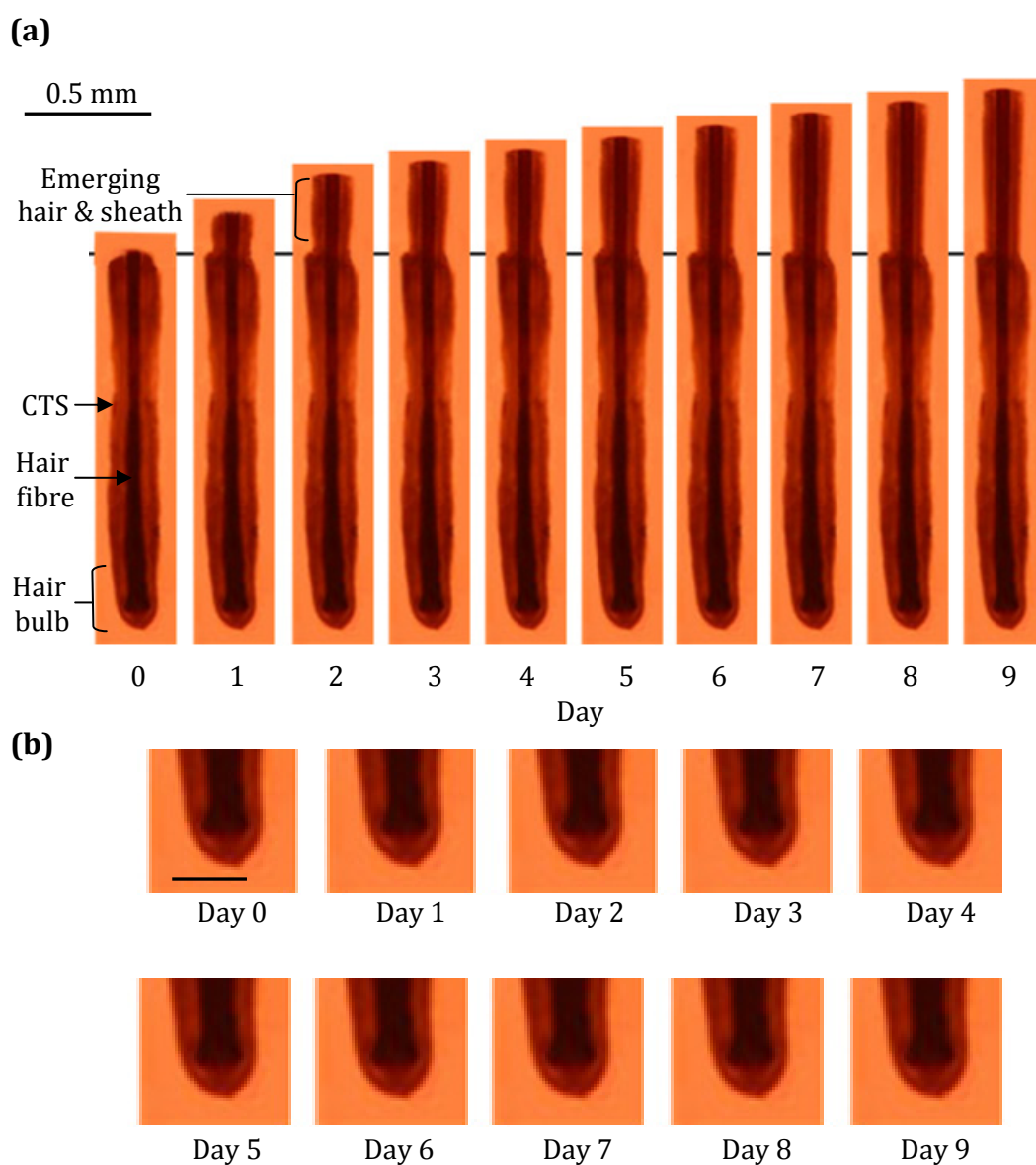
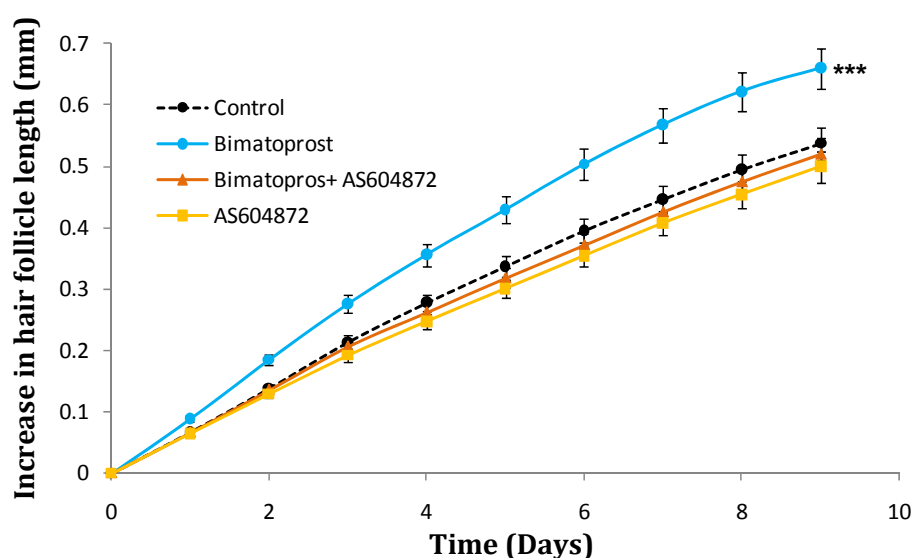




**Figure 62 AS604872 and AGN211336 blocked bimatoprost-stimulation of scalp hair follicle growth rate**

Bimatoprost (100nM) alone significantly increased the hair growth rate by about 27% ( $P < 0.001^{***}$ ) in organ culture. This growth-stimulating effect was abolished when it was combined with the FP antagonist, AS604872, (1 $\mu$ M) (**a**) and the prostamide  $F_{2\alpha}$  receptor antagonist, AGN211336, (1 $\mu$ M) (**b**) ( $P < 0.001^{***}$ ). Results are the mean  $\pm$  SEM of 5 individuals; at least 6 follicles were examined per person per condition. Statistical analysis was performed using a two-factor within-subjects ANOVA using SPSS after confirming normal distribution, using KS-test.

**(a) AS604872**



**(b) AGN211336**

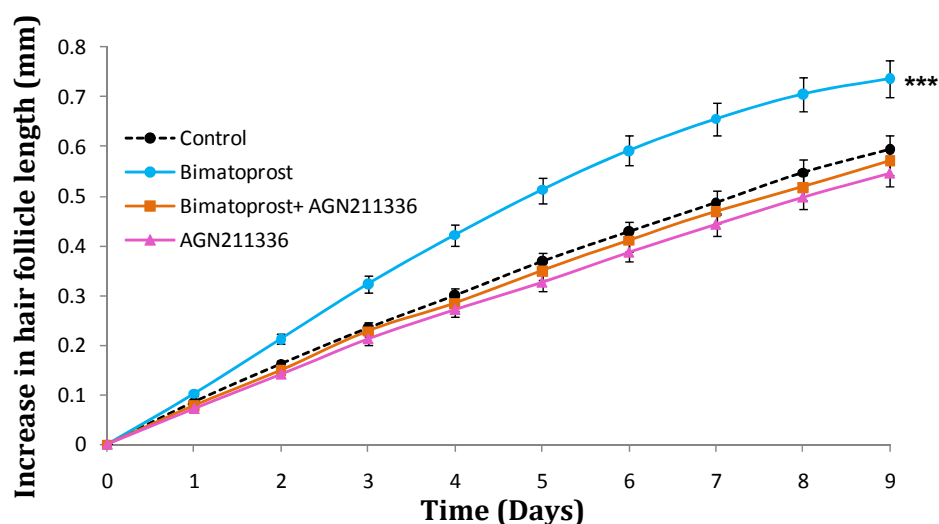
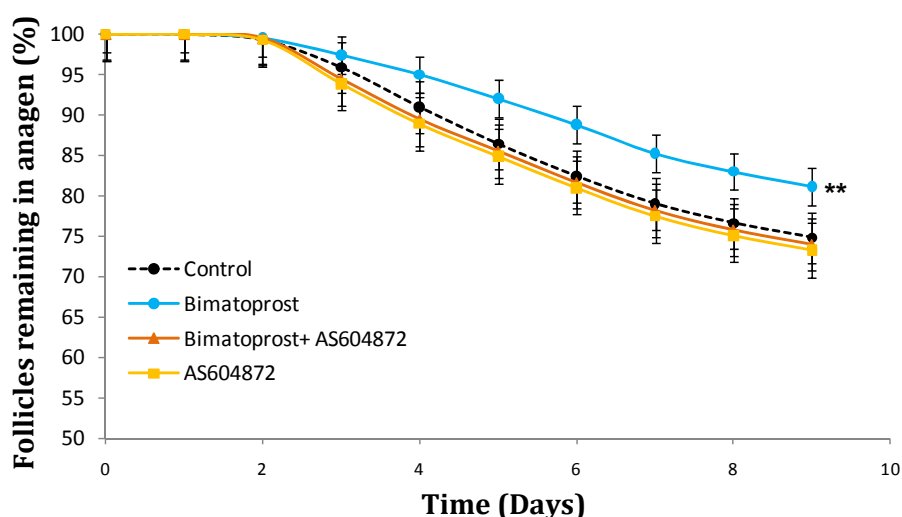


**Figure 63 AS604872 and AGN211336 blocked the bimatoprost-promoted increase in % of scalp hair follicles in anagen**

Bimatoprost (100 nM) alone significantly increased the percentage of follicles in anagen by about 11% ( $P < 0.01^{**}$ ) but this effect was blocked when it was combined with the FP antagonist AS604872 (1 $\mu$ M) (**a**) and the prostamide  $F_{2\alpha}$  receptor antagonist AGN211336 (1 $\mu$ M) (**b**) ( $P < 0.01^{**}$ ). Values are the mean  $\pm$  SEM of 5 individuals; at least 6 follicles were examined per person for each condition. Statistical analysis was performed using a two-factor within-subjects ANOVA using SPSS after confirming normal distribution, using the KS-test.

**(a) AS604872**



**(b) AGN211336**

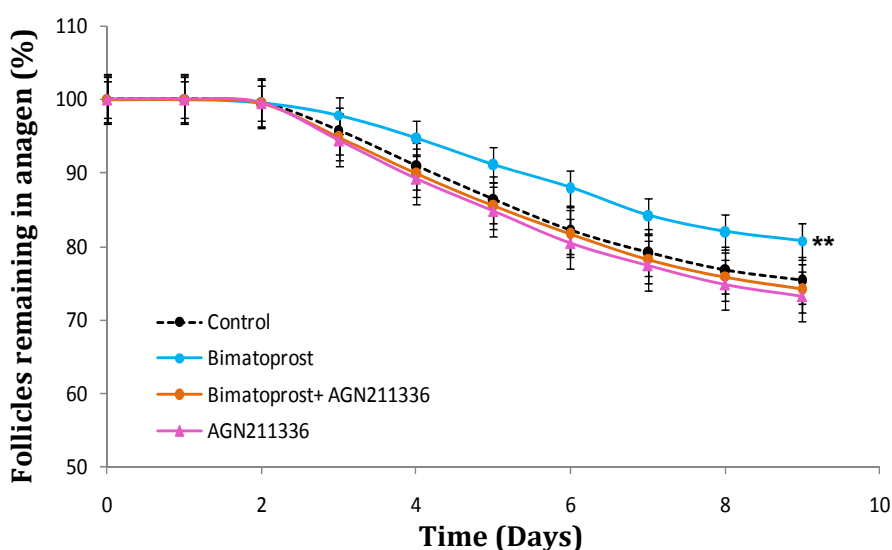
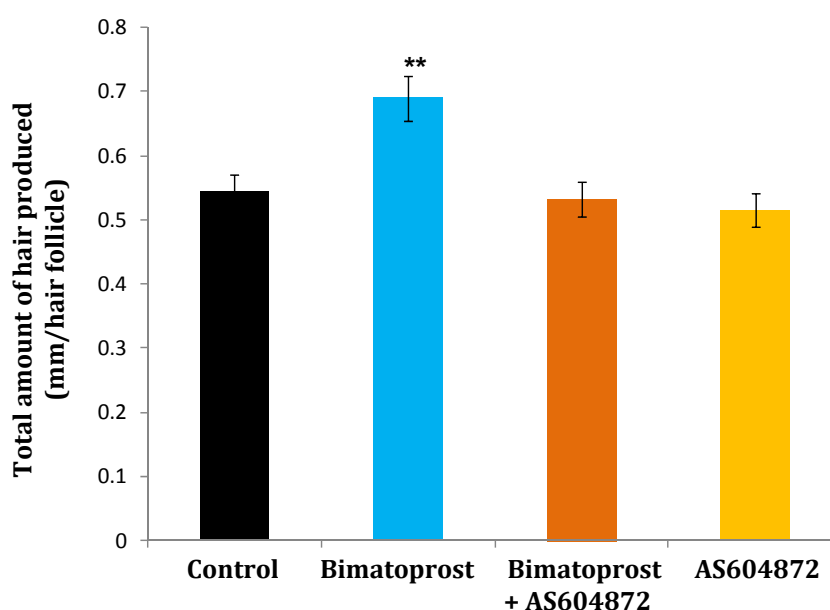


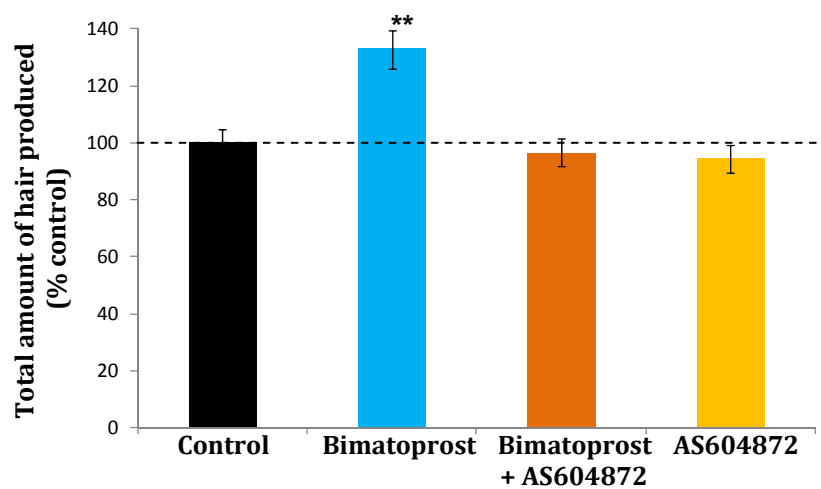
**Figure 64 AS604872 and AGN211336 blocked bimatoprost-stimulated increase in total amount of hair production**

The overall amount of hair produced by all the follicles in organ culture was calculated by recording the final length of each follicle on the last day the follicle maintained a normal anagen morphology. Bimatoprost alone (100 nM) increased the overall amount of hair synthesised expressed as mean actual values (a, c) or as a % of their own control follicles (b, d) by about 35% ( $P < 0.01^{**}$ ), but the FP antagonist AS604872 (1 $\mu$ M) (a, b) and the prostamide  $F_{2\alpha}$  receptor antagonist AGN211336 (1 $\mu$ M) (c, d) both abolished this response ( $P < 0.01^{**}$ ). Values are the mean  $\pm$  SEM of 5 individuals; at least 6 follicles were examined per person for each condition. Statistical analysis was performed using a two-factor within-subjects ANOVA using SPSS after confirming normal distribution, using the KS-test.

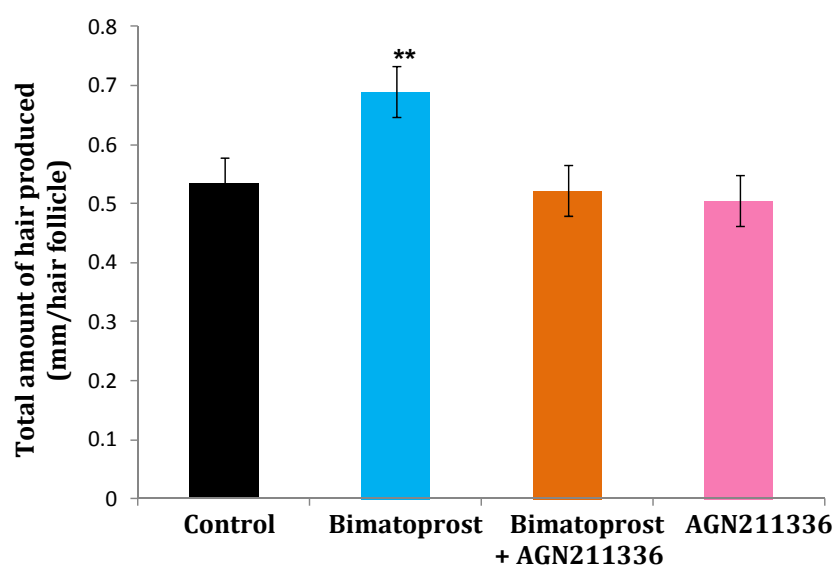
**(a) AS604872**



**(b) AS604872**



**(c) AGN211336**



**(d) AGN211336**

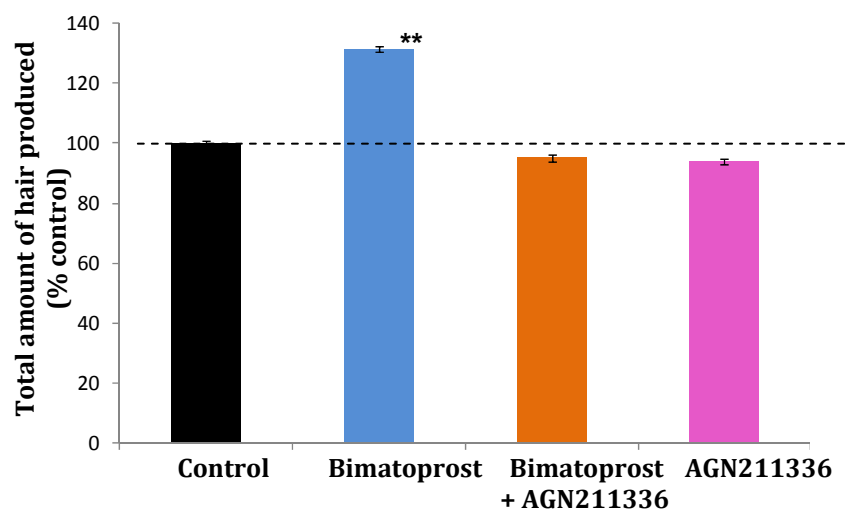
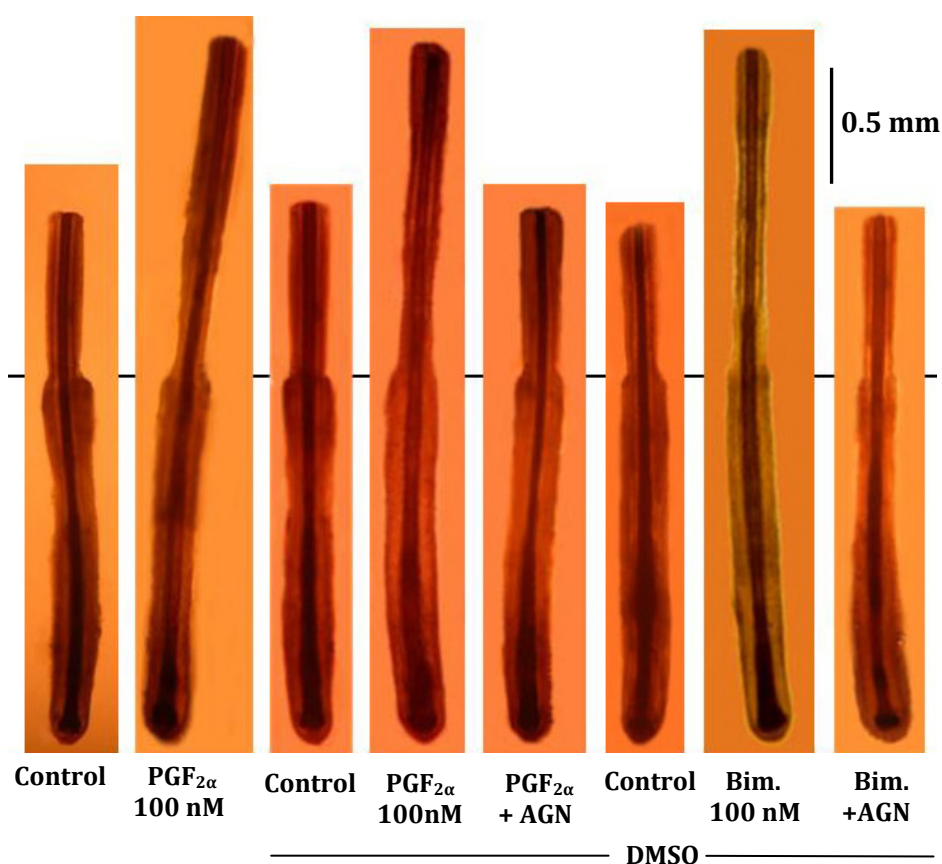


**Figure 65 Photomicrographs of scalp hair follicles after growing in different conditions in organ culture for 9 days**

Photomicrographs of typical scalp hair follicles after 9 days in organ culture in various conditions. From left: control medium, 100 nM  $\text{PGF}_{2\alpha}$ . The remaining follicles were cultured in the presence of 0.01% DMSO to increase drug solubility; these included: control medium containing the vehicle, 100nM  $\text{PGF}_{2\alpha}$ , 100nM  $\text{PGF}_{2\alpha}$  with FP antagonist AS-604872 (1 $\mu\text{M}$ ); control medium containing the vehicle, 100nM bimatoprost, or 100nM bimatoprost with FP antagonist AS-604872 (1 $\mu\text{M}$ ). Scale bar = 0.5 mm



### **3.11 Identification of genes for prostamide F<sub>2α</sub> receptors in human scalp hair follicles using molecular biological methods**

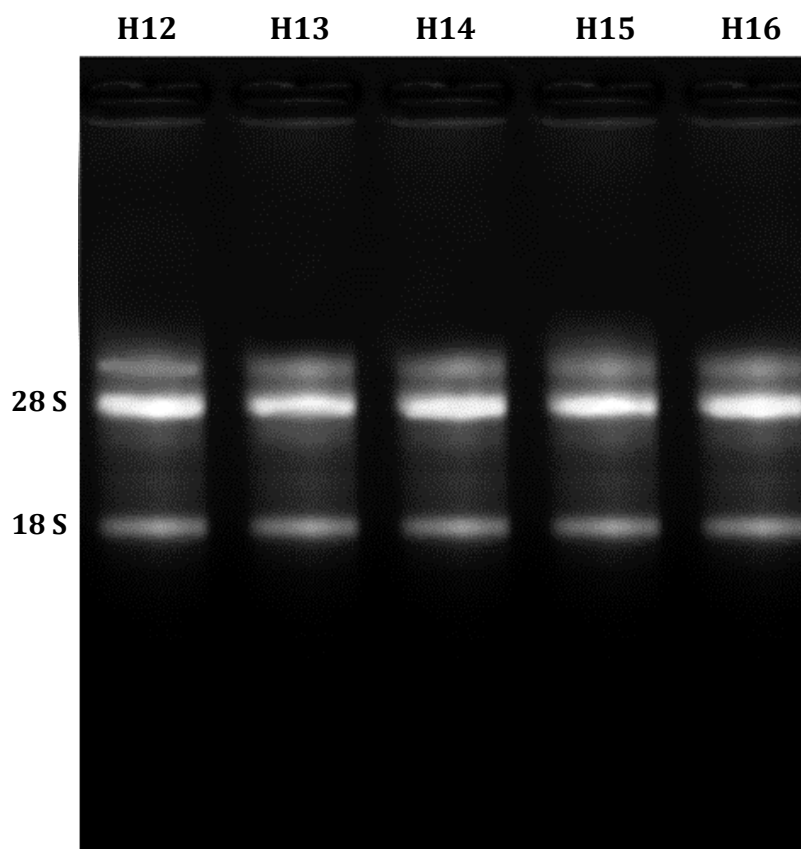
Since bimatoprost interacts with spliced variants of the FP (prostamide receptors) (Liang *et al.*, 2008), RT-PCR was used to investigate the expression of FP variant genes in occipital scalp anagen hair follicles from 5 different adult male individuals. Non balding scalp hair follicles were isolated, poly(A<sup>+</sup>)RNA extracted and cDNA was prepared separately from each individual's sample. Each cDNA was prepared from 65 lower hair follicles per donor and each individual's hair follicles were investigated separately (Table 9). The quality of each RNA sample was checked by gel electrophoresis on a 1.5% agarose gel. The total RNA from each sample had sharp 28S and 18S rRNA bands and the 28S rRNA band was approximately twice as intense as the 18S rRNA band (Figure 66), indicating that the RNA samples were of good quality. The concentration & purity of each total RNA sample was also checked spectrophotometrically (Table 9), followed by further purification to isolate poly(A<sup>+</sup>)RNA. The poly(A<sup>+</sup>)RNA samples were treated with DNase I to remove any contaminating genomic DNA and cDNAs were synthesised immediately.

**Table 9 The concentration and purity of RNA from lower follicles from human scalp skin samples used for prostamide receptor detection**

Human sample number	Gender	Age (years)	Total RNA purity ( $A_{260}/A_{280}$ )	Total RNA concentration ( $\mu\text{g/ml}$ )
H12	Male	33	1.65	162
H13	Male	40	1.8	147
H14	Male	46	1.75	125
H15	Male	38	1.9	132
H16	Male	35	2.0	170

**Figure 66 Gel electrophoresis of RNA from human scalp follicles**

Electrophoresis on a 1.5% agarose gel confirmed successful extraction of RNAs; 10 $\mu\text{l}$  from each total RNA sample was loaded. Two bands of 18S and 28S ribosomal RNA are obvious in the total RNA samples, exhibiting 2:1 ratio.



### **3.11.1 RT-PCR for $\beta$ -actin gene expression from anagen lower hair follicles**

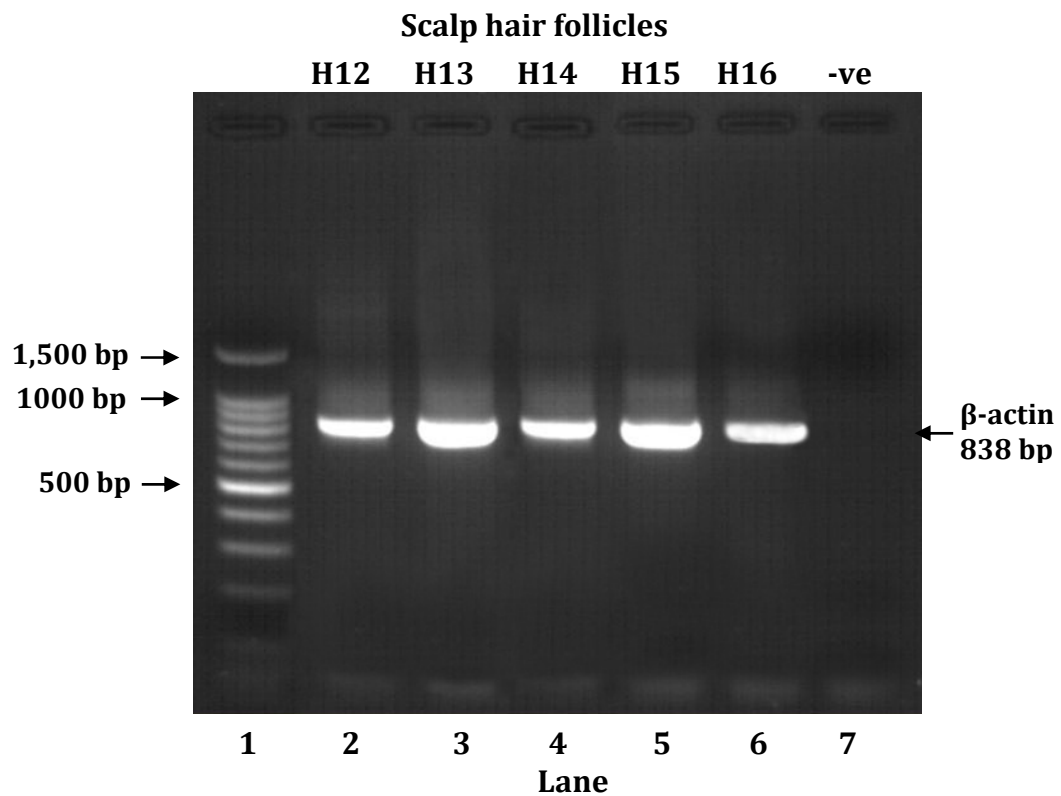
The cDNA qualities from all five lower hair follicle samples were initially checked using the positive control gene,  $\beta$ -actin, prior to investigating the expression of FP variant genes. RT-PCR was carried out using specific primers and 5 $\mu$ l of cDNA from each sample. Agarose gel electrophoresis (1.5% w/v) of the PCR products (30 $\mu$ l) from each of 5 individuals showed appropriately sized bands corresponding to  $\beta$ -actin (838 bp) (Figure 67). No bands were observed in the negative control in which the template cDNA was omitted from the PCR reaction mix. This indicated that the product bands resulted from the direct amplification of cDNA synthesised from the mRNA samples, and the reagents used in the PCR reaction mix were free from any DNA contamination.

The identity of  $\beta$ -actin PCR products were confirmed by sequence analysis of the PCR products. When the sequenced products were aligned with the known human  $\beta$ -actin gene sequences using the NCBI BLAST program (<http://www.ncbi.nlm.nih.gov/blast/bl2seq/wblast2.cgi>),  $\beta$ -actin PCR products showed 96% homology (data not shown).



### Figure 67 $\beta$ -actin gel electrophoresis

$\beta$ -actin gene expression in cDNA from five human scalp anagen lower hair follicles was investigated by RT-PCR using 5 $\mu$ l of cDNA. The resulting PCR products were separated by agarose gel (1.5% w/v) electrophoresis and visualised with ethidium bromide staining. 10 $\mu$ l DNA ladder 100-1500 bp (lane 1) and 30 $\mu$ l of each person's PCR products (lanes 2-6) were loaded on to the gel. A negative control in which cDNA was omitted from the PCR reaction mix was loaded on lane 7. All PCR products showed appropriately sized bands (838 bp) corresponding to  $\beta$ -actin.



### **3.11.2 Expression of the genes for the prostamide F<sub>2α</sub> receptors (FP splice variants) in human hair follicles using RT-PCR**

When the expression of FP gene splice variants were examined in human scalp hair follicles using primers which detects all the known FP splice variants (altFPs) three bands were seen (Figure 68a). Their sizes suggested the wild-type FP, prostamide receptor variant 4 (altFP4) or 3 and small amounts of another prostamide receptor possibly variant 1 (altFP1) or 2. Further RT-PCR reactions using relevant specific primers (Table 2) were carried out to determine which splice variants of variant 5 (altFP5), variant 4 (altFP4), variant 3 (altFP3), variant 2 (altFP2) and variant 1 (altFP1) were expressed in hair follicles. These primers only identified altFP4 and altFP1 genes in cDNA from scalp hair follicles from 5 individuals (Figure 68b, c). The altFP5, altFP3 and altFP2 were not detected (data not shown). There were no bands in the negative controls when the cDNA was replaced with nuclease-free water.

The identities of the PCR products for the splice variants altFP4 and altFP1 were checked by sequence analysis and their identities verified when compared against the relevant human FP gene sequence in GenBank. The altFP4 and altFP1 gene PCR products had 95 & 98 % homology respectively (Figure 69a, b).

**Figure 68 Human scalp anagen hair follicles expressed genes for 2 prostamide F<sub>2α</sub> receptors**

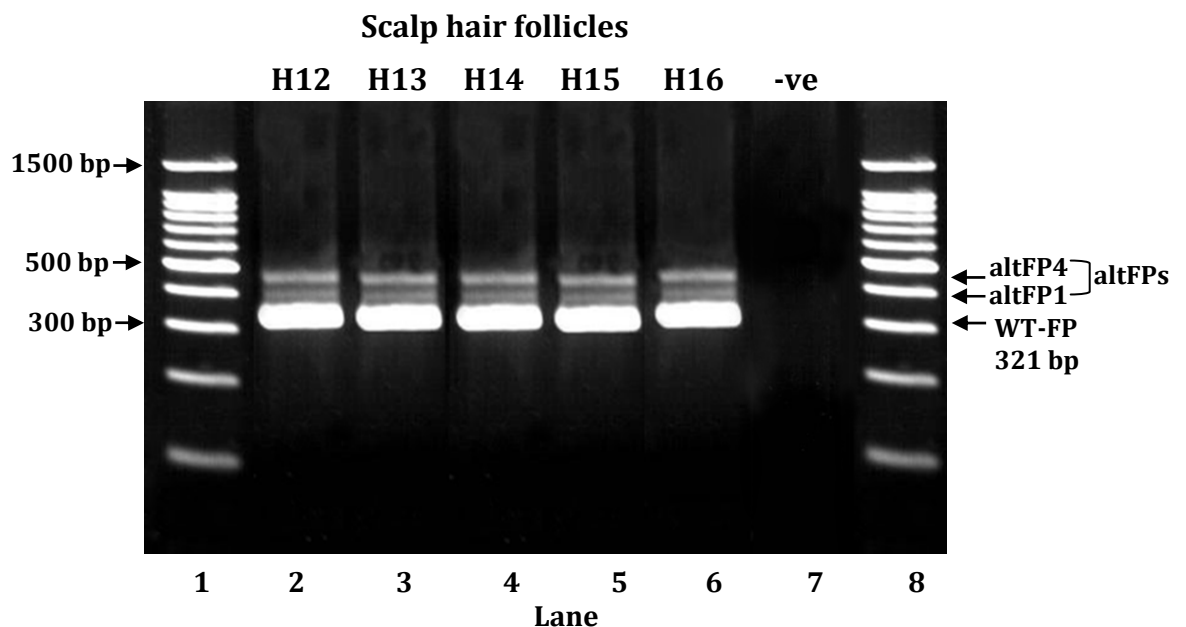
Agarose gel electrophoresis of PCR products (30 µl loaded) of lower hair follicle cDNAs from 5 different individuals showed appropriately sized product bands for FP variant receptors with primers for all FP splice variants (a), altFP4 (b) and altFP1 (c). There were no bands in the negative controls when cDNAs were omitted.

**(a)** Lanes 1 and 8, DNA ladder (100-1500 bp), lanes 2–6, altFPs PCR products showing bands corresponding to wild-type FP (321 bp) at the bottom, altFP1 at the middle and altFP4 at the top; lane 7, negative control.

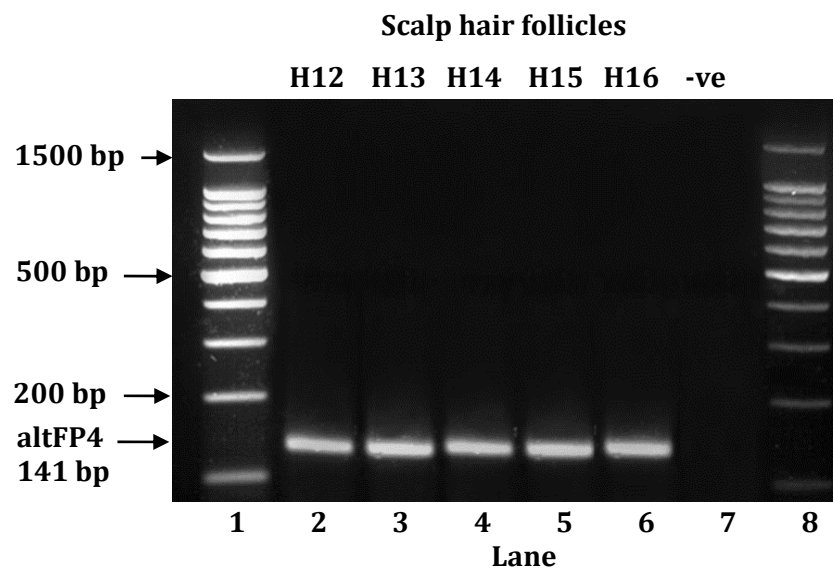
**(b)** Lanes 1 and 8, DNA ladder (100-1500 bp), lanes 2–6, altFP4 PCR products (141bp); lane 7, negative control.

**(c)** Lanes 1 and 8, DNA ladder (100-1500 bp), lanes 2–6, altFP1 PCR products (392bp); lane 7, negative control.

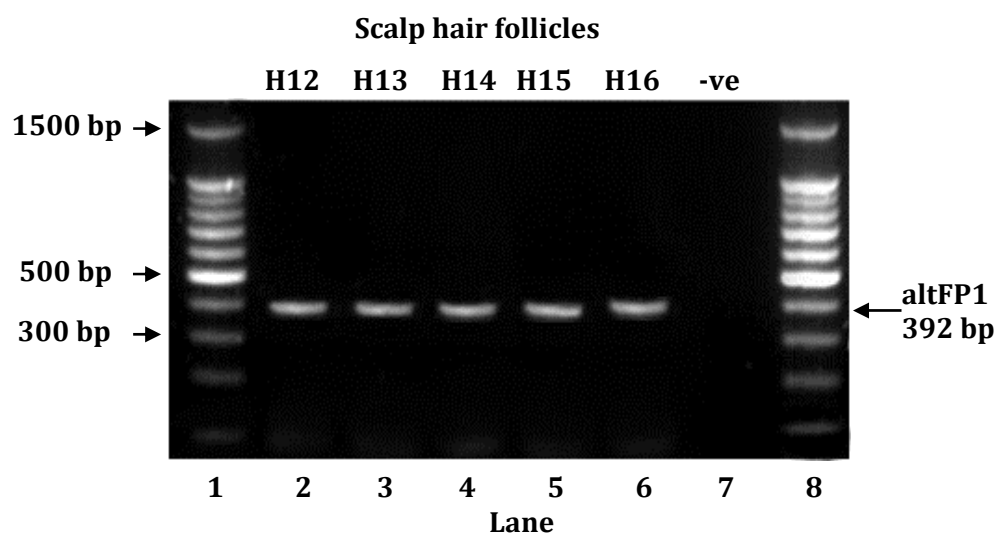
**(a) all FP splice variants**



(b) altFP4



(c) altFP1





### **3.11.3 Location of gene expression for prostamide F<sub>2α</sub> receptors in amplified RNA from human hair follicle components**

Amplified RNA (see section 3.8.5) from human scalp hair follicle components from 3 individuals (Table 7) were used to localise the gene expression of the prostamide F<sub>2α</sub> receptors (FP splice variants) in scalp hair follicle. RT-PCR was carried out using primers for altFPs, altFP5, altFP4, altFP3, altFP2 and altFP1 (see Table 2). When the PCR products were separated using agarose gel electrophoresis, dermal papilla and connective tissue sheath cDNA samples from each of 3 different individuals exhibited 3 bands using primers for altFPs (Figure 70a) which were similar to those of the prostamide F<sub>2α</sub> receptor gene expression in lower hair follicles (Figure 68). None of the other components, the matrix, the follicle from bulge area and the follicle area between the bulge and the bulb, showed any detectable bands (Figure 70, 72). Further RT-PCRs with primers for altFP4 (Figure 70b, 72) and altFP1 (Figure 70c, 72) also paralleled the FP distribution in the DP and CTS, but none of other components expressed either gene splicing variants. None of the hair follicle components cDNA showed detectable PCR products with the other primers for altFP5, altFP3 and altFP2 (data not shown). The negative controls were clear from any bands when cDNAs were omitted.

The identity of altFP4 and altFP1 PCR products from dermal papilla and connective tissue sheath were checked by sequence analysis; when they were aligned with the known human FP gene sequence using NCBI BLAST program, dermal papilla PCR products showed 94 & 91 % and connective tissue sheath PCR products showed 91 & 90 % homology respectively (Figure 71a, b, c, d).

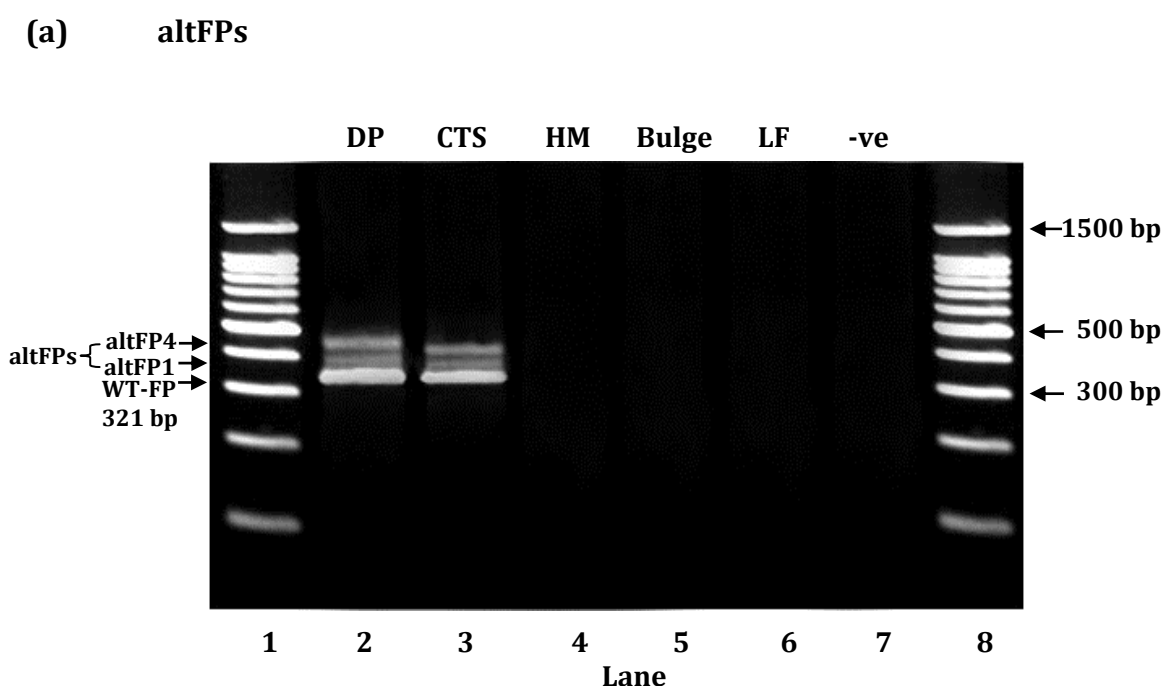
**Figure 70 Dermal papilla and connective tissue sheath cells of human scalp hair follicles expressed genes for 2 prostamide F<sub>2α</sub> receptors**

Typical agarose gel electrophoresis of PCR products from scalp hair follicle components, shows that only dermal papilla (DP) and connective tissue sheath (CTS) cDNA developed appropriately sized product bands for prostamide F<sub>2α</sub> receptor (FP splice variants) with primers for altFPs (a), altFP4 (b) and (altFP1) (c). No detectable bands were produced with cDNA from other components: the hair matrix (HM), the follicle from bulge area and the lower follicle area between the bulge and the bulb (LF).

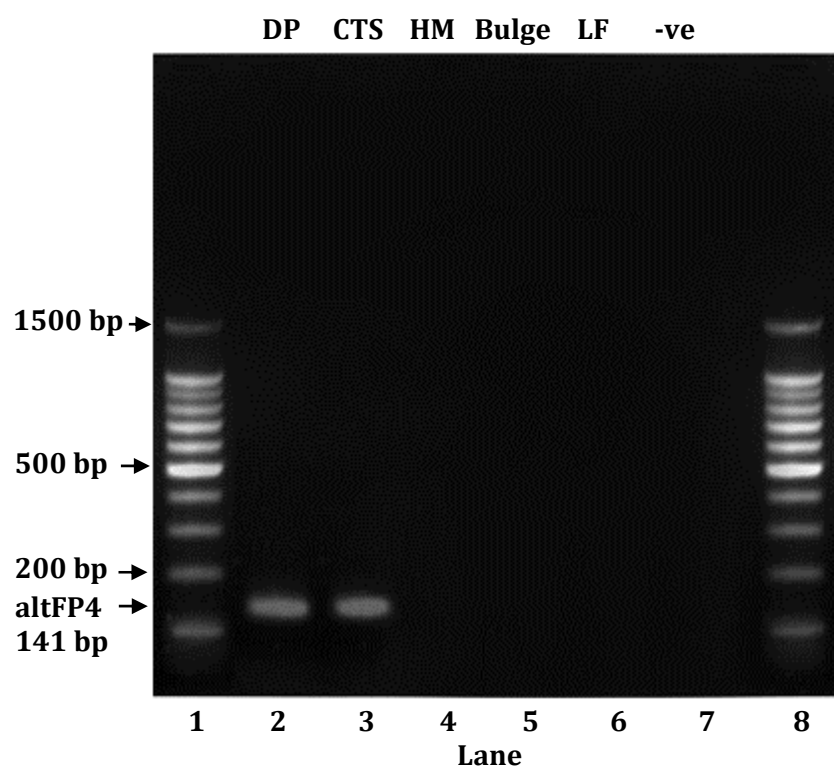
**(a)** Lanes 1 and 8, DNA ladder (100-1500 bp), lanes 2-6, altFPs PCR products from hair follicle components, shows bands for DP and CTS cDNA only corresponded to wild-type FP (321 bp) at the bottom, altFP1 at the middle and altFP4 at the top; lane 7, negative control without cDNA (-ve).

**(b)** Lanes 1 and 8, DNA ladder (100-1500 bp), lanes 2-6, altFP4 PCR products from hair follicle components, show expected size bands (141 bp) with DP and CTS cDNA; lane 7, negative control (-ve).

**(c)** Lanes 1 and 8, DNA ladder (100-1500 bp), lanes 2-6, altFP1 PCR products from hair follicle components, show expected size bands (392 bp) with DP and CTS cDNA only; lane 7, negative control (-ve).



**(b) altFP4**



**(c) altFP1**

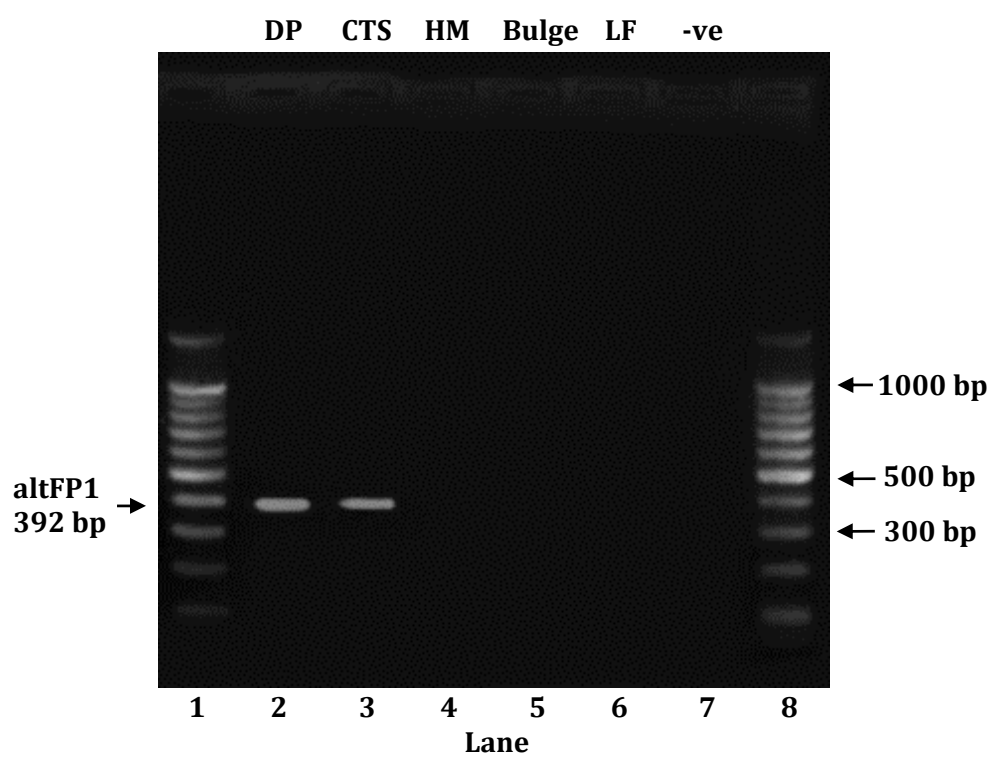




## Figure 71 Sequence analyses for FP splice variants RT-PCR products amplified from scalp hair follicle components cDNA, DP and CTS

The identities of altFP4 and altFP1 PCR products from DP and CTS were confirmed by sequencing. The sequenced products (query: red) were aligned against the known human FP gene sequence (subject: black) using NCBI BLAST programme. The bases that match in the two sequences are shown by a vertical line.

**(a)** The altFP4 PCR product of the human hair follicle DP cells exhibited 94% homology.

**(b)** The altFP4 PCR product of the human hair follicle CTS cells exhibited 91% homology.

**(c)** The altFP1 PCR product of the human hair follicle DP cells exhibited 91% homology.

**(d)** The altFP1 PCR product of the human hair follicle CTS cells exhibited 90% homology.

### (a) altFP4 for DP

```

Query  2      AGTTGTTTGATCCACTTTCATGTTGCCTCTCCATCCACACCTTAGTTCTTTCTGTCATAT  61
          |||
Sbjct  41247  AGTTGTTTGATCCACTTTCATGTTGCCTCTCCATCCACACCTT-GTT-TTTCTGTCAT-T  41191

Query  62      TCTCGATTGAAGTGTCTTATCGC  84
          |||
Sbjct  41190  TCTCG-TTGA-GTGTCTTATCGC  41170

```

### (b) altFP4 for CTS

```

Query  2      AGTTGTTTGATCCACTTTCATNTTGCCTCTCCATCCACACCTTAGAACTTTCTGTCATAT  61
          |||
Sbjct  41247  AGTTGTTTGATCCACTTTCATGTTGCCTCTCCATCCACACCTT-GTT-TTTCTGTCAT-T  41191

Query  62      TCTCGATTGAAGTGTCTTATCGC  84
          |||
Sbjct  41190  TCTCG-TTGA-GTGTCTTATCGC  4117

```

**(c) altFP1 for DP**

```
Query 83 TTTCT-GGTTACAATGGCCAACATTGGAATAAATGGAAATCATTCTCTGGAAACCTGTGA 14
      ||||| |||||||||||||||||||||||||||||||||||||||||||||||||||||||
Sbjct 43002 TTTCTAGGTTACAATGGCCAACATTGGAATAAATGGAAATCATTCTCTGGAAACCTGTGA 43061

Query 142 AACAACTTTTGTCTCTCCGAATGGTTACATGGAATCAAATCTTAGATCATAAAAGTAT 201
      ||||| |||||||||||||||||||||||||||||||||||||||||||||||||||||
Sbjct 43062 AACAACTTTTGTCTCTCCGAATGGTTACATGGAATCAAATCTTAGATCCTTGG-GTAT 43120

Query 202 ATATTCTTCTACGAAAGGCTGTCCTTAAAAATCTCTATAAACTTGCCAGTCAATGCTGT 261
      ||||| |||||||||||||||||||||||||||||||||||||||||||||||||||||
Sbjct 43121 ATATTCTTCTACGAAAGGCTGTCCTTAAAGAATCTCTATAAG-CTTGCCAGTCAATGCTGT 43179

Query 262 GGGAGTG 268
      || ||||
Sbjct 43180 GG-AGTG 43185
```

**(d) altFP1 for CTS**

```
Query 83 TTTCT-GGTTACAATGGCCAACATTGCAATAAATGGAAATCATTCTCTGGAAACCTGTGA 14
      ||||| |||||||||||||||||||||||||||||||||||||||||||||||||||||||
Sbjct 43002 TTTCTAGGTTACAATGGCCAACATTGGAATAAATGGAAATCATTCTCTGGAAACCTGTGA 43061

Query 142 AACAACTTTAGGCTCTCCGAATGGTTACATGGAATCAAATCTTAGATCATAAAAGTAT 201
      ||||| |||||||||||||||||||||||||||||||||||||||||||||||||||||
Sbjct 43062 AACAACTTTTGTCTCTCCGAATGGTTACATGGAATCAAATCTTAGATCCTTGG-GTAT 43120

Query 202 ATATTCTTCTACGTNAGGCTGTCCTTAAAAATCTCTATAAACTTGCCAGTCAATGCTGT 261
      ||||| |||||||||||||||||||||||||||||||||||||||||||||||||||||
Sbjct 43121 ATATTCTTCTACGAAAGGCTGTCCTTAAAGAATCTCTATAAG-CTTGCCAGTCAATGCTGT 43179

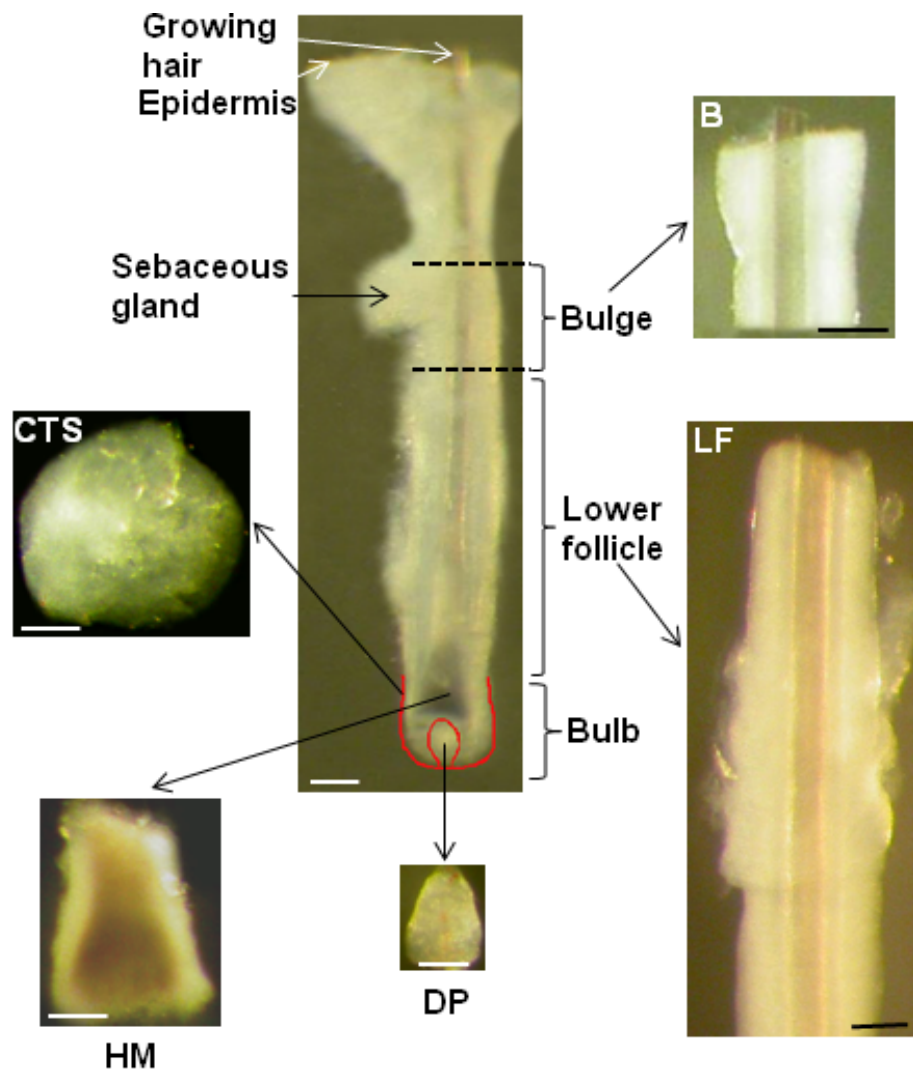
Query 262 GGGAGTG 268
      || ||||
Sbjct 43180 GG-AGTG 43185
```

**Figure 72 Summery of the localisation of the gene expression of prostaglandin and prostamide F<sub>2α</sub> receptors in scalp hair follicle dermal papilla and connective tissue sheath but not in other follicular components**

**(a)** Photomicrographs of an isolated scalp hair follicle and its microdissected components. The hair bulb (outlined in red) was microdissected into the mesenchyme-derived dermal papilla (DP; outlined in red), the hair matrix (HM), containing dividing and differentiating keratinocytes and actively pigmenting melanocytes, and the surrounding connective tissue sheath (CTS); also outlined in red. The sheath is seen dissected flat. Follicles were collected above the bulb up to the top of the sebaceous gland and then separated into the 'bulge' area, containing epithelial and melanocyte stem cells (B) and the remaining lower follicle (LF).

**(b)** Table of results of RT-PCR using specific primers for all splice variants of FP, FP and each of 5 splice variants of FP (see Figure 70) in hair follicle components. Prostamide receptor FP variants 1 & 4 and the prostanoid receptor FP were detected only in the dermal papilla and connective tissue sheath (CTS) components from each of 3 individual's scalp follicles; no expression was seen in the other components examined. CTS: connective tissue sheath;  $\sqrt{\phantom{x}}$  = gene expression in one person's follicles, **x** = no expression.

(a)



(b)

Primers	Dermal papilla	Hair matrix	Bulb CTS	Lower follicle	Bulge region
FP-all v	✓✓✓	xxx	✓✓✓	xxx	xxx
altFP1	✓✓✓	xxx	✓✓✓	xxx	xxx
altFP2	xxx	xxx	xxx	xxx	xxx
altFP3	xxx	xxx	xxx	xxx	xxx
altFP4	✓✓✓	xxx	✓✓✓	xxx	xxx
altFP5	xxx	xxx	xxx	xxx	xxx
FP	✓✓✓	xxx	✓✓✓	xxx	xxx

## 4 Discussion

Hair loss disorders, such as androgenetic alopecia (Hamilton, 1951) or alopecia areata (Randall, 2001b), cause significant psychological distress (Girman et al., 1998; Gulec et al., 2004) and negative effects on the quality of life even in men who have never sought treatment (Girman et al., 1998). Unfortunately, hair loss disorders are currently poorly controlled; available therapies are either limited in their effectiveness or have unwanted side effects (Rogers and Avram, 2008; Garg and Messenger, 2009). Interestingly, two of the main therapies for androgenetic alopecia were developed for other conditions. Minoxidil (Regaine), which opens ATP-sensitive potassium channels (Shorter et al., 2008), was originally an oral antihypertensive drug, but this application was discontinued as it stimulated unacceptable hair growth in many areas (Messenger and Rundegren, 2004). Finasteride (Propecia), which reduces androgen effects by blocking testosterone metabolism to the more active  $5\alpha$ -dihydrotestosterone, was initially designed for prostate disorders (Kaufman et al., 1998; Whiting et al., 2003). The most recent drugs reported to stimulate hair growth as an unexpected side-effect are analogues of  $\text{PGF}_{2\alpha}$  and prostamide  $\text{F}_{2\alpha}$ , such as latanoprost and bimatoprost, used as eyedrops to reduce intraocular pressure in glaucoma. These drugs frequently stimulate eyelashes to lengthen, thicken and darken (Curran, 2009). However, human hair follicles exhibit different behaviour depending on their body site. For example hair greying with age occurs first above the ears before gradually spreading over the scalp (Keogh and Walsh, 1965). There are also extreme differences in response to androgens which stimulate hair growth in many areas, such as the beard, have no effect on eyelashes and, in contrast, inhibit scalp follicles causing balding (Randall, 2007, 2008a). Therefore, it is important to

determine whether  $\text{PGF}_{2\alpha}$  and prostamide  $\text{F}_{2\alpha}$  analogues can also stimulate scalp follicle growth.

Why eyelash stimulation occurs with this glaucoma therapy is unknown; possibilities include stimulating blood flow to the eyelashes or direct effects on the eyelash follicles. Latanoprost has been reported to relax rabbit ciliary arteries (Ishikawa et al., 2002). Although eyelashes are rather specialised hairs which protect the eyes from foreign objects, they are produced by hair follicles and are regularly replaced via the hair cycle (Thibaut et al., 2009). In this way they resemble all other hair follicles, including those on the scalp (Kligman, 1959; Higgins et al., 2009a).

The initial aim of this study was to determine if scalp hair follicles could also respond to  $\text{PGF}_{2\alpha}$  related compounds and therefore could be useful for treating hair loss disorders. Working on the hypotheses that eyelash follicles resemble other hair follicles and that  $\text{PGF}_{2\alpha}$  is acting directly on the eyelash follicles themselves, experiments were carried out to see whether  $\text{PGF}_{2\alpha}$  could stimulate growth in isolated human scalp hair follicles in organ culture. Isolated human scalp anagen hair follicles have an exciting and fascinating ability to grow in organ culture for several days, maintaining the epithelial & mesenchymal interactions (Reynolds et al., 1999; Rendl et al., 2005) and cell division necessary for the ordered synthesis of new pigmented hair as seen *in vivo* (Shorter et al., 2008) (See Figure 19); any stimulation of growth under these conditions cannot be due to effects on the vasculature.

The difference between producing a long or short human hair is primarily due to alterations in the length of anagen, the growing part of the hair growth cycle, rather than the rate of hair growth which is relatively constant *in vivo*. Anagen varies from several years in a large terminal scalp follicle, forming a long hair to only a few weeks for the short hairs on the finger (Saitoh and Sakamoto, 1970). During balding in

androgenetic alopecia, the length of scalp follicle anagen is substantially reduced and the resting phase, telogen, is increased (Whiting, 1993). When hypertrichosis of eyelashes was reported after unilateral topical latanoprost treatment of 89 glaucoma patients; changes to eyelashes including increased number, thickness, length and pigmentation had occurred in 5 of the patients in less than 3 weeks, similar to those patients who had received long term treatment (Johnstone, 1998), suggesting effects on follicles already in anagen. The organ culture method used here is based on that established by Philpott *et al* (Philpott et al., 1990), but was extended to include daily observation of follicle morphology, to monitor if the follicle remained in anagen, and length measurement. These modifications reveal much more detail. They allow assessment of any effects on the length of anagen and provide a more precise rate of growth, since the final length can be related to the number of days the follicle was actually growing. They also enable a more accurate measurement of the increase in hair length, as apparent increases due to the upward movement of the hair when follicles enter the catagen-like stage are avoided. The overall increase in hair length over the experimental period incorporates both the effect on anagen and any alteration in growth rate.

In line with the established method (Philpott et al., 1990), insulin was added to all culture conditions. Insulin advances the movement of ions across the plasma membrane (Irwin and Rippe, 2008) and acts as a stimulant of glucose uptake into cells and storage (Cushman and Wardzala, 1980; Suzuki and Kono, 1980; Leney and Tavaré, 2009). It is not used to supplement the medium in experiments involving minoxidil as it interferes with minoxidil's effects (Shorter et al., 2008).

Follicles grew well in control conditions regularly increasing in length throughout the culture period. Observation of cultured follicles indicated that this increase in hair

follicle length was due to the production of a hair fibre and associated inner and outer root sheathes, but the connective tissue sheath did not increase in length and remained at the same level as in day 0; growth was not due to a loss of follicle morphology during culture (Figure 19). Follicles which showed no increase in length over 3 days were assumed to be damaged and removed from the experiment.

In control conditions human scalp hair follicles grew at a rate of about 0.1 mm per day (Figure 20) and some hair follicles developed catagen-like changes in their bulb morphology, but most follicles (about 70%) maintained their anagen bulb morphology during the nine days of culture (Figure 21). Those follicles which were designated as undergoing catagen-like changes in their hair bulb morphology showed that pigmentation had ceased and the base of the hair fibre moved upward, losing contact with the regulatory mesenchyme-derived dermal papilla, which became rounded up into a ball of cells (Figure 19c, d). After 2 days there was a gradual increase in the number of follicles showing catagen-like changes in the hair bulb region. The overall amount of hair follicle synthesised in organ culture was calculated from the increased length of each follicle on the last day of the experiment, day 9, or the last day that follicle maintained a normal anagen morphology; in control condition about 40% hair fibre was synthesised (Figure 22).

PGF<sub>2α</sub> stimulated individual isolated scalp hair follicles from 10 different people to grow significantly faster and stay in anagen longer in organ culture, resulting in about a third more new hair being synthesised over 9 days especially with 100 & 1000 nM (Figures 23-26). This was a dose-responsive effect, though increasing over 100 nm caused no further enlargement; this would concur with the saturation of a receptor-mediated effect via the PGF<sub>2α</sub> receptor, FP, as reported in other tissues (Sharif et al., 1999; Liang et al., 2003; Woodward et al., 2003).



All 3 concentrations of  $\text{PGF}_{2\alpha}$  stimulated human scalp hair follicles to grow faster *in vitro*; increased growth rate significantly by about 16% with 10 nM ( $P < 0.01^{**}$ ) while 100 & 1000 nM had a similar and greater effect, about 25% ( $P < 0.001^{***}$ ) (Figure 24).  $\text{PGF}_{2\alpha}$  slightly raised the number of follicles remaining in anagen by about 6% with 10 nM ( $P < 0.05^*$ ) and by about 10% with 100 & 1000 nM ( $P < 0.01^{**}$ ) (Figure 25).  $\text{PGF}_{2\alpha}$  also stimulated the overall amount of hair follicle synthesised in organ culture by about 20% with 10 nM ( $P < 0.05^*$ ), by about 32% with 100 nM ( $P < 0.01^{**}$ ) and by about 30% with 1000 nM ( $P < 0.01^{**}$ ) (Figure 26).

To confirm that the  $\text{PGF}_{2\alpha}$  effects was through prostanoid FP receptor in the hair follicles themselves, the ability of the FP antagonists, AS604872 and AL-8810, to block  $\text{PGF}_{2\alpha}$ -stimulated hair growth in organ culture was assessed. Both AS604872 and AL-8810 have been reported to be potent FP antagonists in human and feline ocular tissue (Sharif et al., 1999; Woodward et al., 2007; Woodward and *al.*, in press) with  $\text{pA}_2$  of about 7.33 against the human FP receptor (Cirillo et al., 2007). DMSO (0.01%) was added to the control media as this was necessary to solubilise the FP antagonists, however, it caused no significant differences in growth rate, percentage of follicles remaining in anagen at day 9 nor the overall amount of hair follicle synthesised compared to the original control media (see Figures 20-22; 31-33). Similarly, the presence of 0.01% DMSO did not alter any of responses to 100 nM  $\text{PGF}_{2\alpha}$  (see Figures 24-26; 31-33).  $\text{PGF}_{2\alpha}$  alone again significantly increased all parameters compared to the control (hair growth rate ( $P < 0.001^{***}$ ; Figure 31), the % of follicles remaining in anagen ( $P < 0.01^{**}$ ; Figure 32) and the total amount of hair produced ( $P < 0.01^{**}$ ; Figure 33)), but those stimulatory effects were blocked when combined with either the FP antagonist, AS604872, at 1  $\mu\text{M}$  or AL-8810 at 10  $\mu\text{M}$  ( $P <$

0.01\*\*- 0.001\*\*\*; Figures 30-33). Neither FP antagonist alone significantly inhibited any parameters of scalp hair growth compared to the control conditions.

The saturation of the effect at receptor relevant concentrations and the ability of the potent FP antagonists, AS-604872 and AL-8810, to block the stimulatory effects of  $\text{PGF}_{2\alpha}$  at all hair growth parameters in this dynamic bioassay indicate a receptor-mediated response.

Latanoprost, the  $\text{PGF}_{2\alpha}$  analogue, has also been reported to increase eyelash growth in human beings (Johnstone, 1997). To determine whether latanoprost can stimulate scalp hair growth *in vitro*, the pharmacological responses of different concentrations of latanoprost on human scalp hair follicles was also investigated in organ culture. Latanoprost had similar effects to the natural ligand,  $\text{PGF}_{2\alpha}$ , stimulating individual isolated scalp hair follicles from 10 different people to grow significantly faster by about 18% with 10 nM ( $P < 0.01^{**}$ ) while 100 & 1000 nM had a similar and greater effect, about 26% ( $P < 0.001^{***}$ ) (Figure 27). Latanoprost also slightly raised the number of follicles remaining in anagen by about 6% with 10 nM ( $P < 0.05^{*}$ ) and by about 10% with 100 & 1000 nM ( $P < 0.01^{**}$ ) (Figure 28) and increased the overall amount of hair follicle synthesised in organ culture by about 22% with 10 nM ( $P < 0.05^{*}$ ), by about 33% with 100 nM ( $P < 0.01^{**}$ ) and by about 31% with 1000 nM ( $P < 0.01^{**}$ ) (Figure 29).

This stimulation of the growth of human scalp hair follicles mirrors that seen *in vivo* in monkeys. Uno *et al.*, (2002) also reported that different concentrations of latanoprost had variable responses in scalp hair growth in stump-tailed macaques; the lower concentration (115 nM) caused minimal hair growth, whilst the higher concentration (1.15  $\mu\text{M}$ ) caused significant hair growth. Using a murine model, the stimulatory effects of latanoprost on the hair follicles and the follicular melanocytes

in both the telogen and anagen stages were observed following treatment with  $\text{PGF}_{2\alpha}$  and several analogues including latanoprost; they also stimulated conversion from the telogen to the anagen phase (Sasaki et al., 2005), also indicating a non-eyelash follicle response.

The scalp hair follicle response to latanoprost in organ culture, like that to  $\text{PGF}_{2\alpha}$ , was also a dose-responsive effect, though increasing over 100 nM caused no further stimulation; suggesting the saturation of a receptor-mediated effect.

Importantly, these results indicate that  $\text{PGF}_{2\alpha}$  and latanoprost can stimulate growth in human scalp hair follicles as well as eyelashes. The strong similarities in the responses to a natural ligand,  $\text{PGF}_{2\alpha}$ , and the synthetic analogue, latanoprost, could suggest that both are working through the same receptors in the hair follicles. Alternatively, this could reflect the maximum increase in growth that can be achieved in organ culture under these conditions; recent experiments have highlighted that the conditions employed can affect follicular responses (Shorter et al., 2008). Since this is occurring in isolated follicle organ culture without any possibility of involving alterations in blood supply, interactions with other skin tissues or circulating cells, direct effects via receptors in hair follicle cells seem likely. The  $\text{PGF}_{2\alpha}$  and latanoprost receptor-mediated stimulation of hair growth possibly occur via altering paracrine transcription factors mediated by dermal papilla cells. Interaction of  $\text{PGF}_{2\alpha}$  and latanoprost with their receptor, FP, trigger  $G_q$  protein-coupled activating  $\text{Ca}^{2+}$  signalling pathways, which lead to initiating second messenger production of inositol 1,4,5-triphosphate and activation of protein kinase C. This can cause activation and increase in the cytoplasmic  $\beta$ -catenin protein level. The activated  $\beta$ -catenin protein is then translocates to the nucleus and forms a complex with members of Lef1/Tcf family of transcription factors and subsequently regulates the expression of Wnt-

target genes. The  $\beta$ -catenin is at the core of the Wnt signalling pathway and Wnt/ $\beta$ -catenin signalling pathway has a crucial role in the hair follicle development and cycling (Van Genderen et al., 1994); several studies have suggested that multiple steps in hair follicle development and cycling are dependent upon a change in the transcriptional status of genes that are regulated by Wnt/ $\beta$ -catenin signalling pathway (Reddy et al., 2001; Merrill et al., 2001; DasGupta and Fuchs, 1999). In mice, it was demonstrated that high level of  $\beta$ -catenin cause rapid proliferation of matrix cells (Gat et al., 1998; Chan et al., 1999). Selective ablation of Lef1 gene in the epidermis inhibits hair follicle development (Van Genderen et al., 1994). In contrast, transgenic mice over-expressing Lef1 resulted in *de novo* hair follicle formation in the skin and forced activation of Wnt/ $\beta$ -catenin signalling in the epidermis induced extra hairs (Gat et al., 1998; Millar S 2002; Alonso and Fuchs, 2003). It was demonstrated that increase in the levels of nuclear  $\beta$ -catenin in dermal papilla cells induced stem cell differentiation (Hino et al., 2005) and chronic activation of  $\beta$ -catenin results in proliferation of the outer root sheath and other epithelial components of the hair follicle (Seidensticker and Behrens, 2000). Many studies in mouse models have revealed that Wnt/ $\beta$ -catenin signalling plays a crucial role in hair follicle morphogenesis (DasGupta and Fuchs, 1999; Huelsken et al., 2001). *Dkk4* is a direct target gene of Wnt/ $\beta$ -catenin signalling and is predominantly expressed in the hair follicle placode (Sick et al., 2006; Bazzi et al., 2007). Ablation of  $\beta$ -catenin blocks HF formation all together (Huelsen et al., 2001) and introducing stabilised  $\beta$ -catenin induced resting hair follicles into anagen and promoted growth of existing follicle in mice (Celso et al., 2004).

Another possible mechanism of  $\text{PGF}_{2\alpha}$  and latanoprost receptor-mediated action is via  $\text{Ca}^{2+}$  signalling pathway (Figure 73). Interaction of  $\text{PGF}_{2\alpha}$  and its analogues with FP trigger  $G_q$  protein-coupled activating  $\text{Ca}^{2+}$  signalling pathways which helps releasing of other paracrine regulatory transcription factors by nucleus which may act on the proliferation and differentiation of matrix keratinocytes and melanocytes independent of  $\beta$ -catenin. It has been proposed that intracellular  $\text{Ca}^{2+}$  is involved in the differentiation, proliferation, and gene regulation of precursor cells fated to become hair cells (Correia et al., 2001);  $\text{Ca}^{2+}$  is critical for mechanosensory adaptation and modulation in hair cells. It was demonstrated by a study that a mobile  $\text{Ca}^{2+}$  is highly concentrated in hair cells (Lenzi and Roberts, 1994). Most processes of terminal keratinocyte epidermal differentiation are controlled by the intracellular calcium concentration (Brown et al., 1995). Few Wnt-mediated pathways have been proposed to function independent of  $\beta$ -catenin. One pathway involves activation of calcium/calmodulin-dependent kinase II (CamKII) and protein kinase C (PKC);  $\text{Ca}^{2+}$  has been implicated as an important second messenger in all of these pathways (Kohn and Moon, 2005) supporting the  $\text{Ca}^{2+}$  signalling pathway action independent of  $\beta$ -catenin. Activation of specific prostanoid FP receptor initiate second messenger production (inositol 1,4,5-trisphosphate) which can initiate signalling via extracellular signal-regulated kinase (ERK1/2) pathway to initiate target gene transcription. It has been suggested that target gene transcription can occur via prostanoid-receptor-mediated trans activation of receptor tyrosine kinases (RTKs) such as the epidermal growth factor receptor (EGFR) (Jabbour., 2006). The activation of target genes such as COX-2 can promote prostanoid-receptor signalling and can also in turn elevates the expression of pro-angiogenic genes such as VEGF, bFGF, Ang-1 and Ang-2 (Tsuji et al., 1998; Sales et al., 2002; Jabbour., 2006). The VEGF is one of

the possible paracrine factors which may alter hair growth, therefore, this could also be one of the possible routes for hair growth stimulation via FP. Several studies are supporting the involvement of VEGF in hair growth. Cultured dermal papilla cells had been shown to express VEGF (Hibberts, 1996; Lachgar et al., 1996b; Merrick, 1999) and catagen and telogen phase human scalp hair follicle dermal papilla cells were found to express decreased levels of VEGF mRNA (Lachgar et al., 1996). Minoxidil, a treatment for androgenetic alopecia, has been shown to stimulate VEGF mRNA expression in cultured human dermal papilla cells (Lachgar et al., 1998).

To investigate whether human scalp hair follicles contained  $\text{PGF}_{2\alpha}$  receptor, FP, protein immunohistochemistry was carried out.

Initially, in order to learn the structure of the skin and hair follicle, histological staining of red deer (*Cervus elaphus*) and human skin sections was performed using Saccpic stain. It was more difficult to obtain good vertical sections of human scalp skin than deer skin due to the smaller size of human follicles as well as the small sample sizes and limited availability. Longitudinal and horizontal cross cryosections were stained using the histological stain, Saccpic, which provides a good differentiation of the skin and hair follicle structure (Nixon, 1993; Nutbrown and Randall, 1996). Saccpic staining technique is better than other histochemical staining methods such as haematoxylin and eosin staining because it employs a number of different dyes which successfully highlight the different layers of hair follicles in both longitudinal and cross sections at the level of light microscope. It coloured the dermis an obvious blue/green in both deer and human skin and the hair follicle layers were easily differentiated into the inner root sheath which stained bright red, the outer root sheath (blue) and the connective tissue sheath a darker blue colour with black/blue

nuclei. Fully keratinised parts of the hair fibre and the epidermis were stained yellow (Figure 34). The histological staining of human scalp skin showed a thin epidermis, a collagenous dermis beneath it and the underlying subcutaneous fat layer in which the hair follicle bulb extends down into it (Figure 35). Similar Saccpic staining results in the skin and hair follicles were observed in human skin by Nutbrown and Randall (1996) in deer by Croft (2002) and in sheep by Nixon (1993).

Immunohistochemistry was initially performed using a polyclonal antibody against cytokeratins 5 & 6 to learn the technique as this is a highly expressed cytoskeletal protein in the hair follicle outer root sheath (Hans-Jürgen et al., 1987). The other proteins of interest are much less highly expressed, since FP and EP<sub>2</sub> are cell surface receptors (Srinivasan et al., 2002) while NKI-beteb recognises 7 and 100-Kd cell surface melanosomal antigens on melanocytes (Hayashibe et al., 1986; Randall et al., 2008). Negative controls were carried out on parallel sections to the antibody stained sections for all the immunohistochemistry experiments to detect whether any non-specific staining occurred and to ensure any positive staining was due to the binding of the antibody to the specific antigen (Polak, 2003). Three controls were performed; initially the primary antibody was replaced with 1.5% normal mouse serum or 1% normal goat serum, checking that the secondary antibody or any of the later reagents were not binding non-specifically to the tissue without the presence of the primary antibody. In the second one, the secondary antibody was excluded and replaced with PBS, this checked that the AEC colour system is not binding to the primary antibody without the presence of the secondary antibody. In the third control both primary and secondary antibodies were replaced, this checked that the blocking procedure had been efficient and the AEC colour detection system was not activated alone.

The most important factors which affect the staining result are antibody concentration, the antibody incubation time, the blocking serum types and the blocking serum concentration (Polak, 2003). Although higher primary antibody concentration can give stronger staining results, the antibody concentrations were optimised to balance between gaining the best staining results and reducing the chance of getting non-specific staining. Increasing serum blocking concentration, incubation time and using additional blocking serum can reduce non-specific staining, but too extensive blocking techniques can also reduce the intensity of the positive staining.

When cytokeratins 5 & 6 expression was investigated in human skin and hair follicles using immunohistochemistry, positive staining was detected in the outer root sheath of the hair follicles (Figure 36b, d). The negative controls showed no staining (Figure 36a, c), indicating that the staining seen was due to specific binding of the primary antibody with the target antigen. These results correlate to previous studies using human hair follicles (Stark et al., 1987). Similar results obtained by previous studies in the deer follicle (Croft, 2002) and sheep wool (Bond et al., 1996), in which positive staining for cytokeratin 5/6 occurred in the outer root sheath and hair medulla.

The expression of melanoma associated antigen, a melanocyte marker, was also investigated in human hair follicles using a monoclonal primary antibody to human melanoma associated antigen, NKI-beteb to confirm the location of melanocytes as these are possibly targets of  $\text{PGF}_{2\alpha}$  related drugs as they cause darkening of eyelashes (Reynolds et al., 1998). Staining occurred in the hair follicle bulb matrix above and around the upper part of the dermal papilla (Figure 37b). The negative controls showed no staining (Figure 37a) indicating that the positive staining was due to specific binding of the antibody to melanoma associated antigen. Similar results have



been reported (Horikawa et al., 1996; Commo and Bernard, 2000; Randall et al., 2008) in which positive staining using NKI-beteb antibody occurred in the human hair follicle bulb above and around the upper part of the dermal papilla. The hair bulb melanocytes, around and above the upper outer edges of the dermal papilla are the active hair follicles melanocytes which are necessary for hair pigmentation (Staricco, 1960, 1963); i.e. they would be the direct, or indirect, target of  $\text{PGF}_{2\alpha}$  analogues in eyelash darkening. Melanoma associated antigen was detected in other areas of the hair follicle in the outer layer of the outer root sheath below the level of the sebaceous gland but these cells were not actively pigmenting keratinocytes. NKI-beteb antibody recognises mature and immature melanosomes (premelanosomes) which may be present on very immature melanocytes before starting pigment synthesis (Vennegoor et al., 1988); this area is believed to be the site of melanocyte stem cells (Commo and Bernard, 2000; Nishimura et al., 2002; Nishimura et al., 2005).

To confirm the presence of FP in human scalp hair follicles, the location of FP protein was also investigated by immunohistochemistry using two polyclonal antibodies to FP (goat polyclonal anti-human  $\text{PGF}_{2\alpha}\text{R}$  (N-18 & T-15) antibodies). These antibodies were the only types commercially available and required extensive optimisation. FP was detected in the connective tissue sheath and the dermal papilla of human scalp hair follicle (Figures 38b, c, e, f). There was no sign of staining in areas containing melanocytes. These results suggest that FP protein is located in the mesenchyme-derived components of human hair follicle, but not in the epithelial or melanocyte cells. Since this work was done, a paper was published reporting FP protein expression in the dermal papilla, the connective tissue sheath and the outer root sheath companion layer of human scalp hair follicle by immunohistochemistry using

different polyclonal primary antibodies raised in rabbit; at 1/200 dilution (Colombe et al., 2008).

To confirm the presence and localisation of FP in human scalp hair follicles, the expression of the FP gene was examined in microdissected whole lower anagen scalp hair follicles using RT-PCR.

When cDNA was synthesised from each sample, it was first investigated using the positive control primers specific to cytoskeletal protein,  $\beta$ -actin. RT-PCR results of this positive control highly expressed cytoskeletal protein gene for all cDNAs showed bands of expected product size, 838 bp, indicating that the isolated RNA samples were of sufficient quality for RT-PCR to be performed effectively using different primers (Davies, 2001; Croft, 2002) (Figure 40). A negative control, in which the template cDNA was excluded from the reaction mixture, was used in parallel to all RT-PCR investigations. None of the negative controls generated any PCR product (Figure 40) showing that the  $\beta$ -actin RT-PCR products resulted from the amplification of the cDNA samples and there was no DNA contamination in the reaction mixtures. All the  $\beta$ -actin PCR products from whole hair follicle samples appeared as sharp bands of expected amplification size with no other bands present indicating that primers are binding specifically to the cDNA template and there is no contamination in the positive reaction mixtures, and the cDNA from each sample was of appropriate quality for analysis of the FP gene.

Due to limited work on this gene, a literature search for a specific primer pair to detect FP gene expression from human tissues was unsuccessful. Therefore, specific primers were designed to detect the FP gene from human tissues. There are a number of characteristics that increase the specificity of a primer sequence which were considered while designing the primers. The length of the primer sequences

were 20 as they should be between 17 to 25 nucleotides long; the primers need to be long enough to reduce the chance of mismatching which results from the sequence being found at non-target sites, while too long sequences will decrease the efficiency of the PCR as they take longer to hybridise to the template strand (Dieffenbach et al., 1995). The proportion of guanine (G) and cytosine (C) bases in the primer sequence should be not more than 60%, as high GC ratio affects the melting and denaturing temperature due to the strong three hydrogen bond connections between G and C. Therefore, the primers designed were well matched for GC content and melting temperature to give an annealing temperature which is a few degrees below the lowest melting temperature of the primer pair. The chances of non-specific binding will increase with primers with higher melting temperature (Dieffenbach et al., 1995). The primers were designed avoiding a rich GC composition at the 3' end, as high GC 3' end increases the stability of the two complementary sequences and therefore decreases the ease of releasing them during the denaturation cycle. Also during primer design, repeating any of the bases, or sequence of bases, was avoided as base repetition will increase the primer chance to mismatch (Kwok et al., 1990). The expected size of the base pair PCR product also had to be considered; a very small base pair PCR product e.g. 100 bp would have been difficult to detect as it can be lost easily on the gel. The primer pair were not complementary to each other, especially at the 3' end, as this leads to the formation of primer-dimers (Dieffenbach et al., 1995), meaning that the primers would be in competition with the template DNA for amplification resulting in an inefficient PCR.

The designed new primers to detect the FP gene were tested on GenBank to check they were specific for FP and then first checked on rat liver tissue cDNA which is known to express the FP gene (Arend et al., 2005; Koukoui et al., 2006). Rat liver was

used first as a positive control tissue as it was available and easy to prepare compared to the valuable human hair follicle cDNA. Human hair follicle cDNA samples are also more difficult to prepare due to ethical considerations, the limited sample availability and the long time needed to isolate and prepare the hair follicles before cDNA synthesis. An amplified band of the expected size for FP gene (1100bp in rat) was obtained after agarose gel electrophoresis (Figure 42).

When the methods were optimised successfully they were applied to the human samples. All five human scalp whole hair follicle cDNA samples showed expected size bands (Figure 43). The negative controls, in which the template cDNA was excluded from the reaction mix, were clear of any bands.

The FP RT-PCR products were shown as distinct bands of expected amplification size of 1080 bp on the agarose gel and sequence analysis confirmed the identity of the FP PCR products formed. Human hair follicle FP PCR products demonstrated 99% homology to the known human FP gene sequence (Figure 44).

To localise the expression of the FP gene in scalp hair follicles, gene expression was investigated in hair follicle components: the dermal papilla, the connective tissue sheath surrounding the bulb, the hair bulb matrix, the follicle at the level of the “bulge” area and the lower follicle between the bulb and the “bulge” area. The components were microdissected from isolated hair follicles from three human scalp hair follicle samples using measurements from an experiment done on a fresh scalp hair follicle sample as sebaceous gland is hard to detect from samples treated with *RNAlater*<sup>TM</sup>. The cDNAs were prepared separately from the micro-dissected hair follicle components from each individual and RT-PCR performed first for the positive control gene,  $\beta$ -actin. All hair follicle components expressed the  $\beta$ -actin gene (Figure 46), but the strength of the expression was generally lower than that of the whole

lower hair follicles (Figure 40). The only component with similar levels of expression was the area of the follicle between the “bulge” and the hair bulb. The expression varied between the components with the lower follicle, the hair bulb matrix and the “bulge”, i.e. epithelial cell containing areas, were relatively high while the mesenchyme-derived areas, the dermal papilla and the bulbar connective tissue sheath were much lower (Figure 46). This indicates that the cDNA preparation was successful in general, but the quantities of cDNA were small for the dermal papilla, the connective tissue sheath and the “bulge” area. This related to their composition as all three contain smaller amounts of cells compared to the epithelial hair matrix and lower follicle.

None of PCR of the hair follicle components cDNA using primers for FP showed bands (Figure 47). This would not be expected if sufficient cDNA was available since the whole hair follicle samples all expressed the receptor gene. Since the dermal papilla is the main regulatory part of the hair follicle (Oliver, 1970; Oliver and Jahoda, 1989a; Jahoda, 1992; Jahoda et al., 2001; Yang and Cotsarelis, 2010) and the polyclonal antibody to the FP stained this area, it seemed likely that gene expression of the receptor would have been detected in the dermal papilla samples at least. Similarly, the connective tissue sheath around the bulb could have been expected to exhibit gene expression since it has many similarities to the dermal papilla, including the ability to induce new hair growth (Jahoda and Reynolds, 2001) and some receptor immunostaining was also detected here.

The low cDNA quantity indicated in the  $\beta$ -actin PCR results (Figure 46) seemed a reasonable explanation for these negative results. This is particularly unsurprising for the mesenchyme-derived tissues as hair follicle dermal papilla and connective tissue sheath contain small number of cells and most of their bulk is made of

extracellular proteins. The difference between  $\beta$ -actin and FP gene expression even in the whole follicle samples (compare figures 40 and 43) reflect the much lower expression of FP receptor genes which are encoding receptors for paracrine factors, compared to those for the highly expressed cytoskeletal fibre,  $\beta$ -actin.

Therefore, no conclusions could be drawn about whether there was gene expression of FP in these areas. Since there was more cDNA for the epithelial areas, with the lower follicle between the “bulge” and hair bulb samples containing about the same as the whole follicle extracts, this is less likely to be the explanation for the lack of expression seen. An absence of expression would also concur with the immunohistochemical results. These experiments need to be repeated with either higher number of hair follicle components microdissected from each individual or the RNA samples must be amplified before converting to cDNA. Due to the limited human scalp skin sample sizes and availability, RNA amplification was the only practical route.

Therefore, the experiment was repeated using a further three human scalp skin samples, but the RNA from each hair follicle component was amplified before cDNA synthesis. All samples from each of the 3 individuals showed stronger bands for the positive control,  $\beta$ -actin, gene expression similar to those of intact anagen follicles (Figure 49). However, after PCR to detect FP gene expression, only cDNA from the dermal papilla and the connective tissue sheath around the bulb showed appropriate bands corresponding to FP gene (1080 bp) (Figure 51); none of the other three components, the matrix, the follicle from bulge area and the lower follicle between the bulge and the bulb, showed any detectable bands. When the identities of the dermal papilla and connective tissue sheath PCR products were checked by sequence

analysis, they demonstrated 98% & 95% homology respectively with the known human FP gene sequence (Figure 52).

The expression of the FP gene only in dermal papilla and connective tissue sheath of scalp hair follicles corresponded to the location of prostanoid FP receptor protein in the mesenchyme-derived parts by immunohistochemistry. Colombe *et al* (2008) also observed the expression of the FP gene by RT-PCR in human hair follicle and cultured cells from the dermal papilla and the connective tissue sheath, supporting this receptor gene expression in human scalp follicles and the location.

To investigate the *in vivo* relevance of these *in vitro* organ culture experiments the presence of prostanoid, dihydroprostaglandins and isoprostane lipid mediators were investigated in anagen follicles isolated from human scalp skin from 3 individuals, using lipidomic approaches. Liquid chromatography electrospray tandem mass spectrometry (LC/ESI-MS/MS) of follicle lipid extracts clearly identified 7 prostanoids: PGF<sub>2α</sub>, PGE<sub>1</sub>, PGE<sub>2</sub>, PGD<sub>1</sub>, PGD<sub>2</sub>, TXB<sub>2</sub> and 6-keto PGF<sub>1α</sub>; a dihydroprostaglandin, 13, 14 dihydro-15-keto PGE<sub>2</sub> and an isoprostane, 8-*iso*-PGE<sub>2</sub> (Figure 54). The highest amount of naturally occurring lipid mediators detected in scalp hair follicle were PGE<sub>2</sub> (17.192 ± 2.2 pg/mg protein) and PGF<sub>2α</sub> (13.39 ± 1.8 pg/mg protein) (Figure 55). The levels of the PGF<sub>2α</sub> were lower than those previously reported in human myometrium tissue at term gestation before labour onset (Durn *et al.*, 2010a) only about 25% of the level, whilst, the levels of the PGE<sub>2</sub> were higher than those reported in human non labour myometrium tissue by about 90% of the level. The eicosanoids are known to have significant physiological roles in the skin including repairs of cutaneous integrity and the restoration of skin function following injury (Ziboh *et al.*, 2000).

The presence of high levels of PGE<sub>2</sub> in the isolated scalp hair follicles was interesting. The PGE<sub>2</sub> has been implicated in causing re-growth of hair in mice (Torii et al., 2002) and a prostaglandin E receptor, EP<sub>3</sub>, was localised to the dermal papilla of mouse anagen follicles using *in situ* hybridization. During telogen, the EP<sub>3</sub> mRNA expression disappeared, but was detected again in the dermal papilla of new anagen follicles. PGE<sub>2</sub> production has also been demonstrated in cultured rat vibrissae dermal papilla cells (Lachgar et al., 1996) and human dermal papilla cells (Michelet et al., 1997) by high pressure-liquid chromatography/enzymatic immunoassay (HPLC/EIA) analysis. Therefore, the location of EP<sub>2</sub> receptor protein was also investigated in human scalp hair follicles by immunohistochemistry using a polyclonal antibody to EP<sub>2</sub> (goat polyclonal anti-human PGE<sub>2</sub>αR antibody). After optimisation, EP<sub>2</sub> was detected in the connective tissue sheath and the dermal papilla of human hair follicles (Figures 56b, d), suggesting that EP<sub>2</sub> protein is also located only in the mesenchyme-derived components of human hair follicle. The expression of EP<sub>2</sub> has also been reported in the dermal papilla and the outer root sheath of human scalp hair follicle by immunohistochemistry using different polyclonal primary antibodies raised in rabbit; at 1/200 dilution (Colombe et al., 2008).

Bimatoprost, a prostamide F<sub>2α</sub> analogue related to PGF<sub>2α</sub>, currently the most efficient treatment to reduce intraocular pressure in glaucoma, used as eyedrops, also frequently stimulate eyelashes to lengthen, thicken and darken (Curran, 2009). Bimatoprost was licensed as Latisse for the treatment of hypotrichosis of the eyelashes by the FDA in December 2008 (NDA 022369). Therefore, the last aim of this study was to determine whether the prostamide F<sub>2α</sub> analogue, bimatoprost, can act on scalp hair follicles and therefore could be useful for treating hair loss disorders. Working again on the hypotheses that eyelash follicles resemble other hair follicles



and that bimatoprost is acting directly on the eyelash follicles themselves, we investigated whether this compound could stimulate growth in isolated human scalp hair follicles in organ culture.

Since bimatoprost needed to be solubilised in DMSO, 0.01% DMSO was added to all control conditions used for these experiments on scalp hair follicle samples from a further 10 individuals but this did not cause any difference to control follicles which behaved as they had in the earlier experiments. Most of the hair follicles (>70%) increased in length regularly during the nine day culture period in all conditions.

Bimatoprost caused individual isolated scalp hair follicles from 10 different people to grow significantly faster by about 16% with 10 nM ( $P < 0.01^{**}$ ) while 100 & 1000 nM had a similar and greater effect, about 27% ( $P < 0.001^{***}$ ) (Figure 58). Bimatoprost also slightly raised the number of follicles remaining in anagen by about 7% with 10 nM ( $P < 0.05^{*}$ ) and by about 11% with 100 & 1000 nM ( $P < 0.01^{**}$ ) (Figure 59) and increased the overall amount of hair follicle synthesised in organ culture by about 20% with 10 nM ( $P < 0.05^{*}$ ), by about 35% with 100 nM ( $P < 0.01^{**}$ ) and by about 33% with 1000 nM ( $P < 0.01^{**}$ ) (Figure 60).

This was a dose-responsive effect, though increasing the bimatoprost concentration over 100 nM caused no further enlargement; this would concur with the saturation of a receptor-mediated effect as reported in other tissues (Sharif et al., 1999; Liang et al., 2003; Woodward et al., 2003). To confirm whether the bimatoprost effects were through prostamide  $F_{2\alpha}$  receptors and/or FP in the hair follicles themselves, the effects of the potent prostamide  $F_{2\alpha}$  receptor antagonist, AGN211336, with a  $pA_2$  of 7.6 against the human prostamide receptor (Woodward and *al.*, in press) and the FP antagonist, AS604872, on bimatoprost-stimulated hair growth in organ culture was also studied. Bimatoprost (100 nM) alone again significantly increased all hair

growth parameters compared to the control (hair growth rate ( $P < 0.001^{***}$ ), the % of follicles remaining in anagen ( $P < 0.01^{**}$ ) and the total amount of hair produced ( $P < 0.01^{**}$ )) (Figures 62-65) but these stimulatory effects were blocked when combined with either AGN211336 or AS604872 at (1 $\mu$ M) ( $P < 0.01^{**}$ -  $0.001^{***}$ ) (Figures 61-65). Since the prostamide  $F_{2\alpha}$  receptor antagonist, AGN211336, and the FP antagonist, AS604872, both similarly blocked the stimulatory effects of bimatoprost on scalp hair growth, suggesting the requirement of both receptors for significant bimatoprost action.

Importantly, these results indicate that bimatoprost can stimulate human scalp hair follicles growth as well as that of eyelashes. The saturation of the effect at receptor relevant concentrations and the ability of the potent receptor antagonists, AGN211336 and AS604872, to block the stimulatory effects of bimatoprost on all hair growth parameters in this dynamic bioassay also indicate a receptor-mediated response involving prostamide  $F_{2\alpha}$  and FP receptors. Thus, bimatoprost also act on receptors located within the hair follicle itself to generate paracrine transcription factors to regulate the expression of target genes as mentioned earlier for  $PGF_{2\alpha}$  and latanoprost.

To prove the presence of prostamide  $F_{2\alpha}$  receptors in human scalp hair follicles, the expression of prostamide  $F_{2\alpha}$  receptor genes in isolated scalp hair follicles from another 5 individuals was investigated using molecular biological methods. The prostamide  $F_{2\alpha}$  receptor genes are alternative splicing variants of FP such as FP variant 4, which appears to heterodimerize with FP to create a bimatoprost-sensitive receptor (Liang et al., 2008). Specific primers (Liang et al., 2008) were used first to detect all the 5 splicing variants of FP, altFPs, and this detected three bands from scalp hair follicles cDNA corresponded to wild-type FP and two larger splice variants

of between 321 bp and 462 bp size (Figure 68a). To verify the expression of the FP variants, specific primers were used to detect the expression of the 5 previously reported splice variants, altFP5, altFP4, altFP3, altFP2, altFP1 (Liang et al., 2008). Primers for variants altFP5, altFP3 and altFP2 were taken from (Liang et al., 2008); those for variants altFP4 and altFP1 were designed new as described previously. All scalp hair follicle samples expressed genes for altFP4 and altFP1 only (Figure 68b, c) and sequence analysis of the PCR products confirmed their identities (Figure 69a, b). To localise the expression of prostamide  $F_{2\alpha}$  receptor genes in scalp hair follicles, gene expression was investigated in hair follicle components as described previously for FP. These included: the dermal papilla, the connective tissue sheath surrounding the bulb, the hair bulb matrix, the follicle at the level of the “bulge” area and the lower follicle between the bulb and the “bulge”. The components were microdissected from isolated hair follicles from three individuals and the RNA extracts were each amplified before cDNA synthesis. All cDNA samples gave good bands when RT-PCR was carried out  $\beta$ -actin (Figure 49). However, when the primer set for altFPs were used only the DP and CTS exhibited three bands from all 3 samples (Figure 70a) like those seen in the intact follicle (Figure 68a). When the primers to detect individual FP splice variants: altFP5, altFP4, altFP3, altFP2, altFP1 were used, only the dermal papilla and connective tissue sheath around the bulb expressed genes for altFP4 and altFP1 (Figure 70b, c); the identities of the PCR products were also confirmed by sequence analysis (Figure 71a, b). None of the other scalp hair follicle components, the hair bulb matrix, the follicle at the level of the “bulge” area and the lower follicle between the bulb and the “bulge”, developed any bands (Figure 70). This parallels the location of the FP gene discussed earlier. The alternative splicing variants of the FP gene such as FP variant 4 which appears to heterodimerize with FP to create a

bimatoprost-sensitive receptor, altFP4, (Liang et al., 2008); genes for prostamide  $F_{2\alpha}$  receptor such as altFP4 have been identified in the human ocular tissue (Liang et al., 2008).

The identification of appropriate prostamide  $F_{2\alpha}$  receptor gene expression, FP variants 4 and, to a lesser extent, 1, and native FP genes in scalp hair follicles and in the dermal papilla and connective tissue sheath around the bulb strongly support the hypothesis that  $PGF_{2\alpha}$  and prostamide  $F_{2\alpha}$  analogues act directly on hair follicles via receptors within them. The location of FP protein (Figure 38) and the gene expression of FP and splice variants altFP4 & 1 (Figures 51, 70) only in the mesenchyme-derived dermal papilla and connective tissue sheath of scalp hair follicles is particularly interesting. The dermal papilla determines the type of hair formed by a follicle by producing paracrine signals to control other follicular functions (Jahoda et al., 1984; Jahoda, 1992) and the connective tissue sheath around the bulb can replace this function (Reynolds et al., 1999). Reports of prostaglandin metabolising enzymes and FP in cultured dermal papilla cells from human scalp hair follicles (Colombe et al., 2007; Colombe et al., 2008) support this localisation in the dermal papilla. The absence of any relevant prostanoid receptors from the bulb keratinocytes which form the hair or the melanocytes which produce the pigment and from the “bulge” region, the site of epithelial (Sotiropoulou et al.) and melanocyte stem cells (Nishimura et al., 2005), strongly suggests that the dermal papilla is coordinating follicular responses of increased growth. This is presumably by altering its production of paracrine factors which influence the activity of the bulb keratinocytes and melanocytes. These results suggest that the glaucoma drugs e.g.  $PGF_{2\alpha}$ , latanoprost and bimatoprost which darken eyelashes as well as increasing their length (Curran, 2009; Law, 2010) by actions on the keratinocytes which make

the hair and melanocytes which produce the colour pigments act via the dermal papilla acting as a single regulatory component which interprets the signals to other follicular cell types.

Overall, these experiments demonstrated that the  $\text{PGF}_{2\alpha}$ , its analogue, latanoprost, and the prostamide  $\text{F}_{2\alpha}$  analogue, bimatoprost, can stimulate human scalp hair growth in organ culture i.e. mirroring the stimulation of eyelashes known to occur *in vivo*. These strong similarities in responses by eyelash and scalp follicles contrast with their differing biological responses to androgens (Randall, 2007). From the pharmacological perspective, it was not a certainty that bimatoprost effects on eyelashes would transition into scalp hair growth. There are many instances where the effects of  $\text{PGF}_{2\alpha}$  and its analogues acting via FP expressed in tissues and cells are not reproduced by bimatoprost and its prostamide congeners (Liang et al., 2003; Woodward et al., 2003; Rendl et al., 2005; Woodward and *al.*, in press). The effects of latanoprost, a FP agonist prodrug, and bimatoprost have also been differentiated with respect to ocular hypotension (Jahoda et al., 1984; Sharif et al., 1999; Liang et al., 2008; Woodward and *al.*, in press). Since the development of new treatments for distressing hair growth disorders, such as alopecia and hirsutism, is hampered by our lack of understanding of hair follicle biology, the specific effects of  $\text{PGF}_{2\alpha}$ , prostamide  $\text{F}_{2\alpha}$  and their analogues on hair follicles require further analysis. Interestingly, the current main treatment for alopecia, minoxidil, has been reported to increase prostaglandin synthesis in cultured dermal papilla cells (Michelet et al., 1997).

Overall, these results indicate that  $\text{PGF}_{2\alpha}$  and prostamide  $\text{F}_{2\alpha}$ -related glaucoma drugs do appear to offer a new approach for treating alopecia and merit further investigation.

## General Discussion & Conclusions

Overall, the experiments in this thesis have demonstrated that  $\text{PGF}_{2\alpha}$ , its analogue, latanoprost, and the prostamide  $\text{F}_{2\alpha}$  analogue, bimatoprost, can all stimulate human scalp hair follicle growth in organ culture i.e. they have an effect *in vitro* which mirrors the stimulation of eyelashes known to occur *in vivo*. These strong similarities in responses by eyelash and scalp follicles contrast with their differing biological responses to androgens (Randall, 2007). From the pharmacological perspective, it was also not a certainty that bimatoprost effects on eyelashes would transition into promoting scalp hair growth. There are many instances where the effects of  $\text{PGF}_{2\alpha}$  and its analogues acting via FP expressed in tissues and cells are not reproduced by bimatoprost and its prostamide congeners (Liang et al., 2003; Woodward et al., 2003; Woodward and al., in press). The effects of latanoprost, a FP agonist prodrug, and bimatoprost have also been differentiated with respect to ocular hypotension (Liang et al., 2008; Woodward and al., in press).

The identification of appropriate receptor gene expression, including native FP, FP variant 4 and, to a lesser extent FP variant 1, in scalp hair follicles also strongly support the hypothesis that  $\text{PGF}_{2\alpha}$  and prostamide  $\text{F}_{2\alpha}$  analogues act directly on hair follicles via receptors within them.



The location of FP protein (Figure 38) and the gene expression of FP and splice variants altFP4 & 1 (Figures 51, 70) only in the mesenchyme-derived dermal papilla and connective tissue sheath of scalp hair follicles is particularly interesting. Reports of prostaglandin metabolising enzymes and FP in cultured dermal papilla cells from human scalp hair follicles (Colombe et al., 2007; Colombe et al., 2008) support this

localisation in the dermal papilla. The dermal papilla determines the type of hair formed by a follicle by producing paracrine signals to control other follicular functions (Jahoda et al., 1984; Jahoda, 1992) and the connective tissue sheath around the bulb can replace this function (Reynolds et al., 1999). The absence of any relevant prostanoid receptors from the bulb keratinocytes which form the hair or the melanocytes which produce the pigment and from the “bulge” region, the site of epithelial (Sotiropoulou et al.) and melanocyte stem cells (Nishimura et al., 2005), strongly suggests that action of these prostaglandin-related drugs is via the dermal papilla.

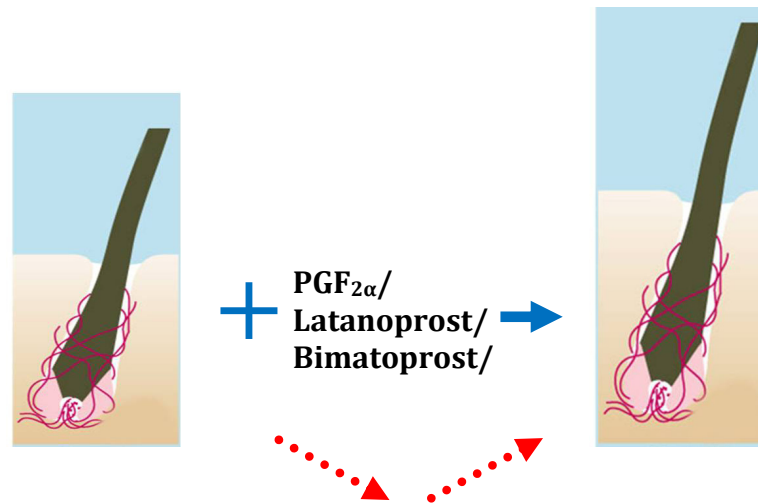
These observations support a hypothesis that stimulation of FP or FP variants would trigger an altered production of paracrine factors in the dermal papilla which cross the dermal papilla basement membrane to increase the activity of the bulb keratinocytes and melanocytes (Figure 73). This would mean that the dermal papilla would coordinate all the follicular responses of increased growth and pigmentation in response to these agents; the response of the target keratinocytes and melanocytes would be an indirect one. The paracrine factors whose production and release by the dermal papilla cells could be altered by  $\text{PGF}_{2\alpha}$  and its related  $\text{PGF}_{2\alpha}$  and prostamide analogues might well include an increase in IGF-I and/or a decrease in TGF- $\beta$ . IGF-I stimulates follicular keratinocyte growth and androgen increases its production in dermal papilla cells from androgen-stimulated hair follicles (reviewed in Randall 2007). The secretion of the keratinocyte inhibitory factor, TGF- $\beta$ , is also stimulated by androgen in balding dermal papilla cells in line with androgen’s inhibitory effect on scalp hair growth (reviewed in Hamada and Randall 2006). However, in contrast it would be predicted in this model that TGF- $\beta$  secretion might be inhibited by  $\text{PGF}_{2\alpha}$  and its related  $\text{PGF}_{2\alpha}$  and prostamide analogues.

**Figure 73 Possible mechanisms for the stimulation of hair growth by  $\text{PGF}_{2\alpha}$ , latanoprost and bimatoprost**

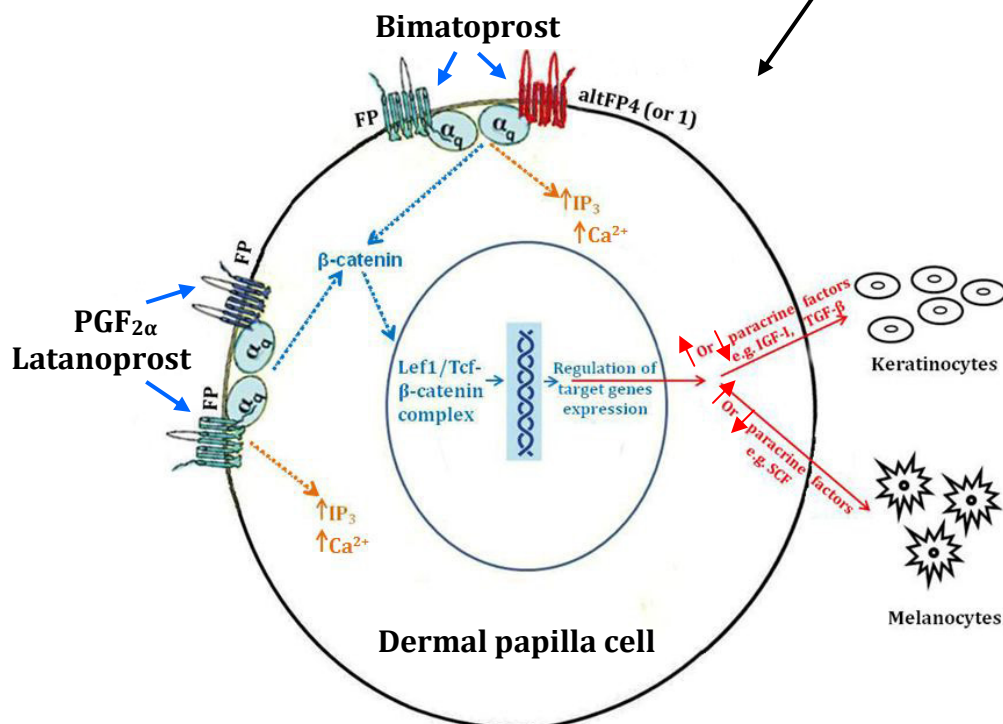
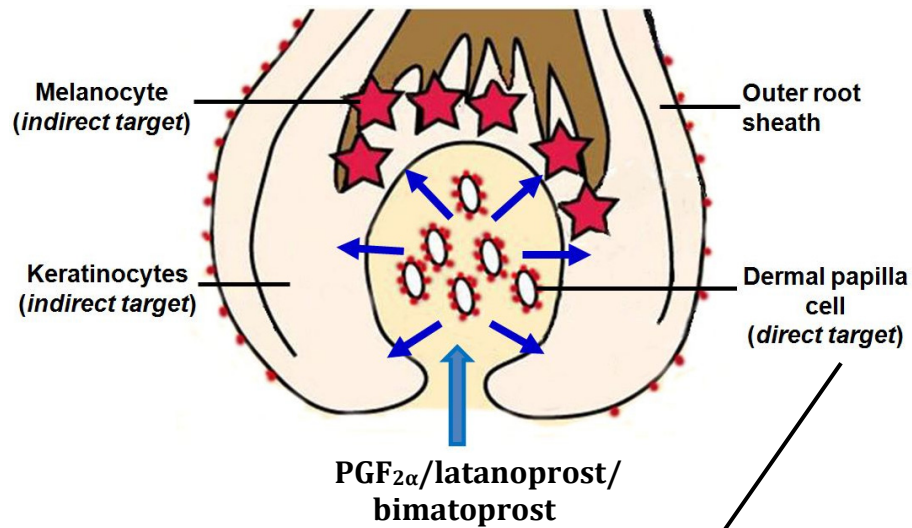
Prostaglandin  $\text{F}_{2\alpha}$  & the related analogues stimulate eyelash hair growth *in vivo* & scalp hair growth in organ culture. This effect is probably by stimulating appropriate receptors in the dermal papilla (middle panel). This may stimulate intracellular signalling pathways resulting in increased intracellular  $\text{Ca}^{++}$  and  $\beta$ -catenin inside the dermal papilla cells. These would trigger the alterations of the gene expression of paracrine signals and their extracellular release so that they could in turn stimulate the activity of the keratinocytes and melanocytes to result in increased hair growth (lower panel).

: FP and/or prostamide  $\text{F}_{2\alpha}$  receptors,  direction of movement of paracrine factors.





Evidence from eyelashes *in vivo*  
scalp follicles in organ culture



Paracrine factors secreted by the dermal papilla have also been implicated in regulating melanocyte activity. Stem cell factor (SCF) is believed to be secreted by dermal papilla cells and to stimulate pigmentary activity in melanocytes via their cell surface c-kit receptors (Hibberts et al., 1996; Randall et al., 2008). SCF is, therefore, also a potential candidate for increased secretion by the dermal papilla under  $\text{PGF}_{2\alpha}$ , latanoprost or bimatoprost.

If this is a correct model, there will have to be intracellular signalling within the dermal papilla cells which ends with the altered synthesis and secretion of paracrine factors. Presumably, interaction of latanoprost with the transmembrane protein  $\text{PGF}_{2\alpha}$  receptor, FP, or bimatoprost with the transmembrane protein FP and prostamide  $\text{F}_{2\alpha}$  receptors, altFP4 or altFP1, trigger  $G_q$  protein-signal pathways (Coleman et al., 1994; Breyer et al., 2001). The observation in the hair growth studies that both AS604872, a FP antagonist (Jones et al., 2009) (Figures 62-64), and AGN211336, a prostamide  $\text{F}_{2\alpha}$  receptor antagonist (Woodward et al., 2007) (Figures 61-64), could block the effect of bimatoprost suggests that these receptors are acting as heterodimers with both types of receptors being necessary for signalling at least *in vitro*. This would parallel reports of heterodimer activity in other tissues e.g. eye (Liang et al., 2008). Once activated the  $G_q$  protein could possibly stimulate two pathways, increasing  $\beta$ -catenin and/or increasing calcium ( $\text{Ca}^{2+}$ ) levels in the cytoplasm. The activated  $\beta$ -catenin protein could then translocate into the nucleus and form a complex with members of Lef1/Tcf family of transcription factors and subsequently up-regulate the expression of target genes producing paracrine factors (see suggestions above) which would pass across the dermal papilla membrane into the surrounding cells (Figure 73).  $\beta$ -catenin has already been identified as a core signalling molecule in the hair follicle.  $\beta$ -catenin is at the core of the Wnt signalling

pathway and the Wnt/ $\beta$ -catenin signalling pathway has a crucial role in hair follicle development and cycling (Van Genderen et al., 1994). Several studies have suggested that multiple steps in hair follicle development and cycling are dependent upon a change in the transcriptional status of genes that are regulated by the Wnt/ $\beta$ -catenin signalling pathway (DasGupta and Fuchs, 1999; Merrill et al., 2001; Reddy et al., 2001). In embryonic mice, high levels of  $\beta$ -catenin caused rapid proliferation of matrix cells (Gat et al., 1998; Chan et al., 1999) and forced activation of Wnt/ $\beta$ -catenin signalling in the epidermis induced extra hairs (Gat et al., 1998; Millar S 2002; Alonso and Fuchs, 2003). In addition, chronic activation of  $\beta$ -catenin in mice during embryonic development resulted in proliferation of the outer root sheath and other epithelial components of the hair follicle (Seidensticker and Behrens, 2000). After hair follicles have formed, deleting of  $\beta$ -catenin led to loss of the hair after the first hair cycle (Huelsenken et al., 2001) and introducing stabilised  $\beta$ -catenin into the epidermis of transgenic mice induced resting hair follicles into anagen and promoted the growth of existing follicles (Celso et al., 2004).

Another possible mechanism is via a  $\text{Ca}^{2+}$  signalling pathway. In this model interaction of latanoprost or bimatoprost with FP or prostamide receptors could trigger  $\text{G}_q$  protein-coupled initiation of second messenger production of inositol 1, 4, 5-triphosphate ( $\text{IP}_3$ ) which would then activate protein kinase C and increase  $\text{Ca}^{2+}$  levels. This could stimulate the release of stored paracrine regulatory factors which may act on the proliferation and differentiation of matrix keratinocytes and melanocytes independent of  $\beta$ -catenin and/or stimulate gene transcription (Figure 73).

These possible mechanisms would allow the fine tuning of the regulatory paracrine pathways to enable the observed alterations in hair growth seen *in vivo* and *in vitro* and in pigmentation reported *in vivo*.

The presence of PGF<sub>2α</sub> and prostamide F<sub>2α</sub> receptors in the connective tissue sheath around the bulb is interesting. However, whether this is actually involved in the immediate response or whether they are there in a reserve role in case the dermal papilla is damaged is not clear. The actual roles of the connective tissue sheath in an anagen follicle is currently one of many aspects of hair follicle biology which are not understood. Connective tissue sheath cells are probably acting as a “pool” of papilla cells in injury situations, and may interchange with dermal papilla cells during the catagen/telogen/early anagen phases of the hair growth cycle (Jahoda and Reynolds, 2001). They probably enable significant hair cycle-associated plasticity which is likely to be involved during clinically important hair follicle transformations, e.g. during vellus-to-terminal changes during adult development and/or terminal-to-vellus changes during androgenetic alopecia (Tobin et al., 2003).

Since the development of new treatments for distressing hair growth disorders, such as alopecia and hirsutism, is hampered by our lack of understanding of hair follicle biology, the specific effects of PGF<sub>2α</sub>, prostamide F<sub>2α</sub> and their analogues on hair follicles require further analysis. Interestingly, the current main treatment for alopecia, minoxidil, has been reported to increase prostaglandin synthesis in cultured dermal papilla cells (Michelet et al., 1997).

In the future, it will be important to clarify what molecular effects these prostaglandin-related drugs have on signalling pathways in the scalp hair follicle. This will include both identifying the intra-dermal papilla signalling in response to these reagents and any alterations in the paracrine molecules produced by the

dermal papilla cells. The easiest way to investigate this would be to use the well established cultured dermal papilla system (Randall, 1999) in the presence, and absence, of prostaglandin-related drugs using a range of techniques including DNA microarray analysis.

Throughout this thesis there has been an assumption that eyelash hair follicles would be similar to scalp hair follicles in their responses to prostaglandin  $F_{2\alpha}$ -related drugs in organ culture and in their possession of receptors. Parallel experiments on eyelash follicles *in vitro* such as organ culture with those prostaglandin-related drugs and investigation of receptor gene expression could have clarified whether our findings in scalp hair follicles directly reflect those in eyelashes. Neither time nor availability of eyelash material permitted this, but the conclusion would be much stronger if this had been carried out. This should be examined in the future.

An interesting observation during this research was the detection of  $PGE_2$  in scalp hair follicles and immunolocation of its receptor,  $EP_2$ , also in the dermal papilla and connective tissue sheath around the bulb. This also merits further investigation to see if  $PGE_2$  can also stimulate scalp hair follicle growth in organ culture or whether it plays another role.

Overall, the results in this thesis, in combination with the observations of eyelash stimulation as a side-effect of glaucoma drugs, indicate that  $PGF_{2\alpha}$  and prostamide  $F_{2\alpha}$ -related glaucoma drugs do appear to be able to stimulate human scalp hair growth via a direct effect on  $PGF_{2\alpha}$  and prostamide  $F_{2\alpha}$  receptors in the follicle mesenchyme-derived tissues including the dermal papilla. They also demonstrate the actual presence of  $PGF_{2\alpha}$  in scalp hair follicles. Thus, all the original aims of this thesis have been met.

These drugs merit investigation in a small clinical trial as a topical application to the scalp of people with early stages of androgenetic alopecia to determine whether these organ culture and molecular biological observations can translate to a novel approach to treating the common, but psychologically distressing forms of hair loss.

## 5 References

- Agnoli, G.C., Borgatti, R., Cacciari, M., Lenzi, P., Marinelli, M., and Stipo, L. (1999). "Renal function and urinary prostanoid excretions in salt-depleted women: comparative effects of enalapril and indomethacin treatments". *Prostaglandins Leukot Essent Fatty Acids* **60**: 87-93.
- Alkhalifah, A., Alsantali, A., Wang, E., McElwee, K.J., and Shapiro, J. (2010). "Alopecia areata update: part II. Treatment". *J Am Acad Dermatol* **62**: 191-202.
- Alm, A., Schoenfelder, J., and McDermott, J. (2004). "A 5-year, multicenter, open-label, safety study of adjunctive latanoprost therapy for glaucoma". *Arch Ophthalmol* **122**: 957-965.
- Anand, B.S., and Graham, D.Y. (1999). "Ulcer and gastritis". *Endoscopy* **31**: 215-225.
- Andersson, S., Berman, D.M., Jenkins, E.P., and Russell, D.W. (1991). "Deletion of steroid 5 alpha-reductase 2 gene in male pseudohermaphroditism". *Nature* **354**: 159-161.
- Angeli, V., Faveeuw, C., Roye, O., Fontaine, J., Teissier, E., Capron, A., Wolowczuk, I., Capron, M., and Trottein, F. (2001). "Role of the parasite-derived prostaglandin D2 in the inhibition of epidermal Langerhans cell migration during schistosomiasis infection". *J Exp Med* **193**: 1135-1147.
- Arend, A., Aunapuu, M., Masso, R., and Selstam, G. (2005). "Prostaglandins of the E-series inhibit connective tissue proliferation in the liver wound of the rat". *Ann Anat* **187**: 57-62.
- Asada, Y., Sonoda, T., Ojio, M., Kurata, S., Sato, T., Ezaki, T., and Takayasu, S. (2001). "5 alpha-reductase type 2 is constitutively expressed in the dermal papilla and connective tissue sheath of the hair follicle in vivo but not during culture in vitro". *J Clin Endocrinol Metab* **86**: 2875-2880.
- Aslan, G., Cimen, S., Yorukoglu, K., Tuna, B., Sonmez, D., Mungan, U., and Celebi, I. (2005). "Vascular endothelial growth factor expression in untreated and androgen-deprived patients with prostate cancer". *Pathol Res Pract* **201**: 593-598.
- Auber, L. (1952). "The anatomy of follicles producing wool-fibres, with special reference to keratinization". *Transactions of the Royal Society of Edinburgh* **62**: 191-254.
- Bazan, N.G., and Flower, R.J. (2002). "Medicine: lipid signals in pain control". *Nature* **420**: 135-138.
- Bernstein, R.M., and Rassman, W.R. (1999). "The logic of follicular unit transplantation". *Dermatol Clin* **17**: 277-295.
- Bikowski, J., Lau, E.G., and Jacob, S.E. (2010). "Eyelash growth: a beneficial side effect of prostaglandin analogues". *Cutis* **85**: 187-188.

Birch, M.P., and Messenger, A.G. (2001). "Genetic factors predispose to balding and non-balding in men". *Eur J Dermatol* **11**: 309-314.

Bishop-Bailey, D., Calatayud, S., Warner, T.D., Hla, T., and Mitchell, J.A. (2002). "Prostaglandins and the regulation of tumor growth". *J Environ Pathol Toxicol Oncol* **21**: 93-101.

Blanchard, Y., Seenundun, S., and Robaire, B. (2007). "The promoter of the rat 5alpha-reductase type 1 gene is bidirectional and Sp1-dependent". *Mol Cell Endocrinol* **264**: 171-183.

Blume-Peytavi, U., and Mandt, N. (2000). "Signalling molecules in human hair follicle cell populations". In *Hair and its disorders: biology, pathology and management*, F.M. Camacho, Randall, V.A., and Price, V.H., ed. (Martin Dunitz, London), pp. 103-113.

Blume, U., Ferracin, J., Verschoore, M., Czernielewski, J.M., and Schaefer, H. (1991). "Physiology of the vellus hair follicle: hair growth and sebum excretion". *Br J Dermatol* **124**: 21-28.

Bolognia, J.L., and Pawelek, J.M. (1988). "Biology of hypopigmentation". *J Am Acad Dermatol* **19**: 217-255.

Bond, J.J., Wynn, P.C., and Moore, G.P. (1996). "Effects of epidermal growth factor and transforming growth factor alpha on the function of wool follicles in culture". *Arch Dermatol Res* **288**: 373-382.

Botchkareva, N.V., Ahluwalia, G., and Shander, D. (2006). "Apoptosis in the hair follicle". *J Invest Dermatol* **126**: 258-264.

Bradfield, R. (1971). "Protein deprivation: comparative response of hair roots, serum protein and urinary nitrogen". *Am J Clin Nutr* **24**: 405-410.

Brodell, L.A., and Mercurio, M.G. (2010). "Hirsutism: Diagnosis and management". *Gend Med* **7**: 79-87.

Bruins, A.P. (1991). "Liquid chromatography-mass spectrometry with ionspray and electrospray interfaces in pharmaceutical and biomedical research". *J Chromatogr* **554**: 39-46.

Bubenik, G.A., and Bubenik, A.B. (1985). "Seasonal variations in hair pigmentation of white-tailed deer and their relationship to sexual activity and plasma testosterone". *J Exp Zool* **235**: 387-395.

Burchill, S.A., and Thody, A.J. (1986). "Melanocyte-stimulating hormone and the regulation of tyrosinase activity in hair follicular melanocytes of the mouse". *J Endocrinol* **111**: 225-232.

Burnett, J.B., Holstein, T.J., and Quevedo, W.C., Jr. (1969). "Electrophoretic variations of tyrosinase in follicular melanocytes during the hair growth cycle in mice". *J Exp Zool* **171**: 369-376.



- Burstein, S.H., Rossetti, R.G., Yagen, B., and Zurier, R.B. (2000). "Oxidative metabolism of anandamide". *Prostaglandins Other Lipid Mediat* **61**: 29-41.
- Camras, C.B. (1996). "Comparison of latanoprost and timolol in patients with ocular hypertension and glaucoma: a six-month masked, multicenter trial in the United States". The United States Latanoprost Study Group. *Ophthalmology* **103**: 138-147.
- Cash, T.F. (1992). "The psychological effects of androgenetic alopecia in men". *J Am Acad Dermatol* **26**: 926-931.
- Cash, T.F., Price, V.H., and Savin, R.C. (1993). "Psychological effects of androgenetic alopecia on women: comparisons with balding men and with female control subjects". *J Am Acad Dermatol* **29**: 568-575.
- Castanet, J., and Ortonne, J.P. (2000). "Hair pigmentation" (London, Martin Dunitz).
- Centofanti, M., Oddone, F., Gandolfi, S., Hommer, A., Boehm, A., Tanga, L., Sangermani, C., Sportelli, V., Haustein, M., Manni, G., *et al.* (2010). "Comparison of Travoprost and Bimatoprost plus Timolol Fixed Combinations in Open-Angle Glaucoma Patients Previously Treated with Latanoprost plus Timolol Fixed Combination". *Am J Ophthalmol*.
- Cha, R.S., and Thilly, W.G. (1995). Specificity, Efficiency and Fidelity of PCR. In *PCR Primer: A Laboratory Manual*, C.W. Dieffenbach, and Dveksler, G.S., ed. (New York, Cold Spring Harbor Laboratory Press), pp. 37-51.
- Chakraborty, A.K., Funasaka, Y., Slominski, A., Ermak, G., Hwang, J., Pawelek, J.M., and Ichihashi, M. (1996). "Production and release of proopiomelanocortin (POMC) derived peptides by human melanocytes and keratinocytes in culture: regulation by ultraviolet B". *Biochim Biophys Acta* **1313**: 130-138.
- Chase, H.B. (1954). "Growth of the hair". *Physiol Rev* **34**: 113-126.
- Chase, H.B. (1958). "The behaviour of pigment cells and epithelial cells in the hair follicle" (New York, Academic Press).
- Chase, H.B., Rauch, R., and Smith, V.W. (1951). "Critical stages of hair development and pigmentation in the mouse". *Physiol Zool* **24**: 1-8.
- Chen, J., Senior, J., Marshall, K., Abbas, F., Dinh, H., Dinh, T., Wheeler, L., and Woodward, D. (2005). "Studies using isolated uterine and other preparations show bimatoprost and prostanoid FP agonists have different activity profiles". *Br J Pharmacol* **144**: 493-501.
- Chenchik, A., and al, e. (1998). "Generation and use of high-quality cDNA from small amounts of total RNA by SMART PCR". In *Gene Cloning and Analysis by RT-PCR* (MA).
- Chuong, C.M., Nickoloff, B.J., Elias, P.M., Goldsmith, L.A., Macher, E., Maderson, P.A., Sundberg, J.P., Tagami, H., Plonka, P.M., Thestrup-Pederson, K., *et al.* (2002). "What is the 'true' function of skin?". *Exp Dermatol* **11**: 159-187.

- Cirillo, R., Tos, E.G., Page, P., Missotten, M., Quattropiani, A., Scheer, A., Schwarz, M.K., and Chollet, A. (2007). "Arrest of preterm labor in rat and mouse by an oral and selective nonprostanoid antagonist of the prostaglandin F2alpha receptor (FP)". *Am J Obstet Gynecol* **197**: 54 e51-59.
- Cohn, B. (1994). "In search of human skin pheromones". *Arch Dermatol* **130**: 1048-1051.
- Colombe, L., Michelet, J.F., and Bernard, B.A. (2008). "Prostanoid receptors in anagen human hair follicles". *Exp Dermatol* **17**: 63-72.
- Colombe, L., Vindrios, A., Michelet, J.F., and Bernard, B.A. (2007). "Prostaglandin metabolism in human hair follicle". *Exp Dermatol* **16**: 762-769.
- Commo, S., and Bernard, B.A. (2000). "Melanocyte subpopulation turnover during the human hair cycle: an immunohistochemical study". *Pigment Cell Res* **13**: 253-259.
- Coronel-Perez, I.M., Rodriguez-Rey, E.M., and Camacho-Martinez, F.M. (2010). "Latanoprost in the treatment of eyelash alopecia in alopecia areata universalis". *J Eur Acad Dermatol Venereol* **24**: 481-485.
- Cotsarelis, G., Sun, T.T., and Lavker, R.M. (1990). "Label-retaining cells reside in the bulge area of pilosebaceous unit: implications for follicular stem cells, hair cycle, and skin carcinogenesis". *Cell* **61**: 1329-1337.
- Cott, H.B. (1940). "Adaptive Coloration in Animals", Methuen, London.
- Couchman, J.R. (1993). "Hair follicle proteoglycans". *J Invest Dermatol* **101**: 60S-64S.
- Courtois, M., Loussouarn, G., Hourseau, S., and Grollier, J.F. (1996). "Periodicity in the growth and shedding of hair". *Br J Dermatol* **134**: 47-54.
- Cracowski, J.L., Durand, T., and Bessard, G. (2002). "Isoprostanes as a biomarker of lipid peroxidation in humans: physiology, pharmacology and clinical implications". *Trends Pharmacol Sci* **23**: 360-366.
- Cravatt, B.F., Giang, D.K., Mayfield, S.P., Boger, D.L., Lerner, R.A., and Gilula, N.B. (1996). "Molecular characterization of an enzyme that degrades neuromodulatory fatty-acid amides". *Nature* **384**: 83-87.
- Croft, N.J. (2002). "Antler velvet is a novel model for the study of hair follicle morphogenesis". In Department of Biomedical Sciences (Bradford, PhD thesis, Department of Biomedical Sciences, University of Bradford), pp. 225.
- Cullinan-Bove, K., and Koos, R.D. (1993). "Vascular endothelial growth factor/vascular permeability factor expression in the rat uterus: rapid stimulation by estrogen correlates with estrogen-induced increases in uterine capillary permeability and growth". *Endocrinology* **133**: 829-837.

Cunha, G.R., Donjacour, A.A., and Cook, P.S., et al (1987). "The endocrinology and development biology of the prostate". *Endocrinology*.

Curran, M.P. (2009). "Bimatoprost: a review of its use in open-angle glaucoma and ocular hypertension". *Drugs Aging* **26**: 1049-1071.

Cushman, S.W., and Wardzala, L.J. (1980). "Potential mechanism of insulin action on glucose transport in the isolated rat adipose cell. Apparent translocation of intracellular transport systems to the plasma membrane". *J Biol Chem* **255**: 4758-4762.

Daray, F.M., Minvielle, A.I., Puppo, S., and Rothlin, R.P. (2004). "Vasoconstrictor effects of 8-iso-prostaglandin E2 and 8-iso-prostaglandin F(2alpha) on human umbilical vein". *Eur J Pharmacol* **499**: 189-195.

Davies, G.C. (2001). "*In vivo* and *in vitro* models of hair growth for the assessment of potassium channel openers". In Department of Biomedical Sciences (Bradford, University of Bradford), pp. 297.

Dawber, R. (2000). "Update on minoxidil treatment of hair loss". In *Hair and its disorders: Biology, research and management*, F.M. Camacho, Randall, V.A., and Price, V.H., ed. (London, Martin Dunitz), pp. 169-173.

De Petrocellis, L., Cascio, M.G., and Di Marzo, V. (2004). "The endocannabinoid system: a general view and latest additions". *Br J Pharmacol* **141**: 765-774.

Delamere, F.M., Sladden, M.M., Dobbins, H.M., and Leonardi-Bee, J. (2008). "Interventions for alopecia areata". *Cochrane Database Syst Rev*, CD004413.

Dieffenbach, C.W., Lowe, T.M.J., and Dveksler, G.S. (1995). "General concepts for PCR primer design". In *PCR Primer: A Laboratory Manual*, C.W. Dieffenbach, and Dveksler, G.S., ed. (Cold Spring Harbor Laboratory Press), pp. 133-142.

Dry, F.W. (1926). "The coat of the mouse (*Mus Musculus*)". *Journal of Genetics* **16**: 287-340.

Durn, J.H. (2008). "Profiling prostanoids in human term pregnant myometrium *in vitro*". In Pharmacy Department (University of Bradford, Bradford).

Durn, J.H., Marshall, K.M., Farrar, D., O'Donovan, P., Scally, A.J., Woodward, D.F., and Nicolaou, A. (2010). "Lipidomic analysis reveals prostanoid profiles in human term pregnant myometrium". *Prostaglandins Leukot Essent Fatty Acids* **82**: 21-26.

Easthope, S.E., and Perry, C.M. (2002). "Topical bimatoprost: a review of its use in open-angle glaucoma and ocular hypertension". *Drugs Aging* **19**: 231-248.

Ebling, F.G., Hale, P.A., and Randall, V.A. (1991). "Hormones and hair growth". In *Biochemistry and Physiology of the Skin*, G. LA, ed. (Oxford: Clarendon Press), pp. 660-690.

Ebling, F.J. (1976). "Hair". *J Invest Dermatol* **67**: 98-105.

- Ebling, F.J.G. (1985). "The mythological evolution of nudity". p 33-41.
- Elgin, U., Batman, A., Berker, N., and Ilhan, B. (2006). "The comparison of eyelash lengthening effect of latanoprost therapy in adults and children". *Eur J Ophthalmol* **16**: 247-250.
- Elliott, K., Stephenson, T.J., and Messenger, A.G. (1999). "Differences in Hair Follicle Dermal Papilla Volume are Due to Extracellular Matrix Volume and Cell Number: Implications for the Control of Hair Follicle Size and Androgen Responses". **113**: 873-877.
- Ellis, J.A., and Harrap, S.B. (2001). "The genetics of androgenetic alopecia". *Clin Dermatol* **19**: 149-154.
- Enshell-Seijffers, D., Lindon, C., Kashiwagi, M., and Morgan, B.A. (2010). "beta-catenin activity in the dermal papilla regulates morphogenesis and regeneration of hair". *Dev Cell* **18**: 633-642.
- Epstein, E. (2001). "Evidence-based treatment of alopecia areata". *J Am Acad Dermatol* **45**: 640-642.
- Epstein, J.S. (2007). "Evolution of techniques in hair transplantation: a 12-year perspective". *Facial Plast Surg* **23**: 51-59.
- Erdemir, F., Harbin, A., and Hellstrom, W.J. (2008). "5-alpha reductase inhibitors and erectile dysfunction: the connection". *J Sex Med* **5**: 2917-2924.
- Faghihi, G., Andalib, F., and Asilian, A. (2009). "The efficacy of latanoprost in the treatment of alopecia areata of eyelashes and eyebrows". *Eur J Dermatol* **19**: 586-587.
- Farrell, R.E. (1998). "RNA methodologies", second edn (New York, Academic press).
- Ferraris, C., Chevalier, G., Favier, B., Jahoda, C.A., and Dhouailly, D. (2000). "Adult corneal epithelium basal cells possess the capacity to activate epidermal, pilosebaceous and sweat gland genetic programs in response to embryonic dermal stimuli". *Development* **127**: 5487-5495.
- Finn, D.A., Beadles-Bohling, A.S., Beckley, E.H., Ford, M.M., Gililand, K.R., Gorin-Meyer, R.E., and Wiren, K.M. (2006). "A new look at the 5alpha-reductase inhibitor finasteride". *CNS Drug Rev* **12**: 53-76.
- Fleischman, R.A., Saltman, D.L., Stastny, V., and Zneimer, S. (1991). "Deletion of the c-kit protooncogene in the human developmental defect piebald trait". *Proc Natl Acad Sci USA* **88**: 10885-10889.
- Foitzik, K., Krause, K., Conrad, F., Nakamura, M., Funk, W., and Paus, R. (2006). "Human scalp hair follicles are both a target and a source of prolactin, which serves as an autocrine and/or paracrine promoter of apoptosis-driven hair follicle regression". *Am J Pathol* **168**: 748-756.

Foitzik, K., Lindner, G., Mueller-Roever, S., Maurer, M., Botchkareva, N., Botchkarev, V., Handjiski, B., Metz, M., Hibino, T., Soma, T., *et al.* (2000). "Control of murine hair follicle regression (catagen) by TGF-beta1 in vivo". *Faseb J* **14**: 752-760.

Forslind, B. (2000). "Structure and function of the hair follicle". In *Hair and its disorders: biology, pathology and management*, F.M. Camacho, Randall, V.A., and Price, V.H., ed. (Martin Dunitz Ltd), pp. 3-15.

Franks, S. (1989). "Polycystic ovary syndrome: a changing perspective (review)". *Clin Endocrinol (Oxf)* **31**: 87-120.

Fuchs, E. (2007). "Scratching the surface of skin development". *Nature* **445**: 834-842.

Galbraith, H. (1998). "Nutritional and hormonal regulation of hair follicle growth and development". *Proc Nutr Soc* **57**: 195-205.

Gandolfi, S.A., and Cimino, L. (2003). "Effect of bimatoprost on patients with primary open-angle glaucoma or ocular hypertension who are nonresponders to latanoprost". *Ophthalmology* **110**: 609-614.

Garg, S., and Messenger, A.G. (2009). "Alopecia areata: evidence-based treatments". *Semin Cutan Med Surg* **28**: 15-18.

Geissler, E.N., Ryan, M.A., and Housman, D.E. (1988). "The dominant-white spotting (W) locus of the mouse encodes the c-kit proto-oncogene". *Cell* **55**: 185-192.

Gilhar, A., Ullmann, Y., Berkutzki, T., Assy, B., and Kalish, R.S. (1998). "Autoimmune hair loss (alopecia areata) transferred by T lymphocytes to human scalp explants on SCID mice". *J Clin Invest* **101**: 62-67.

Girman, C.J., Rhodes, T., Lilly, F.R., Guo, S.S., Siervogel, R.M., Patrick, D.L., and Chumlea, W.C. (1998). "Effects of self-perceived hair loss in a community sample of men". *Dermatology* **197**: 223-229.

Glass, M., Hong, J., Sato, T.A., and Mitchell, M.D. (2005). "Misidentification of prostamides as prostaglandins". *J Lipid Res* **46**: 1364-1368.

Goldyne, M.E. (2000). "Cyclooxygenase isoforms in human skin". *Prostaglandins Other Lipid Mediat* **63**: 15-23.

Goodhart, C.B. (1960). "The evolutionary significance of human hair patterns and skin colouring". 53-58.

Gorpinich, I.V., and Nozdrin, V.I. (2007). "Morpho-functional changes in hair during their renewal". *Morfologija* **132**: 7-17.

Greco, A., and Minghetti, L. (2004). "Isoprostanes as biomarkers and mediators of oxidative injury in infant and adult central nervous system diseases". *Curr Neurovasc Res* **1**: 341-354.

- Grichnik, J.M., Burch, J.A., Burchette, J., and Shea, C.R. (1998). "The SCF/KIT pathway plays a critical role in the control of normal human melanocyte homeostasis". *J Invest Dermatol* **111**: 233-238.
- Grigsby, P.L., Sooranna, S.R., Brockman, D.E., Johnson, M.R., and Myatt, L. (2006). "Localization and expression of prostaglandin E2 receptors in human placenta and corresponding fetal membranes with labor". *Am J Obstet Gynecol* **195**: 260-269.
- Gulec, A.T., Tanriverdi, N., Duru, C., Saray, Y., and Akcali, C. (2004). "The role of psychological factors in alopecia areata and the impact of the disease on the quality of life". *Int J Dermatol* **43**: 352-356.
- Haase, E., Ito, S., and Wakamatsu, K. (1995). "Influences of sex, castration, and androgens on the eumelanin and pheomelanin contents of different feathers in wild mallards". *Pigment Cell Res* **8**: 164-170.
- Haeggstrom, J.Z., Rinaldo-Matthis, A., Wheelock, C.E., and Wetterholm, A. (2010). "Advances in eicosanoid research, novel therapeutic implications". *Biochem Biophys Res Commun* **396**: 135-139.
- Hamada, K., and Randall, V.A. (2006). "Inhibitory autocrine factors produced by the mesenchyme-derived hair follicle dermal papilla may be a key to male pattern baldness". *Br J Dermatol* **154**: 609-618.
- Hamilton, J.B. (1942). "Male hormone stimulation is a prerequisite and an incitant in common baldness". *Am J Anat* **71**: 451-481.
- Hamilton, J.B. (1946). "A secondary sexual character that develops in men but not in women upon aging of an organ present in both sexes". pp. 466-467.
- Hamilton, J.B. (1951). "Patterned loss of hair in man; types and incidence". *Ann N Y Acad Sci* **53**: 708-728.
- Hamilton, J.B. (1958). "Age, sex and genetic factors in the regulation of hair growth in man: A comparison of Caucasian and Japanese populations". pp. 399-433.
- Hamilton, J.B. (1960). "Effect of castration in adolescent and young adult males upon further changes in the proportions of bare and hairy scalp". *J Clin Endocrinol Metab* **20**: 1309-1318.
- Hammerstein, J. (1987). "Cyproterone acetate-the European experience". In *The cause and management of hirsutism : a practical approach to the control of unwanted hair*, [Rev. ed.] edn (Carnforth, UK, Parthenon Publishing Group).
- Handelsman, D.J. (2005). "Androgen action and pharmacologic uses" (Philadelphia, WB Saunders Co).
- Hans-Jürgen, S., Dirk, B., Alain, L., Paul, B., and Norbert, E.F. (1987). "Keratins of the human hair follicle: "Hyperproliferative" keratins consistently expressed in outer root sheath cells in vivo and in vitro". *Differentiation* **35**: 236-248.

- Hansen, W.R., Keelan, J.A., Skinner, S.J., and Mitchell, M.D. (1999). "Key enzymes of prostaglandin biosynthesis and metabolism. Coordinate regulation of expression by cytokines in gestational tissues: a review". *Prostaglandins Other Lipid Mediat* **57**: 243-257.
- Hardy, M.H. (1992). "The secret life of the hair follicle". *Trends Genet* **8**: 55-61.
- Hart, J., and Shafranov, G. (2004). "Hypertrichosis of vellus hairs of the malar region after unilateral treatment with bimatoprost". *Am J Ophthalmol* **137**: 756-757.
- Haworth, R., Oakley, K., McCormack, N., and Pilling, A. (2005). "Differential expression of COX-1 and COX-2 in the gastrointestinal tract of the rat". *Toxicol Pathol* **33**: 239-245.
- Hayashibe, K., Mishima, Y., Ichihashi, M., and Kawai, M. (1986). "Melanosomal antigenic expression on the cell surface and intracellular subunits within melanogenic compartments of pigment cells: analysis by antimelanosome-associated monoclonal antibody". *J Invest Dermatol* **87**: 89-94.
- Hellberg, M.R., McLaughlin, M.A., Sharif, N.A., DeSantis, L., Dean, T.R., Kyba, E.P., Bishop, J.E., Klimko, P.G., Zinke, P.W., Selliah, R.D., *et al.* (2002). Identification and characterization of the ocular hypotensive efficacy of travoprost, a potent and selective FP prostaglandin receptor agonist, and AL-6598, a DP prostaglandin receptor agonist. *Surv Ophthalmol* **47**: 13-33.
- Hibberts, N.A., Kato, S., Messenger, A.G., and Randall, V.A. (1996). "Dermal papilla cells from human hair follicles secrete factors (e.g. VEGF) mitogenic for endothelial cells". *J Invest Dermatol* **106**: 862.
- Hibberts, N.A., Messenger, A.G., and Randall, V.A. (1996). "Dermal papilla cells derived from beard hair follicles secrete more stem cell factor (SCF) in culture than scalp cells or dermal fibroblasts". *Biochem Biophys Res Commun* **222**: 401-405.
- Higgins, C.A., Richardson, G.D., Westgate, G.E., and Jahoda, C.A. (2009a). "Exogen involves gradual release of the hair club fibre in the vibrissa follicle model". *Exp Dermatol* **18**: 793-795.
- Higgins, C.A., Westgate, G.E., and Jahoda, C.A.B. (2009b). "From Telogen to Exogen: Mechanisms Underlying Formation and Subsequent Loss of the Hair Club Fiber". *J Invest Dermatol* **129**: 2100-2108.
- Hirobe, T., Kiuchi, M., Wakamatsu, K., and Ito, S. (2010). "Estrogen increases hair pigmentation in female recessive yellow mice". *Zoolog Sci* **27**: 470-476.
- Hoch, B., Bernhard, M., Seyberth, H.W., Watzer, B., and Schweer, H. (2000). "Neonatal urinary prostanoid excretion". *Prostaglandins Other Lipid Mediat* **60**: 9-14.
- Hoffmann, E.D., and Stroobant, V. (1999). *Mass spectrometry: Principles and applications*. In (Chichester, John Wiley & Sons).

Holbrook, K.A., and Minami, S.I. (1991). "Hair follicle embryogenesis in the human. Characterization of events in vivo and in vitro". *Ann N Y Acad Sci* **642**: 167-196.

Hollo, G. (2007). "The side effects of the prostaglandin analogues". *Expert Opin Drug Saf* **6**: 45-52.

Horikawa, T., Norris, D.A., Johnson, T.W., Zekman, T., Dunscomb, N., Bennion, S.D., Jackson, R.L., and Morelli, J.G. (1996). "DOPA-negative melanocytes in the outer root sheath of human hair follicles express premelanosomal antigens but not a melanosomal antigen or the melanosome-associated glycoproteins tyrosinase, TRP-1, and TRP-2". *J Invest Dermatol* **106**: 28-35.

Houchen, C.W., Stenson, W.F., and Cohn, S.M. (2000). "Disruption of cyclooxygenase-1 gene results in an impaired response to radiation injury". *Am J Physiol Gastrointest Liver Physiol* **279**: 858-865.

Hughes, B.R., and Cunliffe, W.J. (1988). "Tolerance of spironolactone". *Br J Dermatol* **118**: 687-691.

Hunt, G., Todd, C., Cresswell, J.E., and Thody, A.J. (1994). "Alpha-melanocyte stimulating hormone and its analogue Nle4DPhe7 alpha-MSH affect morphology, tyrosinase activity and melanogenesis in cultured human melanocytes". *J Cell Sci* **107**: (Pt 1), 205-211.

Hurley, H.J. (2001). "The eccrine sweat glands: Structure and function". In *The biology of the skin*, R.K. Freinkel, and Woodley, D.T., ed. (The Parthenon Publishing Group), pp. 47-76.

Ibarrola-Villava, M., Fernandez, L.P., Pita, G., Bravo, J., Floristan, U., Sendagorta, E., Feito, M., Aviles, J.A., Martin-Gonzalez, M., Lazaro, P., *et al.* (2010). "Genetic analysis of three important genes in pigmentation and melanoma susceptibility: CDKN2A, MC1R and HERC2/OCA2". *Exp Dermatol* **19**: 836-844.

Ibrahim, L., and Wright, E.A. (1982). "A quantitative study of hair growth using mouse and rat vibrissal follicles. I. Dermal papilla volume determines hair volume". *J Embryol Exp Morphol* **72**: 209-224.

Ikai, K. (1999). "Psoriasis and the arachidonic acid cascade". *J Dermatol Sci* **21**: 135-146.

Imperato-McGinley, J., Guerrero, L., Gautier, T., and Peterson, R.E. (1974). "Steroid 5alpha-reductase deficiency in man: an inherited form of male pseudohermaphroditism". *Science* **186**: 1213-1215.

Inamatsu, M., Tochio, T., Makabe, A., Endo, T., Oomizu, S., Kobayashi, E., and Yoshizato, K. (2006). "Embryonic dermal condensation and adult dermal papilla induce hair follicles in adult glabrous epidermis through different mechanisms". *Dev Growth Differ* **48**: 73-86.

Inui, S., Fukuzato, Y., Nakajima, T., Yoshikawa, K., and Itami, S. (2002). "Androgen-inducible TGF-beta1 from balding dermal papilla cells inhibits epithelial cell growth: a



clue to understand paradoxical effects of androgen on human hair growth". *Faseb J* **16**: 1967-1969.

Inui, S., Fukuzato, Y., Nakajima, T., Yoshikawa, K., and Itami, S. (2003). "Identification of androgen-inducible TGF-beta1 derived from dermal papilla cells as a key mediator in androgenetic alopecia". *J Invest Dermatol Symp Proc* **8**: 69-71.

Irwin, R.S., and Rippe, J.M. (2008). "Irwin and Rippe's intensive care medicine, 6th ed. edn (Philadelphia, Pa. ; London, Lippincott Williams & Wilkins).

Ishikawa, H., Yoshitomi, T., Mashimo, K., Nakanishi, M., and Shimizu, K. (2002). "Pharmacological effects of latanoprost, prostaglandin E2, and F2alpha on isolated rabbit ciliary artery". *Graefes Arch Clin Exp Ophthalmol* **240**: 120-125.

Itami, S., Kurata, S., and Takayasu, S. (1995). "Androgen induction of follicular epithelial cell growth is mediated via insulin-like growth factor-I from dermal papilla cells". *Biochem Biophys Res Commun* **212**: 988-994.

Ito, M., Kizawa, K., Hamada, K., and Cotsarelis, G. (2004). "Hair follicle stem cells in the lower bulge form the secondary germ, a biochemically distinct but functionally equivalent progenitor cell population, at the termination of catagen". *Differentiation* **72**: 548-557.

Jahoda, C.A. (1992). "Induction of follicle formation and hair growth by vibrissa dermal papillae implanted into rat ear wounds: vibrissa-type fibres are specified". *Development* **115**: 1103-1109.

Jahoda, C.A., Horne, K.A., and Oliver, R.F. (1984). "Induction of hair growth by implantation of cultured dermal papilla cells". *Nature* **311**: 560-562.

Jahoda, C.A., and Oliver, R.F. (1984). "Vibrissa dermal papilla cell aggregative behaviour in vivo and in vitro". *J Embryol Exp Morphol* **79**: 211-224.

Jahoda, C.A., Oliver, R.F., Reynolds, A.J., Forrester, J.C., Gillespie, J.W., Cserhalmi-Friedman, P.B., Christiano, A.M., and Horne, K.A. (2001). "Trans-species hair growth induction by human hair follicle dermal papillae". *Exp Dermatol* **10**: 229-237.

Jahoda, C.A., and Reynolds, A.J. (2001). "Hair follicle dermal sheath cells: unsung participants in wound healing". *Lancet* **358**: 1445-1448.

Jahoda, C.A., Reynolds, A.J., and Oliver, R.F. (1993). "Induction of hair growth in ear wounds by cultured dermal papilla cells". *J Invest Dermatol* **101**: 584-590.

Jakobsson, P.J., Thoren, S., Morgenstern, R., and Samuelsson, B. (1999). "Identification of human prostaglandin E synthase: a microsomal, glutathione-dependent, inducible enzyme, constituting a potential novel drug target". *Proc Natl Acad Sci U S A* **96**: 7220-7225.

Jansen, V.A., and van Baalen, M. (2006). "Altruism through beard chromodynamics". *Nature* **440**: 663-666.

- Jindo, T., Tsuboi, R., Imai, R., Takamori, K., Rubin, J.S., and Ogawa, H. (1994). "Hepatocyte growth factor/scatter factor stimulates hair growth of mouse vibrissae in organ culture". *J Invest Dermatol* **103**: 306-309.
- Jindo, T., Tsuboi, R., Imai, R., Takamori, K., Rubin, J.S., and Ogawa, H. (1995). "The effect of hepatocyte growth factor/scatter factor on human hair follicle growth". *J Dermatol Sci* **10**, 229-232.
- Johnstone, M.A. (1997). "Hypertrichosis and increased pigmentation of eyelashes and adjacent hair in the region of the ipsilateral eyelids of patients treated with unilateral topical latanoprost". *Am J Ophthalmol* **124**: 544-547.
- Johnstone, M.A. (1998). "Brief latanoprost therapy induces hypertrichosis". *Invest Ophthalmol Vis Sci* **39**: 258.
- Johnstone, M.A., and Albert, D.M. (2002). "Prostaglandin-induced hair growth". *Surv Ophthalmol* **47**: 185-202.
- Junger, H., and Sorkin, L.S. (2000). "Isoprostanes induce plasma extravasation in rat skin". *Prostaglandins Other Lipid Mediat* **62**: 335-342.
- Kabashima, K., Sakata, D., Nagamachi, M., Miyachi, Y., Inaba, K., and Narumiya, S. (2003). "Prostaglandin E2-EP4 signaling initiates skin immune responses by promoting migration and maturation of Langerhans cells". *Nat Med* **9**: 744-749.
- Kaufman, K.D., Olsen, E.A., Whiting, D., Savin, R., DeVillez, R., Bergfeld, W., Price, V.H., Van Neste, D., Roberts, J.L., Hordinsky, M., *et al.* (1998). "Finasteride in the treatment of men with androgenetic alopecia. Finasteride Male Pattern Hair Loss Study Group". *J Am Acad Dermatol* **39**: 578-589.
- Kawasaki, E.S. (1990). "Amplification of RNA. In PCR protocols: A guide to methods and applications", Innis, ed. (New York: Academic Press), pp. 21-27.
- Kempen, E.C., Yang, P., Felix, E., Madden, T., and Newman, R.A. (2001). "Simultaneous quantification of arachidonic acid metabolites in cultured tumor cells using high-performance liquid chromatography/electrospray ionization tandem mass spectrometry". *Anal Biochem* **297**: 183-190.
- Keogh, E.V., and Walsh, R.J. (1965). "Rate of greying of human hair". *Nature* **207**: 877-878.
- Khuder, S.A., Herial, N.A., Mutgi, A.B., and Federman, D.J. (2005). "Nonsteroidal antiinflammatory drug use and lung cancer: a metaanalysis". *Chest* **127**: 748-754.
- Kligman, A.G. (1959). "The human hair cycle". *J Invest Dermatol* **33**: 307-316.
- Kligman, A.M. (1961). "Pathologic dynamics of human hair loss. I. Telogen effluvium". *Arch Dermatol* **83**: 175-198.

- Koda, N., Tsutsui, Y., Niwa, H., Ito, S., Woodward, D.F., and Watanabe, K. (2004). "Synthesis of prostaglandin F ethanolamide by prostaglandin F synthase and identification of Bimatoprost as a potent inhibitor of the enzyme: new enzyme assay method using LC/ESI/MS". *Arch Biochem Biophys* **424**: 128-136.
- Kohno, S., Endo, H., Hashimoto, A., Hayashi, I., Murakami, Y., Kitasato, H., Kojima, F., Kawai, S., and Kondo, H. (2006). "Inhibition of skin sclerosis by 15deoxy delta12,14-prostaglandin J2 and retrovirally transfected prostaglandin D synthase in a mouse model of bleomycin-induced scleroderma". *Biomed Pharmacother* **60**: 18-25.
- Komoto, J., Yamada, T., Watanabe, K., Woodward, D.F., and Takusagawa, F. (2006). "Prostaglandin F2alpha formation from prostaglandin H2 by prostaglandin F synthase (PGFS): crystal structure of PGFS containing bimatoprost". *Biochemistry* **45**: 1987-1996.
- Koukoui, O., Boucherie, S., Sezan, A., Prigent, S., and Combettes, L. (2006). "Effects of the prostaglandins PGF2alpha and PGE2 on calcium signaling in rat hepatocyte doublets". *Am J Physiol Gastrointest Liver Physiol* **290**: 66-73.
- Kozak, K.R., Crews, B.C., Morrow, J.D., Wang, L.H., Ma, Y.H., Weinander, R., Jakobsson, P.J., and Marnett, L.J. (2002). "Metabolism of the endocannabinoids, 2-arachidonylglycerol and anandamide, into prostaglandin, thromboxane, and prostacyclin glycerol esters and ethanolamides". *J Biol Chem* **277**: 44877-44885.
- Kwok, S., Kellogg, D.E., McKinney, N., Spasic, D., Goda, L., Levenson, C., and Sninsky, J.J. (1990). "Effects of primer-template mismatches on the polymerase chain reaction: human immunodeficiency virus type 1 model studies". *Nucleic Acids Res* **18**: 999-1005.
- Lachgar, S., Charveron, M., Bouhaddioui, N., Neveux, Y., Gall, Y., and Bonafe, J.L. (1996). "Inhibitory effects of bFGF, VEGF and minoxidil on collagen synthesis by cultured hair dermal papilla cells". *Arch Dermatol Res* **288**: 469-473.
- Lachgar, S., Charveron, M., Gall, Y., and Bonafe, J.L. (1998). "Minoxidil upregulates the expression of vascular endothelial growth factor in human hair dermal papilla cells". *Br J Dermatol* **138**: 407-411.
- Law, S.K. (2007). "First-line treatment for elevated intraocular pressure (IOP) associated with open-angle glaucoma or ocular hypertension: focus on bimatoprost". *Clin Ophthalmol* **1**: 225-232.
- Law, S.K. (2010). "Bimatoprost in the treatment of eyelash hypotrichosis". *Clin Ophthalmol* **4**: 349-358.
- Leney, S.E., and Tavare, J.M. (2009). "The molecular basis of insulin-stimulated glucose uptake: signalling, trafficking and potential drug targets". *J Endocrinol* **203**: 1-18.
- Lerner, A.B. (1960). "Hormonal control of pigmentation". *Annu Rev Med* **11**: 187-194.
- Lerner, A.B., and Case, J.D. (1959). "Pigment cell regulatory factors". *J Invest Dermatol* **32**: 211-221.

- Lerner, A.B., and McGuire, J.S. (1961). "Effect of alpha- and betamelanocyte stimulating hormones on the skin colour of man". *Nature* **189**: 176-179.
- Li, H., Lawson, J.A., Reilly, M., Adiyaman, M., Hwang, S.W., Rokach, J., and FitzGerald, G.A. (1999). "Quantitative high performance liquid chromatography/tandem mass spectrometric analysis of the four classes of F(2)-isoprostanes in human urine". *Proc Natl Acad Sci USA* **96**: 13381-13386.
- Li, M., Marubayashi, A., Nakaya, Y., Fukui, K., and Arase, S. (2001). "Minoxidil-induced hair growth is mediated by adenosine in cultured dermal papilla cells: possible involvement of sulfonyleurea receptor 2B as a target of minoxidil". *J Invest Dermatol* **117**: 1594-1600.
- Li, N., Chen, X.M., Zhou, Y., Wei, M.L., and Yao, X. (2006). "Travoprost compared with other prostaglandin analogues or timolol in patients with open-angle glaucoma or ocular hypertension: meta-analysis of randomized controlled trials". *Clin Experiment Ophthalmol* **34**: 755-764.
- Liang, Y., Li, C., Guzman, V.M., Evinger, A.J., 3rd, Protzman, C.E., Krauss, A.H., and Woodward, D.F. (2003). "Comparison of prostaglandin F2alpha, bimatoprost (prostamide), and butaprost (EP2 agonist) on Cyr61 and connective tissue growth factor gene expression". *J Biol Chem* **278**: 27267-27277.
- Liang, Y., Woodward, D.F., Guzman, V.M., Li, C., Scott, D.F., Wang, J.W., Wheeler, L.A., Garst, M.E., Landsverk, K., Sachs, G., *et al.* (2008). "Identification and pharmacological characterization of the prostaglandin FP receptor and FP receptor variant complexes". *Br J Pharmacol* **154**: 1079-1093.
- Libecco, J.F., and Bergfeld, W.F. (2004). "Finasteride in the treatment of alopecia". *Expert Opin Pharmacother* **5**: 933-940.
- Liepa, G.U., Sengupta, A., and Karsies, D. (2008). "Polycystic ovary syndrome (PCOS) and other androgen excess-related conditions: can changes in dietary intake make a difference?". *Nutr Clin Pract* **23**: 63-71.
- Lin, J.Y., and Fisher, D.E. (2007). "Melanocyte biology and skin pigmentation". *Nature* **445**: 843-850.
- Lincoln, G.A., and Kay, R.N.B. (1971). "The seasonal reproductive changes in the red deer stag (*Cervus elaphus*)". *Journal of Zoology* **163**: 105-123.
- Lindner, G., Botchkarev, V.A., Botchkareva, N.V., Ling, G., van der Veen, C., and Paus, R. (1997). "Analysis of apoptosis during hair follicle regression (catagen)". *Am J Pathol* **151**: 1601-1617.
- Lindner, G., Menrad, A., Gherardi, E., Merlino, G., Welker, P., Handjiski, B., Roloff, B., and Paus, R. (2000). "Involvement of hepatocyte growth factor/scatter factor and met receptor signaling in hair follicle morphogenesis and cycling". *Faseb J* **14**: 319-332.

- Link, R.E., Paus, R., Stenn, K.S., Kuklinska, E., and Moellmann, G. (1990). "Epithelial growth by rat vibrissae follicles in vitro requires mesenchymal contact via native extracellular matrix". *J Invest Dermatol* **95**: 202-207.
- Liu, J.P., Baker, J., Perkins, A.S., Robertson, E.J., and Efstratiadis, A. (1993). "Mice carrying null mutations of the genes encoding insulin-like growth factor I (Igf-1) and type 1 IGF receptor (Igf1r)". *Cell* **75**: 59-72.
- Logan, A., and Weatherhead, B. (1981). "Effects of alpha-melanocyte-stimulating hormone and [8-arginine]-vasotocin upon melanogenesis in hair follicle melanocytes in vitro". *J Endocrinol* **91**: 501-507.
- Lowry, O.H., Rosebrough, N.J., Farr, A.L., and Randall, R.J. (1951). "Protein measurement with the Folin phenol reagent". *J Biol Chem* **193**: 265-275.
- Ludwig, E. (1977). "Classification of the types of androgenetic alopecia (common baldness) occurring in the female sex". *Br J Dermatol* **97**: 247-254.
- Lynfield, Y.L. (1960). "Effect of pregnancy on the human hair cycle". *J Invest Dermatol* **35**: 323-327.
- Madani, S., and Shapiro, J. (2000). "Alopecia areata update". *J Am Acad Dermatol* **42**: 549-566.
- Mansberger, S.L., and Cioffi, G.A. (2000). "Eyelash formation secondary to latanoprost treatment in a patient with alopecia". *Arch Ophthalmol* **118**: 718-719.
- Marshall, W.A., and Tanner, J.M. (1969). "Variations in pattern of pubertal changes in girls". *Arch Dis Child* **44**: 291-303.
- Marshall, W.A., and Tanner, J.M. (1970). "Variations in the pattern of pubertal changes in boys". *Arch Dis Child* **45**: 13-23.
- Masoodi, M., and Nicolaou, A. (2006). "Lipidomic analysis of twenty-seven prostanoids and isoprostanes by liquid chromatography/electrospray tandem mass spectrometry". *Rapid Commun Mass Spectrom* **20**: 3023-3029.
- Matias, I., Chen, J., De Petrocellis, L., Bisogno, T., Ligresti, A., Fezza, F., Krauss, A.H., Shi, L., Protzman, C.E., Li, C., *et al.* (2004). "Prostaglandin ethanolamides (prostanamides): in vitro pharmacology and metabolism". *J Pharmacol Exp Ther* **309**: 745-757.
- Matsuo, K., Mori, O., and Hashimoto, T. (1998). "Apoptosis in murine hair follicles during catagen regression". *Arch Dermatol Res* **290**: 133-136.
- Mc Donald, C.J. (1991). "Disorders of pigmentation and hair in black patients", (Michigan, The Upjohn Company).
- McAdam, B.F., Catella-Lawson, F., Mardini, I.A., Kapoor, S., Lawson, J.A., and FitzGerald, G.A. (1999). "Systemic biosynthesis of prostacyclin by cyclooxygenase

(COX)-2: the human pharmacology of a selective inhibitor of COX-2". Proc Natl Acad Sci USA **96**: 272-277.

McElwee, K.J., Kissling, S., Wenzel, E., Huth, A., and Hoffmann, R. (2003). "Cultured peribulbar dermal sheath cells can induce hair follicle development and contribute to the dermal sheath and dermal papilla". J Invest Dermatol **121**: 1267-1275.

McPhaul, M.J. (2004). "Androgen receptors and androgen insensitivity syndromes". In Endocrinology, L.J. Degroot, and Jameson, J.L., ed. (Philadelphia, W B Saunders Co).

McPherson, M.J., and Moller, S.G. (2000). In PCR, A. Boshier, ed. (BIOS Scientific Publishers Ltd.).

Mehlhorn, U., Krahwinkel, A., Geissler, H.J., LaRosee, K., Fischer, U.M., Klass, O., Suedkamp, M., Hekmat, K., Tossios, P., and Bloch, W. (2003). "Nitrotyrosine and 8-isoprostane formation indicate free radical-mediated injury in hearts of patients subjected to cardioplegia". J Thorac Cardiovasc Surg **125**: 178-183.

Mehta, J.S., Raman, J., Gupta, N., and Thoung, D. (2003). "Cutaneous latanoprost in the treatment of alopecia areata". Eye **17**, 444-446.

Merrick, A.E. (2000). "The role of paracrine factors in androgen-regulated human hair growth". In Department of Biomedical Sciences (Ph.D thesis, Department of Biomedical Sciences, University of Bradford).

Merrick, A.E., Hibberts, N.A., Kato, S., Messenger, A.G., Thornton, M.J., and Randall, V.A. (1999). "Both beard and scalp cultured dermal papilla cells express mRNA for, and secrete, VEGF but the levels are unaltered by testosterone *in vitro*". J Invest Dermatol Sym Proc **4**: 352.

Messenger, A.G. (1993). "The control of hair growth: an overview". J Invest Dermatol **101**: 4S-9S.

Messenger, A.G., Elliott, K., Temple, A., and Randall, V.A. (1991). "Expression of basement membrane proteins and interstitial collagens in dermal papillae of human hair follicles". J Invest Dermatol **96**: 93-97.

Messenger, A.G., and Rundegren, J. (2004). "Minoxidil: mechanisms of action on hair growth". Br J Dermatol **150**: 186-194.

Meyer, H.C. (1979). "Alopecia associated with ibuprofen". Jama **242**: 142.

Michelet, J.F., Commo, S., Billoni, N., Mahe, Y.F., and Bernard, B.A. (1997). "Activation of cytoprotective prostaglandin synthase-1 by minoxidil as a possible explanation for its hair growth-stimulating effect". J Invest Dermatol **108**: 205-209.

Mikkola, M.L., and Millar, S.E. (2006). "The mammary bud as a skin appendage: unique and shared aspects of development". J Mammary Gland Biol Neoplasia **11**: 187-203.

Miyata, A., Yokoyama, C., Ihara, H., Bandoh, S., Takeda, O., Takahashi, E., and Tanabe, T. (1994). "Characterization of the human gene (TBXAS1) encoding thromboxane synthase". *Eur J Biochem* **224**: 273-279.

Montagna, W., Chase, H.B., and Lobitz, W.C., Jr. (1952). "Histology and cytochemistry of human skin. II. The distribution of glycogen in the epidermis, hair follicles, sebaceous glands and eccrine sweat glands". *Anat Rec* **114**: 231-247.

Montagna, W., and Van Scott, E.J. (1958). "The anatomy of the hair follicle" In *The Biology of Hair Growth*, W. Montagna, Ellis, R.A. , ed. (New York, New York: Academic Press), pp. 39-64.

Montuschi, P., Ciabattoni, G., Paredi, P., Pantelidis, P., du Bois, R.M., Kharitonov, S.A., and Barnes, P.J. (1998). "8-Isoprostane as a biomarker of oxidative stress in interstitial lung diseases". *Am J Respir Crit Care Med* **158**: 1524-1527.

Morrow, J.D., Hill, K.E., Burk, R.F., Nammour, T.M., Badr, K.F., and Roberts, L.J., 2nd (1990). "A series of prostaglandin F2-like compounds are produced in vivo in humans by a non-cyclooxygenase, free radical-catalyzed mechanism". *Proc Natl Acad Sci USA* **87**: 9383-9387.

Muller-Decker, K., and Furstenberger, G. (2007). "The cyclooxygenase-2-mediated prostaglandin signaling is causally related to epithelial carcinogenesis". *Mol Carcinog* **46**: 705-710.

Muller, S.A., and Winkelmann, R.K. (1963). "Alopecia Areata. an Evaluation of 736 Patients". *Arch Dermatol* **88**: 290-297.

Murphy, R.C., Barkley, R.M., Zemski Berry, K., Hankin, J., Harrison, K., Johnson, C., Krank, J., McAnoy, A., Uhlson, C., and Zarini, S. (2005). "Electrospray ionization and tandem mass spectrometry of eicosanoids". *Anal Biochem* **346**: 1-42.

Namazi, M.R. (2003). "Prostaglandin analogs for hair growth: greater expectations". *Dermatol Online J* **9**: 29.

Naslund, M.J., and Miner, M. (2007). "A review of the clinical efficacy and safety of 5alpha-reductase inhibitors for the enlarged prostate". *Clin Ther* **29**: 17-25.

Netland, P.A., Landry, T., Sullivan, E.K., Andrew, R., Silver, L., Weiner, A., Mallick, S., Dickerson, J., Bergamini, M.V., Robertson, S.M., *et al.* (2001). "Travoprost compared with latanoprost and timolol in patients with open-angle glaucoma or ocular hypertension". *Am J Ophthalmol* **132**: 472-484.

Nicolaou, A. (2005). "In bioactive lipids". In *The oily press*, A.a.K. Nicolaou, G, ed. (Bridgewater), pp. 197-222.

Nishimura, E.K., Granter, S.R., and Fisher, D.E. (2005). "Mechanisms of hair graying: incomplete melanocyte stem cell maintenance in the niche". *Science* **307**: 720-724.

- Nishimura, E.K., Jordan, S.A., Oshima, H., Yoshida, H., Osawa, M., Moriyama, M., Jackson, I.J., Barrandon, Y., Miyachi, Y., and Nishikawa, S. (2002). "Dominant role of the niche in melanocyte stem-cell fate determination". *Nature* **416**: 854-860.
- Nixon, A.J. (1993). "A method for determining the activity state of hair follicles". *Biotech Histochem* **68**: 316-325.
- Noecker, R.J., Bulau, S., and Schwiegerling, J. (1999). "Xalatan-induced changes in periocular skin pigmentation and lash dimensions measured using a digital imaging technique". *Invest Ophthalmol* **40**: S832.
- Nomura, T., Lu, R., Pucci, M.L., and Schuster, V.L. (2004). "The two-step model of prostaglandin signal termination: in vitro reconstitution with the prostaglandin transporter and prostaglandin 15 dehydrogenase". *Mol Pharmacol* **65**: 973-978.
- Norwood, O.T. (1975). "Male pattern baldness: classification and incidence". *South Med J* **68**: 1359-1365.
- Nutbrown, M., and Randall, V.A. (1995). "Differences Between Connective Tissue-Epithelial Junctions in Human Skin and the Anagen Hair Follicle". *J Invest Dermatol* **104**: 90-94.
- Nutbrown, M., and Randall, V.A. (1996). "Recognition of cellular differentiation in the human hair follicle at the light microscope level using SACPIC staining". In *Hair research for the next millenium*, D.J.J. Van Neste, and Randall, V.A. , ed. (Elsevier Science B.V.), pp. 161-166.
- Ohyama, M. (2007). "Hair follicle bulge: A fascinating reservoir of epithelial stem cells". *J Dermatol Sci* **46**: 81-89
- Oka, T., and Yoshimura, M. (1986). "Paracrine regulation of mammary gland growth". *Clin Endocrinol Metab* **15**: 79-97.
- Oliver, R.F. (1966). "Whisker growth after removal of the dermal papilla and lengths of the follicle in the hooded rat". *J Embryol Exp Morph* **15**: 331-347.
- Oliver, R.F. (1967). "The experimental induction of whisker growth in the hooded rat by implantation of dermal papillae". *J Embryol Exp Morphol* **18**: 43-51.
- Oliver, R.F. (1970). "The induction of hair follicle formation in the adult hooded rat by vibrissa dermal papillae". *J Embryol Exp Morphol* **23**: 219-236.
- Oliver, R.F., and Jahoda, C.A.B. (1989). "The dermal papilla and maintenance of hair growth". In *The biology of wool and hair*, G.E. Rogers, Reis, P.J., Ward, K.A. and Marshall, R.C., ed. (Chapman & Hall, London), pp. 51-67.
- Olsen, E.A., Hordinsky, M., Whiting, D., Stough, D., Hobbs, S., Ellis, M.L., Wilson, T., and Rittmaster, R.S. (2006). "The importance of dual 5alpha-reductase inhibition in the treatment of male pattern hair loss: results of a randomized placebo-controlled study of dutasteride versus finasteride". *J Am Acad Dermatol* **55**: 1014-1023.



- Orentreich, D.S., and Orentreich, N. (1985). "Hair transplantation". *J Dermatol Surg Oncol* **11**: 319-324.
- Orentreich, N. (1969). "Scalp hair replacement in men". *Hair growth* **9**: 99-108.
- Orentreich, N., and Durr, N.P. (1982). "Biology of scalp hair growth". *Clin Plast Surg* **9**: 197-205.
- Paus, R. (2000). "Control of the hair follicle growth cycle". In *Hair and its disorders: biology, pathology and management*, F.M. Camacho, Randall, V.A., and Price, V.H., ed. (Martin Dunitz, London), pp. 83-94.
- Paus, R., and Cotsarelis, G. (1999). "The biology of hair follicles". *N Engl J Med* **341**: 491-497.
- Paus, R., Handjiski, B., Czarnetzki, B.M., and Eichmuller, S. (1994). "A murine model for inducing and manipulating hair follicle regression (catagen): effects of dexamethasone and cyclosporin A". *J Invest Dermatol* **103**: 143-147.
- Paus, R., Muller-Rover, S., and Botchkarev, V.A. (1999). "Chronobiology of the hair follicle: hunting the " hair cycle clock". *J Invest Dermatol Symp Proc* **4**: 338-345.
- Pecoraro, V., Astore, I., and Barman, J.M. (1968). "The pre-natal and post-natal hair cycles in man". In *Biopathology of pattern alopecia*, A. Baccaredda-Boy, Moretti, G., and Frey, J.R., ed. (Karger, Basel), pp. 29-38.
- Pentland, A.P., and Mahoney, M.G. (1990). "Keratinocyte prostaglandin synthesis is enhanced by IL-1". *J Invest Dermatol* **94**: 43-46.
- Philpott, M. (2000). "The roles of growth factors in hair follicles: investigations using cultured hair follicles". In *Hair and its disorders: biology, pathology and management*, F.M. Camacho, Randall, V.A., and Price, V.H., ed. (Martin Dunitz, London), pp. 103-113.
- Philpott, M.P., Green, M.R., and Kealey, T. (1990). "Human hair growth in vitro". *J Cell Sci* **97**: 463-471.
- Philpott, M.P., Sanders, D.A., and Kealey, T. (1994). "Effects of insulin and insulin-like growth factors on cultured human hair follicles: IGF-I at physiologic concentrations is an important regulator of hair follicle growth in vitro". *J Invest Dermatol* **102**: 857-861.
- Philpott, M.P., Sanders, D.A., and Kealey, T. (1996). "Whole hair follicle culture". *Dermatol Clin* **14**: 595-607.
- Pillans, P.I., and Woods, D.J. (1995). "Drug-associated alopecia". *Int J Dermatol* **34**: 149-158.
- Pinkus, H. (1958). "Embryology of hair. In *The biology of hair growth*", W. Montagna, and Ellis, R.A., ed. (Academic Press, New York), pp. 1-32.

- Polak, J.M., and Van Noorden, S. (2003). "Introduction to immunocytochemistry", Third edn (BIOS Scientific Publishers Ltd).
- Price, M.L., and Griffiths, W.A. (1985). "Normal body hair--a review". *Clin Exp Dermatol* **10**: 87-97.
- Price, V.H. (2003). "Androgenetic alopecia in women". *J Investig Dermatol Symp Proc* **8**: 24-27.
- Priluck, J.C., and Fu, S. (2010). "Latisse-induced periocular skin hyperpigmentation". *Arch Ophthalmol* **12**: 792-793.
- Ramos-Vara, J.A. (2005). "Technical aspects of immunohistochemistry". *Vet Pathol* **42**: 405-426.
- Randall, V.A. (1994). "Androgens and human hair growth". *Clin Endocrinol (Oxf)* **40**: 439-457.
- Randall, V.A. (2000). "Androgens: the main regulator of human hair growth". 69-82.
- Randall, V.A. (2001a). "Is alopecia areata an autoimmune disease?". *Lancet* **358**: 1922-1924.
- Randall, V.A. (2005). "Physiology and pathophysiology of androgenetic alopecia". In *Endocrinology*, L.J. Degroot, and Jameson, J.L., ed. (Philadelphia, W B Saunders Co.), pp. 3295-3309.
- Randall, V.A. (2007). "Hormonal regulation of hair follicles exhibits a biological paradox". *Semin Cell Dev Biol* **18**: 274-285.
- Randall, V.A. (2008a). "Androgens and hair growth". *Dermatol Ther* **21**: 314-328.
- Randall, V.A., and Ebling, F.J. (1991). "Seasonal changes in human hair growth". *Br J Dermatol* **124**: 146-151.
- Randall, V.A., Hibberts, N.A., Thornton, M.J., Hamada, K., Merrick, A.E., Kato, S., Jenner, T.J., De Oliveira, I., and Messenger, A.G. (2000). "The hair follicle: a paradoxical androgen target organ". *Horm Res* **54**: 243-250.
- Randall, V.A., Hibberts, N.A., Thornton, M.J., Merrick, A.E., Hamada, K., Kato, S., Jenner, T.J., de Oliveira, I., and Messenger, A.G. (2001b). "Do androgens influence hair growth by altering the paracrine factors secreted by dermal papilla cells?". *Eur J Dermatol* **11**: 315-320.
- Randall, V.A., Jenner, T.J., Hibberts, N.A., De Oliveira, I.O., and Vafaei, T. (2008b). "Stem cell factor/c-Kit signalling in normal and androgenetic alopecia hair follicles". *J Endocrinol* **197**: 11-23.
- Rathnayake, D., and Sinclair, R. (2010). "Male androgenetic alopecia". *Expert Opin Pharmacother* **11**: 1295-1304.

- Rendl, M., Lewis, L., and Fuchs, E. (2005). "Molecular dissection of mesenchymal-epithelial interactions in the hair follicle". *PLoS Biol* **3**: e331.
- Reynolds, A., Murray, P.I., and Colloby, P.S. (1998). "Darkening of eyelashes in a patient treated with latanoprost". *Eye* **12** ( 4): 741-743.
- Reynolds, A.J., and Jahoda, C.A. (1991). "Inductive properties of hair follicle cells". *Ann N Y Acad Sci* **642**: 226-241.
- Reynolds, A.J., and Jahoda, C.A. (1992). "Cultured dermal papilla cells induce follicle formation and hair growth by transdifferentiation of an adult epidermis". *Development* **115**: 587-593.
- Reynolds, A.J., and Jahoda, C.A. (1996). "Hair matrix germinative epidermal cells confer follicle-inducing capabilities on dermal sheath and high passage papilla cells". *Development* **122**: 3085-3094.
- Reynolds, A.J., Lawrence, C., Cserhalmi-Friedman, P.B., Christiano, A.M., and Jahoda, C.A. (1999). "Trans-gender induction of hair follicles". *Nature* **402**: 33-34.
- Reynolds, E.L. (1951). "The appearance of adult patterns of body hair in man". *Ann N Y Acad Sci* **53**: 576-584.
- Richter, M., Krauss, A.H., Woodward, D.F., and Lutjen-Drecoll, E. (2003). "Morphological changes in the anterior eye segment after long-term treatment with different receptor selective prostaglandin agonists and a prostamide". *Invest Ophthalmol Vis Sci* **44**: 4419-4426.
- Roberts, L.J., 2nd, Montine, T.J., Markesbery, W.R., Tapper, A.R., Hardy, P., Chemtob, S., Dettbarn, W.D., and Morrow, J.D. (1998). "Formation of isoprostane-like compounds (neuroprostanes) in vivo from docosahexaenoic acid". *J Biol Chem* **273**: 13605-13612.
- Rogers, N.E., and Avram, M.R. (2008). "Medical treatments for male and female pattern hair loss". *J Am Acad Dermatol* **59**: 547-566.
- Rommerts, F.F.G. (2004). "Testosterone: An overview of biosynthesis, transport, metabolism and nongenomic actions". In *Testosterone action - deficiency - substitution*, E. Nieschlag, and Behre, H.M., ed. (Cambridge University Press), pp. 1-37.
- Rook, A., and Dawber, R. (1991). "Colour of the Hair". Second Edition edn (Blackwell Scientific).
- Rousseau, K., Kauser, S., Pritchard, L.E., Warhurst, A., Oliver, R.L., Slominski, A., Wei, E.T., Thody, A.J., Tobin, D.J., and White, A. (2007). "Proopiomelanocortin (POMC), the ACTH/melanocortin precursor, is secreted by human epidermal keratinocytes and melanocytes and stimulates melanogenesis". *Faseb J* **21**: 1844-1856.
- Rushton, H.D. (2003). "Commentary: decreased serum ferritin and alopecia in women". *Invest Dermatol* **121**: pp. xvii–xviii.

- Rutberg, S.E., Kolpak, M.L., Gourley, J.A., Tan, G., Henry, J.P., and Shander, D. (2006). "Differences in expression of specific biomarkers distinguish human beard from scalp dermal papilla cells". *J Invest Dermatol* **126**: 2583-2595.
- Ruzicka, T., and Aulock, J. (1987). "Arachidonic acid metabolism in guinea pig Langerhans cells: studies on cyclooxygenase and lipoxygenase pathways". *J Immunol* **138**: 539-543.
- Saitoh, M., Uzuka, M., and Sakamoto, M. (1970). "Human hair cycle". *J Invest Dermatol* **54**: 65-81.
- Samad, T.A., Sapirstein, A., and Woolf, C.J. (2002). "Prostanoids and pain: unraveling mechanisms and revealing therapeutic targets". *Trends Mol Med* **8**: 390-396.
- Sasaki, S., Hozumi, Y., and Kondo, S. (2005). "Influence of prostaglandin F<sub>2</sub>α and its analogues on hair regrowth and follicular melanogenesis in a murine model". *Exp Dermatol* **14**: 323-328.
- Schlake, T. (2007). "Determination of hair structure and shape". *Semin Cell Dev Biol* **18**: 267-273.
- Schmidt-Ullrich, R., and Paus, R. (2005). "Molecular principles of hair follicle induction and morphogenesis". *Bioessays* **27**: 247-261.
- Schuster, V.L. (1998). "Molecular mechanisms of prostaglandin transport". *Annu Rev Physiol* **60**: 221-242.
- Sengel, P. (1983). "Epidermal-dermal interactions during formation of skin and cutaneous appendages". In *Biochemistry and physiology of the skin*, L.A. Goldsmith, ed. (Oxford University Press, New York), pp. 102-131.
- Shapiro, J., and Lui, H. (2005). "Treatments for unwanted facial hair". *Skin Therapy Lett* **10**: 1-4.
- Shapiro, J., and Price, V.H. (1998). "Hair regrowth. Therapeutic agents". *Dermatol Clin* **16**: 341-356.
- Sharif, N.A., Davis, T.L., and Williams, G.W. (1999). "[<sup>3</sup>H]AL-5848 ([<sup>3</sup>H]9β-(+)-Fluprostenol). Carboxylic acid of travoprost (AL-6221), a novel FP prostaglandin to study the pharmacology and autoradiographic localization of the FP receptor". *J Pharm Pharmacol* **51**: 685-694.
- Sharif, N.A., Kelly, C.R., and Williams, G.W. (2003). "Bimatoprost (Lumigan((R))) is an agonist at the cloned human ocular FP prostaglandin receptor: real-time FLIPR-based intracellular Ca(2+) mobilization studies". *Prostaglandins Leukot Essent Fatty Acids* **68**: 27-33.
- Sharif, N.A., Williams, G.W., and Kelly, C.R. (2001). "Bimatoprost and its free acid are prostaglandin FP receptor agonists". *Eur J Pharmacol* **432**: 211-213.

- Sharma, V.K., Dawn, G., and Kumar, B. (1996). "Profile of alopecia areata in Northern India". *Int J Dermatol* **35**: 22-27.
- Sharov, A., Tobin, D.J., Sharova, T.Y., Atoyan, R., and Botchkarev, V.A. (2005). "Changes in different melanocyte populations during hair follicle involution (catagen)". *J Invest Dermatol* **125**: 1259-1267.
- Sherwood, M., and Brandt, J. (2001). "Six-month comparison of bimatoprost once-daily and twice-daily with timolol twice-daily in patients with elevated intraocular pressure". *Surv Ophthalmol* **45**: S361-368.
- Shifren, J.L., Tseng, J.F., Zaloudek, C.J., Ryan, I.P., Meng, Y.G., Ferrara, N., Jaffe, R.B., and Taylor, R.N. (1996). "Ovarian steroid regulation of vascular endothelial growth factor in the human endometrium: implications for angiogenesis during the menstrual cycle and in the pathogenesis of endometriosis". *J Clin Endocrinol Metab* **81**: 3112-3118.
- Shimaoka, S., Imai, R., and Ogawa, H. (1994). "Dermal papilla cells express hepatocyte growth factor". *J Dermatol Sci* **7**: S79-83.
- Shimaoka, S., Tsuboi, R., Jindo, T., Imai, R., Takamori, K., Rubin, J.S., and Ogawa, H. (1995). "Hepatocyte growth factor/scatter factor expressed in follicular papilla cells stimulates human hair growth in vitro". *J Cell Physiol* **165**: 333-338.
- Shorter, K., Farjo, N.P., Picksley, S.M., and Randall, V.A. (2008). "Human hair follicles contain two forms of ATP-sensitive potassium channels, only one of which is sensitive to minoxidil". *Faseb J* **22**: 1725-1736.
- Shweiki, D., Itin, A., Neufeld, G., Gitay-Goren, H., and Keshet, E. (1993). "Patterns of expression of vascular endothelial growth factor (VEGF) and VEGF receptors in mice suggest a role in hormonally regulated angiogenesis". *J Clin Invest* **91**: 2235-2243.
- Sinclair, R.D., Banfield, C.C., and Dawber, R.P.R. (1999). "Alopecia areata". In *Handbook of diseases of the hair and scalp* (Blackwell Science Ltd), pp. 75-84.
- Skrypina, N.A., Timofeeva, A.V., Khaspekov, G.L., Savochkina, L.P., and Beabealashvili, R.S. (2003). "Total RNA suitable for molecular biology analysis". *Journal of Biotechnology* **105**: 1-9.
- Slater, T., and McDonald-Gibson, R. (1987). "Prostaglandins and related substances: A practical approach" In, B. C., McDonald-Gibson, R., S., N. and Slater, T., ed. (Oxford, IRL Press), pp. 1-4.
- Slominski, A., Ermak, G., Hwang, J., Chakraborty, A., Mazurkiewicz, J.E., and Mihm, M. (1995). "Proopiomelanocortin, corticotropin releasing hormone and corticotropin releasing hormone receptor genes are expressed in human skin". *FEBS Lett* **374**: 113-116.
- Slominski, A., Tobin, D.J., Shibahara, S., and Wortsman, J. (2004). "Melanin pigmentation in mammalian skin and its hormonal regulation". *Physiol Rev* **84**: 1155-1228.

Smith, W.L., DeWitt, D.L., and Garavito, R.M. (2000). "Cyclooxygenases: structural, cellular, and molecular biology". *Annu Rev Biochem* **69**: 145-182.

Smith, W.L., and Song, I. (2002). "The enzymology of prostaglandin endoperoxide H synthases-1 and -2". *Prostaglandins Other Lipid Mediat* **68-69**: 115-128.

Snell, R.S. (1964). "Effect of the Alpha Melanocyte Stimulating Hormone of the Pituitary on Mammalian Epidermal Melanocytes". *J Invest Dermatol* **42**: 337-347.

Snell, R.S., and Bischitz, P.G. (1960). "The effect of large doses of estrogen and estrogen and progesterone on melanin pigmentation". *J Invest Dermatol* **35**: 73-82.

Solish, A.M., James, F., Walt, J.G., and Chiang, T.H. (2010). "Paired-eye comparison of medical therapies for glaucoma". *Clin Ophthalmol* **4**: 1131-1135.

Sonnenberg, E., Meyer, D., Weidner, K.M., and Birchmeier, C. (1993). "Scatter factor/hepatocyte growth factor and its receptor, the c-met tyrosine kinase, can mediate a signal exchange between mesenchyme and epithelia during mouse development". *J Cell Biol* **123**: 223-235.

Spada, C.S., Krauss, A.H., Woodward, D.F., Chen, J., Protzman, C.E., Nieves, A.L., Wheeler, L.A., Scott, D.F., and Sachs, G. (2005). "Bimatoprost and prostaglandin F(2 alpha) selectively stimulate intracellular calcium signaling in different cat iris sphincter cells". *Exp Eye Res* **80**: 135-145.

Sperling, L.C. (1991). "Hair anatomy for the clinician". *J Am Acad Dermatol* **25**: 1-17.

Spielman, A.I., Zeng, X.N., Leyden, J.J., and Preti, G. (1995). "Proteinaceous precursors of human axillary odor: isolation of two novel odor-binding proteins". *Experientia* **51**: 40-47.

Srinivasan, D., Fujino, H., and Regan, J.W. (2002). "Differential internalization of the prostaglandin F<sub>2α</sub> receptor isoforms: role of protein kinase C and clathrin". *J Pharmacol Exp Ther* **302**: 219-224.

Staricco, R.G. (1960). "The melanocytes and the hair follicle". *J Invest Dermatol* **35**: 185-194.

Staricco, R.G. (1963). "The presence of melanocyte in the hair follicle" *AnnNY AcadSci* **100**: 239-255.

Stark, H.J., Breitkreutz, D., Limat, A., Bowden, P., and Fusenig, N.E. (1987). "Keratins of the human hair follicle: "hyperproliferative" keratins consistently expressed in outer root sheath cells in vivo and in vitro". *Differentiation* **35**: 236-248.

Stecchi, G., Saccucci, S., Molinari, S., and De Gregorio, F. (2002). "Eyelash hypertrichosis induced by topical latanoprost: 6-month follow-up study". *Acta Ophthalmol Scand Suppl* **236**: 56-57.

Stenn, K. (2005). "Exogen is an active, separately controlled phase of the hair growth cycle". *J Am Acad Dermatol* **52**: 374-375.

Stenn, K.S., Parimoo, S., and Prouty, S. (1998). "Growth of the hair follicle: a cycling and regenerating biological system". In *Molecular basis of epithelial appendage morphogenesis*, C.M. Chuong, ed. (Landes, Austin), pp. 111-130.

Stenn, K.S., and Paus, R. (2001). "Controls of hair follicle cycling". *Physiol Rev* **81**: 449-494.

Stjernschantz, J.W. (2001). "From PGF(2alpha)-isopropyl ester to latanoprost: a review of the development of xalatan: the Proctor Lecture". *Invest Ophthalmol Vis Sci* **42**: 1134-1145.

Straus, D.S., and Glass, C.K. (2001). "Cyclopentenone prostaglandins: new insights on biological activities and cellular targets". *Med Res Rev* **21**: 185-210.

Strober, B.E., Potash, S., and Grossman, M.E. (2001). "Eyelash hypertrichosis in a patient treated with topical latanoprost". *Cutis* **67**: 109-110.

Sugimoto, M., Sugimoto, M., and Uji, Y. (2002). "Quantitative analysis of eyelash lengthening following topical latanoprost therapy". *Can J Ophthalmol* **37**: 342-345.

Sullivan, M.H., Roseblade, C.K., Rendell, N.B., Taylor, G.W., and Elder, M.G. (1992). "Metabolism of prostaglandins E2 and F2 alpha by human fetal membranes". *Biochim Biophys Acta* **1123**: 342-346.

Suzuki-Yamamoto, T., Nishizawa, M., Fukui, M., Okuda-Ashitaka, E., Nakajima, T., Ito, S., and Watanabe, K. (1999). "cDNA cloning, expression and characterization of human prostaglandin F synthase". *FEBS Lett* **462**: 335-340.

Suzuki, K., and Kono, T. (1980). "Evidence that insulin causes translocation of glucose transport activity to the plasma membrane from an intracellular storage site". *Proc Natl Acad Sci USA* **77**: 2542-2545.

Taylor, A.W., Bruno, R.S., Frei, B., and Traber, M.G. (2006). "Benefits of prolonged gradient separation for high-performance liquid chromatography-tandem mass spectrometry quantitation of plasma total 15-series F-isoprostanes". *Anal Biochem* **350**: 41-51.

Terragno, A., Rydzik, R., and Terragno, N.A. (1981). "High performance liquid chromatography and UV detection for the separation and quantitation of prostaglandins". *Prostaglandins* **21**: 101-112.

Thibaut, S., De Becker, E., Caisey, L., Baras, D., Karatas, S., Jammayrac, O., Pisella, P.J., and Bernard, B.A. (2009). "Human eyelash characterization". *Br J Dermatol* **162**: 304-310.

Thody, A.J., Ridley, K., Penny, R.J., Chalmers, R., Fisher, C., and Shuster, S. (1983). "MSH peptides are present in mammalian skin". *Peptides* **4**: 813-816.

Thornton, M.J., Nelson, L.D., Taylor, A.H., Birch, M.P., Laing, I., and Messenger, A.G. (2006). "The modulation of aromatase and estrogen receptor alpha in cultured human dermal papilla cells by dexamethasone: a novel mechanism for selective action of estrogen via estrogen receptor beta?". *J Invest Dermatol* **126**: 2010-2018.

Thornton, M.J., Taylor, A.H., Mulligan, K., Al-Azzawi, F., Lyon, C.C., O'Driscoll, J., and Messenger, A.G. (2003). "The distribution of estrogen receptor beta is distinct to that of estrogen receptor alpha and the androgen receptor in human skin and the pilosebaceous unit". *J Invest Dermatol Symp Proc* **8**: 100-103.

Tiano, H.F., Loftin, C.D., Akunda, J., Lee, C.A., Spalding, J., Sessoms, A., Dunson, D.B., Rogan, E.G., Morham, S.G., Smart, R.C., *et al.* (2002). "Deficiency of either cyclooxygenase (COX)-1 or COX-2 alters epidermal differentiation and reduces mouse skin tumorigenesis". *Cancer Res* **62**: 3395-3401.

Tiede, S., Kloepper, J.E., Bodo, E., Tiwari, S., Kruse, C., and Paus, R. (2007). "Hair follicle stem cells: walking the maze". *Eur J Cell Biol* **86**: 355-376.

Tilley, S.L., Coffman, T.M., and Koller, B.H. (2001). "Mixed messages: modulation of inflammation and immune responses by prostaglandins and thromboxanes". *J Clin Invest* **108**: 15-23.

Tobin, D.J., and Kauser, S. (2005). "Hair melanocytes as neuro-endocrine sensors--pigments for our imagination". *Mol Cell Endocrinol* **243**: 1-11.

Torii, E., Segi, E., Sugimoto, Y., Takahashi, K., Kabashima, K., Ikai, K., and Ichikawa, A. (2002). "Expression of prostaglandin E(2) receptor subtypes in mouse hair follicles". *Biochem Biophys Res Commun* **290**: 696-700.

Trotter, M. (1924). "The life cycles of hair in selected regions of the body". *Am J Phys Anthropol* **7**: 427-437.

Tsuji, Y., Denda, S., Soma, T., Raftery, L., Momoi, T., and Hibino, T. (2003). "A potential suppressor of TGF-beta delays catagen progression in hair follicles". *J Invest Dermatol Symp Proc* **8**: 65-68.

Uno, H., Zimbric, M.L., Albert, D.M., and Stjernschantz, J. (2002). "Effect of latanoprost on hair growth in the bald scalp of the stump-tailed macaque: a pilot study". *Acta Derm Venereol* **82**: 7-12.

Urade, Y., and Eguchi, N. (2002). "Lipocalin-type and hematopoietic prostaglandin D synthases as a novel example of functional convergence". *Prostaglandins Other Lipid Mediat* **68-69**: 375-382.

Van Scott, E.J., and Ekel, T.M. (1958). "Geometric relationships between the matrix of the hair bulb and its dermal papilla in normal and alopecic scalp". *J Invest Dermatol* **31**: 281-287.

Van Scott EJ, E.T. (1958). "Geometric relationships between the matrix of the hair bulb and its dermal papilla in normal and alopecic scalp". *J Invest Dermatol* **31**: 281-287.



Vaughan, T.A. (1986). "Patterned androgenic alopecia". *J Am Acad Dermatol* **18**: 1073-1077.

Vennegoor, C., Hageman, P., Van Nouhuijs, H., Ruiter, D.J., Calafat, J., Ringens, P.J., and Rumke, P. (1988). "A monoclonal antibody specific for cells of the melanocyte lineage". *Am J Pathol* **130**: 179-192.

Vogt, A., Hadam, S., Heiderhoff, M., Audring, H., Lademann, J., Sterry, W., and Blume-Peytavi, U. (2007). "Morphometry of human terminal and vellus hair follicles". *Exp Dermatol* **16**: 946-950.

Waddington, E., Sienuarine, K., Puddey, I., and Croft, K. (2001). "Identification and quantitation of unique fatty acid oxidation products in human atherosclerotic plaque using high-performance liquid chromatography". *Anal Biochem* **292**: 234-244.

Wan, Z., Woodward, D.F., Cornell, C.L., Fliri, H.G., Martos, J.L., Pettit, S.N., Wang, J.W., Kharlamb, A.B., Wheeler, L.A., Garst, M.E., *et al.* (2007). "Bimatoprost, prostamide activity, and conventional drainage". *Invest Ophthalmol Vis Sci* **48**: 4107-4115.

Wand, M. (1997). "Latanoprost and hyperpigmentation of eyelashes". *Arch Ophthalmol* **115**: 1206-1208.

Wasserman, D., Guzman-Sanchez, D.A., Scott, K., and McMichael, A. (2007). "Alopecia areata". *Int J Dermatol* **46**: 121-131.

Waters, J.M., Richardson, G.D., and Jahoda, C.A. (2007). "Hair follicle stem cells". *Semin Cell Dev Biol* **18**: 245-254.

Watson, A.D. (2006). "Thematic review series: systems biology approaches to metabolic and cardiovascular disorders. Lipidomics: a global approach to lipid analysis in biological systems". *J Lipid Res* **47**: 2101-2111.

Watson, P.G. (1999). "Latanoprost in the treatment of glaucoma and ocular hypertension". *Drugs Today (Barc)* **35**: 449-459.

Weber, A., Ni, J., Ling, K.H., Acheampong, A., Tang-Liu, D.D., Burk, R., Cravatt, B.F., and Woodward, D. (2004). "Formation of prostamides from anandamide in FAAH knockout mice analyzed by HPLC with tandem mass spectrometry". *J Lipid Res* **45**: 757-763.

Weedon, D., and Strutton, G. (1981). "Apoptosis as the mechanism of the involution of hair follicles in catagen transformation". *Acta Derm Venereol* **61**: 335-339.

Wei, B.Q., Mikkelsen, T.S., McKinney, M.K., Lander, E.S., and Cravatt, B.F. (2006). "A second fatty acid amide hydrolase with variable distribution among placental mammals". *J Biol Chem* **281**: 36569-36578.

West, P.M., and Packer, C. (2002). "Sexual selection, temperature, and the lion's mane". *Science* **297**: 1339-1343.

Whiting, D.A. (1993). "Diagnostic and predictive value of horizontal sections of scalp biopsy specimens in male pattern androgenetic alopecia". *J Am Acad Dermatol* **28**: 755-763.

Whiting, D.A., Olsen, E.A., Savin, R., Halper, L., Rodgers, A., Wang, L., Hustad, C., and Palmisano, J. (2003). "Efficacy and tolerability of finasteride 1 mg in men aged 41 to 60 years with male pattern hair loss". *Eur J Dermatol* **13**: 150-160.

Williams, D.E., de Vries, P., Namen, A.E., Widmer, M.B., and Lyman, S.D. (1992). "The Steel factor". *Dev Biol* **151**: 368-376.

Williams, R.D. (2002). "Efficacy of bimatoprost in glaucoma and ocular hypertension unresponsive to latanoprost". *Adv Ther* **19**: 275-281.

Wilson, J.D., Griffin, J.E., and Russell, D.W. (1993). "Steroid 5 alpha-reductase 2 deficiency". *Endocr Rev* **14**: 577-593.

Wise, H., Wong, Y.H., and Jones, R.L. (2002). "Prostanoid signal integration and cross talk". *Neurosignals* **11**: 20-28.

Wiswedel, I., Hirsch, D., Nourooz-Zadeh, J., Flechsig, A., Luck-Lambrecht, A., and Augustin, W. (2002). "Analysis of monohydroxyeicosatetraenoic acids and F2-isoprostanes as markers of lipid peroxidation in rat brain mitochondria". *Free Radic Res* **36**: 1-11.

Wolf, R., Matz, H., Zalish, M., Pollack, A., and Orion, E. (2003). "Prostaglandin analogs for hair growth: great expectations". *Dermatol Online J* **9**: 7.

Woodward, D., and *al., e.* (in press). "Pharmacological differentiation of bimatoprost and latanoprost induced ocular hypotension by a second generation prostamide antagonist (AGN 211336)" (Nova Science Publishers Inc.).

Woodward, D.F., Carling, R.W., Cornell, C.L., Fliri, H.G., Martos, J.L., Pettit, S.N., Liang, Y., and Wang, J.W. (2008a). "The pharmacology and therapeutic relevance of endocannabinoid derived cyclo-oxygenase (COX)-2 products". *Pharmacol Ther* **120**: 71-80.

Woodward, D.F., and Chen, J. (2007). "Fixed-combination and emerging glaucoma therapies". *Expert Opin Emerg Drugs* **12**: 313-327.

Woodward, D.F., Krauss, A.H., Chen, J., Lai, R.K., Spada, C.S., Burk, R.M., Andrews, S.W., Shi, L., Liang, Y., Kedzie, K.M., *et al.* (2001). "The pharmacology of bimatoprost (Lumigan)". *Surv Ophthalmol* **4**: 337-345.

Woodward, D.F., Krauss, A.H., Chen, J., Liang, Y., Li, C., Protzman, C.E., Bogardus, A., Chen, R., Kedzie, K.M., Krauss, H.A., *et al.* (2003). "Pharmacological characterization of a novel antiglaucoma agent, Bimatoprost (AGN 192024)". *J Pharmacol Exp Ther* **305**: 772-785.

- Woodward, D.F., Krauss, A.H., Wang, J.W., Protzman, C.E., Nieves, A.L., Liang, Y., Donde, Y., Burk, R.M., Landsverk, K., and Struble, C. (2007). "Identification of an antagonist that selectively blocks the activity of prostamides (prostaglandin-ethanolamides) in the feline iris". *Br J Pharmacol* **150**: 342-352.
- Woodward, D.F., and Lawrence, R.A. (1994). "Identification of a single (FP) receptor associated with prostanoid-induced Ca<sup>2+</sup> signals in Swiss 3T3 cells". *Biochem Pharmacol* **47**: 1567-1574.
- Woodward, D.F., Liang, Y., and Krauss, A.H. (2008b). "Prostamides (prostaglandin-ethanolamides) and their pharmacology". *Br J Pharmacol* **153**: 410-419.
- Woodward, D.F., Phelps, R.L., Krauss, A.H., Weber, A., Short, B., Chen, J., Liang, Y., and Wheeler, L.A. (2004). "Bimatoprost: a novel antiglaucoma agent". *Cardiovasc Drug Rev* **22**: 103-120.
- Wosicka, H., and Cal, K. (2010). "Targeting to the hair follicles: current status and potential". *J Dermatol Sci* **57**: 83-89.
- Wu-Kuo, T., and Chuong, C.M. (2000). "Developmental biology of hair follicles and other skin appendages". In *Hair and its disorders: biology, pathology and management*, F.M. Camacho, Randall, V.A., and Price, V.H., ed. (Martin Dunitz Ltd), pp. 17-37.
- Yang, C.C., and Cotsarelis, G. (2010). "Review of hair follicle dermal cells". *J Dermatol Sci* **57**: 2-11.
- Yang, P., Felix, E., Madden, T., Fischer, S.M., and Newman, R.A. (2002). "Quantitative high-performance liquid chromatography/electrospray ionization tandem mass spectrometric analysis of 2- and 3-series prostaglandins in cultured tumor cells". *Anal Biochem* **308**: 168-177.
- Yang, W., Ni, J., Woodward, D.F., Tang-Liu, D.D., and Ling, K.H. (2005). "Enzymatic formation of prostamide F2 $\alpha$  from anandamide involves a newly identified intermediate metabolite, prostamide H2". *J Lipid Res* **46**: 2745-2751.
- Young, J.Z. (1957). *The life of mammals*. In, O.U.p. Oxford, ed.
- Yu, M., Ives, D., and Ramesha, C.S. (1997). "Synthesis of prostaglandin E2 ethanolamide from anandamide by cyclooxygenase-2". *J Biol Chem* **272**: 21181-21186.
- Yue, H., Jansen, S.A., Strauss, K.I., Borenstein, M.R., Barbe, M.F., Rossi, L.J., and Murphy, E. (2007). "A liquid chromatography/mass spectrometric method for simultaneous analysis of arachidonic acid and its endogenous eicosanoid metabolites prostaglandins, dihydroxyeicosatrienoic acids, hydroxyeicosatetraenoic acids, and epoxyeicosatrienoic acids in rat brain tissue". *J Pharm Biomed Anal* **43**: 1122-1134.
- Ziboh, V.A., Miller, C.C., and Cho, Y. (2000). "Significance of lipoxygenase-derived monohydroxy fatty acids in cutaneous biology". *Prostaglandins Other Lipid Mediat* **63**: 3-13.

## **6 Appendices**

### **6.1 Saccpic stain**

Preparation of solutions:

#### **Celestine blue**

A 5% aqueous solution of ferric ammonium sulphate (500 ml) was added to 2.5g Celestine blue (C1 51050). After boiling for 3 min, the solution was allowed to cool, and filtered (grade 595 paper, Schleicher and Schuell, supplied by SLS, Nottingham, UK) before the addition of 70ml glycerol.

#### **Picric acid/ethanol**

A saturated alcoholic solution of picric acid (5ml) was mixed with 300 ml absolute ethanol.

#### **Picro-indigo carmine**

A saturated aqueous solution of picric acid (300 ml) was mixed thoroughly with 1 g of indigo carmine (C1 73015); this solution was filtered before use.

#### **Safranin**

Safranin (6 g; C150240) was dissolved in 300ml of a 1:1 ethanol:distilled water solution. The solution was filtered before use.

#### **Scott's tap water**

Sodium hydrogen carbonate (2 g) and magnesium sulphate (20 g) were dissolved in 1 ml distilled water, filtered and stored at 4°C until use.

### **6.2 Preparation of phosphate buffered saline**

NaCl (8g), KCl (0.2g), Na<sub>2</sub>HPO<sub>4</sub> (1.44g) and KH<sub>2</sub>PO<sub>4</sub> (0.24g) were dissolved in 800 ml distilled water and the pH controlled at 7.4.

### **6.3 Lowry method for protein content estimation**

Principle: In biological samples, under alkaline conditions divalent copper ions form a complex with peptide bonds to form a monovalent copper ion. The monovalent copper ion and the radical groups of tyrosine, tryptophan, and cysteine react with Folin reagent to produce an unstable product (chromophore) that becomes reduced to molybdenum/tungsten blue, which allows an absorbance to be read at a wavelength of 650nm.

Serial dilutions of bovine serum albumin (BSA; stock concentration 1.5mg/ml) was prepared in 0.5M sodium hydroxide (NaOH) to give different concentrations (0.25, 0.5, 0.75, 1.0 and 1.5 mg/ml). The reagents were added stepwise according to the Lowry method (Lowry et al., 1951) and the absorbances were measured. This enabled a standard calibration line of BSA to be constructed (see appendix 6.4) and thus scalp anagen hair follicle protein content to be estimated.

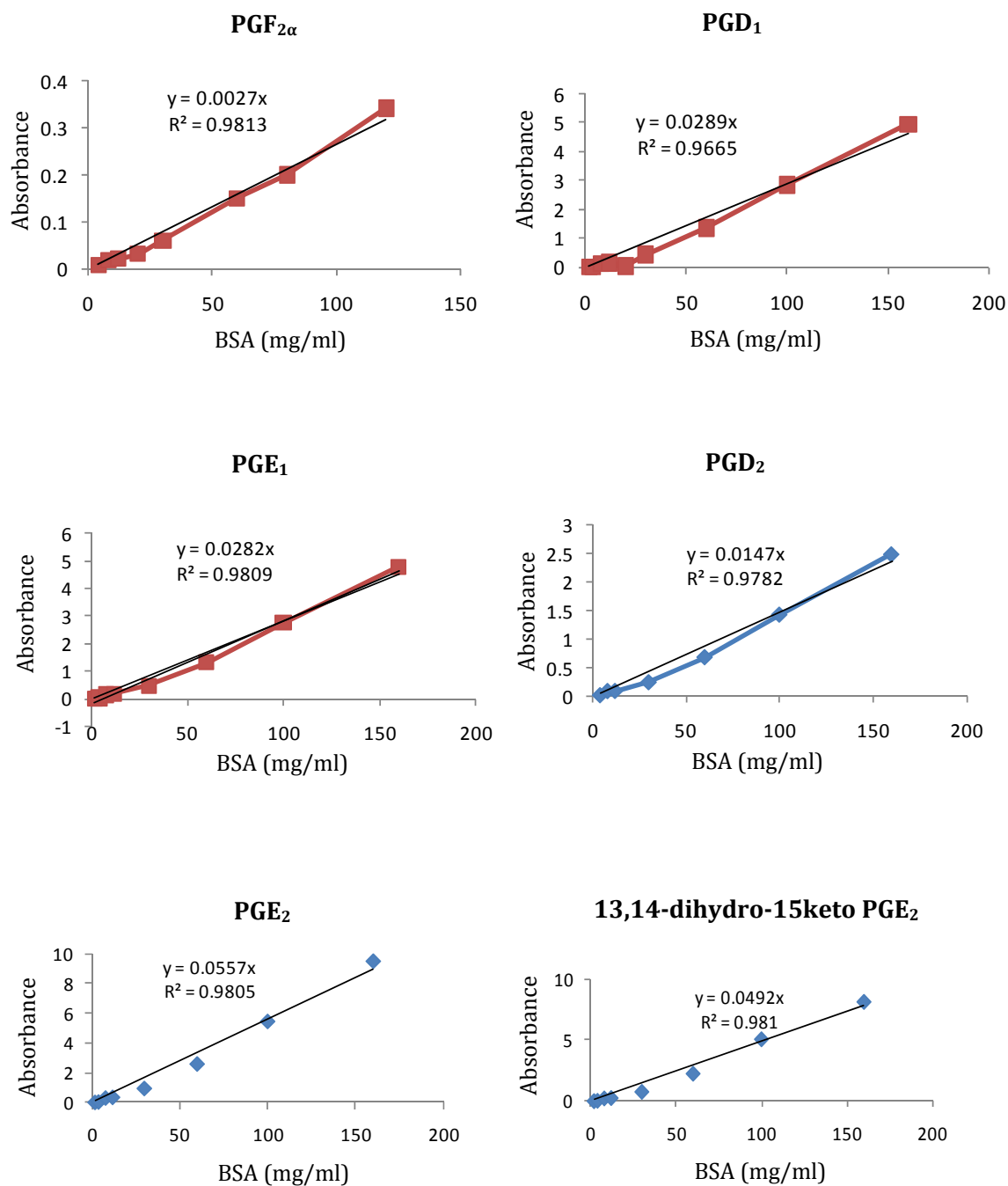
Three different scalp hair follicle samples HF1, HF2, HF3 (5µl) were added in triplicate (Table 10) into a 96 wells plate. Standard dilutions of BSA were also pipetted at the same volume in triplicate into wells as the diagram below shows. Solution A and S comprised alkaline copper tartrate solution and surfactant respectively. Reagents were subsequently added to the wells as follow: 20µl A mixed with 1000µl S to make solution AS, of which 25µl was pipetted into assay wells and 200µl B (Folin reagent) was added to assay wells as a final step.

**Table 10 Representation of a 96 well plate used to estimate protein content**

A	1	3	4	5	6	7	8	9	10	11	12
B	HF1	HF2	HF3				Hair follicle samples (red)				
C	HF1	HF2	HF3								
D	HF1	HF2	HF3								
E											
F	0	0.25	0.5	0.75	1.0	1.5	BSA standards mg/ml				
G	0	0.25	0.5	0.75	1.0	1.5					
H	0	0.25	0.5	0.75	1.0	1.5					

The plate was left in the dark for 20 minutes; a blue colour developed proportionally with the amount of protein in the biological samples. A reading of absorbance at 650nm wavelength was then taken using spectrophotometer. The absorbance of 100% 0.5M NaOH (background) was subtracted from each reading taken to normalise data. Absorbences for the standards were plotted against known concentration of BSA, to construct a calibration line (Figure 79). Using linear regression, the concentration of protein in each sample was estimated.

#### 6.4 Representative calibration lines for PGF<sub>2α</sub>, PGD<sub>1</sub>, PGE<sub>1</sub>, PGD<sub>2</sub>, PGE<sub>2</sub> and 13,14-dihydro-15keto PGE<sub>2</sub>



## 6.5 Materials presented from this thesis

### Papers

**Karzan G Khidhir**, David F Woodward, Nilofer P Farjo, Bessam K Farjo, Jenny W Wang, Steven M Picksley and Valerie A Randall. Is a prostaglandin-related glaucoma therapy the next approach for treating alopecia? (submitted)

### Conference contributions

**1. K.G. Khidhir**, N.P. Farjo, D. F. Woodward, S.M. Picksley and V.A. Randall (2009)

Human scalp hair follicles express the genes for prostanoid FP receptor, *Journal of Investigative Dermatology*, **129**, S102

Poster presentation at 69<sup>th</sup> Society for Investigative Dermatology's Annual Conference, Montreal, Canada, 6-9 May 2009.

**2. Karzan Khidhir**, Nilofer Farjo, David Woodward, Steven Picksley and Valerie A

Randall (2009) Prostaglandin can act directly on human hair follicles: scalp follicles increase growth and in organ culture and express receptor genes, *International Journal of Trichology*, **1**, 69-70

Oral and poster presentaion at 14<sup>th</sup> European Hair Research Society's Annual Conference, Graz, Austria, 2-4 July 2009.

**3. K.G. Khidhir**, N.P. Farjo, S. Picksley and V.A. Randall (2010) Prostaglandin F<sub>2α</sub>

stimulates human hair follicles via receptors located within the follicle itself, *British Journal of Dermatology*, **162**, 916

Oral presentaion at British Society for Investigative Dermatology's 2010 Conference, Edinbrough, United Kingdom, 12-14 April 2010.



**4. K.G. Khidhir**, N.P. Farjo, B. Farjo, D. F. Woodward S.M. Picksley, and V.A. Randall (2010) A prostaglandin  $F_{2\alpha}$  analogue, bimatoprost, used for glaucoma stimulates scalp hair follicle growth in organ culture; is this a new approach for alopecia therapy? *Journal of Experimental Dermatology*, **19**, 571

Oral presentation at 6<sup>th</sup> World Congress for Hair Research, Cairns, Australia, 16-19 Jun 2010.

**5. KG Khidhir**, NP Farjo, BK Farjo, DF Woodward, SM Picksley and VA Randall (2011) Bimatoprost, a prostamide  $F_{2\alpha}$  analogue used for glaucoma, stimulates scalp hair follicle growth via follicular receptors; is this a new approach for alopecia? *Journal of Investigative Dermatology*, **131**, S79

Poster presentaion at 71<sup>st</sup> Society for Investigative Dermatology's Annual Conference, Phoenix, Arizona, USA 4-7 May 2011.